Summer 2020

Temporal Differences in the Emission and Atmospheric Dispersion of Particulate Matter From Waste and Drinking Water Treatment Facilities

Abdulmalik Alsaif

TEMPORAL DIFFERENCES IN THE EMISSION AND ATMOSPHERIC DISPERSION OF PARTICULATE MATTER FROM WASTE AND DRINKING WATER TREATMENT FACILITIES

by

Abdulmalik Alsaif

Bachelor of Science
King Faisal University, 2008

Master of Science
University of Findlay, 2013

Submitted in Partial Fulfillment of the Requirements

For the Degree of Doctor of Philosophy in

Environmental Health Sciences

The Norman J. Arnold School of Public Health

University of South Carolina

2020

Accepted by:

Robert Sean Norman, Major Professor

Dwayne E. Porter, Major Professor

Geoff Scott, Committee Member

Shamia Hoque, Committee Member

Kenneth Mundt, Committee Member

Cheryl L. Addy, Vice Provost and Dean of the Graduate School

DEDICATION

I dedicate this dissertation to my parents, my wife and my daughters, my brothers and sisters and my whole family, and to my country. I dedicate this work to Imam Abdulrahman Bin Faisal University.

ACKNOWLEDGEMENTS

I would like to thank the following people and institutions, without whom I would not have been able to complete this research. I would like to thank Imam Abdulrahman Bin Faisal University for its full support to accomplish this work. I would love to thank my family in the US and back in Saudi Arabia. First and special thanks to my wife for her ultimate support during the whole master and PhD journey and for her patience through the tough times and her full motivation all the time. I would love to thank my two daughters who lighten my life with their smiles and enthusiasm which help me go through stress and give me happiness. I would love to thank my parents for their full support and prayers and being my role models in every life aspect. I would like to thank my brothers and sisters, the rest of my family and my friends in the US and Saudi Arabia for their prayers. I would like to give a big thank you to my adviser Dr. Sean Norman, who invited me to come and work in his lab and for being my guidance until I finish my PhD, it has been a pleasure being your student. I would like to thank my committee members Dr. Dwayne Porter, Dr. Shamia Hoque, Dr. Geoff Scott and Dr. Kenneth Mundt, I learned a lot from you. Big thanks also to my lab peers Mirza Isanovic, Karlen E Correa Velez, Cassie Bailey, Dahae Seong and Gabriel Kenne for their help in sampling trips and data analysis. I would like to thank Peng Gao who was a big help in GIS.

ABSTRACT

Many countries encounter a growing shortage of water, and the reuse of treated or untreated wastewater is their main source. Wastewater Treatment Plants (WWTPs) are mainly designed to remove organic nutrients, large solids, and chemical substances. There are some possible issues regarding WWTPs that are close to residential areas around the world. One of the environmental effects from WWTP that might cause air pollution would be the emission of toxic chemical gases and microorganisms via aerosols that transport bacteria as well as viruses and fungal spores which can be harmful to human health. Therefore, particulate matters (PM) and metrological parameters samples were collected from four WWTPs to examine the spatial and temporal differences in their emissions and dispersions. Geographic Information System (GIS) was used to visualize the predicted PM concentrations from 50 meters to 500 meters around WWTPs sites. We found that there are some seasonal, treatment methods and daily statistical significance variations in the total particulate matters and particulate number by diameter between the four sites.

TABLE OF CONTENTS

LIST OF TABLES

LIST OF FIGURES

CHAPTER 1

INTRODUCTION

1.1. Wastewater Treatment Plant

1.1.1. Wastewater Treatment Plants Process

Many countries encounter a growing shortage of water, and the reuse of treated or untreated wastewater is their main source. Wastewater is using water from homes, industries, and other sources. It includes human wastes, chemicals, and several substances that must be treated before releasing to protect the environment and human health. Therefore, wastewater treatment is necessary to remove as much waste from the water before discharging it into the environment (USGS).

Wastewater Treatment Plants (WWTPs) are mainly designed to remove organic nutrients, large solids, and chemical substances. Generally, municipal WWTPs process wastewater through the conventional method of treatment, which consists of primary, secondary, and tertiary treatment processes (Tran, et al., 2018). Primary treatment aims to remove the suspended solids such as oils, fats, grease, sand, grit, and settable solids. The primary treatment of the water uses screening and filtration to remove bulky solids followed by flotation and sedimentation to remove suspended solids (Godoi, et al., 2018). Moreover, Tran et al. (2018) stated that the removal efficiencies for benzophenones group UV filters are from 10 to 27% after primary treatment. Also, over 75% amount of

triclocarban and triclosan in the influents was removed after primary treatment. The primary purpose of the secondary treatment stage in WWTPs is to remove organic matter and/or nutrients through biological processes such as activated sludge, membrane bioreactors, moving bed biofilm reactor, or fixed bed bioreactors, etc. In this process, bacteria use dissolved oxygen for the biodegradation of organic matters in the wastewater (Kumara and Pal, 2018). As an example of biological treatment, (Godoi, et al., 2018) mentioned that the Upflowx Anaerobic Sludge Blanket (UASB) has 65 to 75% efficiency of organic matter removal with a tank retention time between 8 to 10 hours. Moreover, sludge produced from the secondary treatment is also treated using thickening, dewatering, drying and digestion methods to reduce the volume and to stabilize its biological content so it can be used as fertilizer or it will be sent to landfills (Godoi, et al., 2018).

The tertiary treatment process is used to remove nutrients and contaminants that may escape from secondary treatment such as nitrogen, phosphorous, remaining suspended solids, and unmanageable inorganics and organics. Finally, the disinfection (such as chlorine, UV radiation, and ozonization) removes pathogens from the wastewater before its release into the environment (Kumara, et al., 2018).

1.1.2. Wastewater Treatment Plants Location

According to previous studies, there are some possible issues regarding WWTPs that are close to residential areas around the world. One of the main problems is the public health issues of WWTP pollution that affect the surrounding environmental and human health. Some of these issues are air pollution, discharge of partially treated water, and unpleasant odor. Besides, several studies have stated that WWTP workers have more

gastrointestinal symptoms than the general population due to relationships of occupational exposure to bioaerosols. This could be seen through the occurrence of diarrhea, which is approximately 45% in Swedish Sewage workers compared to 3% in the population (Masclaux, et al., 2014).

Moreover, studies showed a higher rate of mental disorders to the population living near a WWTP. On the other hand, even though there was a significant presence of pathogenic microorganisms in the aerosols close to WWTP, there was no significant association of the WWTP and the incidence of gastrointestinal or myoskeletal diseases to the residents. Likewise, some studies' results acquired at the position located 100 m away from the sewage treatment plant show that the facility does not pose a risk in regard of the emission of bioaerosols and that the near people are not threatened (Vantarakis, et al., 2016).

1.1.3. Wastewater Treatment Plants Environmental Issues

Since conventional municipal wastewater treatment can partially remove solids and nutrients, some contaminants will remain in the effluent and will be discharged into the environment. These pollutants include antibiotics, emerging contaminants (EC) and pharmaceuticals chemicals which can be introduced to the environments via a direct discharge of treated wastewater to the aquatic environment (Tran, et al., 2018) and air emissions from moving mechanical equipment such as screens and aerators during treatment processes (Godoi, et al., 2018).

According to (Miklos, et al., 2018), trace organic chemicals such as pharmaceuticals products have been detected in the aquatic environment, and WWTPs

are one of the leading emitters of those materials because conventional municipal WWTPs are incapable to remove them from the effluent. Moreover, one of the most recent and significant environmental and sanitary concerns are antibiotics. Bacteria that are exposed to antibiotics can develop Antibiotics Resistance (AR), which allows them to survive against medications. WWTPs effluents have an important role in the spreading and dispersions of AR and considered as a major source of Antibiotic Resistance Bacteria (ARB) and Antibiotics Resistance Genes (ARG) into the environment (Turolla, et al., 2018). In addition, (Barancheshme and Munir, 2018) study showed that the concentration of ARGs in WWTPs effluents is higher than the level of ARGs in the natural rivers and environments. They have found that the concentration of total tetracycline resistance genes was 6.4 × 103 copies/ml in the effluent. Also, at WWTP that used activated sludge, chlorination and UV irradiation, the concentrations of ARGs in effluent were 3.4 × 104 copies/ml. Additionally, microbial analysis of water samples from a river showed that all the isolates have the antibiotic-resistant ability. For example, resistance to aztreonam was (63%), gentamicin (50%), oxacillin (46%), penicillin (38%) and ampicillin (38%).

Furthermore, (Chonova, et al., 2018) stated that pharmaceutical contaminants had been detected with concentrations of 192 ng/l and they were concentrated more in the surface waters sampled close downstream of the WWTP. Also, the impact of those contaminants on the ecosystem has been recognized as an international concern because they can alter microbial activity, community composition in the environment. Moreover, Bacteria resistant to antibiotics were found downstream of a wastewater treatment plant, drinking water and in water sprayed on vegetables in developing countries and Europe (Kumar, et al., 2018)

In addition, the impact of WWTPs is not limited to the effluents, but it also includes air emissions from moving equipment from the treatment processes. Significant amounts of bioaerosols can be produced during the wastewater treatment process such as discharging, mixing, aerating and spraying of sewage which can cause a high health risk to workers and could be dispersed over considerable distances to pose adverse effects on humans(Li, et al., 2016). Moreover, Anaerobic wastewater treatment plants (WWTPs) are significant sources of Hydrogen sulphide (H2S). H2S emission is a result of physicochemical processes in the treatment and can be found in the atmosphere causing unpleasant odors, which might lead to environmental, social, and economic impacts on the neighboring area (Godoi, et al., 2018).

1.1.4. Wastewater Treatment Plants Human Health Issues

One of the environmental effects from WWTP that might cause air pollution would be the emission of toxic chemical gases and microorganisms via aerosols that transport bacteria as well as viruses and fungal spores which can be harmful to human health (Filipkowska, et al., 2000). In fact, exposure to bioaerosol pollution is now unavoidable for urban residents around the world, and it is associated with many adverse health effects such as infectious diseases, acute toxic effects, allergies, and cancer (Mouli, et al., 2005). Wastewater treatment plants (WWTPs) release aerosol particles into the ambient air, and they contain harmful substances and various pathogenic microbes, such as viruses, fungi, and bacteria. They can cause infection to humans through inhalation, ingestion, and skin contact (Wang, et al., 2018). Exposure to WWTPs' air emissions has significant human health impacts. According to (Wang, et al., 2018), there are many diseases associated with the exposure to bioaerosols such as respiratory diseases,

allergies, and skin rashes, and tuberculosis. Also, some studies have found Streptococcus pneumoniae, Shigella, and Escherichia coli in bioaerosols of municipal WWTPs, which can cause pneumonia, diarrhea, and food poisoning, respectively.

(Han, et al., 2019) studied aerosols emitted from WWTPs based on the particulate size and their depositions in the respiratory system. Particulate larger than 0.5 μm are accumulated in the upper airways where particulate smaller than 0.5 μm can reach the lower airways of the lungs, and both sizes can cause respiratory and cardiovascular illnesses. Also, they found many microorganisms (such as Enterobacter, Enterococcus, Pseudomonas, and Penicillium) and chemicals and toxic metals (such as As, Mn, Ni, Co, and Cr) in the aerosols. These aerosols can stay suspended in the air for long times and travel for long distances by the wind.

Moreover, (Wang, et al., 2018) have investigated the concentration and the distribution of particles in the air over and near WWTP. They discovered that there is a health risk for adults and children living nearby a WWTP from exposure to airborne bacteria, and the significance of the exposure through inhalation is higher than the skin contact exposure. As a result, there were increased incidences of respiratory and intestinal diseases among WWTP workers and residents in the neighboring area.

In addition, there are toxicity concerns to humans' health-related to chemicals emissions from WWTP. For example, exposure to H2S can cause eye damage, respiratory irritation, and death in the acute high concentrations' doses. However, exposure to chronic long-term with low concentrations doses can cause nausea, headaches, and respiratory problems (Godoi, et al., 2018).

1.2. Air Pollution Modeling

Air pollution modeling is a mathematical tool used to explain the relationship between emissions, meteorology, concentrations, and other factors. Likewise, it can give more description of the air quality problems through the analysis of factors and causes such as emission sources, meteorological factors, and physicochemical changes. Air pollution models have an essential role in science, regulations, research, and other applications because they are capable of quantifying the relationship between emissions and concentrations/dispersion for the past and future situations (Daly and Zannetti, 2007). Moreover, one of the most fundamental objectives of air pollution models is to predict pollutant concentrations and dispersions changes and patterns after their emissions from the source. According to (Ni, et al., 2018), Weather Research and Forecasting with Chemistry (WRF-Chem) model have been used in China to provide a useful prediction of particulate pollution over studying the relations between atmospheric physics, dynamics and composition. In this model, aerosols were predicted by simulating physical processes (such as condensation and deposition), cloud interaction, and chemical processes by observing the daily variations and the different metrological conditions. As a result, by using air pollution models, the total PM2.5 concentration was declined by 15%, which proves the effectiveness of the control measures applied. In addition, air pollution models are beneficial in performing exposure and Health Risk Assessment (HRA) studies to provide mitigation measures and policy procedures to protect human health. For example, atmospheric dispersion modeling (AERMOD) system evaluated PM10 emissions from industrial activities, and the results revealed that 30% of the total PM10 is emitted from

industries which were similar to the ground monitoring station data (Amoatey, et al., 2018).

Air dispersion models have been commonly used to predict air pollutant concentrations such as the Gaussian dispersion model, Box model, Lagrangian model, and Eulerian model (Saha, et al., 2018). Furthermore, the box model is including source emissions, advective inflow, and outflow to and from the sides, diffusion of pollutants through increasing and decreasing of mixed height or vertical height, chemical transformations, and wind direction. The model can predict the average volume concentration as a function of time because the mixing is mostly considered uniformed, and all sources of emissions are estimated as a single source. Also, the rate of change of mass must be equal to the sum of the rates by adding all the emission sources mass within the box (Singh, 2018). On the other hand, the lagrangian model is used to calculate the rate of changes of property in a material system, i.e., following particles in the air as they move. The model describes the vertical diffusion of pollutants, deposition, and emissions into the air parcel. However, the Eulerian model is used to determine the changes of particles in one point of space. The atmosphere over the modeling region is supposed as a defined box, and the evolution of pollutants in the box includes emissions, deposition, chemical reactions, and the change in the mixing height (Singh, 2018). Thus, Lagrangian models describe atmospheric transport and dispersion more than Eulerian models. However, they both need a complex meteorological data set, a detailed understanding of the atmospheric processes, and prolonged computation times. Therefore, Eulerian models are commonly utilized than Lagrangian models in different areas such as long-term population exposure and regulatory processes (Teggi, et al., 2018).

1.2.1. Gaussian Dispersion Model

Gaussian dispersion model is a mathematical equation that is applied to point source emitters. This model is used to calculate the maximum ground-level impact of plumes and the distance of maximum effect from the source at full mixing conditions (Matacchiera, et al., 2019). This model can be described experimentally by plotting the standard deviation of its concentration distribution in the vertical and horizontal direction by taking into account the atmospheric stability and downwind distance from the source (Singh, 2018). Gaussian model is quick to run, and it is preferred over more complex models because it allows a wide range of scenarios. Also, Gaussian model is efficient in point source emission prediction on flat terrain and has the highest calculation efficiency among dispersion models (Ma, Zhang, 2016) and commonly used for long term average concentrations modeling (Bitta, et al., 2018).

Currently, Gaussian models are generally used in air quality modeling because of their efficiency and accuracy and easier computational time. According to (Maués, et al., 2019), the Gaussian dispersion model has been developed to examine pollutant dispersion in Santa Cecilia, Mexico. The study has found that high concentrations of particulate matter to the south of the steel complex and showed a substantial contribution of sintering and coke processes in the increase of pollutants in the air.

1.2.2. Air Pollution Modeling Visualization

Geographic Information Systems (GIS) is defined as a computer-based information system that is designed to work with spatial or geographic data. The use of GIS is rapidly increasing in regional and environmental planners, resource managers, and the scientific communities around the world. GIS is composed of three major components which

include the digital map data, the hardware used to enter, store, process and display these data and all the computer software used to perform GIS operations (Eslami, et al, 2011). ArcGIS system allowed the application of a spatially-based dispersion model, which is useful in research fields such as social sciences, public health, geography, and emergency management. Moreover, using spatial and temporal methods in GIS modeling to demonstrate the transport and dispersion of aerosolized pollutants helps to visualize pollutant exposure and potential health outcomes and can minimize the need to run hundreds of equations in case of using other systems. Furthermore, predictive models combined with GIS technology will improve model performance, and eventually, it will improve decision-making capability (Dickman, 2013).

Moreover, using GIS applications in the public health field has been successful and proved that it is a vital tool in solving public health issues and in decision support making processes. Risk analysis and GIS were used to evaluate the public health issues of water sources that are accessible to rural populations in Nigeria. Using spatial analysis approaches, they were able to estimate the probability of the risk of diarrheal infections, and they proposed different solutions to eliminate those risks (Rushton, 2003). Furthermore, there is one remarkable example of how GIS has been used for infectious diseases in the World Health Organization (WHO)'s where they established web GIS-based Public Health Surveillance Systems (WGPHSSs). As an example, the World Health Organization (WHO)'s DengueNet which is a centralized data management system that contains a database and GIS for the global epidemiological and virological surveillance of dengue fever (DF) and dengue haemorrhagic fever (DHF). Data in the system are reported at the country level, standardized to be comparable for different

geographical areas, and used as early warning information for public health to be prepared for management, control, and prevention. As a result, the application of GIS technology for dengue fever has enhanced the understanding of the disease prevalence, disease distribution, and spatial relationship between incidence and risk factors, which was very useful to form control programs (Fletcher-Lartey and Caprarelli, 2016).

In recent years, GIS has been used in several epidemiologic applications, which include disease mapping, cluster analysis, and spatial modeling, which is called "spatial epidemiology". In other words, GIS is used to create spatially variables such as constructed environmental measures (e.g., land use), environmental exposures (e.g., air pollutant concentrations), and demographic indicators (e.g., percent of persons in poverty). Spatial epidemiology, defined as "concerns the analysis of the spatial/geographical distribution of the incidence of disease," and its primary purpose is to measure and determine the degree of spatial relationships for the infectious diseases. Moreover, the field of spatial epidemiology has acknowledged four types of spatial analyses in epidemiology: 1) disease mapping, 2) geographical correlation studies, 3) risk assessment in relation to point or line sources, and 4) cluster detection and disease clustering (Kirby, et al., 2017).

CHAPTER 2

SEASONAL VARIATION OF PARTICULSTE MATTER EMISSION FROM WASTEWATER TREATMENT PLANTS AND PREDICTING THEIR DISPERSION

2.1. Introduction

Generally, particulate matter (PMs) concentrations in the air vary due to several factors. These factors are emission sources, metrological parameters (such as temperature, relative humidity [RH], and wind speed) (Nathan, 2018), human activities and seasonal variations (Li, et al., 2019). According to (Han, et al., 2019) study, they studied concentration, size distribution, population, and exposure risk from bacteria and fungi in bioaerosols of WWTPs that use anaerobic-anoxic-oxic (A2O) process, which uses the activated sludge method to treat wastewater and it is the most widely used process in WWTPs, and they found that the airborne bacteria concentrations were different due to the seasonal variations. The maximum level was in summer with a range of 5.36×10^2 to 1.00×10^4 CFU/m^3 followed by relatively high amounts in autumn with a range of 2.23×10^3 to 7.51×10^3 CFU/m^3 and in spring with a range of 1.14×10^3 to 5.58×10^3 CFU/m^3. Additionally, the minimum concentration of airborne bacteria was found in winter within the range of 194 to 1472 CFU/m^3. Moreover, (Tang, et al., 2020) conducted a study to evaluate the effects of climate such as temperature, relative humidity and wind speed on the concentrations of total suspended particulates (TSP),

PM10, PM4, PM2.5, and PM1that emitted from pig nursery houses. Their study found that the concentration of airborne Escherichia coli was higher in the summer than in other seasons.

Furthermore, a study in Urumqi, China, showed that the average PM10 concentration was higher in January, February, March, November, and December with a highest average value of 338.2 $\mu g/m^3$ in January, 293.5 $\mu g/m^3$ in December and 210.7 $\mu g/m^3$ in November, respectively. On the other hand, the PM10 concentration was lower from April to October, with a minimum of 60.9 $\mu g/m^3$ in June. Based on the division of the seasons on China, spring (March, April, and May), summer (June, July, and August), autumn (September, October, and November), and winter (December, January, and February). Thus, their results showed that summer is the clearest season with lower PM10 concentrations in the air, while winter in the lowest season with the higher PM10 levels in the air. (Meng, et al., 2019).

Moreover, previous studies showed that meteorological factors have a significant impact on the concentrations of the airborne particles in the surrounding area of the WWTPs atmosphere. The correlation between meteorological conditions and particulate concentrations was measured in autumn, winter, and spring and the results showed that relative humidity has a significant correlation with the concentration of airborne particles in autumn ($p < 0.05$, $r = 0.310$) and spring ($p < 0.05$, $r = 0.380$) and no significant correlation in winter ($p = 0.360$, $r = 0.090$). Also, The results demonstrated a significant correlation between the particulate concentrations and ultraviolet (UV) index in winter ($p < 0.05$, $r = –0.270$) and autumn ($p < 0.05$, $r = –0.230$) and no significant correlation in spring ($p > 0.05$, $r = 0.120$) (Dehghani, et al., 2018). Furthermore, Tang et al. (2020)

found that wind speed in summer was significantly higher than in other seasons and that there were no statistical significant differences between seasons. However, they conclude that the concentrations of TSP and PM10 had the same variation trend among different seasons where PM2.5 and PM1 concentration had a similar change trend between seasons. In addition, a previous study showed the variability of the particulate size distributions for bioaerosols by season. For bioaerosols with aerodynamic diameters between 0.65 μm and 3.3 μm, the amounts of particulate in autumn were 2.21×10^4 CFU/m^3, summer was 7.37×10^3 CFU/ m^3 and spring was 4.75×10^3 CFU/m^3 which were higher than winter 3.64×10^3 CFU/m^3. On the other hand, a different phenomenon was found in the seasonal variation of airborne fungal size distribution. The percentage of airborne fungi in bioaerosols was 68.15% in winter, followed by summer with 66.67%, 60.60% in autumn, and the lowest in spring with 59.30%. Overall, the largest concentrations of airborne bacteria and fungi were detected in autumn and summer (Han et al., 2019). Thus, a full understanding of particle concentrations variation during different seasons is important in assessing their impacts on environmental and human health.

2.2. Materials and Methods

2.2.1. Sampling sites

The field sites used for this study consisted of three wastewater treatment plants (WWTPs) and one drinking water treatment plant (DWTP). The DWTP was used as a control for the background concentration of environmental particulate matter (PM) as compared to WWTPs. Though all the WWTPs included in this study use activated sludge treatment processes for their biological treatment, they use different methods of aeration.

WWTP site 1 (Figure 2.1A), located in Mount Pleasant, SC uses bubble aeration in the activated sludge process and treats approximately 3 million gallons per day (MGD). WWTP site 2 (Figure 2.1B), also located in Mount Pleasant, SC, treats approximately 5 MGD and employs mixed methods in the same aeration tank. The injection of the air occurs through bubble aeration from the bottom of the tank and impellers from the top (surface agitation) are used for additional aeration. WWTP site 3 (Figure 2.1C) is located in Columbia, SC and serves around 60,000 customers and covers 120 square miles. The plant has a capacity of 60 MGD and treats an average of 35 MGD of wastewater. This site splits raw sewage into 2 separate treatment trains. Treatment train 1 uses surface agitation for the aeration of activated sludge tanks and the treatment train 2 uses bubble aeration in the activated sludge tanks. The drinking water treatment facility used as a control in this study (site 4, Figure 2.1D) is located in Columbia, SC and has a total treatment capacity of 23 MGD. This facility uses a combination of chemical treatment for initial coagulation followed by mixing and sedimentation, chlorine addition and then a final filtration process.

Figure 2.1: Sampling sites. Panel A, Wastewater Treatment Plant (Site 1); Panel B, Wastewater Treatment plant (Site 2); Panel C, Wastewater Treatment Plant (Site 3); Panel D, Drinking Water Treatment Plant]

2.2.2. Meteorological Data Measurement

Meteorological conditions and particulate matter concentrations were monitored at each site across winter, spring, summer, and fall seasons to examine seasonal variability in particulate emissions (Figures 2.2 – 2.5). During each seasonal sampling event, monitoring occurred across three consecutive days to further examine daily variation in particulate emissions. Meteorological conditions (i.e., wind speed, wind direction, temperature, relative humidity, and barometric pressure) were measured using the Kestrel 4500 Pocket Weather Tracker and the Kestrel 5500 Weather Meter. The Kestrel 4500 Pocket Weather Tracker was placed at the highest location at the center of the testing area to measure the overall prevailing site meteorological parameters across the entire site and sampling period. The Kestrel 5500 Weather Meter was used to collect individual metrological data at each unique sampling location within each field site. Individual meteorological measurements were used to examine within site variation across the different sampling locations to better model particulate emissions and dispersion.

2.2.3. Measurement of Particulate Matter Emissions

To measure particulate emissions, particle concentrations were obtained using the TSI Model 3330 Optical Particle Sizer Spectrometer (OPS). The TSI instrument has 12 channels that separate particles into 12 particle diameters (0.3, 0.4, 0.55, 0.7, 1, 1.3, 1.6, 2.2, 3, 4, 5.5, 7 and 10 micrometers [μm]). The sampling duration was one hour at each sampling location within each site, and the sampling location was varied each day based on the prevailing wind direction measured using the Kestrel 4500 to ensure isolation of downwind and upwind locations. Based on wind direction, one TSI instrument was

placed in the upwind location while another TSI unit was placed in the downwind location to provide simultaneous measurement of upwind and downwind particulate matter concentration (Figures 2.2 - 2.5).

Figure 2.2: Field site 1 sampling location by seasons. Panel A, winter; Panel B, summer; Panel C, spring; Panel D, fall. White circles show the locations of the TSI upwind locations; red rectangles show the locations of the TSI downwind locations; Yellow stars represent the location of Kestrel weather meter measurements).

Figure 2.3: Field site 2 sampling location by seasons. Panel A, winter; Panel B, summer; Panel C, spring; Panel D, fall. White circles show the locations of the TSI upwind locations; red rectangles show the locations of the TSI downwind locations; Yellow stars represent the location of Kestrel weather meter measurements).

Figure 2.4: Field site 3 sampling location by seasons. Panel A, winter; Panel B, summer; Panel C, spring; Panel D, fall. White circles show the locations of the TSI upwind locations; red rectangles show the locations of the TSI downwind locations; Yellow stars represent the location of Kestrel weather meter measurements).

Figure 2.5: Field site 4 sampling location by seasons. Panel A, spring; Panel B, fall; Panel White circles show the locations of the TSI upwind locations; red rectangles show the locations of the TSI downwind locations; Yellow stars represent the location of Kestrel weather meter measurements).

2.2.4. Model Developing

The Gaussian dispersion model is one of the mathematical models that can be used to evaluate the concentration of pollutants downwind from a point source, and it is based on the concept of a normal distribution of the particles downwind from a stack plume. Below is the Gaussian dispersion equation for contaminants emitted at ground level (H=0) (Wark, et al., 1998):

$$C(x,y,z) = \frac{Q}{2\pi\mu\sigma_y\sigma_z} * \exp\left[\frac{-(y-y_0)^2}{2\sigma_y^2}\right] * \exp\left[\frac{-(z-z_0)^2}{2\sigma_z^2}\right]$$

Where:

C = concentration of pollutant at point (x,y,z)

Q = emission rate of the source (mass/time)

μ = average wind speed

x = coordinate position of a point of interest downwind

y = distance of a point of interest perpendicular to plume direction

y_0 = location on plume where a point of interest is perpendicular

z = distance of a point of interest in a vertical direction

z_0 = location on plume where a vertical point of interest is perpendicular

σ_y = horizontal dispersion coefficient

σ_z = vertical dispersion coefficient

Using the equation above, the particulate matter dispersion model used for this study was developed using Microsoft Office Excel to predict the concentration (C) in microgram per cubic meter ($\mu m/m^3$) after dispersion. The total mass of PM at each sampling location was used to estimate the emission rate of the source (Q), and the concentration was converted from microgram per cubic meter per hour ($\mu m/m^3/h$) to gram per second (g/s). The average wind speed (meter per second [m/s]) of each day of sampling was used to estimate overall wind speed (μ). For the recipient height (z), the average person height, which is 1.524 m (5 feet), was used to estimate the breathing zone for the average person. Moreover, different scenarios were used to predict the concentration (C) of PMs at different distances (x) and vertical distance from the plume center (y). For the distance between the source and the recipient (x), we plot 50 meters (m), 60 m, 70 m, 80 m, 90 m, 100 m, 200 m, 300 m, 400 m, and 500 m and the initial concentration of PMs at the sampling location was considered the predicted concentration (C) at a distance 0. However, for the perpendicular distance from the plume centerline (y) which is how far the recipient is located vertically to the right and the left side of the centerline of the emission, we used 1 m, 2 m, 3 m, 4 m, 5 m, 6 m, 7 m, 8 m, 9 m, and 10

m. To generate GIS maps, the coordinates (longitude and latitude) of the treatment tank was collected via Google Earth and then converted to GIS degree decimal to locate the original location of the emission source in the GIS map. Next, the Geographical Coordinates system was adjusted to convert the degree decimal of the longitude and latitude to meters, which aided in identifying the accurate locations of (x) and (y) distances from the original source for each site.

2.2.5. Statistical Analysis

Microsoft Office Excel was used to develop the model and for the calculation of the predicted concentration (C). RStudio software (Version 1.2.5019, 2009-2019 RStudio, Inc) was used for the statistical analysis of the data. Analysis of variance (ANOVA) and Tukey tests were utilized to find the significant difference between study sites, seasons, the process of treatment, and different particulate diameters. The resultant data were plotted using Tableau 2020.2.1 software. Below, the statistical differences between seasons within each treatment site and between all sites together were examined using total particulate counts and particulate counts for each diameter. Additionally, the Gaussian dispersion model was used to predict the dispersion of particulate matter into the surrounding area, which may help to identify environmental and human health concerns spatially and temporally.

2.3. Results

2.3.1. Seasonal Variation in Total PM Counts

Measurements of total particulate matter counts across seasons was used to examine the temporal variation in PM emissions at each site (Figures 2.6 – 2.9). Site 1

has the higher median total particulate count was in summer (12394215.5) followed by fall (8092593), spring (7427707.5) and winter (5172864). For site 2, the higher median total particulate count was in fall (17169109), summer (12889068), winter (11632140), and spring (9193843). On the other hand, the higher median total particulate count in Site 3 was in summer (17626641), spring (16938645), winter (16314349), and fall (15608775). However, fall (4495514) was higher in the median total particulate count for Site 4 than in spring (1792427).

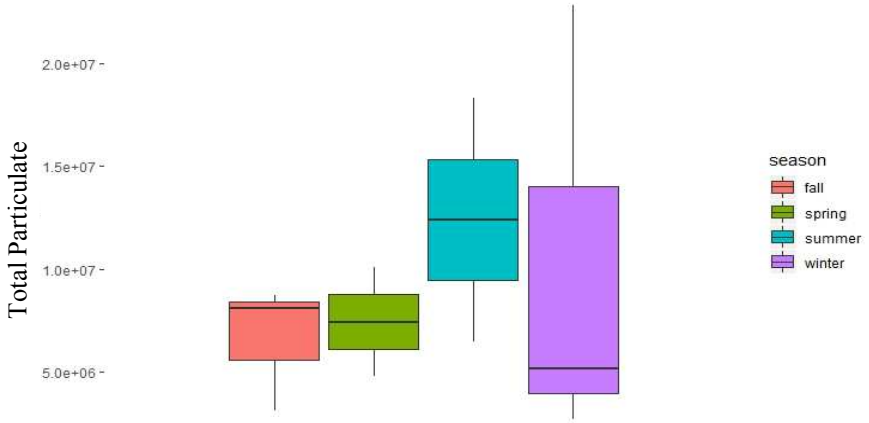

Figure 2.6: Total Particulate Matter (PMs) Count for Site 1 by Seasons

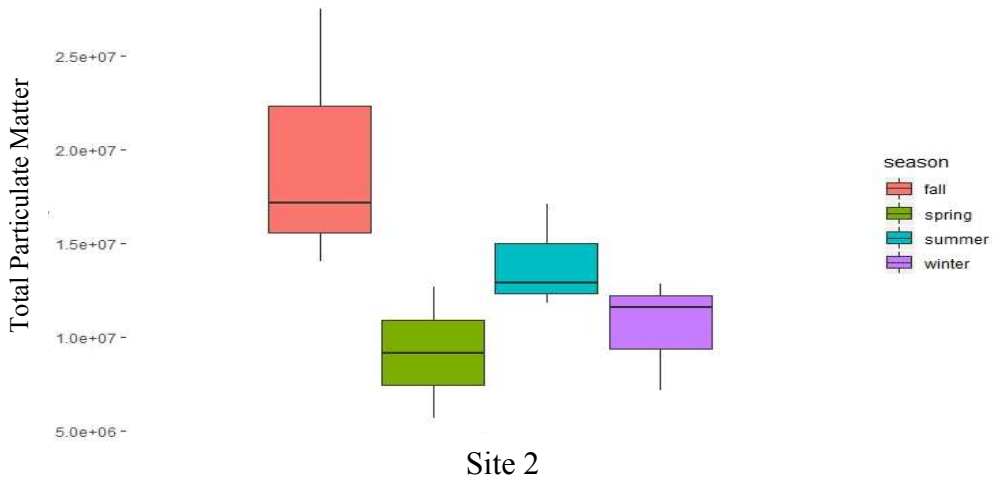

Figure 2.7: Total Particulate Matter (PMs) Count for Site 2 by Seasons

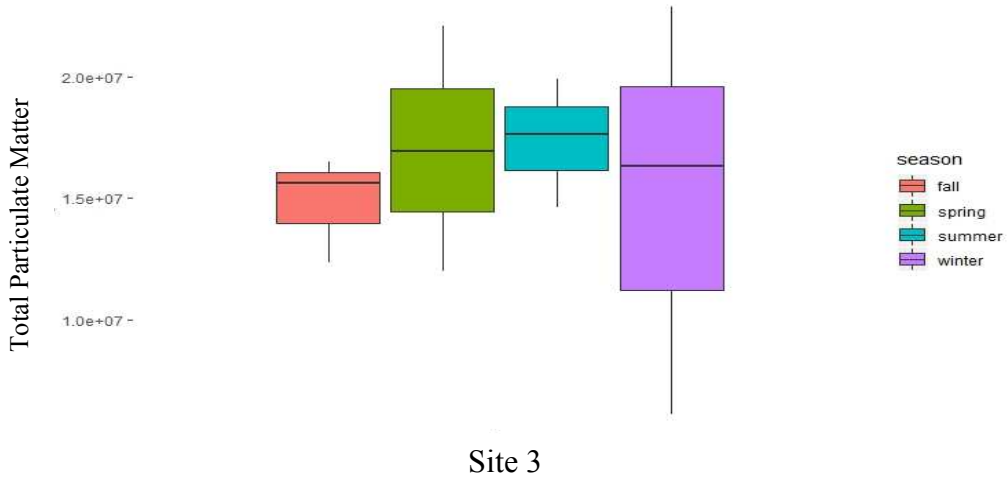

Figure 2.8: Total Particulate Matter (PMs) Count for Site 3 by Seasons

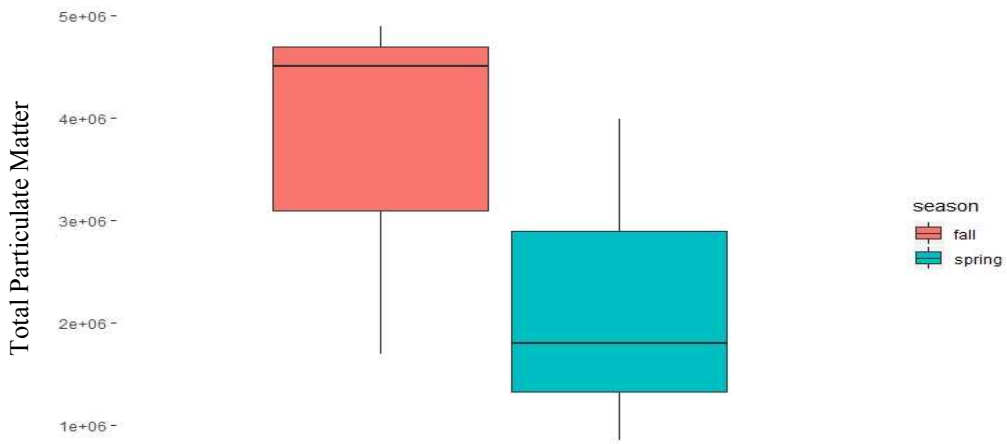

Figure 2.9: Total Particulate Matter (PMs) Count for Site 4 by Seasons

2.3.2. Spatial Variation in Total PM Counts

To examine the spatial variation in PM emissions, total PM counts for each site were compared during each season. Due to sampling collection arrangements, there is data for 4 sites in winter and summer and 3 sites in spring and fall. Comparison among sites showed that site 3 had the highest median PM counts followed by site 2, site 1, and site 4 during winter, spring, and summer seasons (Figures 2.10-2.12) However, during fall season, site 2 showed a higher median of total PM counts compared to the other sites (Figure 2.13).

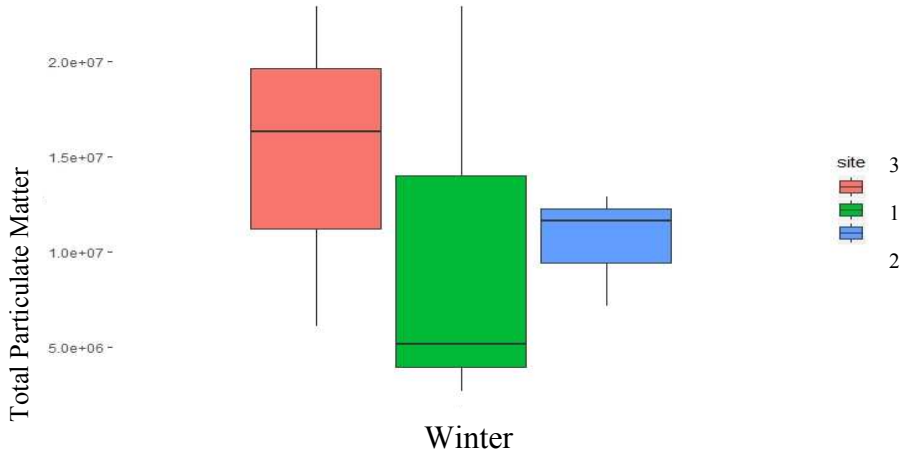

Figure 2.10: Total Particulate Matter (PMs) Count for winter by Sites

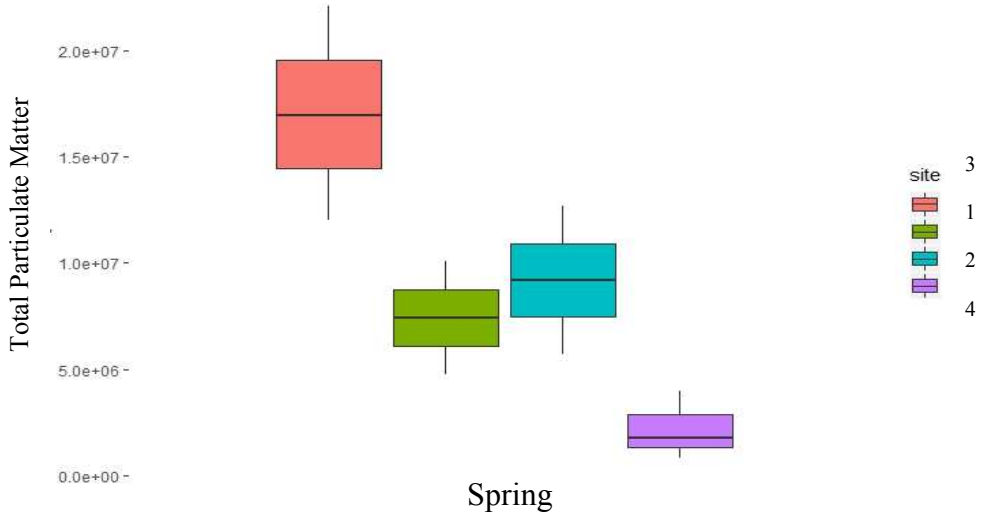

Figure 2.11: Total Particulate Matter (PMs) Count for Spring by Sites

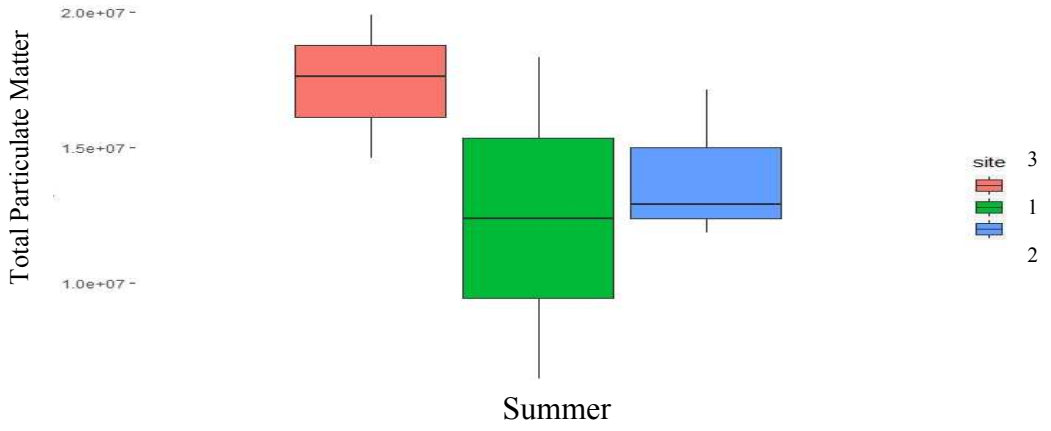

Figure 2.12: Total Particulate Matter (PMs) Count for Summer by Sites

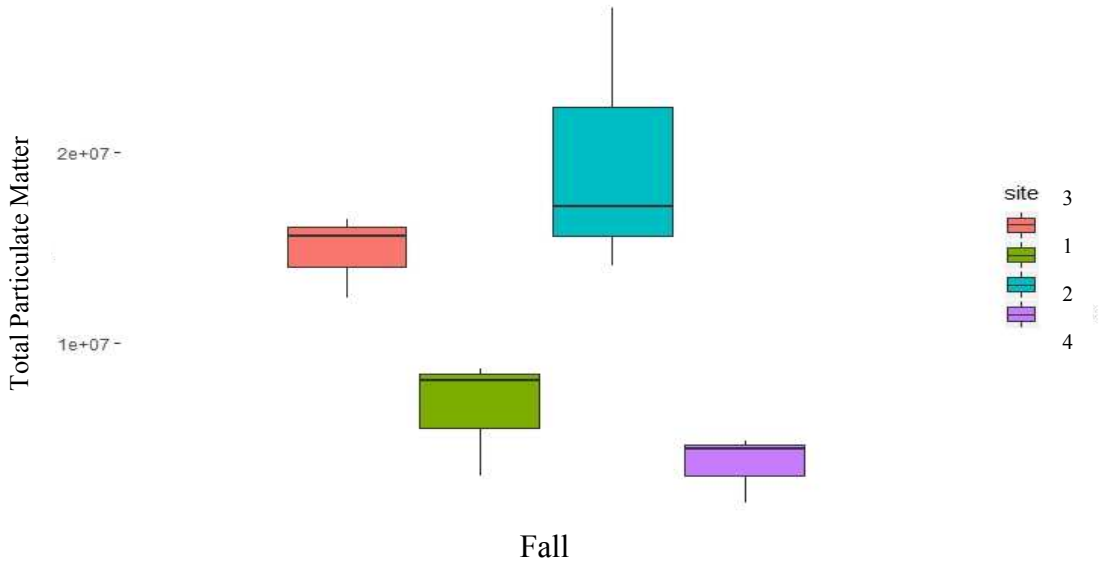

Figure 2.13: Total Particulate Matter (PMs) Count for fall by Sites

2.3.3. Spatial and Temporal Variation by PM Diameter

The TSI instrument is capable of monitoring the abundance of PM based on size, resulting in abundance data for PM of diameters 0.3, 0.4, 0.55, 0.7, 1, 1.3, 1.6, 2.2, 3, 4,

5.5, 7 and 10 micrometers [μm]). This higher resolution data was examined to gain a better understanding of the variation in PM sizes across sites (as compared to the total distribution discussed above). Results indicated that PM within the range of 0.3 μm and 0.4 μm were the most abundant PM sizes across all sites and seasons (Figures 2.14, 2.16, 2.18, 2.20, 2.22, 2.24, 2.26, and 2.28). Because the high abundance of the 0.3 μm and 0.4 μm diameter particulate made the observation of trends in the lower abundant particulate sizes difficult, data were also plotted excluding the more abundant smaller PM sizes. For site 1, winter has the higher particulate counts with higher particulate diameter abundance followed by fall, spring, and summer. The most particulate sizes have been found in the air are 0.55 μm, 2.2 μm, and 5.5 μm, respectively (Figure 2.15). Moreover, fall has the higher particulate counts in Site 2 (Figure 2.17) with more particulate in diameter 4 μm, 2.2 μm, 3 μm, and 5.5 μm. Winter has slightly higher particulate numbers than spring after removing the smaller particulate, and summer changed from the second season when we have all particulate sizes to the lowest season of particle numbers. In addition, 0.55 μm particulate are high in all seasons in Site 3 compared to the other particulate diameters. 0.7 μm particulate are more in summer followed by fall, spring, and winter. In the fall, the most abundant particulate sizes are 2.2 μm, 3 μm, and 4 μm (Figure 2.19). On the other hand, the particulate count for the size 0.55 μm in Site 4 is almost similar, and the higher total particulate in fall are due to the higher abundance of the 0.7 μm particulate size compared to the spring (Figure 2.21).

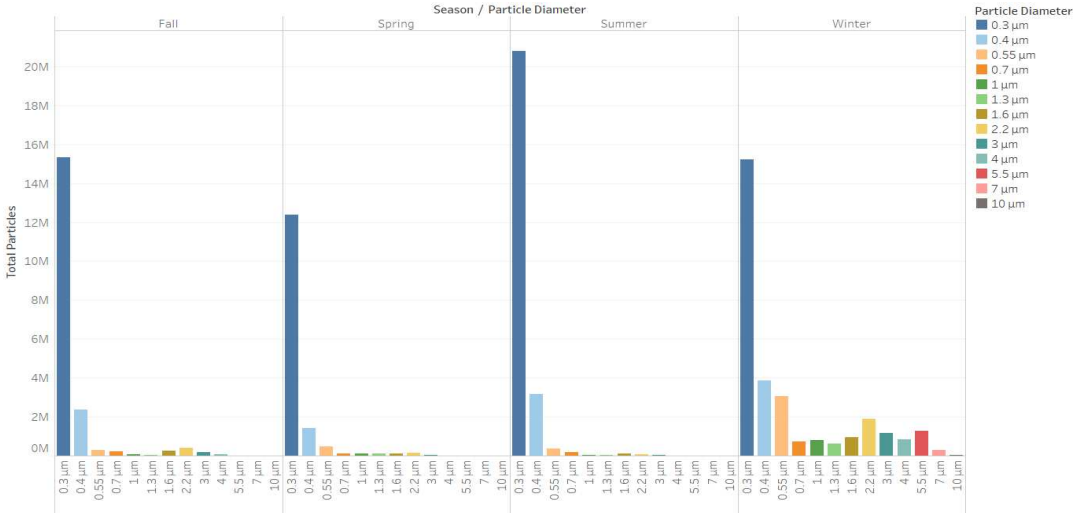

Figure 2.14: Total Particulate Matter (PMs) for each diameter for Site 1 by seasons

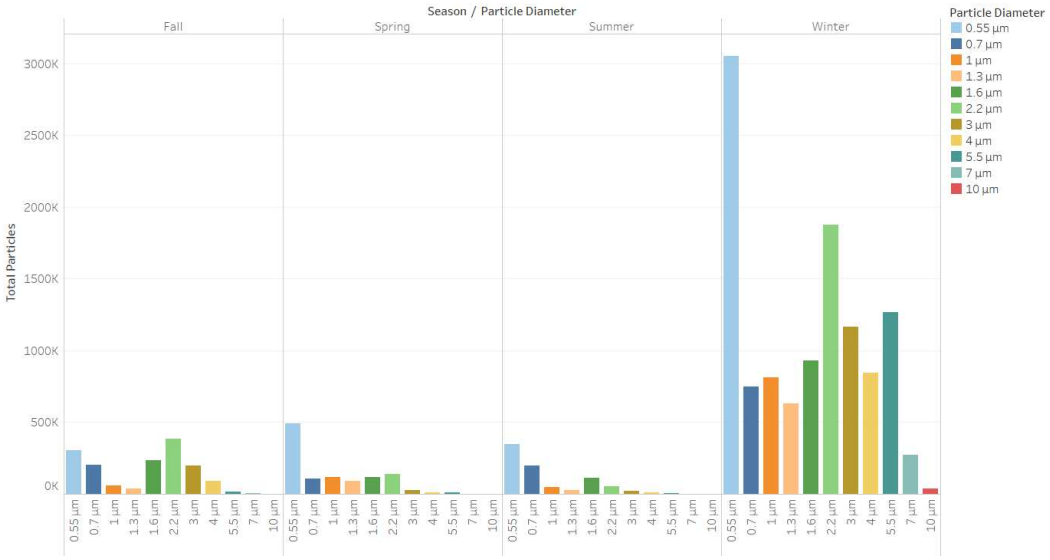

Figure 2.15: Total Particulate Matter (PMs) for each diameter for Site 1 by seasons (excluding 0.3 µm & 0.4 µm)

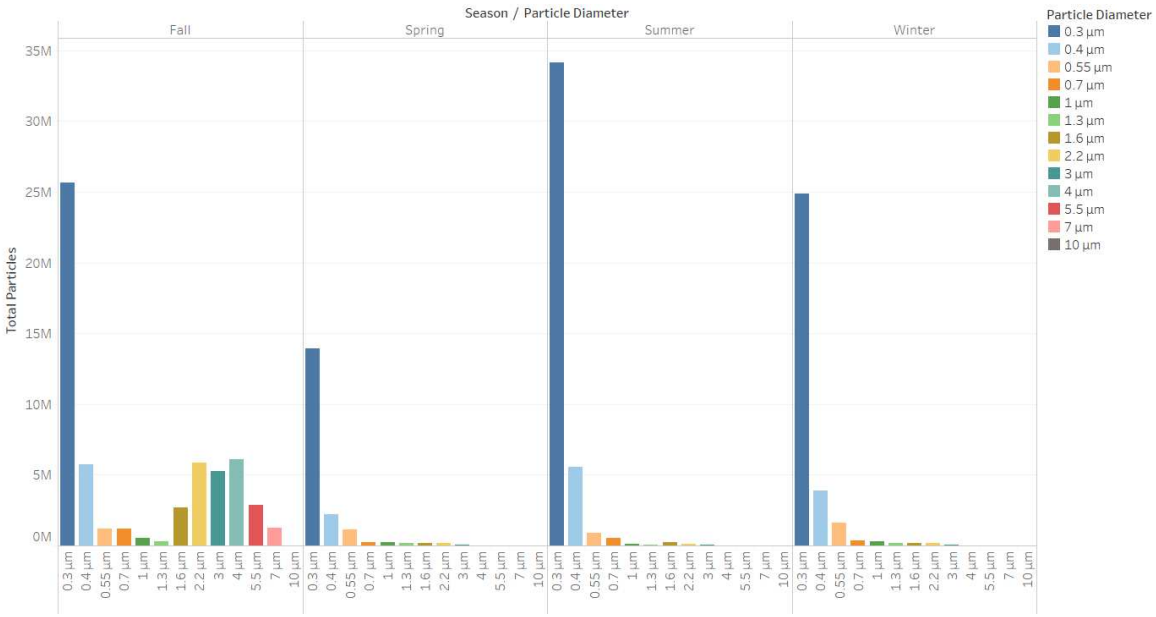

Figure 2.16: Total Particulate Matter (PMs) for each diameter for Site 2 by seasons

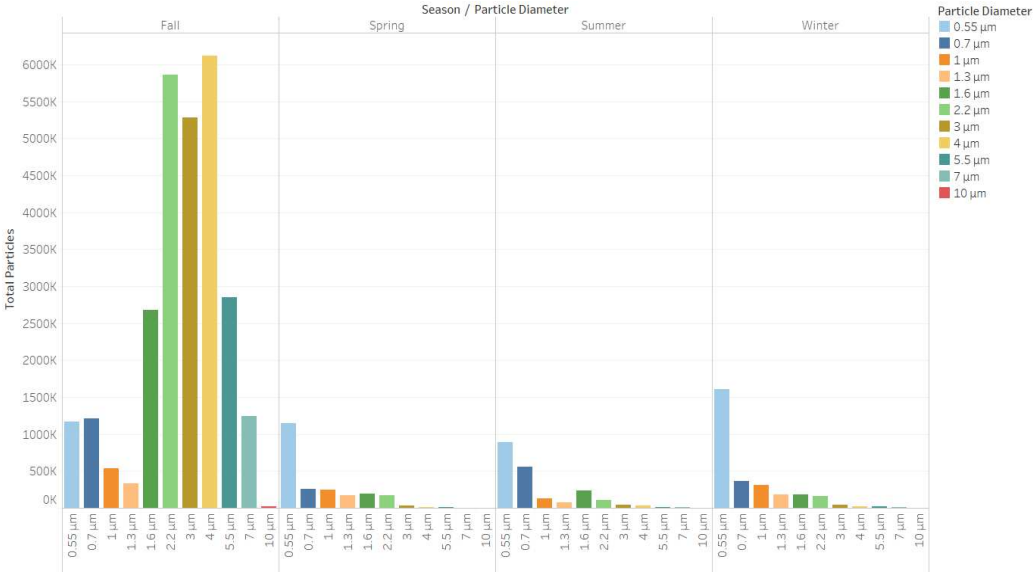

Figure 2.17: Total Particulate Matter (PMs) for each diameter for Site 2 by seasons (excluding 0.3 µm & 0.4 µm)

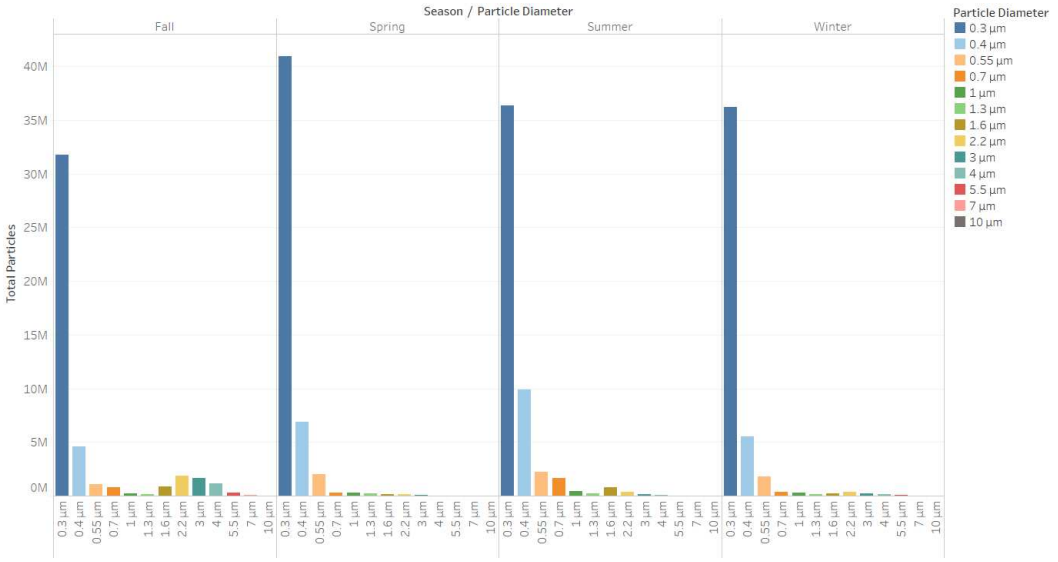

Figure 2.18: Total Particulate Matter (PMs) for each diameter for Site 3 by seasons

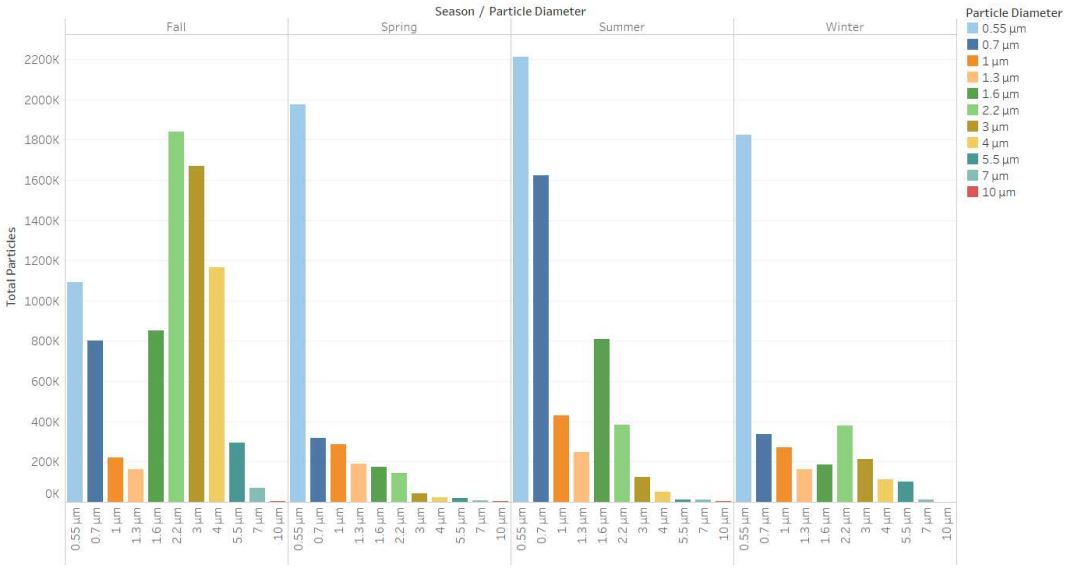

Figure 2.19: Total Particulate Matter (PMs) for each diameter for Site 3 by seasons (excluding 0.3 µm & 0.4 µm)

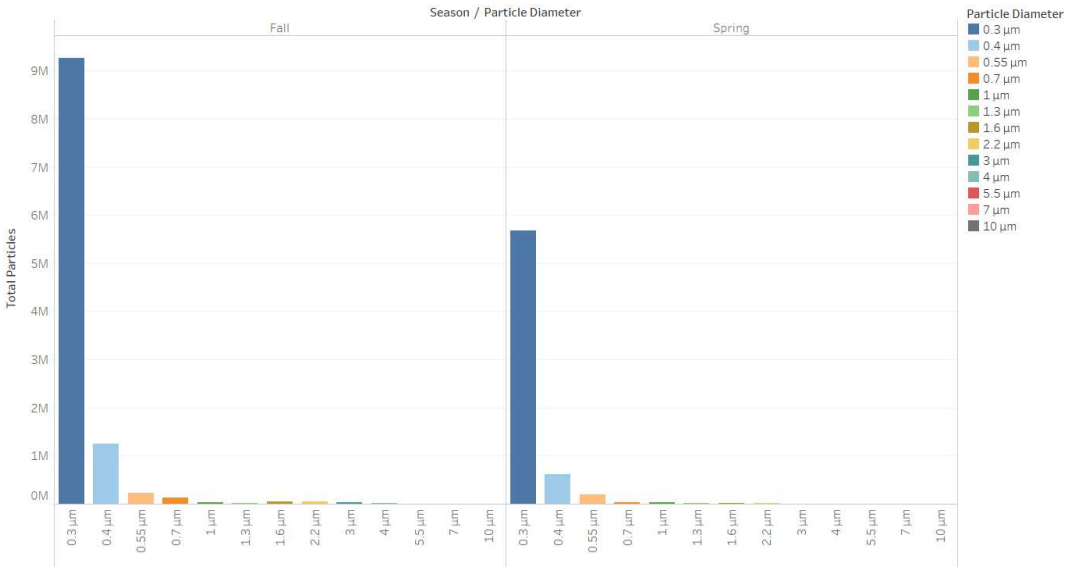

Figure 2.20: Total Particulate Matter (PMs) for each diameter for Site 4 by seasons

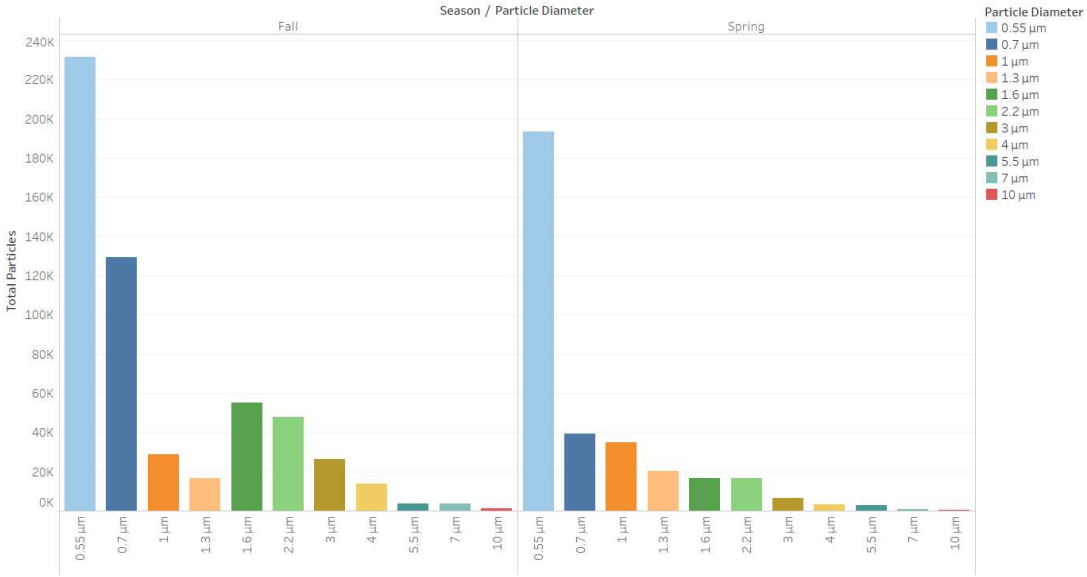

Figure 2.21: Total Particulate Matter (PMs) for each diameter for Site 4 by seasons (excluding 0.3 µm & 0.4 µm)

Furthermore, we analyzed the data to examine the seasonal difference in the total particulate numbers based on the particulate diameter between sites. We found that in winter, Site 1 has higher total counts due to the abundance in 0.55 µm, 2.2 µm, and 5.5 µm sizes (Figure 2.23). For spring, 0.55 µm particulate size is high in all sites (Figure 2.25), and Site 3 has the greater abundance followed by Site 2, Site 1, and Site 4. Also, Site 3 has more significant particulate numbers in summer than Site 2, and Site 1 and the most particulate diameters have been measured are 0.55. µm, 0.7 µm, 1.6 µm, and 2.2 µm (Figure 2.37). In addition, the presence of particulate with diameter 2.2 µm, 3 µm, 4 µm and 5.5 µm in high numbers made Site 2 total particulate counts larger than Site 3, Site 1 and Site 4 in fall (Figure 2.29).

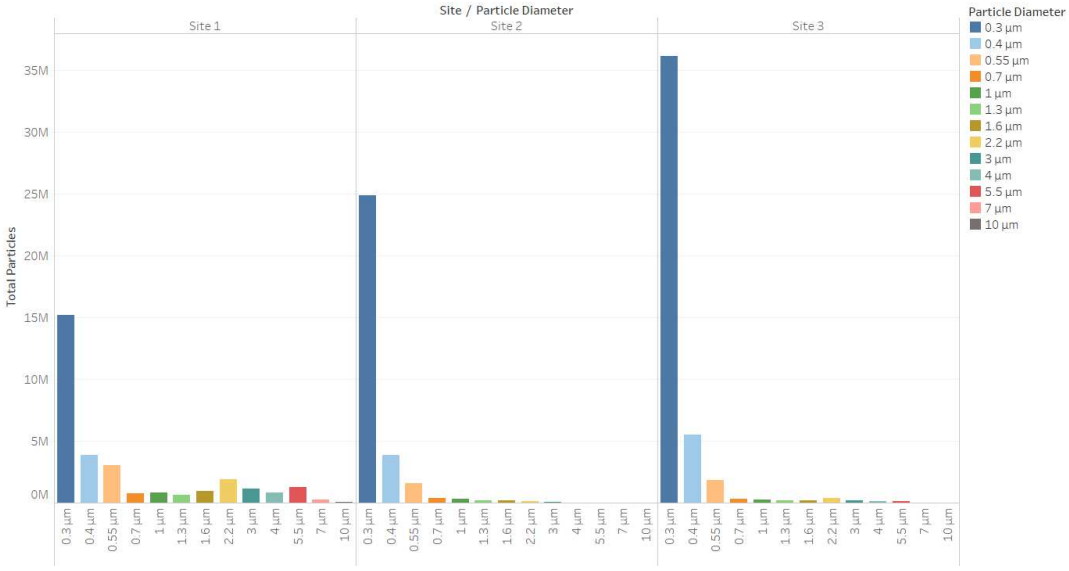

Figure 2.22: Total Particulate Matter (PMs) for each diameter for winter by sites

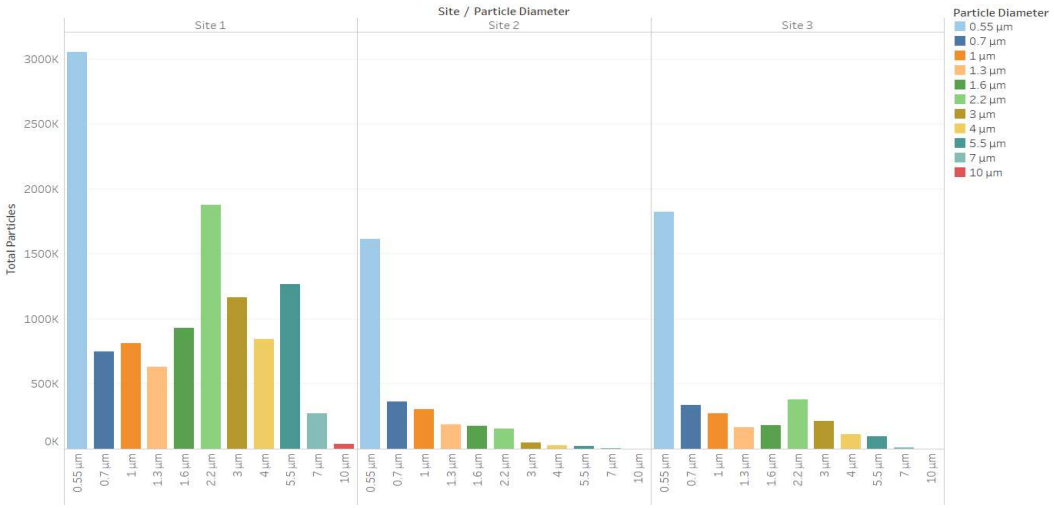

Figure 2.23: Total Particulate Matter (PMs) for each diameter for winter by sites (excluding 0.3 µm & 0.4 µm)

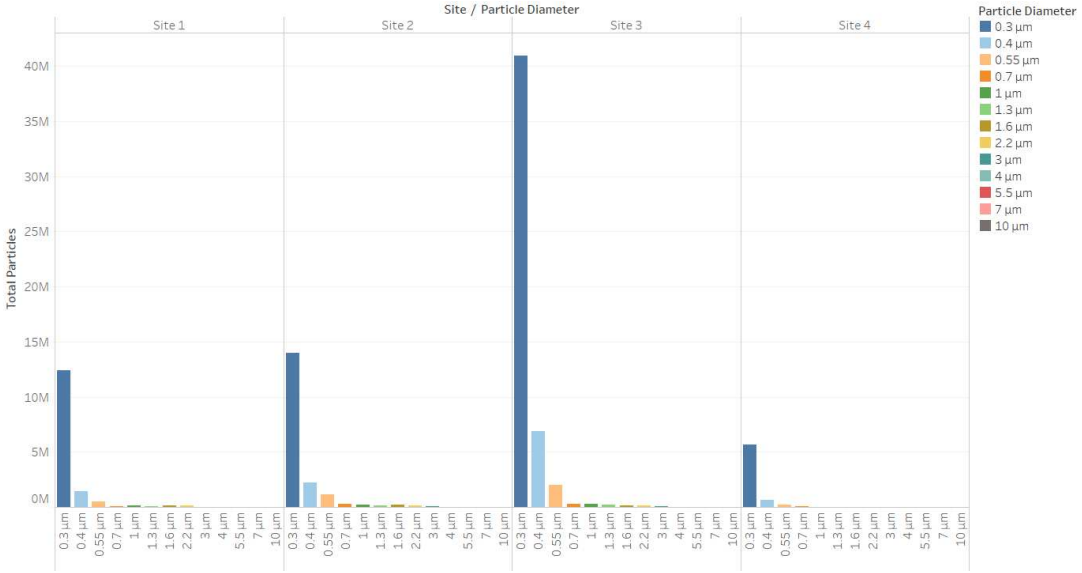

Figure 2.24: Total Particulate Matter (PMs) for each diameter for spring by sites

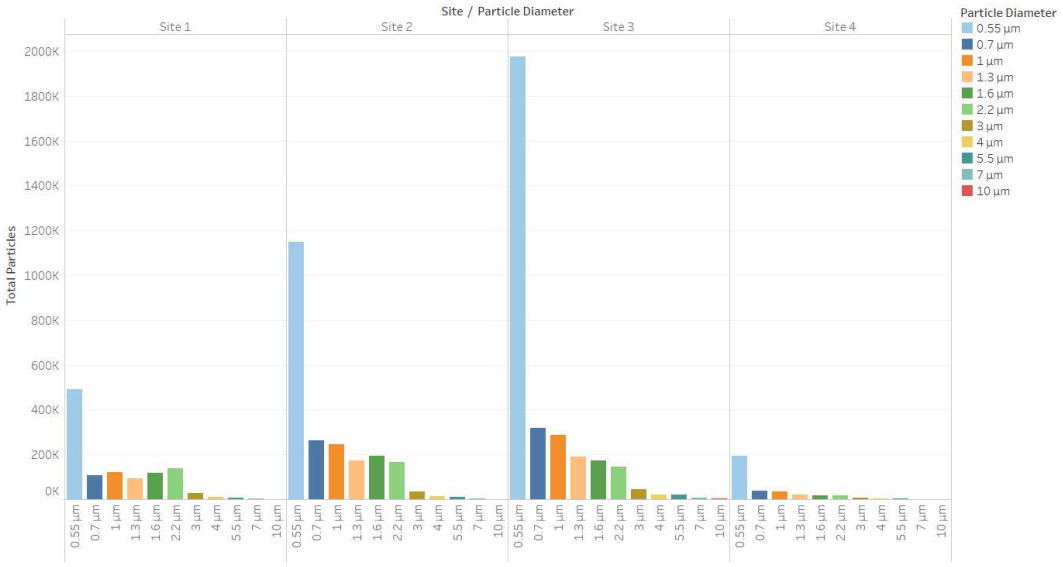

Figure 2.25: Total Particulate Matter (PMs) for each diameter for spring by sites (excluding 0.3 µm & 0.4 µm)

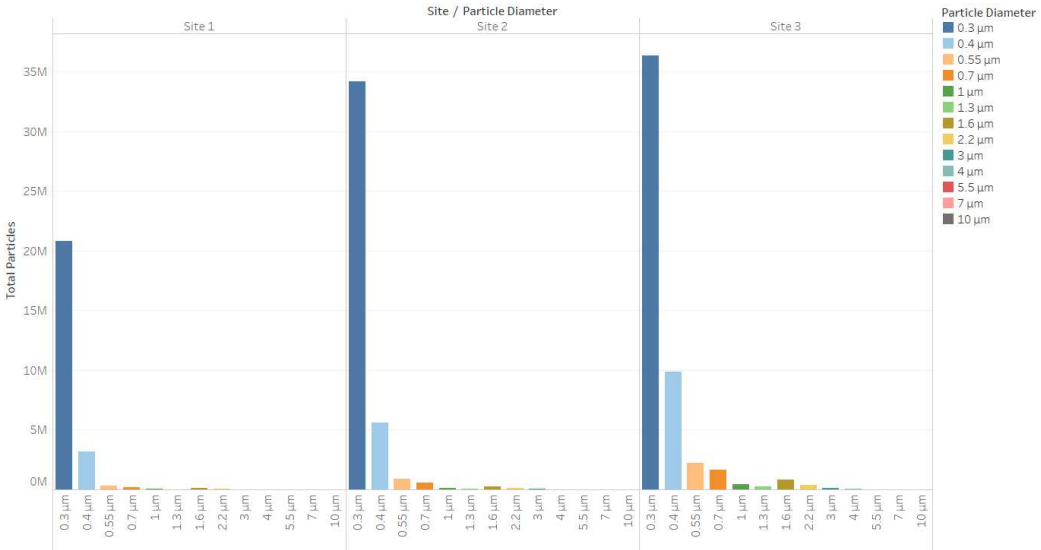

Figure 2.26: Total Particulate Matter (PMs) for each diameter for summer by sites

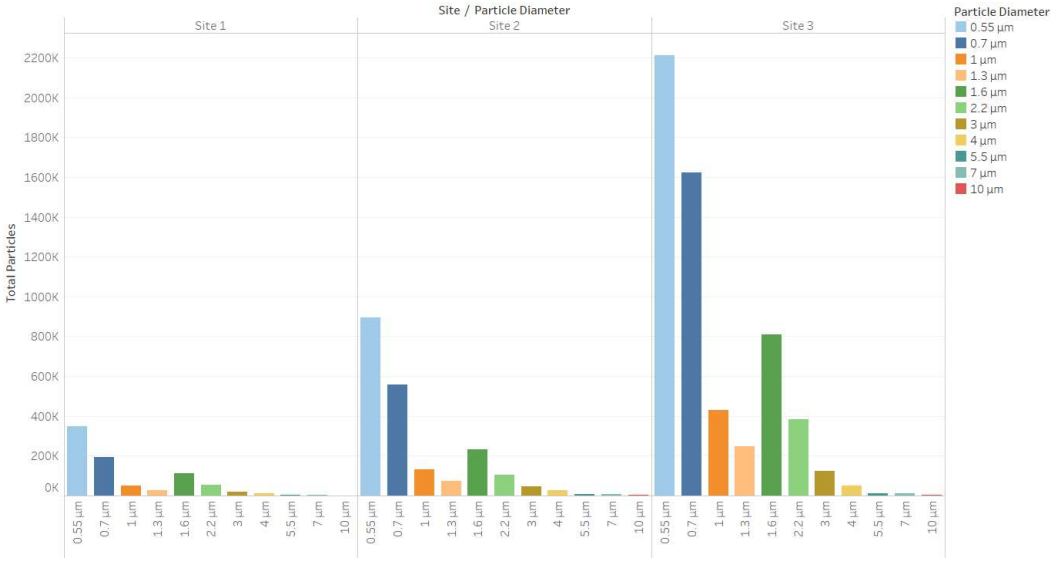

Figure 2.27: Total Particulate Matter (PMs) for each diameter for summer by sites (excluding 0.3 µm & 0.4 µm)

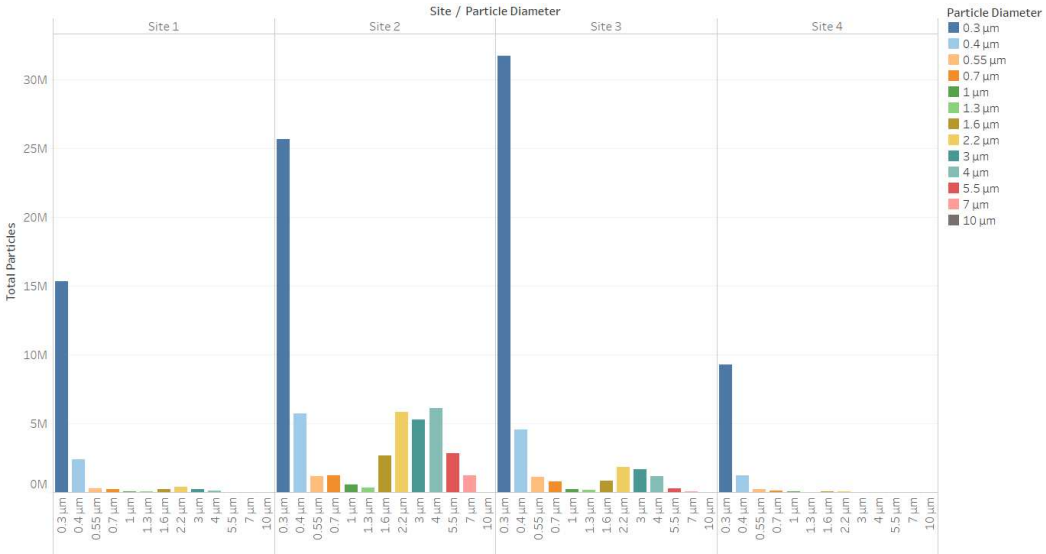

Figure 2.28: Total Particulate Matter (PMs) for each diameter for fall by sites

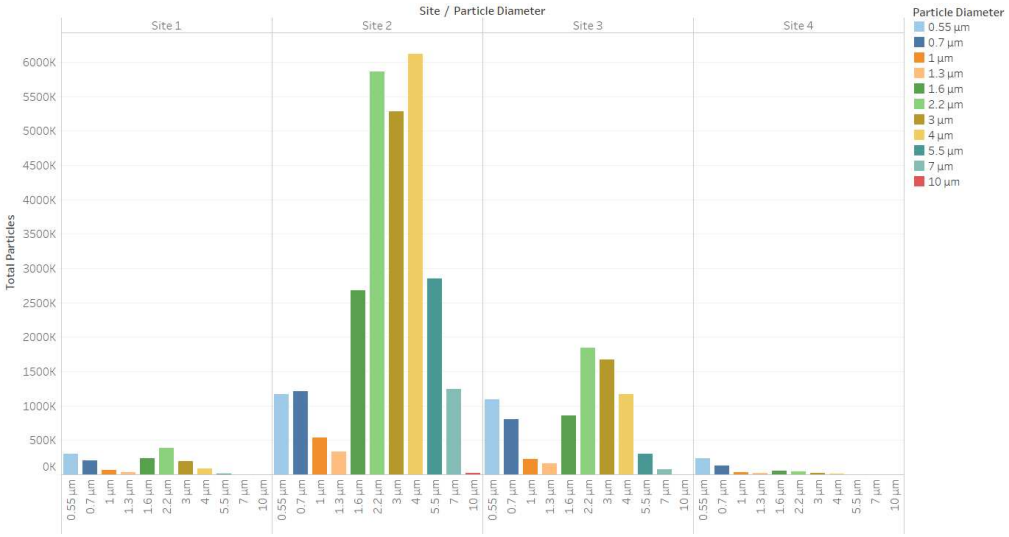

Figure 2.29: Total Particulate Matter (PMs) for each diameter for fall by sites (excluding 0.3 µm & 0.4 µm)

2.3.4. Statistical analysis results

We applied ANOVA and Tukey test to observe the statistical differences for the total particulate numbers spatially and temporally. We found that there is no significant difference between seasons within each site, as shown in (Tables 2.1, 2.2, 2.3, 2.4, 2.5, 2.6 & 2.7). The P-value for Site 1 is 0.872 ($P > 0.05$), Site 2 is 0.131 ($P > 0.05$), Site 3 is 0.832 ($P > 0.05$) and 0.343 ($P > 0.05$) for Site 4. On the other hand, there is a significant difference between sites in some seasons. In spring (p-value is 0.0178 [$P < 0.05$]), there is a significant difference in the total particulate numbers between Site 4 and Site 3 with adjusted P-value 0.0131378 (Table 2.10 & 2.11). Moreover, there is a significant difference in the total particulate numbers between Site 4 and Site 3 (adjusted P-value is 0.0164405) and Site 4 and Site 2 (adjusted P-value is 0.0069676) in fall with p-value 0.00541($P < 0.05$) as shown in (Tables 2.14 & 2.15). However, there is no significant

difference between sites in the total particulate numbers in winter and summer, and their P-value is 0.6 (P > 0.05) and 0.441 (P > 0.05), respectively (Table 2.8, 2.9, 2.12 & 2.13).

Table 2.1: Analysis of variance (ANOVA) test results for Site 1 of total particulate matter

	Df	Sum Sq	Mean Sq	F value	P- value < 0.05
Seasons	3	0.0845	0.02817	0.231	0.872
Residuals	6	0.7310	0.12184		

Table 2.2: Tukey test results for Site 1 of total particulate matter

Seasons	Difference	Lower	Upper	P- value < 0.05
Spring-Fall	0.060903313	-1.0421506	1.1639573	0.9972498
Summer-Fall	0.256983956	-0.8460700	1.3600379	0.8493959
Winter-Fall	0.054514386	-0.9320871	1.0411158	0.9972437
Summer-Spring	0.196080643	-1.0122544	1.4044157	0.9398948
Winter-Spring	-0.006388926	-1.1094429	1.0966650	0.9999968
Winter-Summer	-0.202469570	-1.3055235	0.9005844	0.9168528

Table 2.3: Analysis of variance (ANOVA) test results for Site 2 of total particulate matter

	Df	Sum Sq	Mean Sq	F value	P- value < 0.05
Seasons	3	0.1771	0.05904	2.646	0.131
Residuals	7	0.1562	0.02231		

Table 2.4: Tukey test results for Site 2 of total particulate matter

Seasons	Difference	Lower	Upper	P- value < 0.05
Spring-Fall	-0.34378860	-0.7951821	0.1076049	0.1403906
Summer-Fall	-0.13454562	-0.5382842	0.2691930	0.6990997
Winter-Fall	-0.26354138	-0.6672800	0.1401972	0.2235107
Summer-Spring	0.20924298	-0.2421505	0.6606365	0.4680114
Winter-Spring	0.08024722	-0.3711463	0.5316407	0.9324393
Winter-Summer	-0.12899576	-0.5327344	0.2747428	0.7237990

Table 2.5: Analysis of variance (ANOVA) test results for Site 3 of total particulate matter

	Df	Sum Sq	Mean Sq	F value	P- value < 0.05
Seasons	3	0.02496	0.008321	0.289	0.832
Residuals	8	0.23059	0.028823		

Table 2.6: Tukey test results for Site 3 of total particulate matter

Seasons	Difference	Lower	Upper	P- value < 0.05
Spring-Fall	0.04954450	-0.3943663	0.4934553	0.9832419
Summer-Fall	0.06900284	-0.3749080	0.5129137	0.9573373
Winter-Fall	0.04834561	-0.4922564	0.3955652	0.9843815
Summer-Spring	0.01945834	-0.4244525	0.4633692	0.9989276
Winter-Spring	-0.09789011	-0.5418009	0.3460207	0.8918933
Winter-Summer	-0.11734845	-0.5612593	0.3265624	0.8312697

Table 2.7: Analysis of variance (ANOVA) test results for Site 4 of total particulate matter

	Df	Sum Sq	Mean Sq	F value	P- value < 0.05
Season	1	0.1031	0.10314	1.158	0.343
Residuals	4	0.3564	0.08909		

Table 2.8: Analysis of variance (ANOVA) test results for Winter of total particulate matter

	Df	Sum Sq	Mean Sq	F value	P- value < 0.05
Sites	2	0.1238	0.06189	0.557	0.6
Residuals	6	0.6664	0.11107		

Table 2.9: Tukey test results for Winter of total particulate matter

Sites	Difference	Lower	Upper	P- value < 0.05
Site 1- Site 3	-0.2847021	-1.1196307	0.5502265	0.5777475
Site 2- Site 3	-0.1091581	-0.9440867	0.7257704	0.9163161
Site 2- Site 1	0.1755439	-0.6593846	1.0104725	0.8018285

Table 2.10: Analysis of variance (ANOVA) test results for Spring of total particulate matter

	Df	Sum Sq	Mean Sq	F value	P- value < 0.05
Sites	3	1.4306	0.4769	7.673	**0.0178**
Residuals	6	0.3729	0.0621		

Bold: Significant difference

Table 2.11: Tukey test results for Spring of total particulate matter

Sites	Difference	Lower	Upper	P- value < 0.05
Site 1- Site 3	-0.3762033	-1.1639928	0.4115862	0.4198591
Site 2- Site 3	-0.2872955	-1.0750850	0.5004940	0.6150378
Site 4- Site 3	-0.9561512	-1.6607715	-0.2515309	**0.0131378**
Site 2- Site 1	0.0889078	-0.7740723	0.9518879	0.9830026
Site 4- Site 1	-0.5799479	-1.3677374	0.2078415	0.1482092
Site 4- Site 2	-0.6688557	-1.4566452	0.1189337	0.0925396

Bold: Significant difference

Table 2.12: Analysis of variance (ANOVA) test results for Summer of total particulate matter

	Df	Sum Sq	Mean Sq	F value	P- value < 0.05
Sites	2	0.04839	0.02419	0.968	0.441
Residuals	5	0.12495	0.02499		

Table 2.13: Tukey test results for Summer of total particulate matter

Sites	Difference	Lower	Upper	P- value < 0.05
Site 1- Site 3	-0.19958096	-0.6691462	0.2699843	0.4160384
Site 2- Site 3	-0.09751083	-0.5175028	0.3224811	0.7438134
Site 2- Site 1	0.10207014	-0.3674951	0.5716354	0.7700407

Table 2.14: Analysis of variance (ANOVA) test results for Fall of total particulate matter

	Df	Sum Sq	Mean Sq	F value	P- value < 0.05
Sites	3	1.0871	0.3624	9.353	**0.00541**
Residuals	8	0.3099	0.0387		

Bold: Significant difference

Table 2.15: Tukey test results for Fall of total particulate matter

Sites	Difference	Lower	Upper	P- value < 0.05
Site 1- Site 3	-0.3875621	-0.90221119	0.1270870	0.1519502
Site 2- Site 3	0.1060376	-0.40861147	0.6206867	0.9091778
Site 4- Site 3	-0.6443824	-1.15903152	-0.1297333	**0.0164405**
Site 2- Site 1	0.4935997	-0.02104939	1.0082488	0.0601370
Site 4- Site 1	-0.2568203	-0.77146943	0.2578288	0.4308865
Site 4- Site 2	-0.7504200	-1.26506915	-0.2357709	**0.0069676**

Bold: Significant difference

Furthermore, statistical analysis (ANOVA and Tukey tests) have been performed to test the significant difference for each particulate diameter spatially for each site and temporally for each season. We discovered that there is no significant difference in seasons for the particulate diameter in Site 1(Table 2.16) and the P-value is 0.0648 ($P > 0.05$), Site 3 (Table 2.24) and the P-value is 0.489 ($P > 0.05$), and Site 4 (Table 2.28) and the P-value is 0.161($P > 0.05$). On the other hand, there is a statistical significance difference between seasons in Site 2 (Table 2.20) with P-value 0.0028 ($P < 0.05$). The difference is between spring and fall with adjusted P-value 0.0286154, between summer and fall with adjusted P-value 0.0111765 and between winter and fall with adjusted P-value 0.0075554 (Table 2.21). In addition, statistical analysis has been done to assess the significant difference between particulate diameter inside the sites. For Site 1 (Table 2.18 & 2.19) showed that there is a significant difference with a P-value <2e-16 ($P < 0.05$) and the difference is between 0.3 µm and 0.55 µm, 0.7 µm, 1 µm, 1.3 µm, 1.6 µm, 2.2 µm, 3 µm, 4 µm, 5.5 µm, 7 µm and 10 µm, between 0.4 µm and 1 µm, 1.3 µm, 1.6 µm, 2.2 µm, 3 µm, 4 µm, 5.5 µm, 7 µm, and 10 µm, between 0.55 µm and 3 µm, 4 µm, 5.5 µm 7 µm and 10 µm, 0.7 µm and 5.5 µm, 7 µm and 10 µm, between 1 µm and 7 µm and 10 µm, between 1.3 µm and 7 µm and 10 µm, between 1.6 µm and 5.5 µm, 7 µm and 10 µm,

between 2.2 µm and 5.5 µm, 7 µm and 10 µm, between 3 µm and 7 µm and 10 µm, between 4 µm and 10 µm and between 5.5 µm and 10 µm. Also, the P value of Site 2 (Table 2.22) is <2e-16 ($P < 0.05$) and the difference is in the particulate with diameter 0.3 µm and 0.55 µm, 0.7 µm, 1 µm, 1.3 µm, 1.6 µm, 2.2 µm, 3 µm, 4 µm, 5.5 µm, 7 µm, and 10 µm, particulate of diameter 0.4 µm and 1 µm, 1.3 µm, 1.6 µm, 2.2 µm, 3 µm, 4 µm, 5.5 µm, 7 µm, and 10 µm, particulate size of 0.55 µm and 3 µm, 4 µm, 5.5 µm, 7 µm, and 10 µm, between particulate size of 0.7 µm and 5.5 µm, 7 µm and 10 µm, particulate dimeter 1 µm and 7 µm and 10 µm, particulate size of 1.3 µm and 7 µm and 10 µm, between particulate size of 1.6 µm and 5.5 µm, 7 µm and 10 µm, particulate with 2.2 µm and 5.5 µm, 7 µm and 10 µm, the particulate diameter of 3 µm and 7 µm and 10 µm, between particulate size 4 µm and 10 µm and between 5.5 µm and 10 µm (Table 2.23). Moreover, there is a significant difference in particulate sizes for Site 3 with P-value <2e-16 ($P < 0.05$) (Table 2.26). We found that particulate with dimeter 0.3 µm are statistically different from 0.4 µm, 0.55 µm, 0.7 µm, 1 µm, 1.3 µm, 1.6 µm, 2.2 µm, 3 µm, 4 µm, 5.5 µm, 7 µm, and 10 µm, particulate size 0.4 µm is different from 0.7 µm, 1 µm, 1.3 µm, 1.6 µm, 2.2 µm, 3 µm, 4 µm, 5.5 µm, 7 µm, and 10 µm. There is a difference between particulate of 0.55 µm diameter and 1 µm, 1.3 µm, 1.6 µm, 2.2 µm, 3 µm, 4 µm, 5.5 µm, 7 µm, and 10 µm, between 0.7 µm and 3 µm, 4 µm, 5.5 µm, 7 µm, and 10 µm, between particulate size of 1 µm and 4 µm, 5.5 µm, 7 µm, and 10 µm, particulate of 1.3 µm and 5.5 µm, 7 µm and 10 µm, the particulate diameter of 1.6 µm and 4 µm, 5.5 µm, 7 µm, and 10 µm, between 2.2 µm and 4 µm, 5.5 µm, 7 µm, and 10 µm, between 3 µm and 5.5 µm, 7 µm and 10 µm, between 4 µm and 7 µm and 10 µm, particulate diameter of 5.5 µm and 10 µm and between particulate of 7 µm and 10 µm

(Table 2.27). For Site 4, (Table 2.29) shows that there is a significant difference in the particulate bin size, and the P-value is <2e-16 ($P < 0.05$). The difference is between particulate diameter 0.3 µm and 0.4 µm, 0.55 µm, 0.7 µm, 1 µm, 1.3 µm, 1.6 µm, 2.2 µm, 3 µm, 4 µm, 5.5 µm, 7 µm, and 10 µm, particulate size 0.4 µm and 0.7 µm, 1 µm, 1.3 µm, 1.6 µm, 2.2 µm, 3 µm, 4 µm, 5.5 µm, 7 µm, and 10 µm, particulate of diameter 0.55 µm and 1 µm, 1.3 µm, 1.6 µm, 2.2 µm, 3 µm, 4 µm, 5.5 µm, 7 µm, and 10 µm, between 0.7 µm and 3 µm, 4 µm, 5.5 µm, 7 µm, and 10 µm, between 1 µm and 4 µm, 5.5 µm, 7 µm, and 10 µm, between 1.3 µm and 5.5 µm, 7 µm and 10 µm, between 1.6 µm and 4 µm, 5.5 µm, 7 µm, and 10 µm, particulate of 2.2 µm and 4 µm, 5.5 µm 7 µm and 10 µm, between 3 µm and 7 µm and 10 µm, between 4 µm and 7 µm and 10 µm and particulate of diameter 5.5 µm and 10 µm (Table 2.30).

Table 2.16: Analysis of variance (ANOVA) test results for Site 1 of particulate dimeter by season

	Df	Sum Sq	Mean Sq	F value	P- value < 0.05
Season	3	11.18	3.727	2.472	0.0648
Residuals	126	189.95	1.508		

Table 2.17: Tukey test results for Site 1 of particulate dimeter by season

Seasons	Difference	Lower	Upper	P- value < 0.05
Spring-Fall	0.18224617	-0.627141296	0.9916336	0.9360702
Summer-Fall	0.16539793	-0.643989537	0.9747854	0.9511188
Winter-Fall	0.71962765	-0.004310512	1.4435658	0.0520059
Summer-Spring	-0.01684824	-0.903487789	0.8697913	0.9999563
Winter-Spring	0.53738148	-0.272005992	1.3467689	0.3132398
Winter-Summer	0.55422972	-0.255157751	1.3636172	0.2863817

Table 2.18: Analysis of variance (ANOVA) test results for Site 1 of particulate dimeter by bin size

	Df	Sum Sq	Mean Sq	F value	P- value < 0.05
Bin Size	12	146.62	12.218	26.22	**<2e-16**
Residuals	117	54.52	1.488e+12		

Bold: Significant difference

Table 2.19: Tukey test results for Site 1 of particulate dimeter by bin size

Bin Size	Difference	Lower	Upper	P- value < 0.05
0.3 µm – 0.4 µm	-0.80068360	-1.83322956	0.231862357	0.3089590
0.3 µm – 0.55 µm	-1.37300147	-2.40554742	-0.340455508	**0.0011197**
0.3 µm – 0.7 µm	-1.79497021	-2.82751617	-0.762424252	**0.0000030**
0.3 µm – 1 µm	-2.08166281	-3.11420877	-1.049116857	**0.0000000**
0.3 µm – 1.3 µm	-2.27553918	-3.30808514	-1.242993225	**0.0000000**
0.3 µm – 1.6 µm	-1.90725367	-2.93979962	-0.874707710	**0.0000005**
0.3 µm – 2.2 µm	-1.97320510	-3.00575106	-0.940659145	**0.0000002**
0.3 µm – 3 µm	-2.45662704	-3.48917300	-1.424081088	**0.0000000**
0.3 µm – 4 µm	-2.79653755	-3.82908351	-1.763991591	**0.0000000**
0.3 µm – 5.5 µm	-3.11010124	-4.14264719	-2.077555278	**0.0000000**
0.3 µm – 7 µm	-3.51062860	-4.54317456	-2.478082646	**0.0000000**
0.3 µm – 10 µm	-4.17487968	-5.20742564	-3.142333720	**0.0000000**
0.4 µm – 0. 55 µm	-0.57231787	-1.60486382	0.460228092	0.8063414
0.4 µm – 0.7 µm	-0.99428661	-2.02683257	0.038259348	0.0710162
0.4 µm – 1 µm	-1.28097921	-2.31352517	-0.248433257	**0.0034733**
0.4 µm – 1.3 µm	-1.47485558	-2.50740154	-0.442309625	**0.0002968**

0.4 µm – 1.6 µm	-1.10657007	-2.13911602	-0.074024110	**0.0241467**
0.4 µm – 2.2 µm	-1.17252150	-2.20506746	-0.139975545	**0.0120079**
0.4 µm – 3 µm	-1.65594344	-2.68848940	-0.623397488	**0.0000237**
0.4 µm – 4 µm	-1.99585395	-3.02839991	-0.963307991	**0.0000001**
0.4 µm – 5.5 µm	-2.30941764	-3.34196359	-1.276871678	**0.0000000**
0.4 µm – 7 µm	-2.70994500	-3.74249096	-1.677399046	**0.0000000**
0.4 µm – 10 µm	-3.37419608	-4.40674204	-2.341650120	**0.0000000**
0.55 µm – 0.7 µm	-0.42196874	-1.45451470	0.610577214	0.9749613
0.55 µm – 1 µm	-0.70866135	-1.74120731	0.323884609	0.5064936
0.55 µm – 1.3 µm	-0.90253772	-1.93508367	0.130008241	0.1524764
0.55 µm – 1.6 µm	-0.53425220	-1.56679817	0.498293756	0.8693669
0.55 µm – 2.2 µm	-0.60020364	-1.63274959	0.432342320	0.7522148
0.55 µm – 3 µm	-1.08362558	-2.11617154	-0.051079622	**0.0304590**
0.55 µm – 4 µm	-1.42353608	-2.45608204	-0.390990125	**0.0005849**
0.55 µm – 5.5 µm	-1.73709977	-2.76964573	-0.704553812	**0.0000072**
0.55 µm – 7 µm	-2.13762714	-3.17017309	-1.105081180	**0.0000000**
0.55 µm – 10 µm	-2.80187821	-3.83442417	-1.769332255	**0.0000000**
0.7 µm – 1 µm	-0.28669261	-1.31923856	0.745853352	0.9992301
0.7 µm – 1.3 µm	-0.48056897	-1.51311493	0.551976984	0.9342692
0.7 µm – 1.6 µm	-0.11228346	-1.14482942	0.920262499	1.0000000
0.7 µm – 2,2 µm	-0.17823489	-1.21078085	0.854311064	0.9999951
0.7 µm – 3 µm	-0.66165684	-1.69420279	0.370889121	0.6164109
0.7 µm – 4 µm	-1.00156734	-2.03411330	0.030978618	0.0665219

0.7 µm – 5.5 µm	-1.31513103	-2.34767698	-0.282585069	**0.0023002**
0.7 µm – 7 µm	-1.71565839	-2.74820435	-0.683112437	**0.0000099**
0.7 µm – 10 µm	-2.37990947	-3.41245543	-1.347363511	**0.0000000**
1 µm – 1.3 µm	-0.19387637	-1.22642233	0.838669589	0.9999875
1 µm – 1.6 µm	0.17440915	-0.85813681	1.206955104	0.9999961
1 µm – 2.2 µm	0.10845771	-0.92408825	1.141003669	1.0000000
1 µm – 3 µm	-0.37496423	-1.40751019	0.657581727	0.9905806
1 µm – 4 µm	-0.71487473	-1.74742069	0.317671223	0.4920965
1 µm – 5.5 µm	-1.02843842	-2.06098438	0.004107536	0.0519640
1 µm – 7 µm	-1.42896579	-2.46151175	-0.396419832	**0.0005448**
1 µm – 10 µm	-2.09321686	-3.12576282	-1.060670906	**0.0000000**
1.3 µm – 1.6 µm	0.36828551	-0.66426044	1.400831472	0.9919433
1.3 µm – 2.2 µm	0.30233408	-0.73021188	1.334880037	0.9987027
1.3 µm – 3 µm	-0.18108786	-1.21363382	0.851458095	0.9999941
1.3 µm – 4 µm	-0.52099837	-1.55354432	0.511547591	0.8880431
1.3 µm – 5.5 µm	-0.83456205	-1.86710801	0.197983904	0.2486526
1.3 µm – 7 µm	-1.23508942	-2.26763538	-0.202543464	**0.0059481**
1.3 µm – 10 µm	-1.89934050	-2.93188645	-0.866794538	**0.0000006**
1.6 µm – 2.2 µm	-0.06595144	-1.09849739	0.966594522	1.0000000
1.6 µm – 3 µm	-0.54937338	-1.58191933	0.483172580	0.8459563
1.6 µm – 4 µm	-0.88928388	-1.92182984	0.143262076	0.1686376
1.6 µm – 5.5 µm	-1.20284757	-2.23539353	-0.170301611	**0.0085823**
1.6 µm – 7 µm	-1.60337494	-2.635920890.	-0.570828979	**0.0000504**
1.6 µm – 10 µm	-2.26762601	-3.30017197	-1.235080053	**0.0000000**

2.2 µm – 3 µm	-0.48342194	-1.51596790	0.549124015	0.9315283
2.2 µm – 4 µm	-0.82333245	-1.85587840	0.209213512	0.2677507
2.2 µm – 5.5 µm	-1.13689613	-2.16944209	-0.104350175	**0.0176107**
2.2 µm – 7 µm	-1.53742350	-2.56996946	-0.504877543	**0.0001268**
2.2 µm – 10 µm	2.20167458	1.16912862	3.234220532	**0.0000000**
3 µm – 4 µm	-0.33991050	-1.37245646	0.692635454	0.9960737
3 µm – 5.5 µm	-0.65347419	-1.68602015	0.379071767	0.6353478
3 µm – 7 µm	-1.05400156	-2.08654752	-0.021455601	**0.0407523**
3 µm – 10 µm	1.71825263	0.68570668	2.750798590	**0.0000095**
4 µm – 5.5 µm	-0.31356369	-1.34610964	0.718982270	0.9981564
4 µm – 7 µm	-0.71409106	-1.74663701	0.318454902	0.4939078
4 µm – 10 µm	1.37834213	0.34579617	2.410888087	**0.0010464**
5.5 µm – 7 µm	-0.40052737	-1.43307333	0.632018589	0.9835608
5.5 µm – 10 µm	1.06477844	0.03223249	2.097324400	**0.0366994**
7 µm – 10 µm	0.66425107	-0.36829488	1.696797032	0.6103774

Bold: Significant difference

Table 2.20: Analysis of variance (ANOVA) test results for Site 2 of particulate dimeter by season

	Df	Sum Sq	Mean Sq	F value	P- value < 0.05
Season	3	19.43	6.475	4.921	**0.0028**
Residuals	139	182.92	1.316		

Bold: Significant difference

Table 2.21: Tukey test results for Site 2 of particulate dimeter by season

Seasons	Difference	Lower	Upper	P- value < 0.05
Spring-Fall	-0.816288326	-1.5715461	-0.06103055	**0.0286154**
Summer-Fall	-0.814232143	-1.4897552	-0.13870905	**0.0111765**
Winter-Fall	-0.847022396	-1.5225455	-0.17149930	**0.0075554**
Summer-Spring	0.002056183	-0.7532016	0.75731396	0.9999999
Winter-Spring	-0.030734069	-0.7859918	0.72452371	0.9995739
Winter-Summer	-0.032790253	-0.7083133	0.64273284	0.9992782

Bold: Significant difference

Table 2.22: Analysis of variance (ANOVA) test results for Site 2 of particulate dimeter by bin size

	Df	Sum Sq	Mean Sq	F value	P- value < 0.05
Bin Size	12	146.49	12.21	28.41	**<2e-16**
Residuals	130	55.85	0.43		

Bold: Significant difference

Table 2.23: Tukey test results for Site 2 of particulate dimeter by bin size

Bin Size	Difference	Lower	Upper	P- value < 0.05
0.3 µm – 0.4 µm	-0.77126862	-1.71463996	0.17210273	0.2344297
0.3 µm – 0.55 µm	-1.32930578	-2.27267712	-0.38593444	**0.0003683**
0.3 µm – 0.7 µm	-1.68120604	-2.62457739	-0.73783470	**0.0000013**
0.3 µm – 1 µm	-1.98672369	-2.93009503	-1.04335234	**0.0000000**
0.3 µm – 1.3 µm	-2.20629164	-3.14966298	-1.26292029	**0.0000000**
0.3 µm – 1.6 µm	-1.83748203	-2.78085337	-0.89411068	**0.0000001**
0.3 µm – 2.2 µm	-1.88136866	-2.82474001	-0.93799732	**0.0000000**
0.3 µm – 3 µm	-2.29102678	-3.23439812	-1.34765544	**0.0000000**
0.3 µm – 4 µm	-2.53996678	-3.48333813	-1.59659544	**0.0000000**

0.3 µm – 5.5 µm	-2.86093629	-3.80430763	-1.91756495	**0.0000000**
0.3 µm – 7 µm	-3.26906067	-4.21243201	-2.32568933	**0.0000000**
0.3 µm – 10 µm	-4.11923268	-5.06260402	-3.17586134	**0.0000000**
0.4 µm – 0. 55 µm	-0.55803716	-1.50140851	0.38533418	0.7331061
0.4 µm – 0.7 µm	-0.90993743	-1.85330877	0.03343391	0.0700956
0.4 µm – 1 µm	-1.21545507	-2.15882641	-0.27208373	**0.0018538**
0.4 µm – 1.3 µm	-1.43502302	-2.37839436	-0.49165168	**0.0000742**
0.4 µm – 1.6 µm	-1.06621341	-2.00958475	-0.12284207	**0.0126275**
0.4 µm – 2.2 µm	-1.11010005	-2.05347139	-0.16672871	**0.0073713**
0.4 µm – 3 µm	-1.51975816	-2.46312951	-0.57638682	**0.0000193**
0.4 µm – 4 µm	-1.76869817	-2.71206951	-0.82532683	**0.0000003**
0.4 µm – 5.5 µm	-2.08966767	-3.03303902	-1.14629633	**0.0000000**
0.4 µm – 7 µm	-2.49779206	-3.44116340	-1.55442071	**0.0000000**
0.4 µm – 10 µm	-3.34796407	-4.29133541	-2.40459272	**0.0000000**
0.55 µm – 0.7 µm	-0.35190026	-1.29527161	0.59147108	0.9884720
0.55 µm – 1 µm	-0.65741791	-1.60078925	0.28595344	0.4841181
0.55 µm – 1.3 µm	-0.87698585	-1.82035720	0.06638549	0.0961554
0.55 µm – 1.6 µm	-0.50817625	-1.45154759	0.43519510	0.8370077
0.55 µm – 2.2 µm	0.55206288	-1.49543423	0.39130846	0.7467506
0.55 µm – 3 µm	-0.96172100	-1.90509234	-0.01834966	**0.0412473**
0.55 µm – 4 µm	-1.21066100	-0.26728966	-0.26728966	**0.0019789**
0.55 µm – 5.5 µm	-1.53163051	-2.47500185	-0.58825917	**0.0000159**
0.55 µm – 7 µm	-1.93975489	-2.88312623	-0.99638355	**0.0000000**

0.55 µm – 10 µm	-2.78992690	-3.73329824	-1.84655556	**0.0000000**
0.7 µm – 1 µm	-0.30551764	-1.24888898	0.63785370	0.9967297
0.7 µm – 1.3 µm	-0.52508559	-1.46845693	0.41828575	0.8045036
0.7 µm – 1.6 µm	-0.15627598	-1.09964733	0.78709536	0.9999970
0.7 µm – 2,2 µm	-0.20016262	-1.14353396	0.74320872	0.9999546
0.7 µm – 3 µm	-0.60982073	-1.55319208	0.33355061	0.6059593
0.7 µm – 4 µm	-0.85876074	-1.80213208	0.08461060	0.1136706
0.7 µm – 5.5 µm	-1.17973024	-2.12310159	-0.23635890	**0.0029997**
0.7 µm – 7 µm	-1.58785463	-2.53122597	-0.64448328	**0.0000063**
0.7 µm – 10 µm	-2.43802664	-3.38139798	-1.49465529	**0.0000000**
1 µm – 1.3 µm	-0.21956795	-1.16293929	0.72380339	0.9998783
1 µm – 1.6 µm	0.14924166	0.79412968	1.09261300	0.9999982
1 µm – 2.2 µm	0.10535502 -	-0.83801632	1.04872636	1.0000000
1 µm – 3 µm	-0.30430309	-1.24767444	0.63906825	0.9968485
1 µm – 4 µm	-0.55324310	-1.49661444	0.39012825	0.7440774
1 µm – 5.5 µm	-0.87421260	-1.81758395	0.06915874	0.0986698
1 µm – 7 µm	-1.28233699	-2.22570833	-0.33896564	**0.0007278**
1 µm – 10 µm	-2.13250900	-3.07588034	-1.18913765	**0.0000000**
1.3 µm – 1.6 µm	0.36880961 -	-0.57456173	1.31218095	0.9829246
1.3 µm – 2.2 µm	0.32492297	-0.61844837	1.26829431	0.9942620
1.3 µm – 3 µm	-0.08473514	-1.02810649	0.85863620	1.0000000
1.3 µm – 4 µm	-0.33367515	-1.27704649	0.60969619	0.9927311
1.3 µm – 5.5 µm	-0.65464465	-1.59801600	0.28872669	0.4911308
1.3 µm – 7 µm	-1.06276904	-2.00614038	-0.11939769	**0.0131595**

1.3 µm – 10 µm	-1.91294105	-2.85631239	-0.96956970	**0.0000000**
1.6 µm – 2.2 µm	-0.04388664	-0.98725798	0.89948470	1.0000000
1.6 µm – 3 µm	-0.45354475	-1.39691610	0.48982659	0.9195786
1.6 µm – 4 µm	-0.70248476	-1.64585610	0.24088659	0.3747769
1.6 µm – 5.5 µm	-1.02345426	-1.96682561	-0.08008292	**0.0208558**
1.6 µm – 7 µm	-1.43157865	-2.37494999	-0.48820730	**0.0000783**
1.6 µm – 10 µm	-2.28175066	-3.22512200	-1.33837931	**0.0000000**
2.2 µm – 3 µm	-0.40965811	-1.35302946	0.53371323	0.9609781
2.2 µm – 4 µm	-0.65859812	-1.60196946	0.28477322	0.4811408
2.2 µm – 5.5 µm	-0.97956762	-1.92293897	-0.03619628	**0.0340494**
2.2 µm – 7 µm	-1.38769201	-2.33106335	-0.44432066	**0.0001538**
2.2 µm – 10 µm	2.23786402	1.29449267	3.18123536	**0.0000000**
3 µm – 4 µm	-0.24894000	-1.19231135	0.69443134	0.9995545
3 µm – 5.5 µm	-0.56990951	-1.51328085	0.37346183	0.7052150
3 µm – 7 µm	-0.97803389	-0.03466255	-0.03466255	**0.0346213**
3 µm – 10 µm	1.82820590	0.88483456	2.77157725	**0.0000001**
4 µm – 5.5 µm	-0.32096950	-1.26434085	0.62240184	0.9948608
4 µm – 7 µm	-0.72909389	-1.67246523	0.21427746	0.3160236
4 µm – 10 µm	1.57926590	0.63589455	2.52263724	**0.0000073**
5.5 µm – 7 µm	-0.40812438	-1.35149573	0.53524696	0.9620621
5.5 µm – 10 µm	1.25829639	0.31492505	2.20166774	**0.0010235**
7 µm – 10 µm	0.85017201	-0.09319933	1.79354335	0.1227635

Bold: Significant difference

Table 2.24: Analysis of variance (ANOVA) test results for Site 3 of particulate dimeter by season

	Df	Sum Sq	Mean Sq	F value	P- value < 0.05
Season	3	3.07	1.022	0.813	0.489
Residuals	152	191.12	1.257		

Table 2.25: Tukey test results for Site 3 of particulate dimeter by season

Seasons	Difference	Lower	Upper	P- value < 0.05
Spring-Fall	-0.34507085	-1.0047004	0.3145587	0.5270628
Summer-Fall	-0.11162495	-0.7712545	0.5480046	0.9715056
Winter-Fall	-0.30098262	-0.9606122	0.3586469	0.6370579
Summer-Spring	0.23344590	-0.4261837	0.8930755	0.7945629
Winter-Spring	0.04408823	-0.6155413	0.7037178	0.9981325
Winter-Summer	-0.18935767	-0.8489872	0.4702719	0.8783689

Table 2.26: Analysis of variance (ANOVA) test results for Site 3 of particulate dimeter by bin size

	Df	Sum Sq	Mean Sq	F value	P- value < 0.05
Bin Size	12	167.64	13.970	75.27	**<2e-16**
Residuals	143	26.54	0.186		

Bold: Significant difference

Table 2.27: Tukey test results for Site 3 of particulate dimeter by bin size

Bin Size	Difference	Lower	Upper	P- value < 0.05
0.3 µm – 0.4 µm	-0.74467948	-1.33734091	-0.15201806	**0.0027275**
0.3 µm – 0.55 µm	-1.31816656	-1.91082799	-0.72550514	**0.0000000**
0.3 µm – 0.7 µm	-1.77509746	-2.36775888	-1.18243604	**0.0000000**

0.3 µm – 1 µm	-2.10707305	-2.69973447	-1.51441163	**0.0000000**
0.3 µm – 1.3 µm	-2.30516102	-2.89782244	-1.71249960	**0.0000000**
0.3 µm – 1.6 µm	-2.02336691	-2.61602833	-1.43070549	**0.0000000**
0.3 µm – 2.2 µm	-2.06907747	-2.66173889	-1.47641605	**0.0000000**
0.3 µm – 3 µm	-2.44863367	-3.04129509	-1.85597224	**0.0000000**
0.3 µm – 4 µm	-2.74862929	-3.34129071	-2.15596787	**0.0000000**
0.3 µm – 5.5 µm	-3.05658966	-3.64925108	-2.46392823	**0.0000000**
0.3 µm – 7 µm	-3.42332349	-4.01598491	-2.83066207	**0.0000000**
0.3 µm – 10 µm	-4.04794745	-4.64060887	-3.45528603	**0.0000000**
0.4 µm – 0. 55 µm	-0.57348708	-1.16614850	0.01917434	0.0682036
0.4 µm – 0.7 µm	-1.03041798	-1.62307940	-0.43775656	**0.0000023**
0.4 µm – 1 µm	-1.36239357	-1.95505499	-0.76973215	**0.0000000**
0.4 µm – 1.3 µm	-1.56048153	-2.15314295	-0.96782011	**0.0000000**
0.4 µm – 1.6 µm	-1.27868743	-1.87134885	-0.68602601	**0.0000000**
0.4 µm – 2.2 µm	-1.32439799	-1.91705941	-0.73173657	**0.0000000**
0.4 µm – 3 µm	-1.70395418	-2.29661560	-1.11129276	**0.0000000**
0.4 µm – 4 µm	-2.00394980	-2.59661122	-1.41128838	**0.0000000**
0.4 µm – 5.5 µm	-2.31191017	-2.90457159	-1.71924875	**0.0000000**
0.4 µm – 7 µm	-2.67864401	-3.27130543	-2.08598259	**0.0000000**
0.4 µm – 10 µm	-3.30326796	-3.89592939	-2.71060654	**0.0000000**
0.55 µm – 0.7 µm	-0.45693090	-1.04959232	0.13573052	0.3214260
0.55 µm – 1 µm	-0.78890649	-1.38156791	-0.19624507	**0.0010299**
0.55 µm – 1.3 µm	-0.98699445	-1.57965587	-0.39433303	**0.0000076**

0.55 µm – 1.6 µm	-0.70520035	-1.29786177	-0.11253893	**0.0062213**
0.55 µm – 2.2 µm	-0.75091091	-1.34357233	-0.15824948	**0.0023852**
0.55 µm – 3 µm	-1.13046710	-1.72312852	-0.53780568	**0.0000001**
0.55 µm – 4 µm	-1.43046272	-2.02312414	-0.83780130	**0.0000000**
0.55 µm – 5.5 µm	-1.73842309	-2.33108451	-1.14576167	**0.0000000**
0.55 µm – 7 µm	-2.10515693	-2.69781835	-1.51249551	**0.0000000**
0.55 µm – 10 µm	-2.72978088	-3.32244231	-2.13711946	**0.0000000**
0.7 µm – 1 µm	-0.33197559	-0.92463701	0.26068583	0.7998737
0.7 µm – 1.3 µm	-0.53006356	-1.12272498	0.06259787	0.1304341
0.7 µm – 1.6 µm	-0.24826945	-0.84093087	0.34439197	0.9709195
0.7 µm – 2,2 µm	-0.29398001	-0.88664143	0.29868141	0.9026702
0.7 µm – 3 µm	-0.67353620	-1.26619763	-0.08087478	**0.0116614**
0.7 µm – 4 µm	-0.97353183	-1.56619325	-0.38087040	**0.0000109**
0.7 µm – 5.5 µm	-1.28149219	-1.87415362	-0.68883077	**0.0000000**
0.7 µm – 7 µm	-1.64822603	-2.24088745	-1.05556461	**0.0000000**
0.7 µm – 10 µm	-2.27284999	-2.86551141	-1.68018857	**0.0000000**
1 µm – 1.3 µm	-0.19808796	-0.79074938	0.39457346	0.9957387
1 µm – 1.6 µm	0.08370614 -	-0.50895528	0.67636756	0.9999995
1 µm – 2.2 µm	0.03799558 -	-0.55466584	0.63065700	1.0000000
1 µm – 3 µm	-0.34156061	-0.93422203	0.25110081	0.7676842
1 µm – 4 µm	-0.64155623	-1.23421765	-0.04889481	**0.0213008**
1 µm – 5.5 µm	-0.94951660	-1.54217802	-0.35685518	**0.0000205**
1 µm – 7 µm	-1.31625044	-1.90891186	-0.72358902	**0.0000000**
1 µm – 10 µm	-1.94087440	-2.53353582	-1.34821298	**0.0000000**

1.3 µm – 1.6 µm	0.28179410	0.31086732	0.87445553	0.9265409
1.3 µm – 2.2 µm	0.23608355 -	-0.35657787	0.82874497	0.9805182
1.3 µm – 3 µm	-0.14347265	-0.73613407	0.44918877	0.9998221
1.3 µm – 4 µm	-0.44346827	-1.03612969	0.14919315	0.3688594
1.3 µm – 5.5 µm	-0.75142864	-1.34409006	-0.15876722	**0.0023587**
1.3 µm – 7 µm	-1.11816248	-1.71082390	-0.52550106	**0.0000002**
1.3 µm – 10 µm	-1.74278643	-2.33544785	-1.15012501	**0.0000000**
1.6 µm – 2.2 µm	-0.04571056	-0.63837198	0.54695086	1.0000000
1.6 µm – 3 µm	-0.42526675	-1.01792818	0.16739467	0.4377514
1.6 µm – 4 µm	-0.72526237	-1.31792380	-0.13260095	**0.0041143**
1.6 µm – 5.5 µm	-1.03322274	-1.62588417	-0.44056132	**0.0000022**
1.6 µm – 7 µm	-1.39995658	-1.99261800	-0.80729516	**0.0000000**
1.6 µm – 10 µm	-2.02458054	-2.61724196	-1.43191912	**0.0000000**
2.2 µm – 3 µm	-0.37955620	-0.97221762	0.21310523	0.6229187
2.2 µm – 4 µm	-0.67955182	-1.27221324	-0.08689040	**0.0103738**
2.2 µm – 5.5 µm	-0.98751219	-0.39485076	-0.39485076	**0.0000075**
2.2 µm – 7 µm	-1.35424602	-1.94690744	-0.76158460	**0.0000000**
2.2 µm – 10 µm	1.97886998	1.38620856	2.57153140	**0.0000000**
3 µm – 4 µm	-0.29999562	-0.89265704	0.29266580	0.8892400
3 µm – 5.5 µm	-0.60795599	-1.20061741	-0.01529457	**0.0386432**
3 µm – 7 µm	-0.97468983	-1.56735125	-0.38202841	**0.0000106**
3 µm – 10 µm	1.59931378	1.00665236	2.19197520	**0.0000000**
4 µm – 5.5 µm	-0.30796037	-0.90062179	0.28470105	0.8697739
4 µm – 7 µm	-0.67469421	-1.26735563	-0.08203279	**0.0114027**

4 µm – 10 µm	1.29931816	0.70665674	1.89197958	**0.0000000**
5.5 µm – 7 µm	-0.36673384	-0.95939526	0.22592758	0.6740907
5.5 µm – 10 µm	0.99135779	0.39869637	1.58401921	**0.0000068**
7 µm – 10 µm	0.62462396	0.03196254	1.21728538	**0.0289006**

Bold: Significant difference

Table 2.28: Analysis of variance (ANOVA) test results for Site 4 of particulate dimeter by season

	Df	Sum Sq	Mean Sq	Lower	Upper	F value	P- value < 0.05
Season	1	2.37	2.368	-0.8391892	0.1422085	2.001	0.161
Residuals	76	89.96	1.184				

Table 2.29: Analysis of variance (ANOVA) test results for Site 4 of particulate dimeter by bin size

	Df	Sum Sq	Mean Sq	F value	P- value < 0.05
Bin Size	12	86.33	7.194	78.03	**<2e-16**
Residuals	65	5.99	0.092		

Bold: Significant difference

Table 2.30: Tukey test results for Site 4 of particulate dimeter by bin size

Bin Size	Difference	Lower	Upper	p adj
0.3 µm – 0.4 µm	-0.90610091	-1.5089701 -	-0.303231741	**0.0001717**
0.3 µm – 0.55 µm	-1.49857956	-2.1014487	-0.895710397	**0.0000000**
0.3 µm – 0.7 µm	-1.95713345	-2.5600026	-1.354264281	**0.0000000**
0.3 µm – 1 µm	-2.31249396	-2.9153631	-1.709624797	**0.0000000**
0.3 µm – 1.3 µm	-2.54914565	-3.1520148	-1.946276487	**0.0000000**
0.3 µm – 1.6 µm	-2.33081619	-2.9336854	-1.727947020	**0.0000000**

0.3 µm – 2.2 µm	-2.35663356	-2.9595027	-1.753764393	**0.0000000**
0.3 µm – 3 µm	-2.68983292	-3.2927021	-2.086963758	**0.0000000**
0.3 µm – 4 µm	-2.97925368	-3.5821228	-2.376384512	**0.0000000**
0.3 µm – 5.5 µm	-3.28964954	-3.8925187	-2.686780371	**0.0000000**
0.3 µm – 7 µm	-3.61475887	-4.2176280	-3.011889703	**0.0000000**
0.3 µm – 10 µm	-4.04318002	-4.6460492	3.440310853	**0.0000000**
0.4 µm – 0. 55 µm	-0.59247866	-1.1953478	0.010390511	0.0585727
0.4 µm – 0.7 µm	-1.05103254	-1.6539017	-0.448163374	**0.0000073**
0.4 µm – 1 µm	-1.40639306	-2.0092622	-0.803523890	**0.0000000**
0.4 µm – 1.3 µm	-1.64304475	-2.2459139	-1.040175580	**0.0000000**
0.4 µm – 1.6 µm	-1.42471528	-2.0275844	-0.821846113	**0.0000000**
0.4 µm – 2.2 µm	-1.45053265	-2.0534018	-0.847663486	**0.0000000**
0.4 µm – 3 µm	-1.78373202	-2.3866012	-1.180862851	**0.0000000**
0.4 µm – 4 µm	-2.07315277	-2.6760219	-1.470283605	**0.0000000**
0.4 µm – 5.5 µm	-2.38354863	-2.9864178	-1.780679464	**0.0000000**
0.4 µm – 7 µm	-2.70865796	-3.3115271	-2.105788796	**0.0000000**
0.4 µm – 10 µm	-3.13707911	-3.7399483	-2.534209946	**0.0000000**
0.55 µm – 0.7 µm	-0.45855388	-1.0614231	0.144315282	0.3224516
0.55 µm – 1 µm	-0.81391440	-1.4167836	-0.211045234	**0.0011421**
0.55 µm – 1.3 µm	-1.05056609	-1.6534353	-0.447696924	**0.0000074**
0.55 µm – 1.6 µm	-0.83223662	-1.4351058	-0.229367457	**0.0007908**
0.55 µm – 2.2 µm	-0.85805400	-1.4609232	-0.255184830	**0.0004674**
0.55 µm – 3 µm	-1.19125336	-1.7941225	-0.588384195	**0.0000003**

0.55 µm – 4 µm	-1.48067412	-2.0835433	-0.877804949	**0.0000000**
0.55 µm – 5.5 µm	-1.79106997	-2.3939391	-1.188200808	**0.0000000**
0.55 µm – 7 µm	-2.11617931	-2.7190485	-1.513310141	**0.0000000**
0.55 µm – 10 µm	-2.54460046	-3.1474696	-1.941731290	**0.0000000**
0.7 µm – 1 µm	-0.35536052	-0.9582297	0.247508650	0.7116595
0.7 µm – 1.3 µm	-0.59201221	-1.1948814	0.010856960	0.0589857
0.7 µm – 1.6 µm	-0.37368274	-0.9765519	0.229186427	0.6419973
0.7 µm – 2,2 µm	-0.39950011	-1.0023693	0.203369054	0.5400013
0.7 µm – 3 µm	-0.73269948	-1.3355686	-0.129830311	**0.0054564**
0.7 µm – 4 µm	-1.02212023	-1.6249894	-0.419251065	**0.0000139**
0.7 µm – 5.5 µm	-1.33251609	-1.9353853	-0.729646924	**0.0000000**
0.7 µm – 7 µm	-1.65762542	-2.2604946	-1.054756256	**0.0000000**
0.7 µm – 10 µm	-2.08604657	-2.6889157	-1.483177405	**0.0000000**
1 µm – 1.3 µm	-0.23665169	-0.8395209	0.366217477	0.9778284
1 µm – 1.6 µm	-0.01832222	-0.6211914	0.584546944	1.0000000
1 µm – 2.2 µm	-0.04413960	-0.6470088	0.558729570	1.0000000
1 µm – 3 µm	-0.37733896	-0.9802081	0.225530205	0.6277016
1 µm – 4 µm	-0.66675971	-1.2696289	-0.063890548	**0.0176857**
1 µm – 5.5 µm	-0.97715557	-1.5800247	-0.374286407	**0.0000373**
1 µm – 7 µm	-1.30226491	-1.9051341	-0.699395740	**0.0000000**
1 µm – 10 µm	-1.73068606	-2.3335552	-1.127816889	**0.0000000**
1.3 µm – 1.6 µm	0.21832947	-0.3845397	0.821198633	0.9885074
1.3 µm – 2.2 µm	0.19251209	-0.4103571	0.795381260	0.9961870
1.3 µm – 3 µm	-0.14068727	-0.7435564	0.462181895	0.9998228

1.3 µm – 4 µm	-0.43010803	-1.0329772	0.172761141	0.4218537
1.3 µm – 5.5 µm	-0.74050388	-1.3433731	-0.137634718	**0.0047190**
1.3 µm – 7 µm	-1.06561322	-1.6684824	-0.462744050	**0.0000053**
1.3 µm – 10 µm	-1.49403437	-2.0969035	-0.891165199	**0.0000000**
1.6 µm – 2.2 µm	-0.02581737	-0.6286865	0.577051793	1.0000000
1.6 µm – 3 µm	-0.35901674	-0.9618859	0.243852428	0.6980893
1.6 µm – 4 µm	-0.64843749	-1.2513067	-0.045568326	**0.0240896**
1.6 µm – 5.5 µm	-0.95883335	-1.5617025	-0.355964184	**0.0000556**
1.6 µm – 7 µm	-1.28394268	-1.8868118	-0.681073517	**0.0000000**
1.6 µm – 10 µm	-1.71236383	-2.3152330	-1.109494666	**0.0000000**
2.2 µm – 3 µm	-0.33319936	-0.9360685	0.269669802	0.7888779
2.2 µm – 4 µm	-0.62262012	-1.2254893	-0.019750952	**0.0366910**
2.2 µm – 5.5 µm	-0.93301598	-1.5358851	-0.330146811	**0.0000969**
2.2 µm – 7 µm	-1.25812531	-1.8609945	-0.655256144	**0.0000001**
2.2 µm – 10 µm	1.68654646	1.0836773	2.289415626	**0.0000000**
3 µm – 4 µm	-0.28942075	-0.8922899	0.313448413	0.9062917
3 µm – 5.5 µm	-0.59981661	-1.2026858	0.003052554	0.0523969
3 µm – 7 µm	-0.92492595	-1.5277951	-0.322056779	**0.0001152**
3 µm – 10 µm	1.35334709	0.7504779	1.956216261	**0.0000000**
4 µm – 5.5 µm	-0.31039586	-0.9132650	0.292473308	0.8566303
4 µm – 7 µm	-0.63550519	-1.2383744	-0.032636025	**0.0298075**
4 µm – 10 µm	1.06392634	0.4610572	1.666795507	**0.0000055**
5.5 µm – 7 µm	-0.32510933	-0.9279785	0.277759834	0.8144394
5.5 µm – 10 µm	0.75353048	0.1506613	1.356399648	**0.0036940**

7 µm – 10 µm	0.42842115	-0.1744480	1.031290316	0.4281290

Bold: Significant difference

For the seasonal variation in the particulate size between sites, we noted that there is no significant difference between sites for the particulate diameter in winter (Table 2.31) and the P-value is 0.43 (P > 0.05) and summer (Table 2.24) and the P-value is 0.151 (P > 0.05). On the other hand, there is a statistically significant difference in spring (Table 2.35) with P-value 0.00214 (P < 0.05), and the difference is between Site 2 and Site 1 with adjusted P-value 0.0022804 and between Site 4 and Site 2 with adjusted P-value 0.0195006 (Table 2.36). Also, there is a significant difference in fall with a P-value 1.61e-07 (P < 0.05) (Table 2.43) between Site 1 and Site 3 with adjusted P-value 0.0071814, Site 4 and Site 3 and the adjusted P-value is 0.0015965, between Site 2 and Site 1 with a P-value 0.0000249 and between Site 4 and Site 2 and the P-value is 0.0000034 (Table 2.44). In addition, statistical analysis has been done to assess the significant difference between particulate diameter among seasons. For Winter (Table 2.33 & 2.43) showed that there is a significant difference with a P-value <2e-16 (P < 0.05) and the difference is between 0.3 µm and 0.55 µm, 0.7 µm, 1 µm, 1.3 µm, 1.6 µm, 2.2 µm, 3 µm, 4 µm, 5.5 µm, 7 µm, and 10 µm, between 0.4 µm and 0.7 µm, 1 µm, 1.3 µm, 1.6 µm, 2.2 µm, 3 µm, 4 µm, 5.5 µm, 7 µm, and 10 µm, between 0.55 µm and 3 µm, 4 µm, 5.5 µm 7 µm and 10 µm, 0.7 µm and 5.5 µm, 7 µm and 10 µm, between 1 µm and 7 µm and 10 µm, between 1.3 µm and 7 µm and 10 µm, between 1.6 µm and 7 µm and 10 µm, between 2.2 µm and 7 µm and 10 µm, between 3 µm and 7 µm and 10 µm, between 4 µm and 10 µm and between 5.5 µm and 10 µm. Also, the P value of spring (Table 2.37) is <2e-16 (P < 0.05) and the difference is in the particulate with diameter 0.3 µm and 0.4 µm, 0.55 µm, 0.7 µm, 1 µm, 1.3 µm, 1.6 µm, 2.2 µm, 3 µm, 4 µm, 5.5

µm, 7 µm and 10 µm, particulate of diameter 0.4 µm and 0.7 µm, 1 µm, 1.3 µm, 1.6 µm, 2.2 µm, 3 µm, 4 µm, 5.5 µm, 7 µm and 10 µm, particulate size of 0.55 µm and 1 µm, 1.3 µm , 1.6 µm , 2.2 µm, 3 µm, 4 µm, 5.5 µm, 7 µm and 10 µm, between particulate size of 0.7 µm and 3 µm, 4 µm, 5.5 µm, 7 µm and 10 µm, particulate dimeter 1 µm and 3 µm, 4 µm, 5.5 µm, 7 µm and 10 µm, particulate size of 1.3 µm and 4 µm, 5.5 µm, 7 µm and 10 µm, between particulate size of 1.6 µm and 4 µm, 5.5 µm, 7 µm and 10 µm, particulate with 2.2 µm and 4 µm, 5.5 µm, 7 µm and 10 µm, particulate diameter of 3 µm and 7 µm and 10 µm, between particulate size 4 µm and 10 µm and between 5.5 µm and 10 µm (Table 2.38). Moreover, there is a significant difference in particulate sizes for summer with P-value <2e-16 ($P < 0.05$) (Table 2.41). We found that particulate with diameter 0.3 µm are statistically different from 0.4 µm, 0.55 µm, 0.7 µm, 1 µm, 1.3 µm, 1.6 µm, 2.2 µm, 3 µm, 4 µm, 5.5 µm, 7 µm, and 10 µm, particulate size 0.4 µm is different from 0.55 µm, 0.7 µm, 1 µm, 1.3 µm, 1.6 µm, 2.2 µm, 3 µm, 4 µm, 5.5 µm, 7 µm, and 10 µm. There is a difference between particulate of 0.55 µm diameter and 1 µm, 1.3 µm, 1.6 µm, 2.2 µm, 3 µm, 4 µm, 5.5 µm, 7 µm, and 10 µm, between 0.7 µm and 1 µm, 1.3 µm, 2.2 µm, 3 µm, 4 µm, 5.5 µm, 7 µm, and 10 µm, between particulate size of 1 µm and 4 µm, 5.5 µm, 7 µm, and 10 µm, particulate of 1.3 µm and 1.6 µm, 4 µm, 5.5 µm, 7 µm, and 10 µm, the particulate diameter of 1.6 µm and 3 µm, 4 µm, 5.5 µm, 7 µm, and 10 µm, between 2.2 µm and 4 µm, 5.5 µm, 7 µm, and 10 µm, between 3 µm and 5.5 µm, 7 µm and 10 µm, between 4 µm and 5.5 µm, 7 µm and 10 µm and between particulate diameter of 5.5 µm and 10 µm (Table 2.42). For fall, (Table 2.45) show that there is a significant difference in the particulate bin size, and the P-value is <2e-16 ($P < 0.05$). the difference is between particulate diameter 0.3 µm and 0.4 µm, 0.55 µm, 0.7 µm, 1 µm, 1.3 µm, 1.6

µm, 2.2 µm, 3 µm, 4 µm, 5.5 µm, 7 µm, and 10 µm, particulate size 0.4 µm and 1 µm, 1.3 µm, 3 µm, 4 µm, 5.5 µm, 7 µm, and 10 µm, particulate of diameter 0.55 µm and 5.5 µm, 7 µm and 10 µm, between 0.7 µm and 7 µm and 10 µm, between 1 µm and 10 µm, between 1.3 µm and 10 µm, between 1.6 µm and 7 µm and 10 µm, particulate of 2.2 µm and 7 µm and 10 µm, between 3 µm and 10 µm, between 4 µm and 10 µm and particulate of diameter 5.5 µm and 10 µm (Table 2.46).

Table 2.31: Analysis of variance (ANOVA) test results for Winter of particulate dimeter by site

	Df	Sum Sq	Mean Sq	F value	P- value < 0.05
Site	2	2.34	1.172	0.849	0.43
Residuals	114	157.40	1.381		

Table 2.32: Tukey test results for Winter of particulate dimeter by site

Sites	Difference	Lower	Upper	P- value < 0.05
Site 1- Site 3	0.1844971	-0.4473896	0.8163837	0.7678432
Site 2- Site 3	-0.1620250	-0.7939117	0.4698616	0.8155508
Site 2- Site 1	-0.3465221	-0.9784088	0.2853646	0.3968501

Table 2.33: Analysis of variance (ANOVA) test results for Winter of particulate dimeter by bin size

	Df	Sum Sq	Mean Sq	F value	P- value < 0.05
Bin Size	12	121.25	10.10	27.3	**<2e-16**
Residuals	104	38.49	0.37		

Bold: Significant difference

Table 2.34: Tukey test results for Winter of particulate dimeter by bin size

Bin Size	Difference	Lower	Upper	P- value < 0.05
0.3 µm – 0.4 µm	-0.77673021	-1.7492223	0.195761899	0.2633566

0.3 µm – 0.55 µm	-1.10506576	-2.0775579	-0.132573651	**0.0120599**
0.3 µm – 0.7 µm	-1.75113487	-2.7236270	-0.778642765	**0.0000014**
0.3 µm – 1 µm	-1.79660170	-2.7690938	-0.824109594	**0.0000007**
0.3 µm – 1.3 µm	-1.98260727	-2.9550994	-1.010115158	**0.0000000**
0.3 µm – 1.6 µm	-1.94838367	-2.9208758	-0.975891561	**0.0000001**
0.3 µm – 2.2 µm	-1.90424971	-2.8767418	-0.931757604	**0.0000001**
0.3 µm – 3 µm	-2.38361779	-3.3561099	-1.411125679	**0.0000000**
0.3 µm – 4 µm	-2.69509973	-3.6675918	-1.722607622	**0.0000000**
0.3 µm – 5.5 µm	-2.75324119	-3.7257333	-1.780749075	**0.0000000**
0.3 µm – 7 µm	-3.35871098	-4.3312031	-2.386218867	**0.0000000**
0.3 µm – 10 µm	-4.00813773	-4.9806298	-3.035645621	**0.0000000**
0.4 µm – 0. 55 µm	-0.32833555	-1.3008277	0.644156560	0.9948637
0.4 µm – 0.7 µm	-0.97440466	-1.9468968	-0.001912554	**0.0490598**
0.4 µm – 1 µm	-1.01987149	-1.9923636	-0.047379384	**0.0308137**
0.4 µm – 1.3 µm	-1.20587706	-2.1783692	-0.233384948	**0.0035969**
0.4 µm – 1.6 µm	-1.17165346	-2.1441456	-0.199161350	**0.0054849**
0.4 µm – 2.2 µm	-1.12751950	-2.1000116	-0.155027393	**0.0092932**
0.4 µm – 3 µm	-1.60688758	-2.5793797	-0.634395469	**0.0000130**
0.4 µm – 4 µm	-1.91836952	-2.8908616	-0.945877412	**0.0000001**
0.4 µm – 5.5 µm	-1.97651097	-2.9490031	-1.004018865	**0.0000000**
0.4 µm – 7 µm	-2.58198077	-3.5544729	-1.609488657	**0.0000000**
0.4 µm – 10 µm	-3.23140752	-4.2038996	-2.258915410	**0.0000000**
0.55 µm – 0.7 µm	-0.64606911	-1.6185612	0.326422996	0.5558014

0.55 µm – 1 µm	-0.69153594	-1.6640281	0.280956166	0.4445395
0.55 µm – 1.3 µm	-0.87754151	-1.8500336	0.094950603	0.1204211
0.55 µm – 1.6 µm	-0.84331791	-1.8158100	0.129174200	0.1599996
0.55 µm – 2.2 µm	-0.79918395	-1.7716761	0.173308157	0.2244881
0.55 µm – 3 µm	-1.27855203	-2.2510441	-0.306059918	**0.0014176**
0.55 µm – 4 µm	-1.59003397	-2.5625261	-0.617541862	**0.0000168**
0.55 µm – 5.5 µm	-1.64817542	-2.6206675	-0.675683315	**0.0000069**
0.55 µm – 7 µm	-2.25364522	-3.2261373	-1.281153106	**0.0000000**
0.55 µm – 10 µm	-2.90307197	-3.8755641	-1.930579860	**0.0000000**
0.7 µm – 1 µm	-0.04546683	-1.0179589	0.927025280	1.0000000
0.7 µm – 1.3 µm	-0.23147239	-1.2039645	0.741019716	0.9998320
0.7 µm – 1.6 µm	-0.19724880	-1.1697409	0.775243314	0.9999694
0.7 µm – 2,2 µm	-0.15311484	-1.1256069	0.819377271	0.9999981
0.7 µm – 3 µm	-0.63248291	-1.6049750	0.340009196	0.5895539
0.7 µm – 4 µm	-0.94396486	-1.9164570	0.028527252	0.0659822
0.7 µm – 5.5 µm	-1.00210631	-1.9745984	-0.029614201	**0.0370691**
0.7 µm – 7 µm	-1.60757610	-2.5800682	-0.635083992	**0.0000128**
0.7 µm – 10 µm	-2.25700286	-3.2294950	-1.284510746	**0.0000000**
1 µm – 1.3 µm	-0.18600556	-1.1584977	0.786486546	0.9999838
1 µm – 1.6 µm	-0.15178197	-1.1242741	0.820710144	0.9999983
1 µm – 2.2 µm	-0.10764801	-1.0801401	0.864844101	1.0000000
1 µm – 3 µm	-0.58701608	-1.5595082	0.385476025	0.6996241
1 µm – 4 µm	-0.89849803	-1.8709901	0.073994082	0.1002957
1 µm – 5.5 µm	-0.95663948	-1.9291316	0.015852629	0.0584110

1 µm – 7 µm	-1.56210927	-2.5346014	-0.589617163	**0.0000256**
1 µm – 10 µm	-2.21153603	-3.1840281	-1.239043917	**0.0000000**
1.3 µm – 1.6 µm	0.03422360	-0.9382685	1.006715707	1.0000000
1.3 µm – 2.2 µm	0.07835755	-0.8941346	1.050849664	1.0000000
1.3 µm – 3 µm	-0.40101052	-1.3735026	0.571481589	0.9723053
1.3 µm – 4 µm	-0.71249246	-1.6849846	0.259999646	0.3957285
1.3 µm – 5.5 µm	-0.77063392	-1.7431260	0.201858193	0.2746093
1.3 µm – 7 µm	-1.37610371	-2.3485958	-0.403611599	**0.0003795**
1.3 µm – 10 µm	-2.02553046	-2.9980226	-1.053038353	**0.0000000**
1.6 µm – 2.2 µm	0.04413396	-0.9283582	1.016626067	1.0000000
1.6 µm – 3 µm	-0.43523412	-1.4077262	0.537257992	0.9488489
1.6 µm – 4 µm	-0.74671606	-1.7192082	0.225776048	0.3215384
1.6 µm – 5.5 µm	-0.80485751	-1.7773496	0.167634595	0.2153155
1.6 µm – 7 µm	-1.41032731	-2.3828194	-0.437835196	**0.0002350**
1.6 µm – 10 µm	-2.05975406	-3.0322462	-1.087261950	**0.0000000**
2.2 µm – 3 µm	-0.47936808	-1.4518602	0.493124035	0.9013361
2.2 µm – 4 µm	-0.79085002	-1.7633421	0.181642091	0.2384376
2.2 µm – 5.5 µm	-0.84899147	-1.8214836	0.123500638	0.1528309
2.2 µm – 7 µm	-1.45446126	-2.4269534	-0.481969153	**0.0001252**
2.2 µm – 10 µm	2.10388802	1.1313959	3.076380127	**0.0000000**
3 µm – 4 µm	-0.31148194	-1.2839741	0.661010167	0.9968277
3 µm – 5.5 µm	-0.36962340	-1.3421155	0.602868714	0.9856437
3 µm – 7 µm	-0.97509319	-1.9475853	-0.002601078	**0.0487251**
3 µm – 10 µm	1.62451994	0.6520278	2.597012052	**0.0000099**

4 µm – 5.5 µm	-0.05814145	-1.0306336	0.914350657	1.0000000
4 µm – 7 µm	-0.66361124	-1.6361034	0.308880865	0.5123309
4 µm – 10 µm	1.31303800	0.3405459	2.285530109	**0.0008972**
5.5 µm – 7 µm	-0.60546979	-1.5779619	0.367022318	0.6558273
5.5 µm – 10 µm	1.25489655	0.2824044	2.227388655	**0.0019291**
7 µm – 10 µm	0.64942675	-0.3230654	1.621918864	0.5474584

Bold: Significant difference

Table 2.35: Analysis of variance (ANOVA) test results for Spring of particulate dimeter by site

	Df	Sum Sq	Mean Sq	F value	P- value < 0.05
Site	3	20.79	6.931	5.157	**0.00214**
Residuals	126	169.35	1.344		

Bold: Significant difference

Table 2.36: Tukey test results for Spring of particulate dimeter by site

Sites	Difference	Lower	Upper	P- value < 0.05
Site 1- Site 3	-0.30879619	-1.073038	0.4554461	0.7191632
Site 2- Site 3	-0.08720273	-0.851445	0.6770395	0.9908407
Site 4- Site 3	-0.3465221	-0.9784088	0.2853646	0.3968501
Site 2- Site 1	-0.95351859	-1.637078	-0.2699595	**0.0022804**
Site 4- Site 1	0.22159345	-0.615592	1.0587789	0.9010723
Site 4- Site 2	-0.86631585	-1.630558	-0.1020736	**0.0195006**

Bold: Significant difference

Table 2.37: Analysis of variance (ANOVA) test results for Spring of particulate dimeter by bin size

	Df	Sum Sq	Mean Sq	F value	P- value < 0.05
Bin Size	12	162.4	13.537	57.18	**<2e-16**
Residuals	117	27.7	0.237		

Bold: Significant difference

Table 2.38: Tukey test results for Spring of particulate dimeter by bin size

Bin Size	Difference	Lower	Upper	P- value < 0.05
0.3 µm – 0.4 µm	-0.86823733	-1.6042278	-0.132246813	**0.0072261**
0.3 µm – 0.55 µm	-1.30770508	-2.0436956	-0.571714569	**0.0000016**
0.3 µm – 0.7 µm	-2.01416595	-2.7501565	-1.278175435	**0.0000000**
0.3 µm – 1 µm	-2.05149689	-2.7874874	-1.315506380	**0.0000000**
0.3 µm – 1.3 µm	-2.23875140	-2.9747419	-1.502760883	**0.0000000**
0.3 µm – 1.6 µm	-2.26091816	-2.9969087	-1.524927641	**0.0000000**
0.3 µm – 2.2 µm	-2.27608185	-3.0120724	-1.540091335	**0.0000000**
0.3 µm – 3 µm	-2.79366565	-3.5296562	-2.057675134	**0.0000000**
0.3 µm – 4 µm	-3.13991315	-3.8759037	-2.403922631	**0.0000000**
0.3 µm – 5.5 µm	-3.21577705	-3.9517676	-2.479786540	**0.0000000**
0.3 µm – 7 µm	-3.77676080	-4.5127513	-3.040770283	**0.0000000**
0.3 µm – 10 µm	-4.25162278	-4.9876133	-3.515632269	**0.0000000**
0.4 µm – 0. 55 µm	-0.43946776	-1.1754583	0.296522758	0.7179198
0.4 µm – 0.7 µm	-1.14592862	-1.8819191	-0.409938109	**0.0000474**
0.4 µm – 1 µm	-1.18325957	-1.9192501	-0.447269053	**0.0000223**
0.4 µm – 1.3 µm	-1.37051407	-2.1065046	-0.634523556	**0.0000004**
0.4 µm – 1.6 µm	-1.39268083	-2.1286713	-0.656690314	**0.0000003**
0.4 µm – 2.2 µm	-1.40784452	-2.1438350	-0.671854008	**0.0000002**
0.4 µm – 3 µm	-1.92542832	-2.6614188	-1.189437807	**0.0000000**
0.4 µm – 4 µm	-2.27167582	-3.0076663	-1.535685304	**0.0000000**
0.4 µm – 5.5 µm	-2.34753973	-3.0835302	-1.611549213	**0.0000000**

0.4 µm – 7 µm	-2.90852347	-3.6445140	-2.172532956	**0.0000000**
0.4 µm – 10 µm	-3.38338546	-4.1193760	-2.647394942	**0.0000000**
0.55 µm – 0.7 µm	-0.70646087	-1.4424514	0.029529648	0.0730507
0.55 µm – 1 µm	-0.74379181	-1.4797823	-0.007801297	**0.0450773**
0.55 µm – 1.3 µm	-0.93104631	-1.6670368	-0.195055800	**0.0025644**
0.55 µm – 1.6 µm	-0.95321307	-1.6892036	-0.217222558	**0.0017514**
0.55 µm – 2.2 µm	-0.96837677	-1.7043673	-0.232386252	**0.0013433**
0.55 µm – 3 µm	-1.48596057	-2.2219511	-0.749970051	**0.0000000**
0.55 µm – 4 µm	-1.83220806	-2.5681986	-1.096217548	**0.0000000**
0.55 µm – 5.5 µm	-1.90807197	-2.6440625	-1.172081457	**0.0000000**
0.55 µm – 7 µm	-2.46905571	-3.2050462	-1.733065200	**0.0000000**
0.55 µm – 10 µm	-2.94391770	-3.6799082	-2.207927186	**0.0000000**
0.7 µm – 1 µm	-0.03733094	-0.7733215	0.698659570	1.0000000
0.7 µm – 1.3 µm	-0.22458545	-0.9605760	0.511405066	0.9980696
0.7 µm – 1.6 µm	-0.24675221	-0.9827427	0.489238309	0.9953611
0.7 µm – 2,2 µm	-0.26191590	-0.9979064	0.474074615	0.9921017
0.7 µm – 3 µm	-0.77949970	-1.5154902	-0.043509184	**0.0275574**
0.7 µm – 4 µm	-1.12574720	-1.8617377	-0.389756682	**0.0000707**
0.7 µm – 5.5 µm	-1.20161110	-1.9376016	-0.465620591	**0.0000154**
0.7 µm – 7 µm	-1.76259485	-2.4985854	-1.026604333	**0.0000000**
0.7 µm – 10 µm	-2.23745683	-2.9734473	-1.501466319	**0.0000000**
1 µm – 1.3 µm	-0.18725450	-0.9232450	0.548736011	0.9996811
1 µm – 1.6 µm	-0.20942126	-0.9454118	0.526569253	0.9990193

1 μm – 2.2 μm	-0.22458496	-0.9605755	0.511405559	0.9980697
1 μm – 3 μm	-0.74216875	-1.4781593	-0.006178240	**0.0460653**
1 μm – 4 μm	-1.08841625	-1.8244068	-0.352425737	**0.0001464**
1 μm – 5.5 μm	-1.16428016	-1.9002707	-0.428289646	**0.0000328**
1 μm – 7 μm	-1.72526390	-2.4612544	-0.989273389	**0.0000000**
1 μm – 10 μm	-2.20012589	-2.9361164	-1.464135375	**0.0000000**
1.3 μm – 1.6 μm	-0.02216676	-0.7581573	0.713823756	1.0000000
1.3 μm – 2.2 μm	-0.03733045	-0.7733210	0.698660063	1.0000000
1.3 μm – 3 μm	-0.55491425	-1.2909048	0.181076264	0.3525931
1.3 μm – 4 μm	-0.90116175	-1.6371523	-0.165171234	**0.0042339**
1.3 μm – 5.5 μm	-0.97702566	-1.7130162	-0.241035143	**0.0011528**
1.3 μm – 7 μm	-1.53800940	-2.2739999	-0.802018886	**0.0000000**
1.3 μm – 10 μm	-2.01287139	-2.7488619	-1.276880871	**0.0000000**
1.6 μm – 2.2 μm	-0.01516369	-0.7511542	0.720826820	1.0000000
1.6 μm – 3 μm	-0.53274749	-1.2687380	0.203243021	0.4185610
1.6 μm – 4 μm	-0.87899499	-1.6149855	-0.143004476	**0.0060809**
1.6 μm – 5.5 μm	-0.95485890	-1.6908494	-0.218868385	**0.0017020**
1.6 μm – 7 μm	-1.51584264	-2.2518332	-0.779852128	**0.0000000**
1.6 μm – 10 μm	-1.99070463	-2.7266951	-1.254714113	**0.0000000**
2.2 μm – 3 μm	-0.51758380	-1.2535743	0.218406715	0.4662448
2.2 μm – 4 μm	-0.86383130	-1.5998218	-0.127840782	**0.0077506**
2.2 μm – 5.5 μm	-0.93969521	-1.6756857	-0.203704691	**0.0022120**
2.2 μm – 7 μm	-1.50067895	-2.2366695	-0.764688434	**0.0000000**
2.2 μm – 10 μm	1.97554093	1.2395504	2.711531448	**0.0000000**

3 µm – 4 µm	-0.34624750	-1.0822380	0.389743017	0.9292223
3 µm – 5.5 µm	-0.42211141	-1.1581019	0.313879108	0.7683712
3 µm – 7 µm	-0.98309515	-1.7190857	-0.247104635	**0.0010348**
3 µm – 10 µm	1.45795713	0.7219666	2.193947649	**0.0000001**
4 µm – 5.5 µm	-0.07586391	-0.8118544	0.660126605	1.0000000
4 µm – 7 µm	-0.63684765	-1.3728382	0.099142862	0.1634196
4 µm – 10 µm	1.11170964	0.3757191	1.847700152	**0.0000932**
5.5 µm – 7 µm	-0.56098374	-1.2969743	0.175006771	0.3354732
5.5 µm – 10 µm	1.03584573	0.2998552	1.771836243	**0.0003959**
7 µm – 10 µm	0.47486199	-0.2611285	1.210852500	0.6058372

Bold: Significant difference

Table 2.39: Analysis of variance (ANOVA) test results for Summer of particulate dimeter by site

	Df	Sum Sq	Mean Sq	F value	P- value < 0.05
Site	2	5.1	2.548	1.927	0.151
Residuals	101	133.6	1.322		

Table 2.40: Tukey test results for Summer of particulate dimeter by site

Sites	Difference	Lower	Upper	P- value < 0.05
Site 1- Site 3	-0.5590903	-1.2516374	0.1334568	0.1381966
Site 2- Site 3	-0.3185925	-0.9380254	0.3008405	0.4421678
Site 2- Site 1	0.2404979	-0.4520492	0.9330450	0.6877850

Table 2.41: Analysis of variance (ANOVA) test results for Summer of particulate dimeter by bin size

	Df	Sum Sq	Mean Sq	F value	P- value < 0.05
Bin Size	12	131.1	10.921	130.8	**<2e-16**
Residuals	91	7.6	0.083		

Bold: Significant difference

Table 2.42: Tukey test results for Summer of particulate dimeter by bin size

Bin Size	Difference	Lower	Upper	P- value < 0.05
0.3 µm – 0.4 µm	-0.71952946	-1.211093499	-0.22796543	**0.0002139**
0.3 µm – 0.55 µm	-1.49132722	-1.982891255	-0.99976319	**0.0000000**
0.3 µm – 0.7 µm	-1.68517376	-2.176737798	-1.19360973	**0.0000000**
0.3 µm – 1 µm	-2.29072735	-2.782291386	-1.79916332	**0.0000000**
0.3 µm – 1.3 µm	-2.53273570	-3.024299734	-2.04117167	**0.0000000**
0.3 µm – 1.6 µm	-2.00553876	-2.497102798	-1.51397473	**0.0000000**
0.3 µm – 2.2 µm	-2.33144353	-2.823007568	-1.83987950	**0.0000000**
0.3 µm – 3 µm	-2.75354649	-3.245110528	-2.26198246	**0.0000000**
0.3 µm – 4 µm	-3.05169116	-3.543255197	-2.56012713	**0.0000000**
0.3 µm – 5.5 µm	-3.57964323	-4.071207269	-3.08807920	**0.0000000**
0.3 µm – 7 µm	-3.62095408	-4.112518112	-3.12939004	**0.0000000**
0.3 µm – 10 µm	-4.10880950	-4.600373537	-3.61724547	**0.0000000**
0.4 µm – 0. 55 µm	-0.77179776	-1.263361791	-0.28023372	**0.0000493**
0.4 µm – 0.7 µm	-0.96564430	-1.457208333	-0.47408026	**0.0000001**
0.4 µm – 1 µm	-1.57119789	-2.062761922	-1.07963385	**0.0000000**
0.4 µm – 1.3 µm	-1.81320624	-2.304770270	-1.32164220	**0.0000000**
0.4 µm – 1.6 µm	-1.28600930	-1.777573334	-0.79444526	**0.0000000**
0.4 µm – 2.2 µm	-1.61191407	-2.103478104	-1.12035003	**0.0000000**
0.4 µm – 3 µm	-2.03401703	-2.525581064	-1.54245299	**0.0000000**
0.4 µm – 4 µm	-2.33216170	-2.823725733	-1.84059766	**0.0000000**
0.4 µm – 5.5 µm	-2.86011377	-3.351677805	-2.36854974	**0.0000000**

0.4 µm – 7 µm	-2.90142461	-3.392988648	-2.40986058	**0.0000000**
0.4 µm – 10 µm	-3.38928004	-3.880844073	-2.89771600	**0.0000000**
0.55 µm – 0.7 µm	-0.19384654	-0.685410577	0.29771749	0.9797612
0.55 µm – 1 µm	-0.79940013	-1.290964166	-0.30783610	**0.0000222**
0.55 µm – 1.3 µm	-1.04140848	-1.532972513	-0.54984444	**0.0000000**
0.55 µm – 1.6 µm	-0.51421154	-1.005775577	-0.02264751	**0.0318028**
0.55 µm – 2.2 µm	-0.84011631	-1.331680347	-0.34855228	**0.0000067**
0.55 µm – 3 µm	-1.26221927	-1.753783307	-0.77065524	**0.0000000**
0.55 µm – 4 µm	-1.56036394	-2.051927976	-1.06879991	**0.0000000**
0.55 µm – 5.5 µm	-2.08831601	-2.579880048	-1.59675198	**0.0000000**
0.55 µm – 7 µm	-2.12962686	-2.621190891	-1.63806282	**0.0000000**
0.55 µm – 10 µm	-2.61748228	-3.109046316	-2.12591825	**0.0000000**
0.7 µm – 1 µm	-0.60555359	-1.097117623	-0.11398955	**0.0040999**
0.7 µm – 1.3 µm	-0.84756194	-1.339125971	-0.35599790	**0.0000053**
0.7 µm – 1.6 µm	-0.32036500	-0.811929035	0.17119903	0.5814299
0.7 µm – 2,2 µm	-0.64626977	-1.137833805	-0.15470574	**0.0014915**
0.7 µm – 3 µm	-1.06837273	-1.559936765	-0.57680870	**0.0000000**
0.7 µm – 4 µm	-1.36651740	-1.858081434	-0.87495336	**0.0000000**
0.7 µm – 5.5 µm	-1.89446947	-2.386033506	-1.40290544	**0.0000000**
0.7 µm – 7 µm	-1.93578031	-2.427344349	-1.44421628	**0.0000000**
0.7 µm – 10 µm	-2.42363574	-2.915199774	-1.93207170	**0.0000000**
1 µm – 1.3 µm	-0.24200835	-0.733572382	0.24955569	0.8993377
1 µm – 1.6 µm	0.28518859	-0.206375446	0.77675262	0.7465136

1 µm – 2.2 µm	-0.04071618	-0.532280216	0.45084785	1.0000000
1 µm – 3 µm	-0.46281914	-0.954383176	0.02874489	0.0855725
1 µm – 4 µm	-0.76096381	-1.252527845	-0.26939978	**0.0000672**
1 µm – 5.5 µm	-1.28891588	-1.780479917	-0.79735185	**0.0000000**
1 µm – 7 µm	-1.33022673	-1.821790760	-0.83866269	**0.0000000**
1 µm – 10 µm	-1.81808215	-2.309646185	-1.32651812	**0.0000000**
1.3 µm – 1.6 µm	0.52719694	0.035632901	1.01876097	**0.0242723**
1.3 µm – 2.2 µm	0.20129217 -	-0.290271868	0.69285620	0.9727333
1.3 µm – 3 µm	-0.22081079	-0.712374828	0.27075324	0.9456905
1.3 µm – 4 µm	-0.51895546	-1.010519497	-0.02739143	**0.0288388**
1.3 µm – 5.5 µm	-1.04690753	-1.538471569	-0.55534350	**0.0000000**
1.3 µm – 7 µm	-1.08821838	-1.579782412	-0.59665434	**0.0000000**
1.3 µm – 10 µm	-1.57607380	-2.067637837	-1.08450977	**0.0000000**
1.6 µm – 2.2 µm	-0.32590477	-0.817468804	0.16565926	0.5542617
1.6 µm – 3 µm	-0.74800773	-1.239571764	-0.25644369	**0.0000969**
1.6 µm – 4 µm	-1.04615240	-1.537716433	-0.55458836	**0.0000000**
1.6 µm – 5.5 µm	-1.57410447	-2.065668505	-1.08254044	**0.0000000**
1.6 µm – 7 µm	-1.61541531	-2.106979348	-1.12385128	**0.0000000**
1.6 µm – 10 µm	-2.10327074	-2.594834773	-1.61170670	**0.0000000**
2.2 µm – 3 µm	-0.42210296	-0.913666994	0.06946107	0.1694183
2.2 µm – 4 µm	-0.72024763	-1.211811663	-0.22868359	**0.0002097**
2.2 µm – 5.5 µm	-1.24819970	-1.739763735	-0.75663567	**0.0000000**
2.2 µm – 7 µm	-1.28951054	-1.781074579	-0.79794651	**0.0000000**
2.2 µm – 10 µm	1.77736597	1.285801935	2.26893000	**0.0000000**
3 µm – 4 µm	-0.29814467	-0.789708704	0.19341937	0.6882344

3 µm – 5.5 µm	-0.82609674	-1.317660776	-0.33453271	**0.0000101**
3 µm – 7 µm	-0.86740758	-1.358971619	-0.37584355	**0.0000029**
3 µm – 10 µm	1.35526301	0.863698975	1.84682704	**0.0000000**
4 µm – 5.5 µm	-0.52795207	-1.019516107	-0.03638804	**0.0238883**
4 µm – 7 µm	-0.56926292	-1.060826950	-0.07769888	**0.0096245**
4 µm – 10 µm	1.05711834	0.565554306	1.54868238	**0.0000000**
5.5 µm – 7 µm	-0.04131084	-0.532874878	0.45025319	1.0000000
5.5 µm – 10 µm	0.52916627	0.037602234	1.02073030	**0.0232824**
7 µm – 10 µm	0.48785543	-0.003708609	0.97941946	0.0537175

Bold: Significant difference

Table 2.43: Analysis of variance (ANOVA) test results for Fall of particulate dimeter by site

	Df	Sum Sq	Mean Sq	F value	P- value < 0.05
Site	3	49.05	16.350	12.83	**1.61e-07**
Residuals	152	193.65	1.274		

Bold: Significant difference

Table 2.44: Tukey test results for Fall of particulate dimeter by site

Sites	Difference	Lower	Upper	P- value < 0.05
Site 1- Site 3	-0.8361132	-1.5000917	-0.1721347	**0.0071814**
Site 2- Site 3	0.3840147	-0.2799638	1.0479932	0.4386018
Site 4- Site 3	-0.9500991	-1.6140776	-0.2861206	**0.0015965**
Site 2- Site 1	1.2201280	0.5561494	1.8841065	**0.0000249**
Site 4- Site 1	-0.1139859	-0.7779644	0.5499926	0.9703142
Site 4- Site 2	-1.3341138	-1.9980923	-0.6701353	**0.0000034**

Bold: Significant difference

Table 2.45: Analysis of variance (ANOVA) test results for Fall of particulate dimeter by bin size

	Df	Sum Sq	Mean Sq	F value	P- value < 0.05
Bin Size	12	145.79	12.150	17.93	**<2e-16**
Residuals	143	96.91	0.678		

Bold: Significant difference

Table 2.46: Tukey test results for Fall of particulate dimeter by bin size

Bin Size	Difference	Lower	Upper	P- value < 0.05
0.3 µm – 0.4 µm	-1.51738283	-2.6498207	-0.38494496	**0.0009152**
0.3 µm – 0.55 µm	-1.67530628	-2.8077441	-0.54286840	**0.0001292**
0.3 µm – 0.7 µm	-2.23501883	-3.3674567	-1.10258096	**0.0000000**
0.3 µm – 1 µm	-2.45737841	-3.5898163	-1.32494054	**0.0000000**
0.3 µm – 1.3 µm	-1.78009953	-2.9125374	-0.64766165	**0.0000325**
0.3 µm – 1.6 µm	-1.51738283	-2.6498207	-0.38494496	**0.0009152**
0.3 µm – 2.2 µm	-1.73710193	-2.8695398	-0.60466406	**0.0000577**
0.3 µm – 3 µm	-1.98938150	-3.1218194	-0.85694363	**0.0000017**
0.3 µm – 4 µm	-2.22462711	-3.3570650	-1.09218923	**0.0000001**
0.3 µm – 5.5 µm	-2.78451646	-3.9169543	-1.65207859	**0.0000000**
0.3 µm – 7 µm	-3.07256243	-4.2050003	-1.94012456	**0.0000000**
0.3 µm – 10 µm	-4.03623853	-5.1686764	-2.90380066	**0.0000000**
0.4 µm – 0. 55 µm	-0.73118540	-1.8636233	0.40125247	0.6103014
0.4 µm – 0.7 µm	-0.88910885	-2.0215467	0.24332903	0.2936560
0.4 µm – 1 µm	-1.44882141	-2.5812593	-0.31638353	**0.0020344**
0.4 µm – 1.3 µm	-1.67118098	-2.8036189	-0.53874311	**0.0001363**

0.4 µm – 1.6 µm	-0.99390210	-2.1263400	0.13853578	0.1495334
0.4 µm – 2.2 µm	-0.95090450	-2.0833424	0.18153337	0.2006511
0.4 µm – 3 µm	-1.20318407	-2.3356219	-0.07074620	**0.0264082**
0.4 µm – 4 µm	-1.43842968	-2.5708676	-0.30599180	**0.0022896**
0.4 µm – 5.5 µm	-1.99831903	-3.1307569	-0.86588116	**0.0000015**
0.4 µm – 7 µm	-2.28636500	-3.4188029	-1.15392713	**0.0000000**
0.4 µm – 10 µm	-3.25004110	-4.3824790	-2.11760323	**0.0000000**
0.55 µm – 0.7 µm	-0.15792345	-1.2903613	0.97451443	0.9999996
0.55 µm – 1 µm	-0.71763601	-1.8500739	0.41480187	0.6389734
0.55 µm – 1.3 µm	-0.93999558	-2.0724335	0.19244229	0.2153891
0.55 µm – 1.6 µm	-0.26271670	-1.3951546	0.86972118	0.9998862
0.55 µm – 2.2 µm	-0.21971910	-1.3521570	0.91271877	0.9999834
0.55 µm – 3 µm	-0.47199867	-1.6044365	0.66043920	0.9720418
0.55 µm – 4 µm	-0.70724428	-1.8396822	0.42519360	0.6606760
0.55 µm – 5.5 µm	-1.26713363	-2.3995715	-0.13469576	**0.0142323**
0.55 µm – 7 µm	-1.55517960	-2.6876175	-0.42274173	**0.0005811**
0.55 µm – 10 µm	-2.51885570	-3.6512936	-1.38641783	**0.0000000**
0.7 µm – 1 µm	-0.55971256	-1.6921504	0.57272532	0.9049114
0.7 µm – 1.3 µm	-0.78207214	-1.9145100	0.35036574	0.5014723
0.7 µm – 1.6 µm	-0.10479325	-1.2372311	1.02764462	1.0000000
0.7 µm – 2,2 µm	-0.06179565	-1.1942335	1.07064222	1.0000000
0.7 µm – 3 µm	-0.31407523	-1.4465131	0.81836265	0.9992870
0.7 µm – 4 µm	-0.54932083	-1.6817587	0.58311704	0.9159400

0.7 µm – 5.5 µm	-1.10921019	-2.2416481	0.02322769	0.0609779
0.7 µm – 7 µm	-1.39725615	-2.5296940	0.0036282	**0.0036282**
0.7 µm – 10 µm	-2.36093225	-3.4933701	-1.22849438	**0.0000000**
1 µm – 1.3 µm	-0.22235958	-1.3547975	0.91007830	0.9999811
1 µm – 1.6 µm	0.45491931	-0.6775186	1.58735718	0.9791413
1 µm – 2.2 µm	0.49791690	-0.6345210	1.63035478	0.9579610
1 µm – 3 µm	0.24563733	-0.8868005	1.37807521	0.9999443
1 µm – 4 µm	0.01039173	-1.1220461	1.14282960	1.0000000
1 µm – 5.5 µm	-0.54949763	-1.6819355	0.58294025	0.9157598
1 µm – 7 µm	-0.83754360	-1.9699815	0.29489428	0.3878099
1 µm – 10 µm	-1.80121969	-2.9336576	-0.66878182	**0.0000244**
1.3 µm – 1.6 µm	0.67727888	-0.4551590	1.80971676	0.7211636
1.3 µm – 2.2 µm	0.72027648 -	-0.4121614	1.85271436	0.6334151
1.3 µm – 3 µm	0.46799691	-0.6644410	1.60043478	0.9738496
1.3 µm – 4 µm	0.23275131	-0.8996866	1.36518918	0.9999689
1.3 µm – 5.5 µm	-0.32713805	-1.4595759	0.80529982	0.9989330
1.3 µm – 7 µm	-0.61518402	-1.7476219	0.51725385	0.8310079
1.3 µm – 10 µm	-1.57886012	-2.7112980	-0.44642224	**0.0004352**
1.6 µm – 2.2 µm	0.04299760	-1.0894403	1.17543547	1.0000000
1.6 µm – 3 µm	-0.20928198	-1.3417198	0.92315590	0.9999903
1.6 µm – 4 µm	-0.44452758	-1.5769655	0.68791029	0.9827216
1.6 µm – 5.5 µm	-1.00441693	-2.1368548	0.12802094	0.1386750
1.6 µm – 7 µm	-1.29246290	-2.4249008	-0.16002503	**0.0110290**
1.6 µm – 10 µm	-2.25613900	-3.3885769	-1.12370113	**0.0000000**

2.2 µm – 3 µm	-0.25227957	-1.3847174	0.88015830	0.9999259
2.2 µm – 4 µm	-0.48752518	-1.6199630	0.64491270	0.9641213
2.2 µm – 5.5 µm	-1.04741453	-2.1798524	0.08502334	0.1004989
2.2 µm – 7 µm	-1.33546050	-2.4678984	-0.20302263	**0.0070649**
2.2 µm – 10 µm	2.29913660	1.1666987	3.43157447	**0.0000000**
3 µm – 4 µm	-0.23524560	-1.3676835	0.89719227	0.9999651
3 µm – 5.5 µm	-0.79513496	-1.9275728	0.33730291	0.4739137
3 µm – 7 µm	-1.08318093	-2.2156188	0.04925695	0.0756489
3 µm – 10 µm	2.04685703	0.9144192	3.17929490	**0.0000008**
4 µm – 5.5 µm	-0.55988936	-1.6923272	0.57254852	0.9047161
4 µm – 7 µm	-0.84793532	-1.9803732	0.28450255	0.3677715
4 µm – 10 µm	1.81161142	0.6791735	2.94404930	**0.0000212**
5.5 µm – 7 µm	-0.28804597	-1.4204838	0.84439190	0.9997031
5.5 µm – 10 µm	1.25172207	0.1192842	2.38415994	**0.0165750**
7 µm – 10 µm	0.96367610	-0.1687618	2.09611397	0.1843157

Bold: Significant difference

2.3.5. Model Prediction

Model results showed that Site 1 and Site 2 might pose potential human and environmental issues to the close communities due to the highest particulate distribution around the sites. For Site 1, the higher particulate dispersion occurred on the third day in winter with a maximum concentration 18303 µm/m³ after 500 m (Figure 2.35) followed by the second day of fall with 332 µm/m³ maximum concentration after 500 m (Figure 2.41) . On the other hand, the lower particulate dispersion is on fall first day with 7.1 µg/m³ (Figure 2.40) and fall third day with 7.3 µg/m³ (Figure 42) after 500 m. The most concern seasons of the for the residents around Site 1 are winter and summer, where the

prevailing wind is blowing toward the community close to the site. Moreover, Site 2 higher dispersion is in the second day of fall with 39535 μg/m³ after 500 m (Figure 2.52) and the first day of fall with 2964 μg/m³ (Figure 2.51), while the lower particulate dispersal happened in winter third day with 20.5 μg/m³ (Figure 2.45) and winter second day with 26 μg/m³ (Figure 2.44) after 500 m. The potential environmental and human health issues for the neighboring residences and school are possibly higher in winter, summer, and fall based on the wind direction measurements.

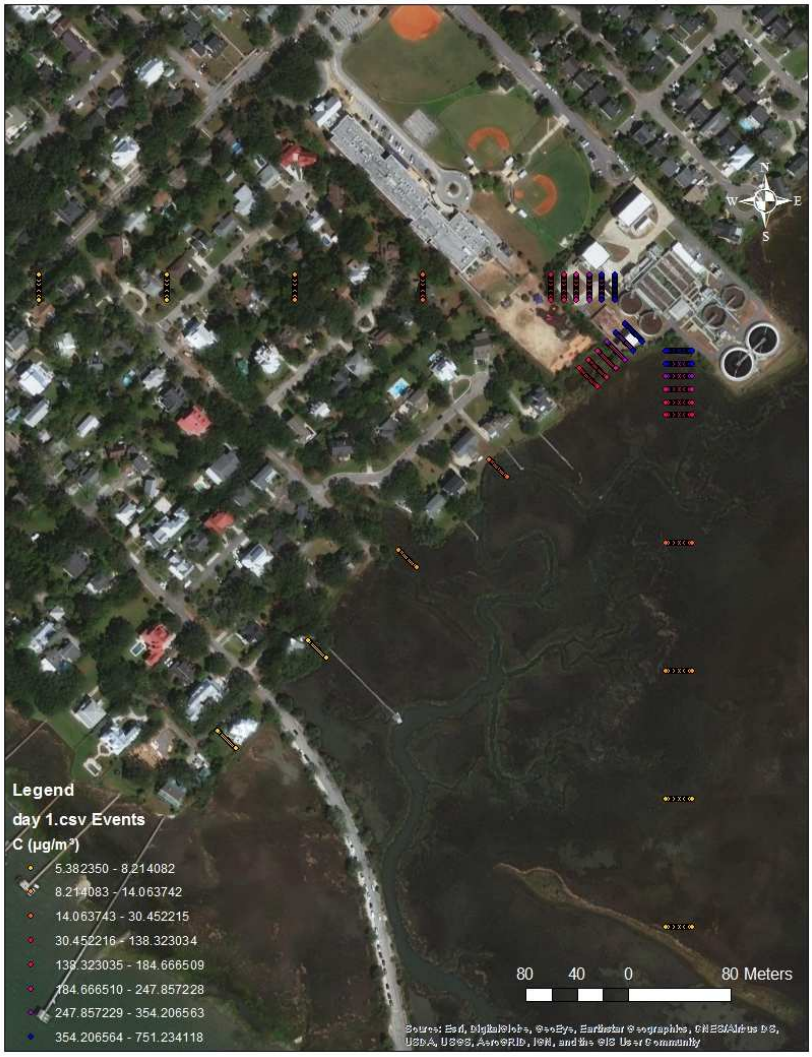

Figure 2.30: Winter first day PM dispersion model for Site 1

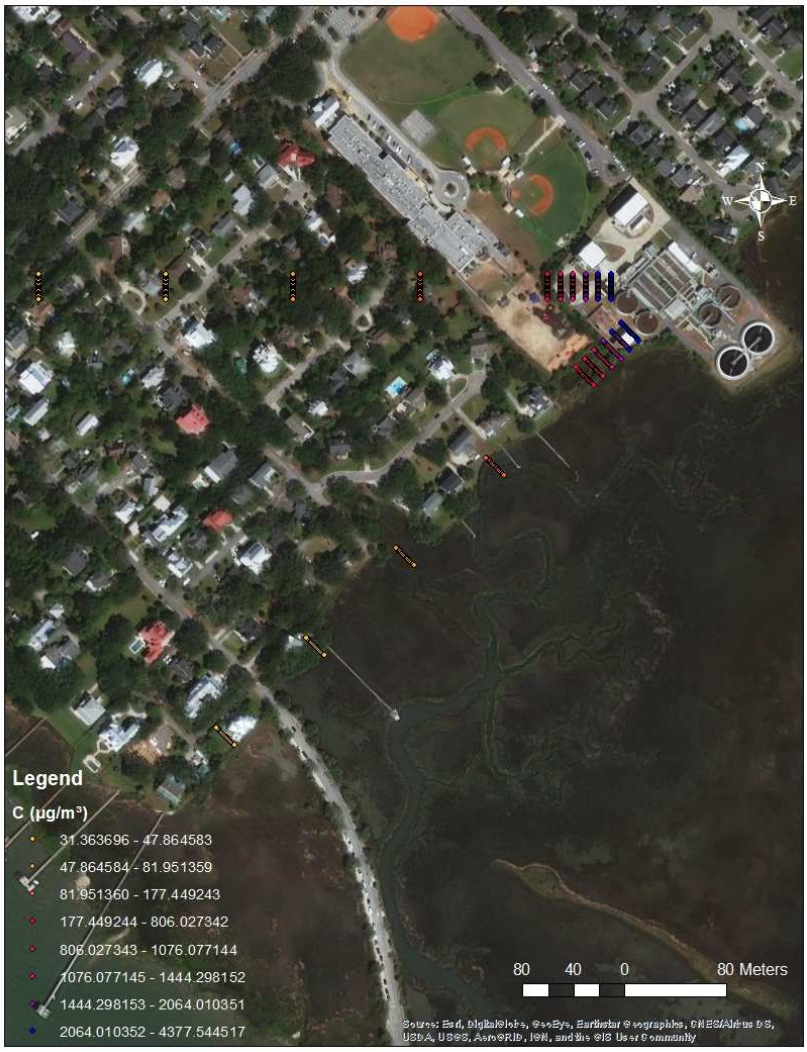

Figure 2.31: Winter second day PM dispersion model for Site 1

Figure 2.32: Winter third day PM dispersion model for Site 1

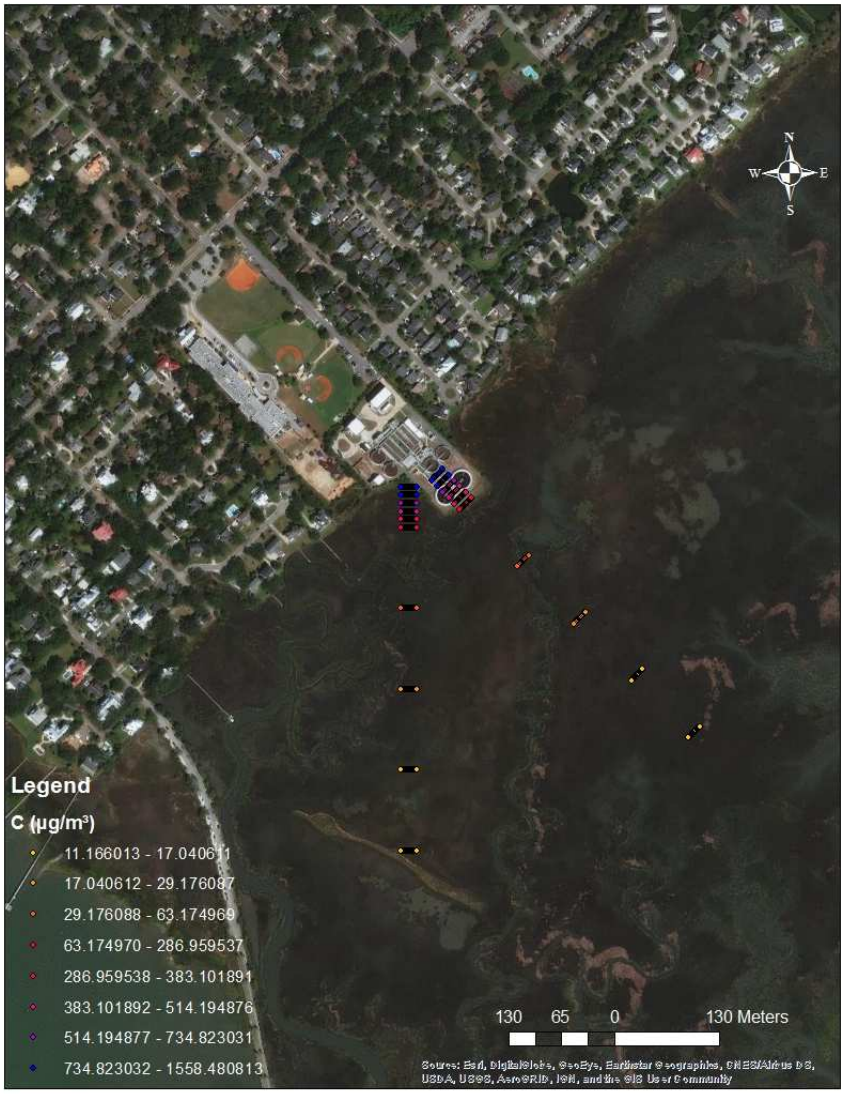

Figure 2.33: Spring second day PM dispersion model for Site 1

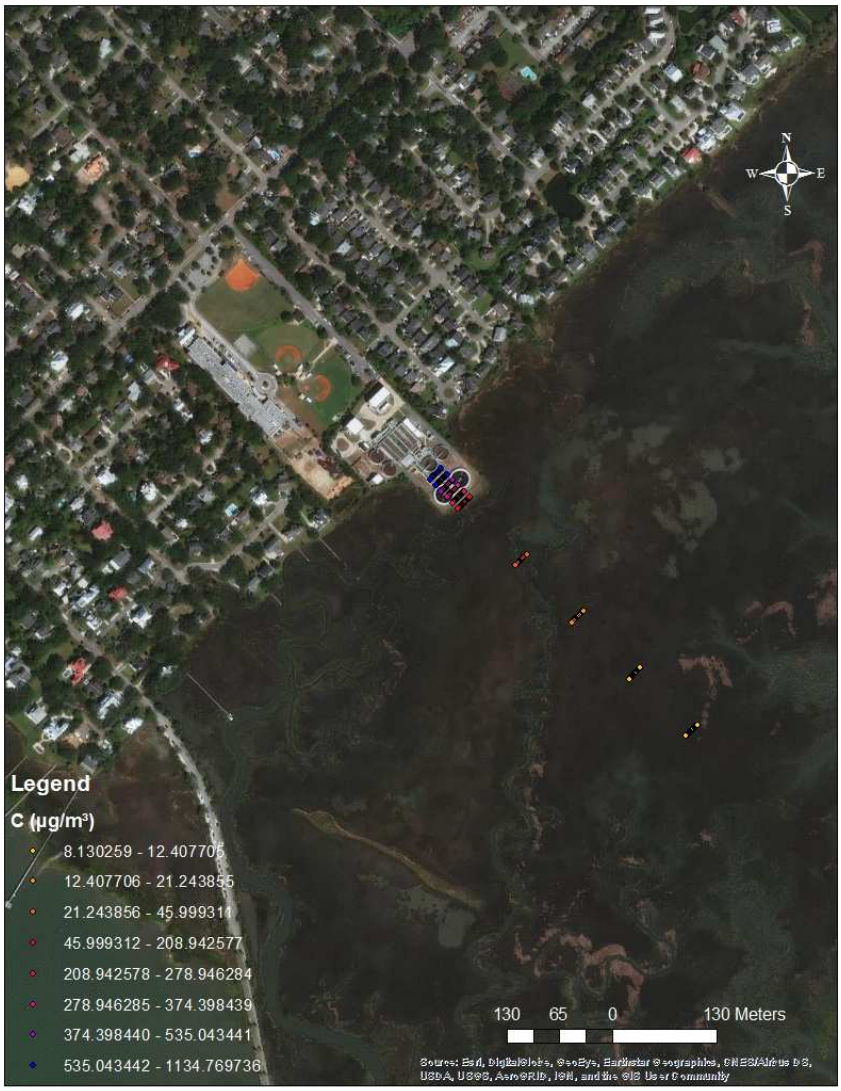

Figure 2.34: Spring third day PM dispersion model for Site 1

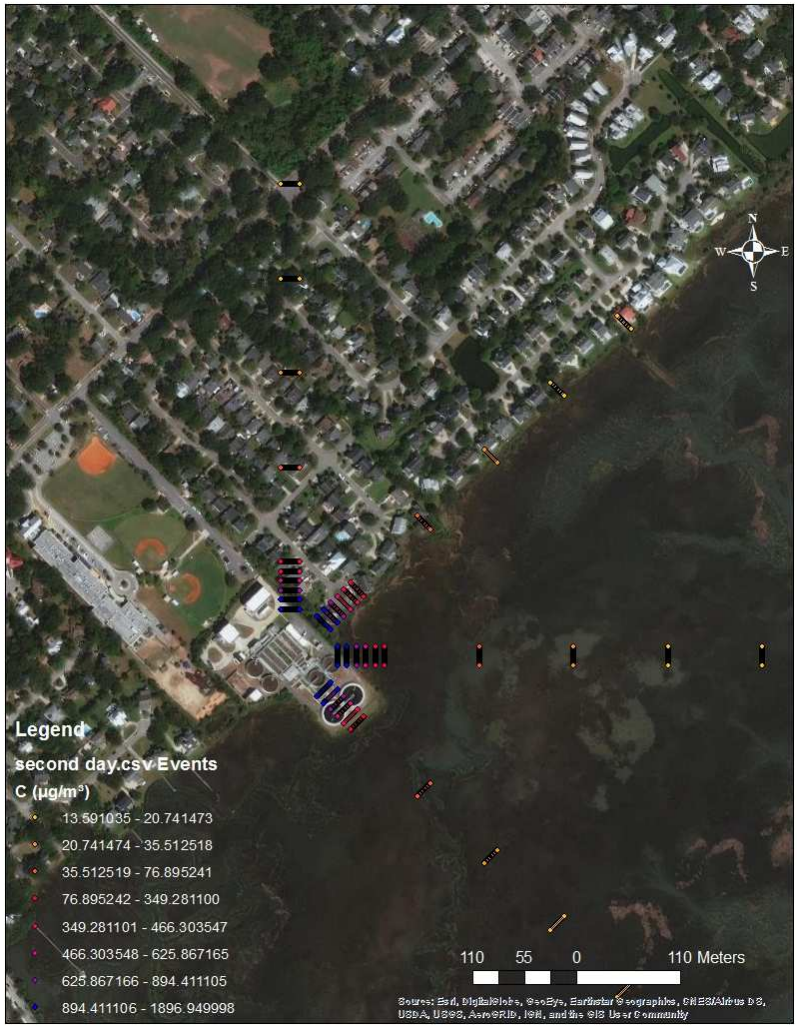

Figure 2.35: Summer second day PM dispersion model for Site 1

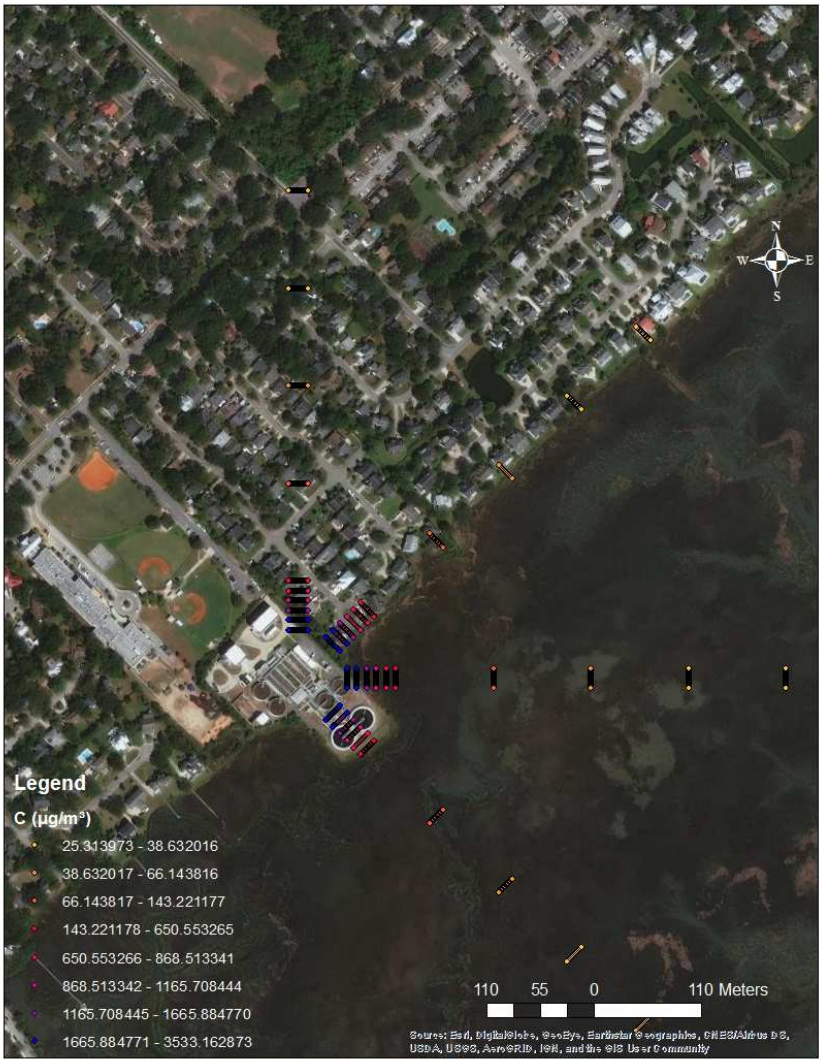

Figure 2.36: Summer third day PM dispersion model for Site 1

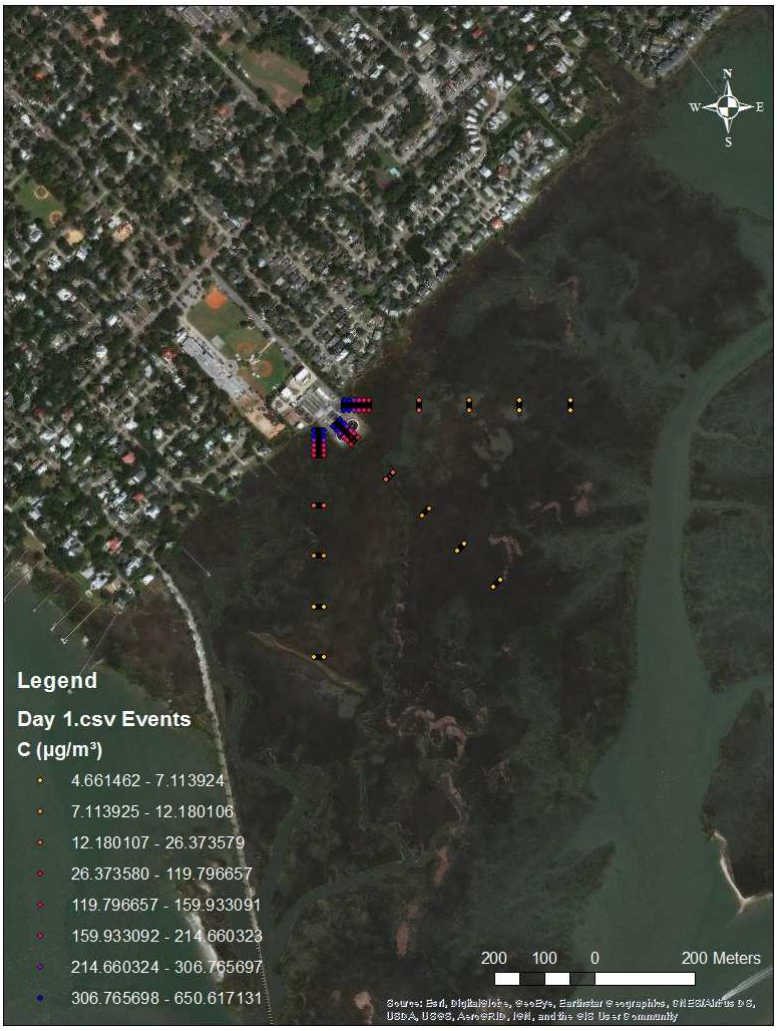

Figure 2.37: Fall first day PM dispersion model for Site 1

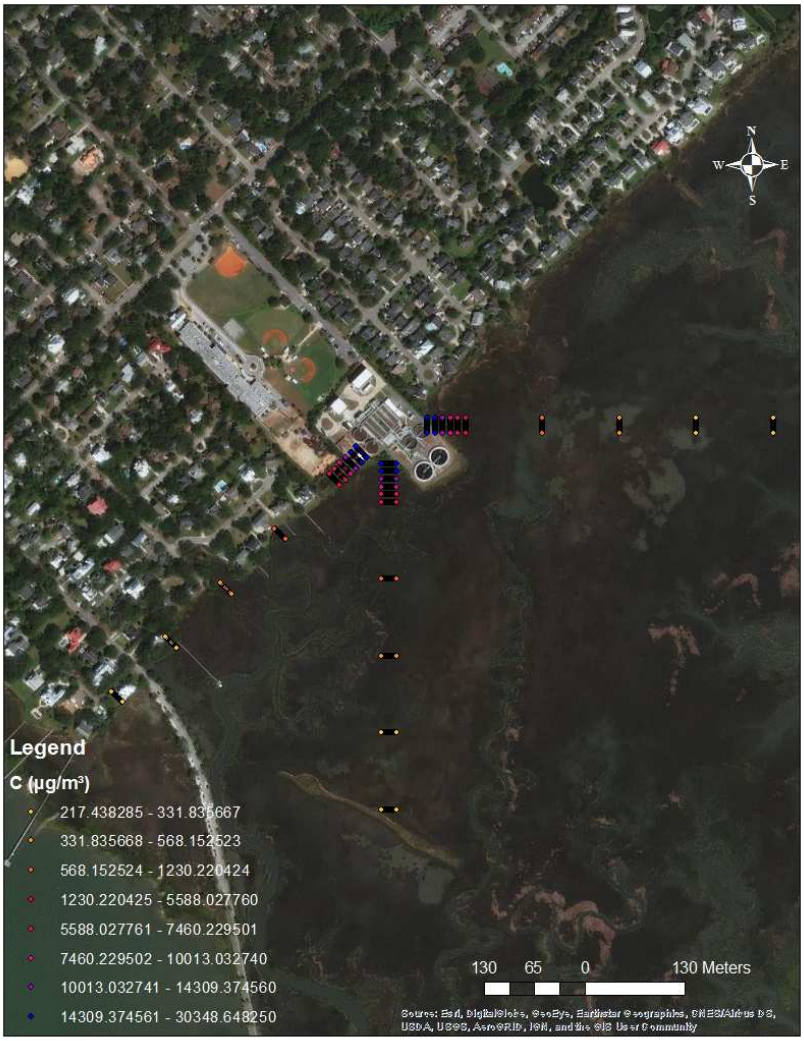

Figure 2.38: Fall second day PM dispersion model for Site 1

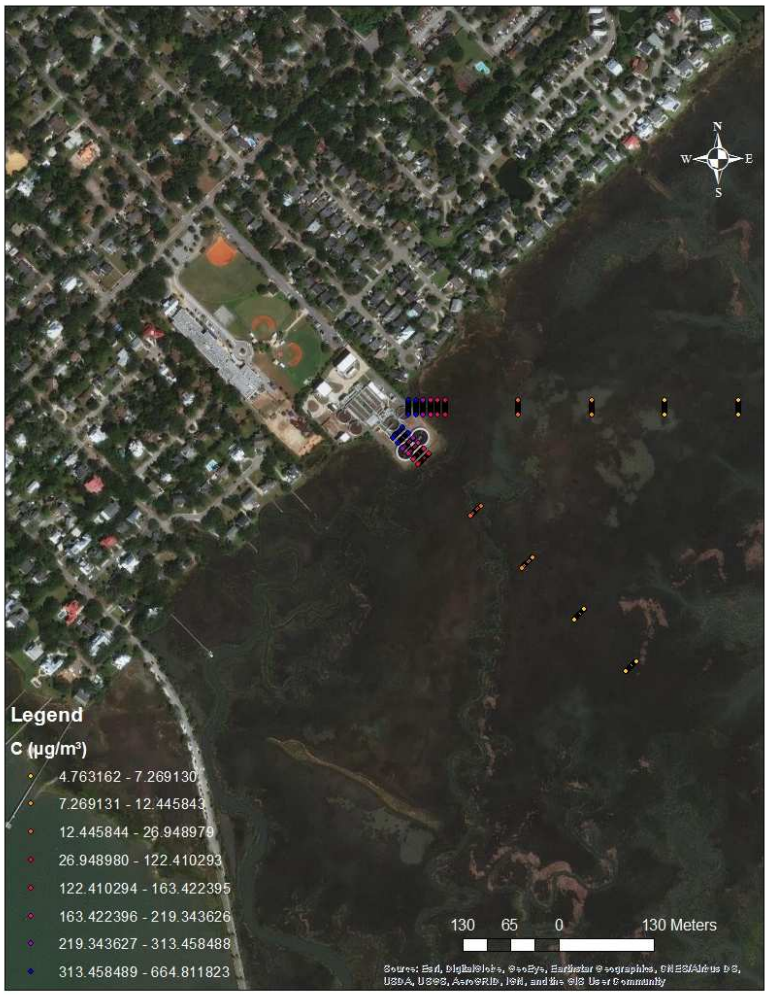

Figure 2.39: Fall third day PM dispersion model for Site 1

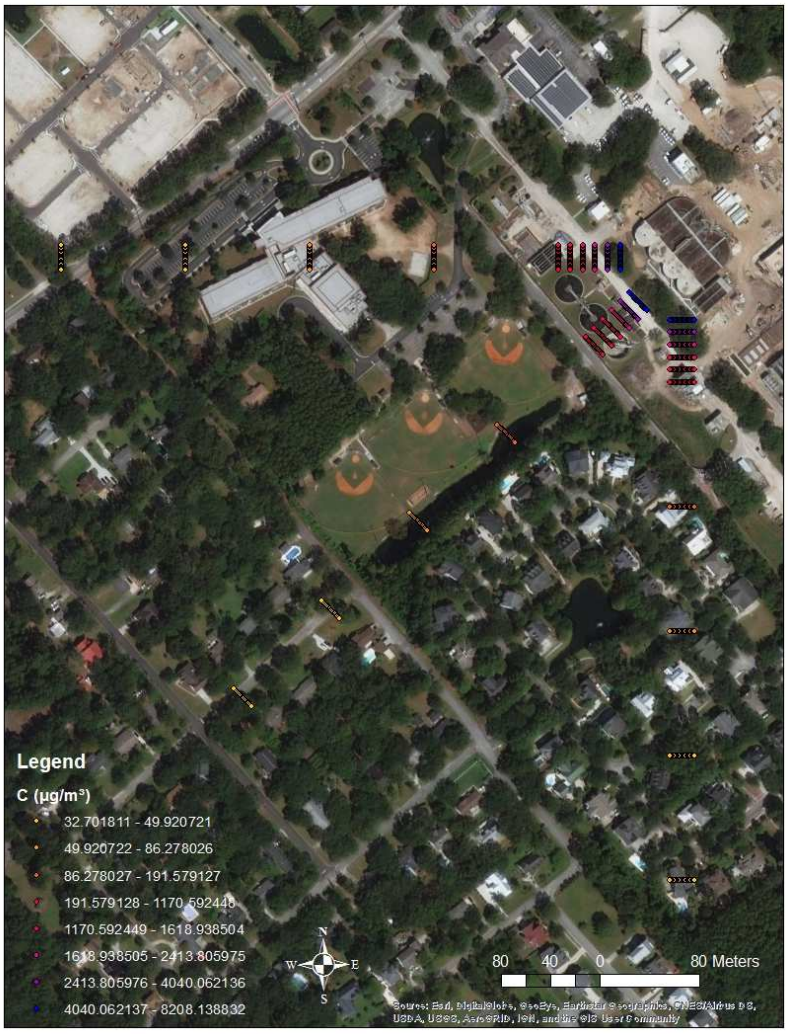

Figure 2.40: Winter first day PM dispersion model for Site 2

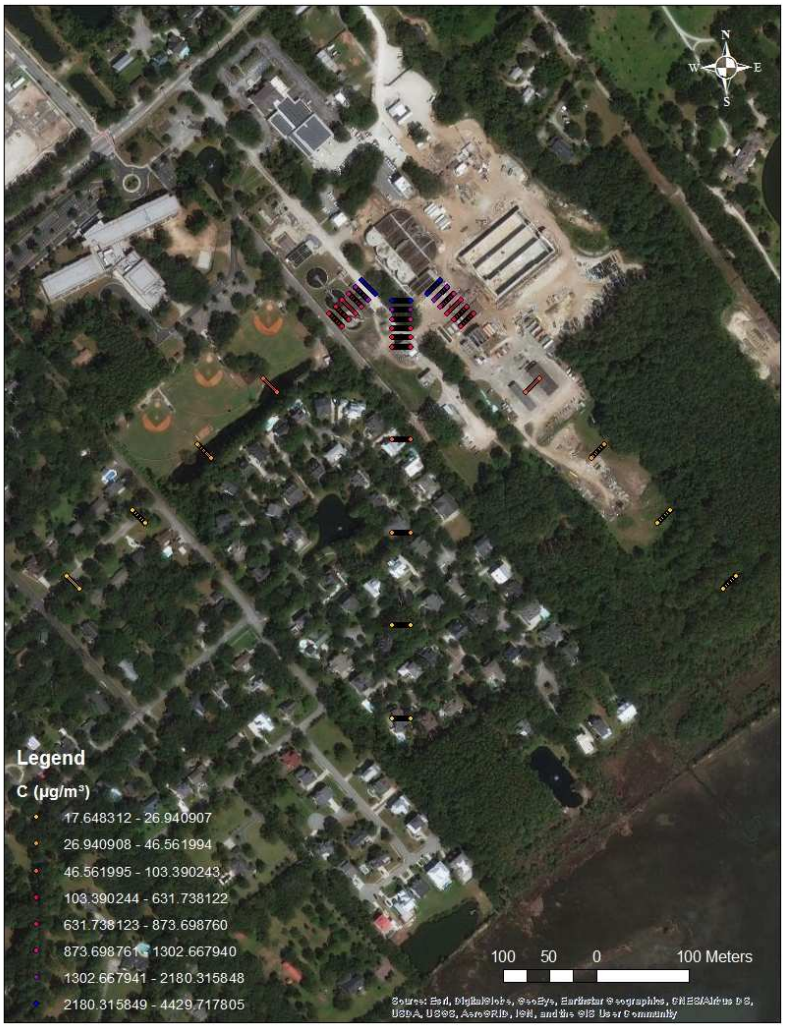

Figure 2.41: Winter second day PM dispersion model for Site 2

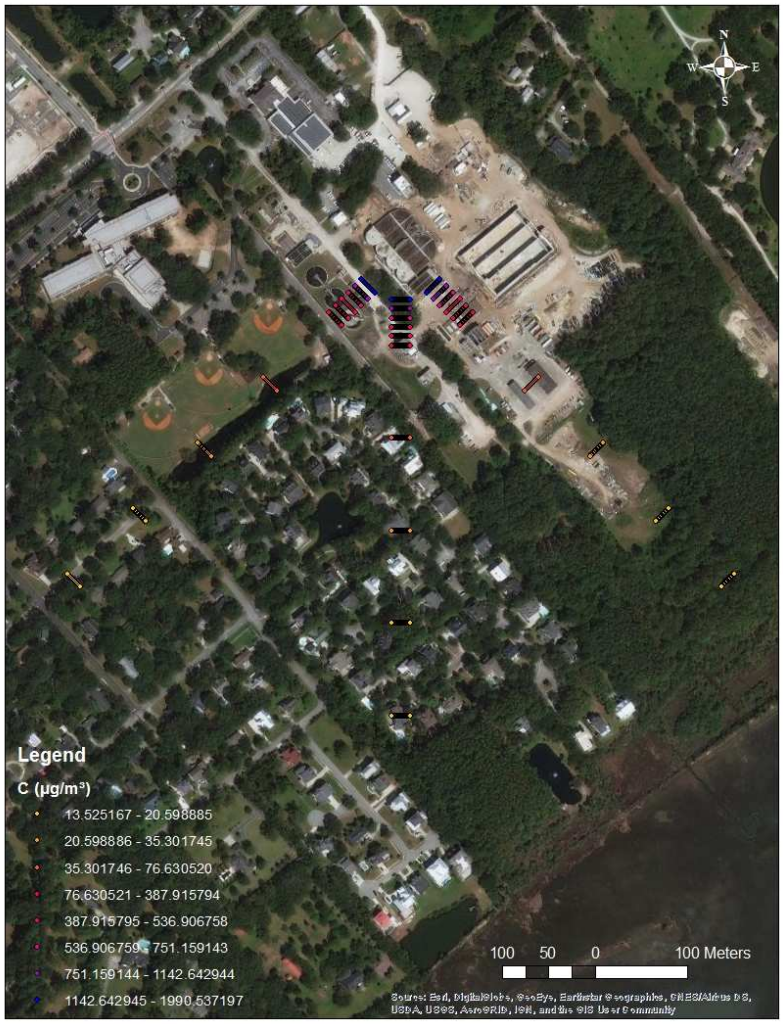

Figure 2.42: Winter third day PM dispersion model for Site 2

Figure 2.43: Spring second day PM dispersion model for Site 2

Figure 2.44: Spring third day PM dispersion model for Site 2

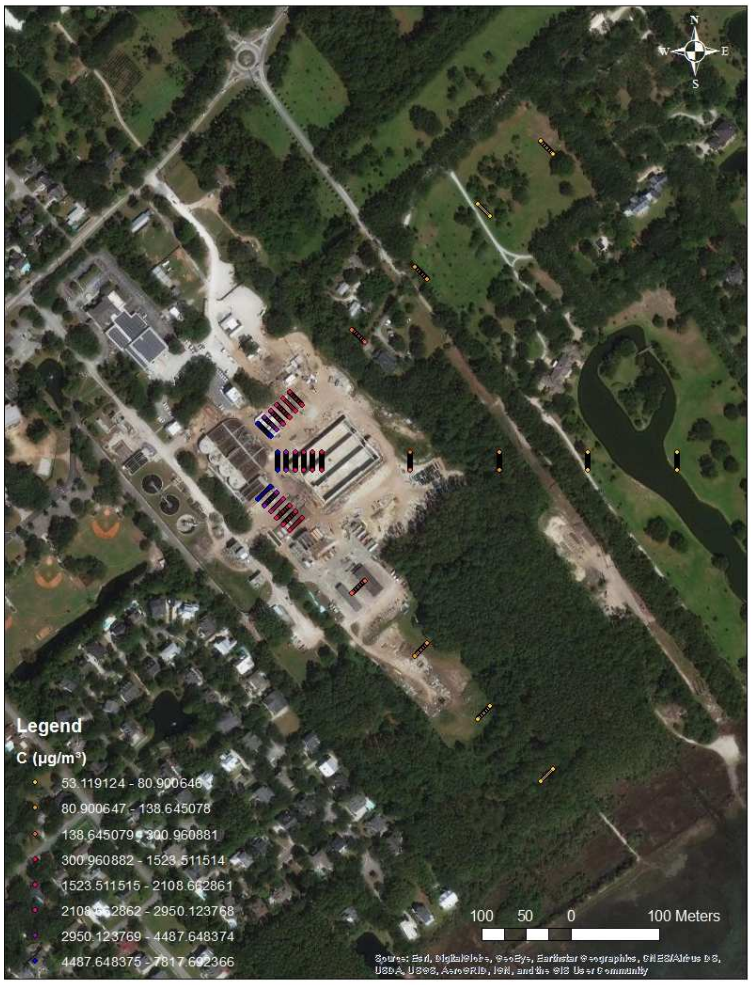

Figure 2.45: Summer first day PM dispersion model for Site 2

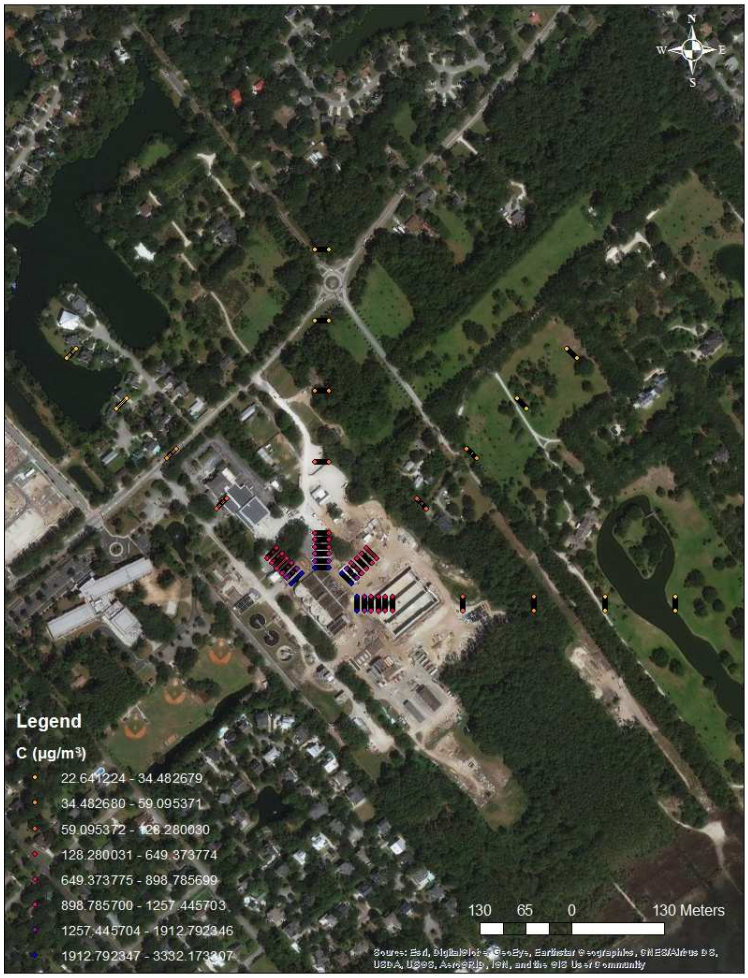

Figure 2.46: Summer second day PM dispersion model for Site 2

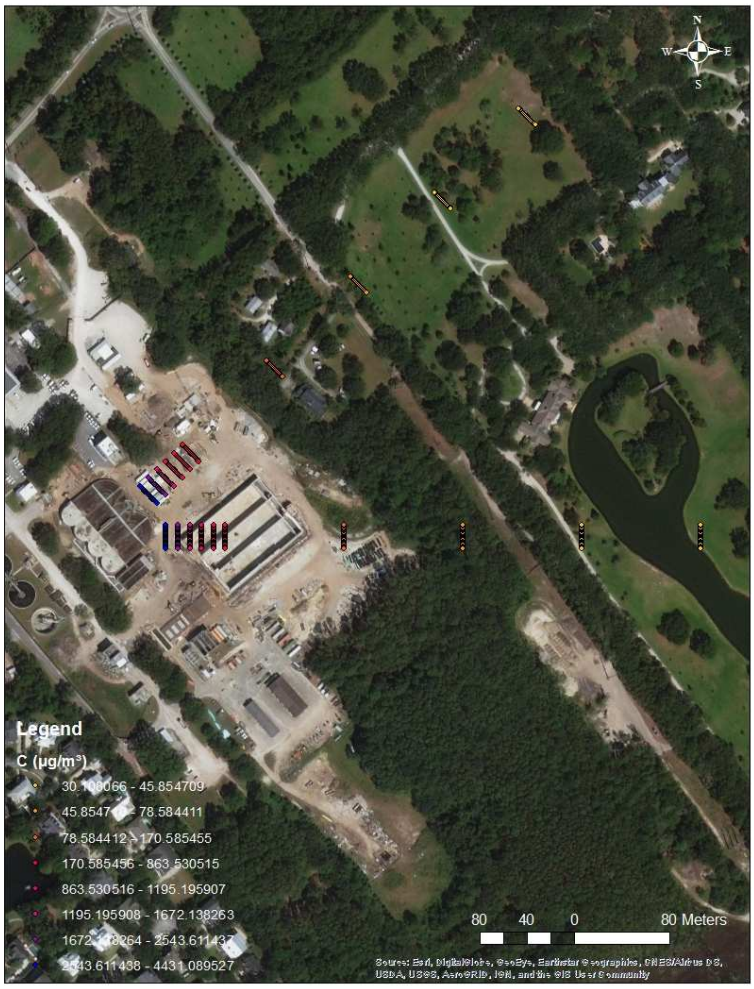

Figure 2.47: Summer third day PM dispersion model for Site 2

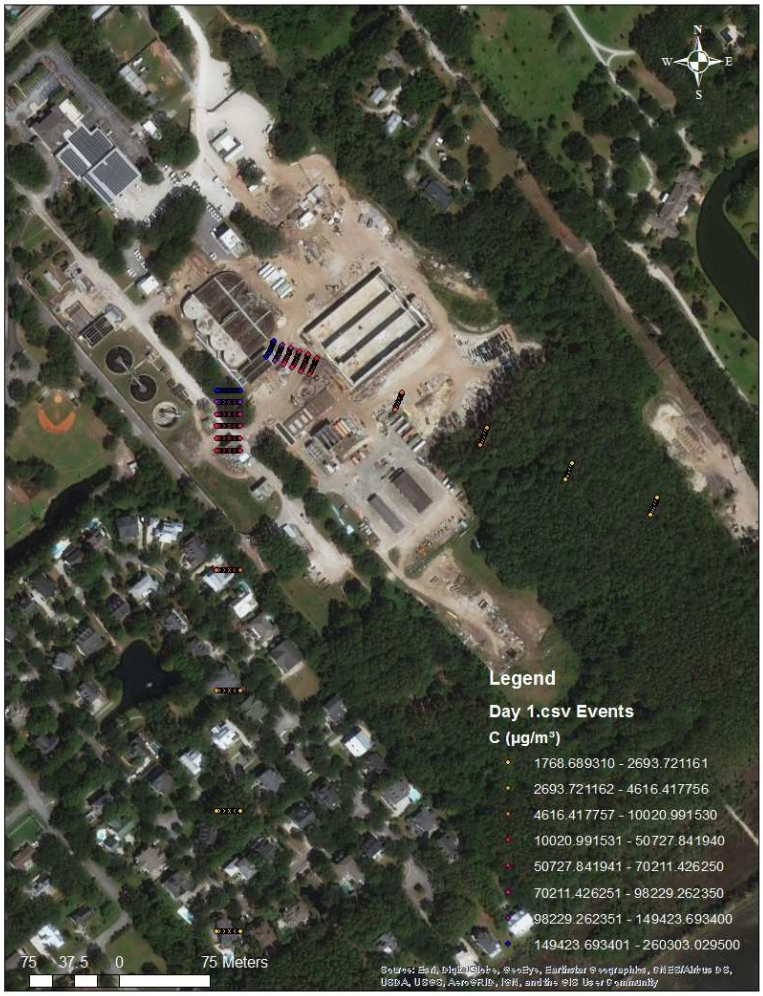

Figure 2.48: Fall first day PM dispersion model for Site 2

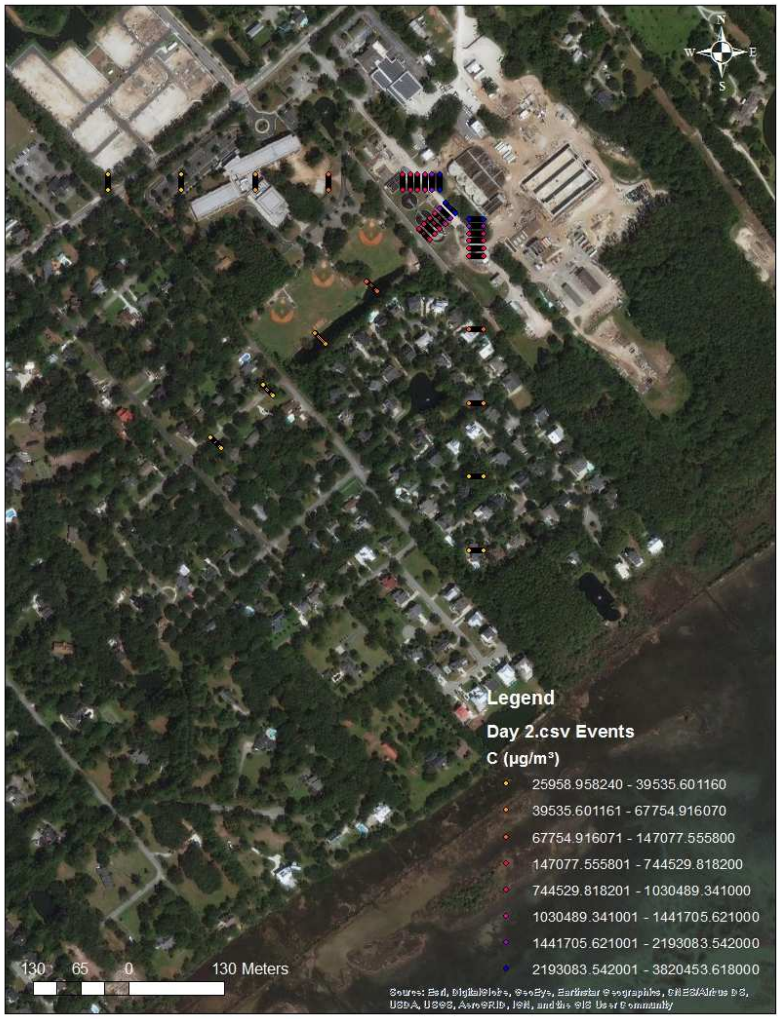

Figure 2.49: Fall second day PM dispersion model for Site 2

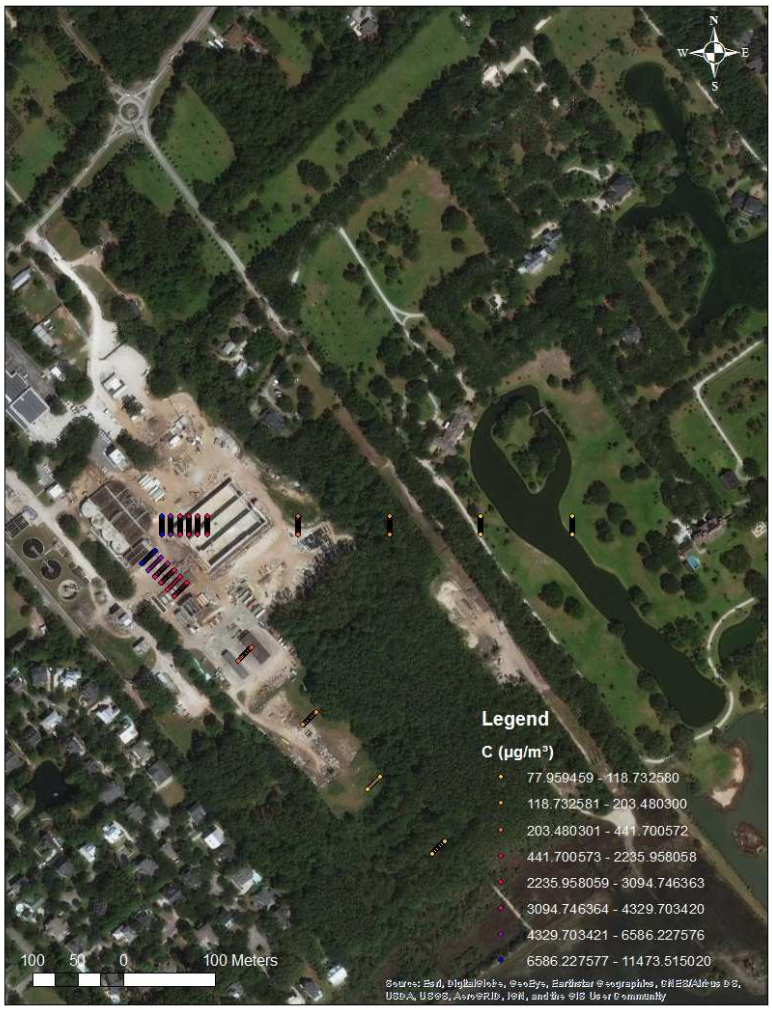

Figure 2.50: Fall third day PM dispersion model for Site 2

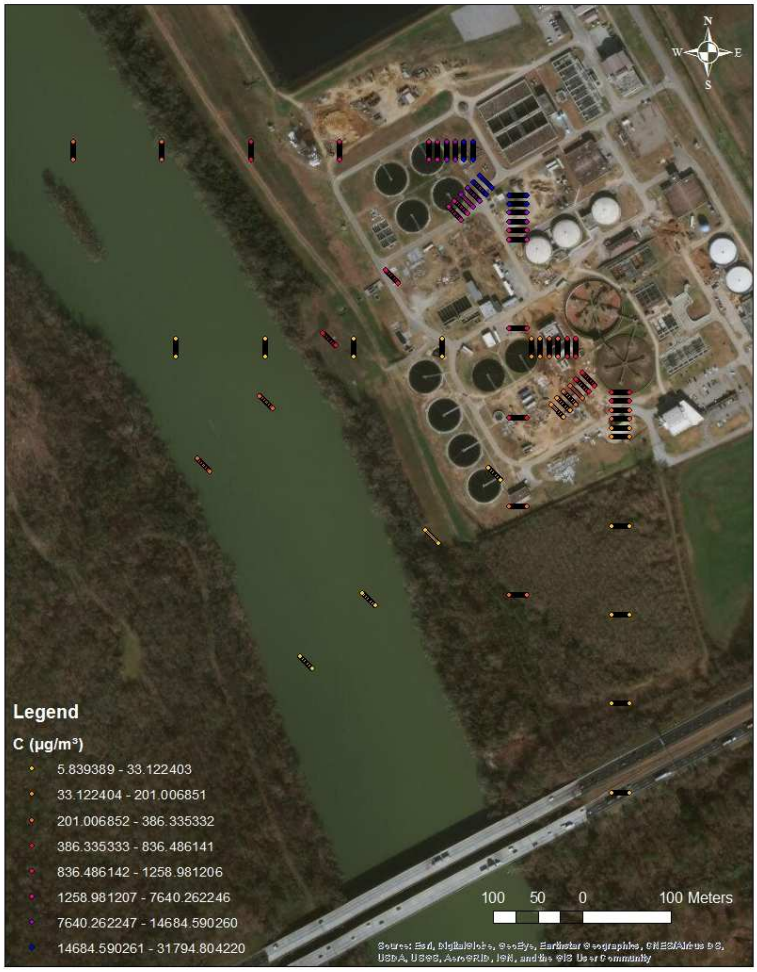

Figure 2.51: Winter first day PM dispersion model for Site 3

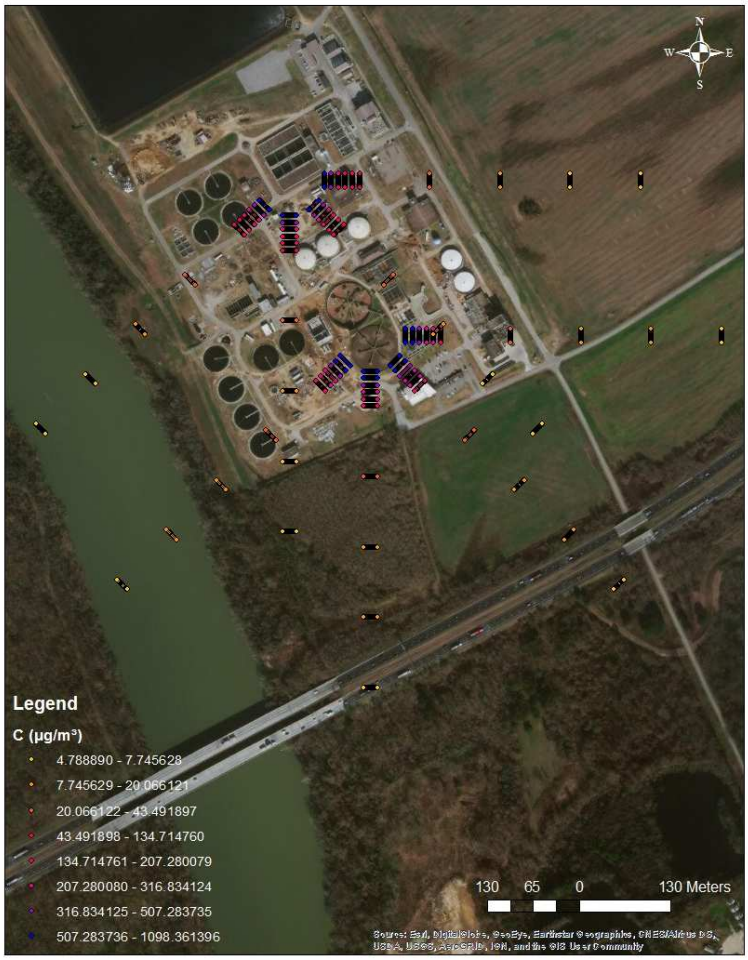

Figure 2.52: Winter second day PM dispersion model for Site 3

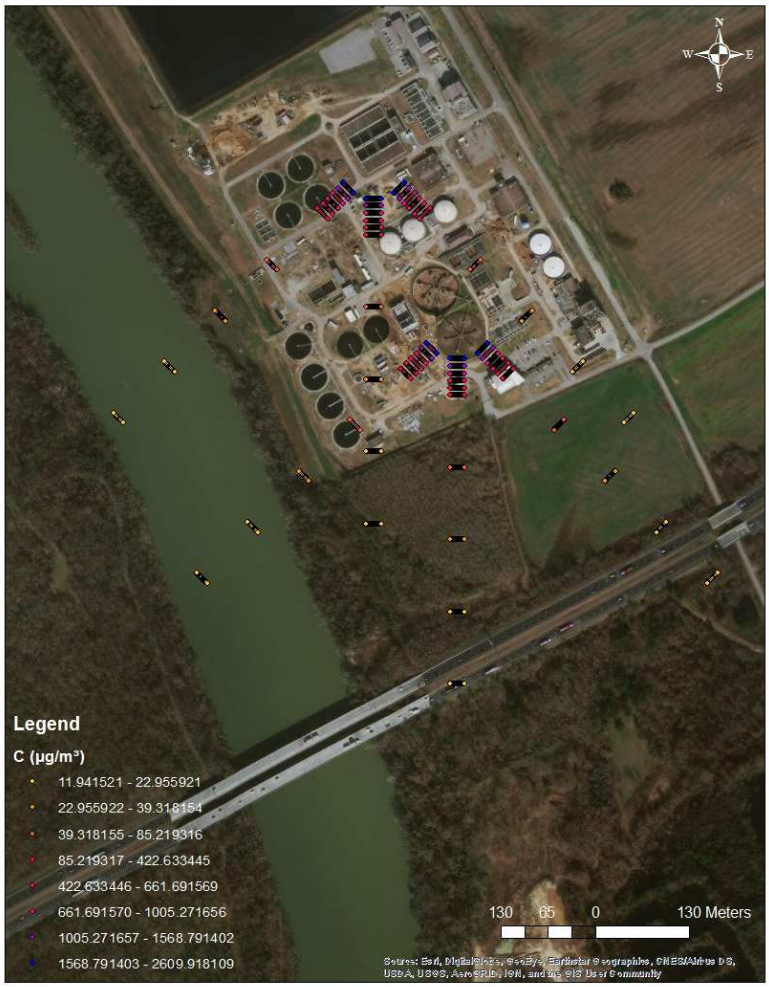

Figure 2.53: Winter third day PM dispersion model for Site 3

Figure 2.54: Spring first day PM dispersion model for Site 3

Figure 2.55: Spring second day PM dispersion model for Site 3

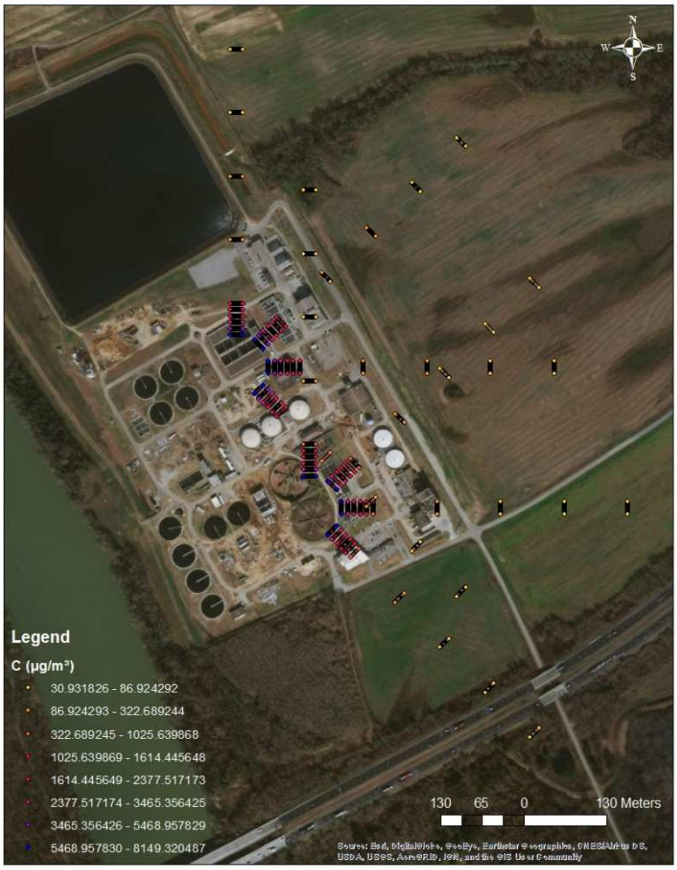

Figure 2.56: Spring third day PM dispersion model for Site 3

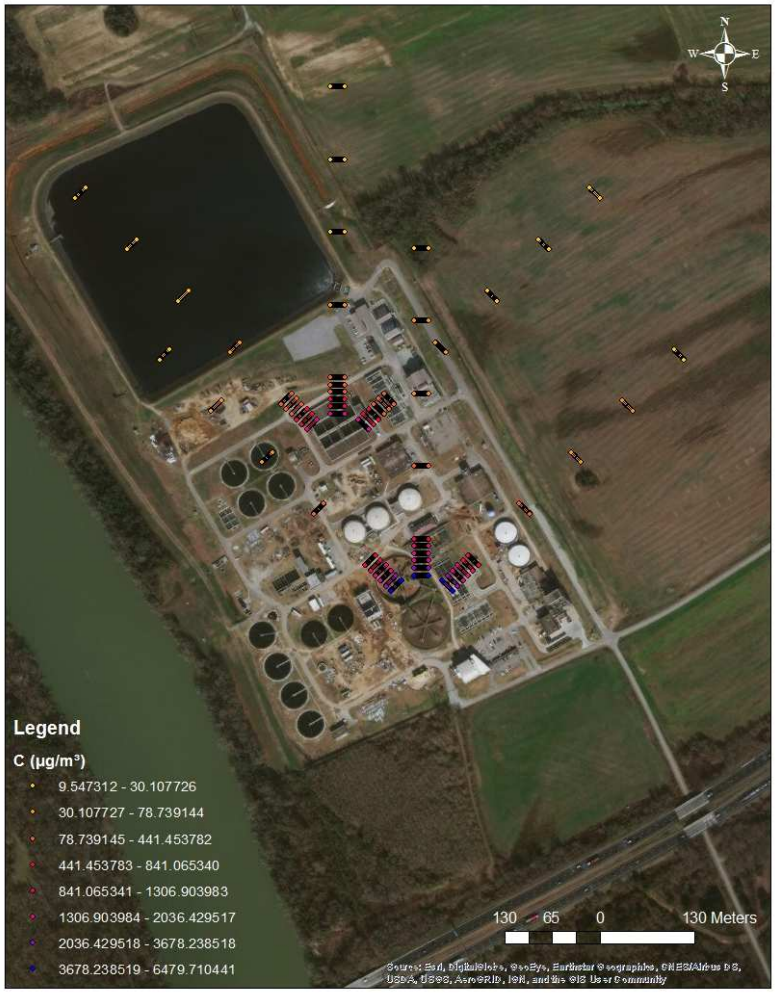

Figure 2.57: Summer first day PM dispersion model for Site 3

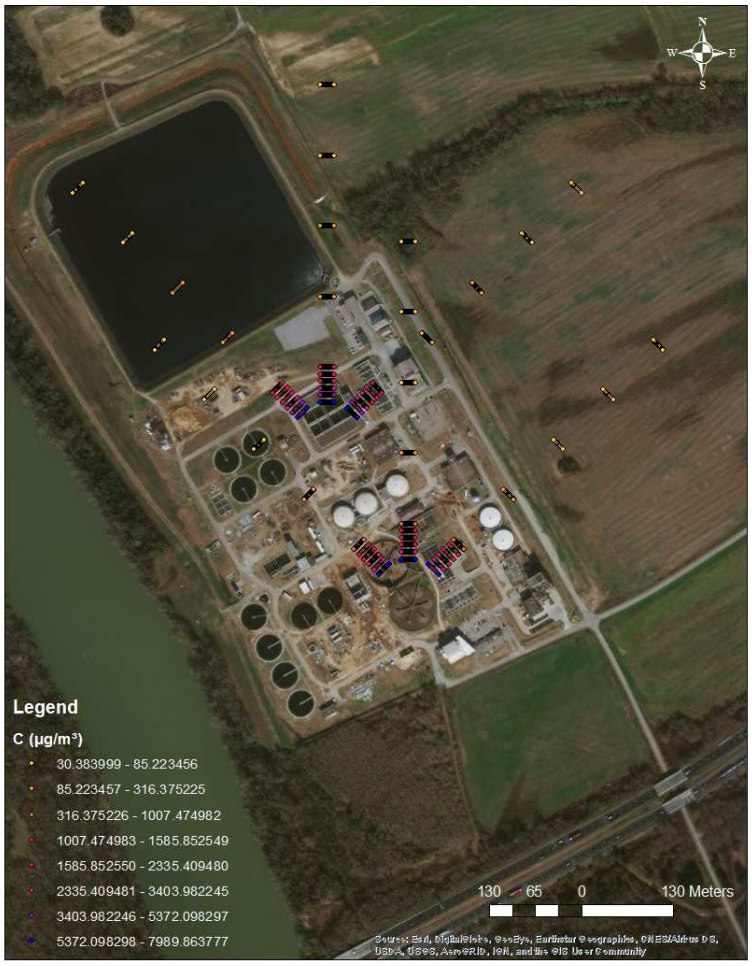

Figure 2.58: Summer second day PM dispersion model for Site 3

Figure 2.59: Summer third day PM dispersion model for Site 3

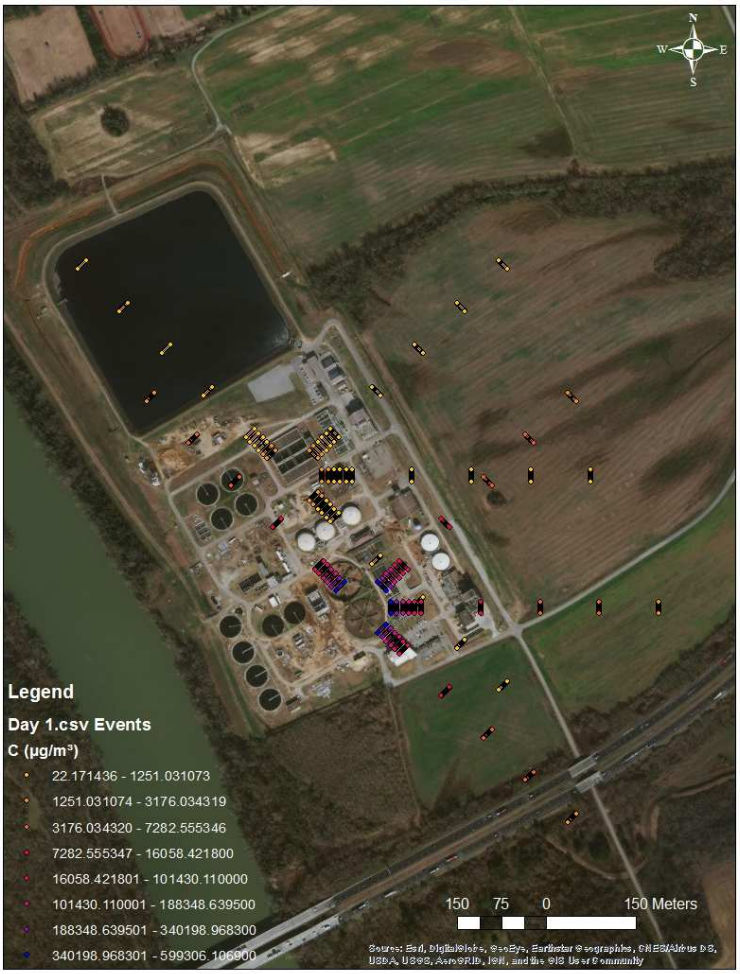

Figure 2.60: Fall first day PM dispersion model for Site 3

Figure 2.61: Fall second day PM dispersion model for Site 3

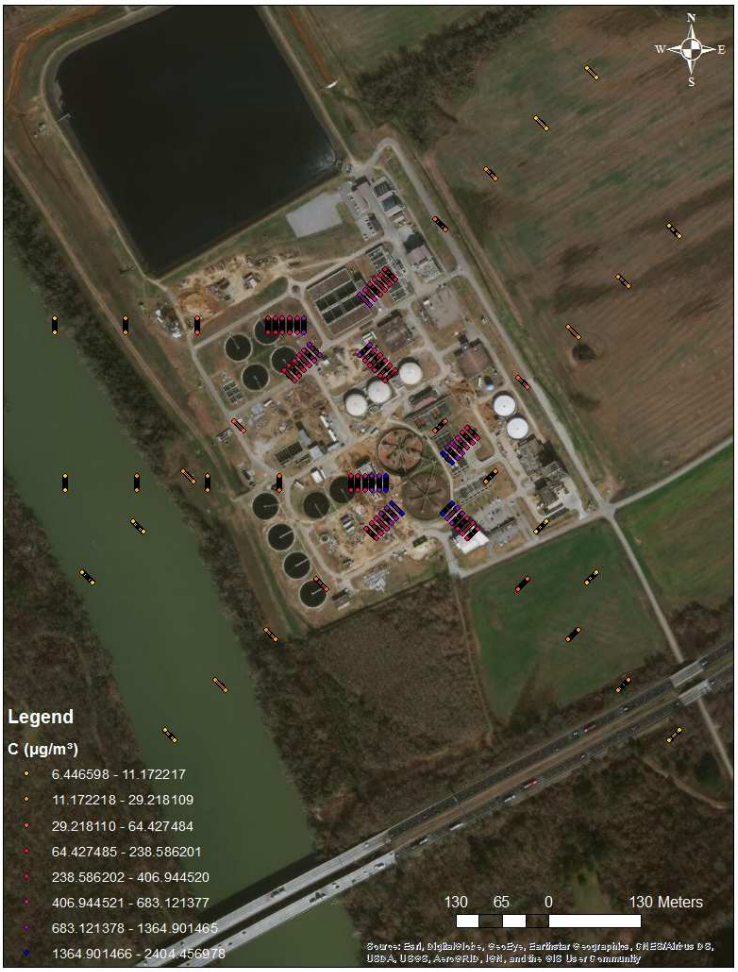

Figure 2.62: Fall third day PM dispersion model for Site 3

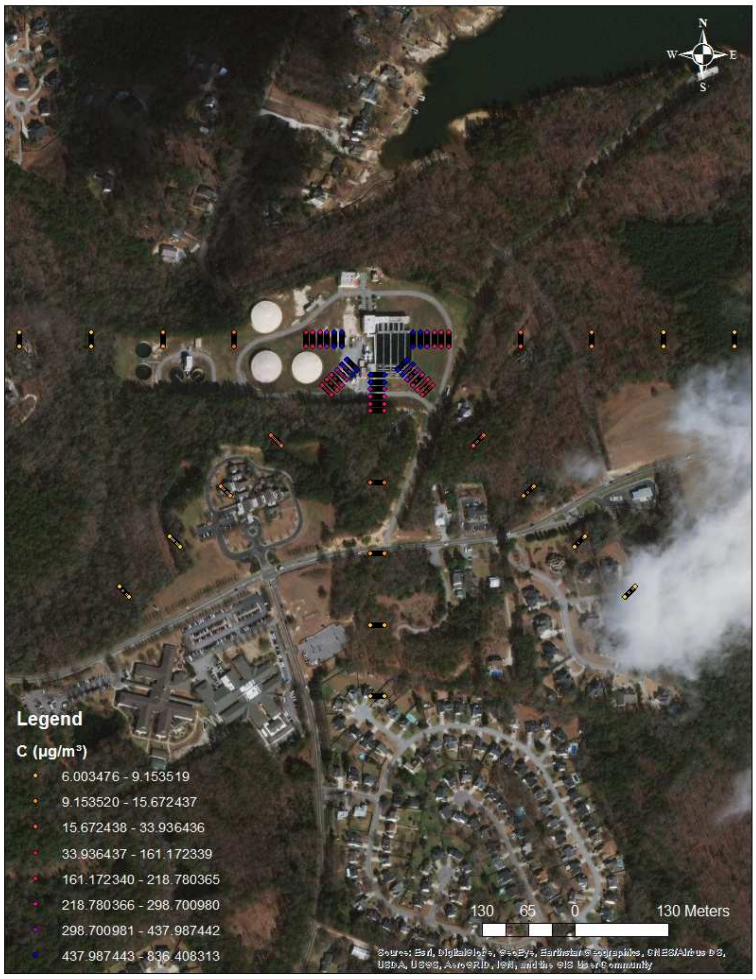

Figure 2.63: Spring first day PM dispersion model for Site 4

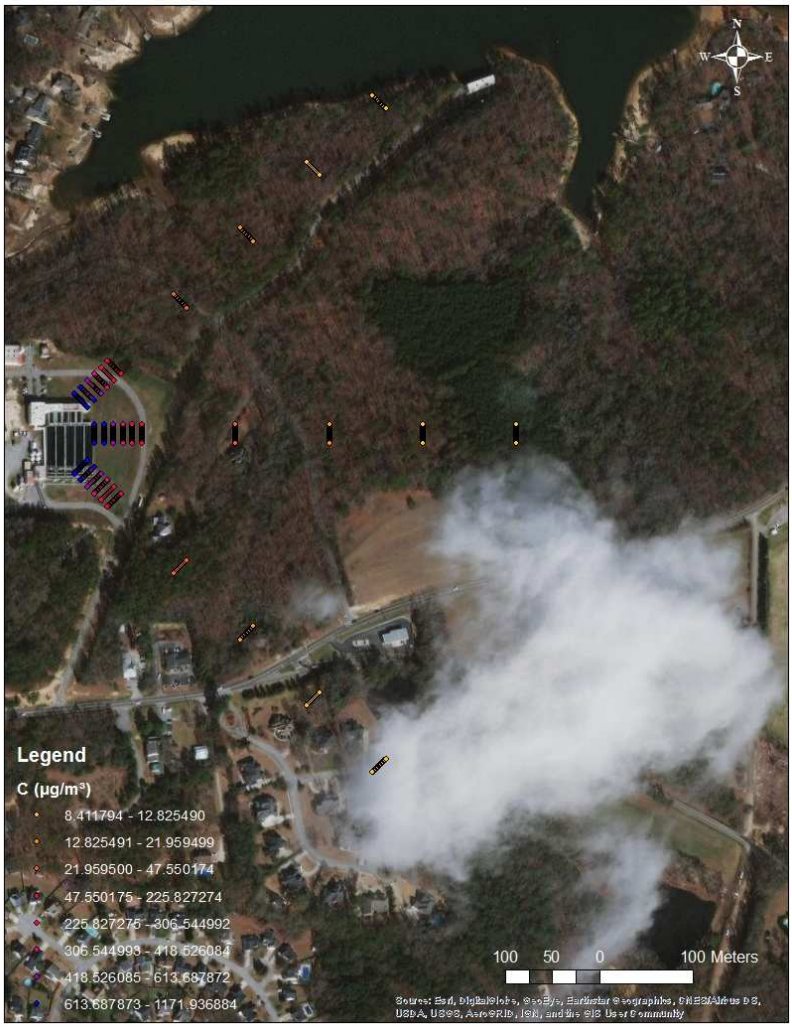

Figure 2.64: Spring second day PM dispersion model for Site 4

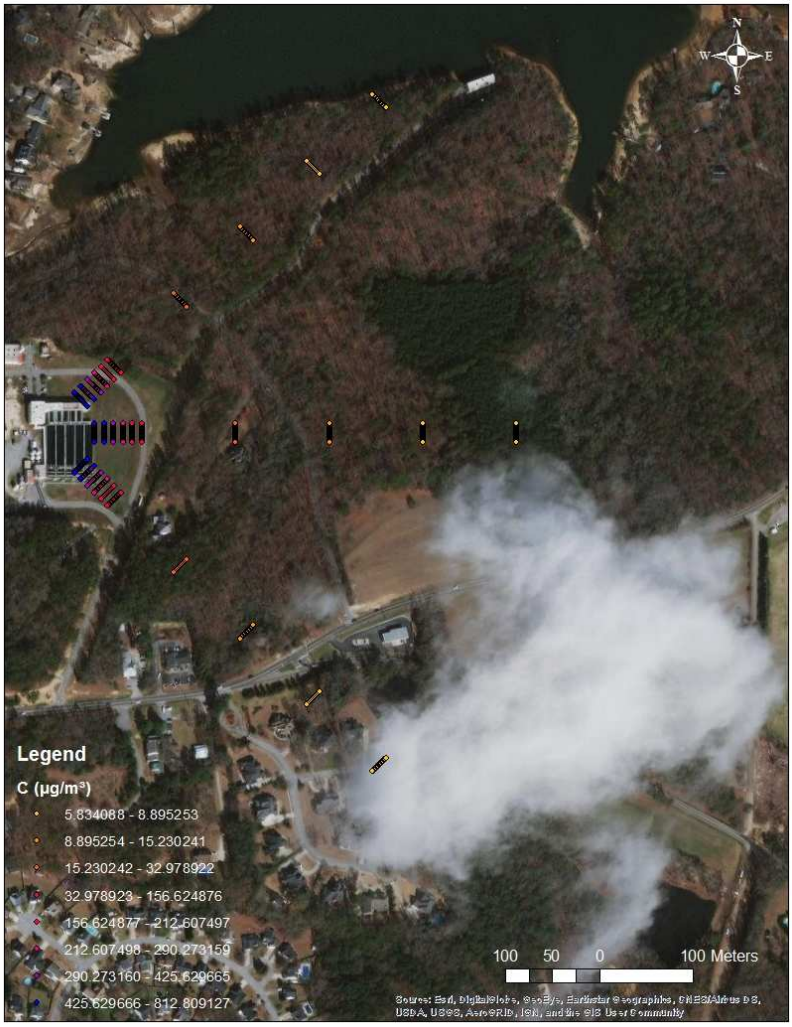

Figure 2.65: Spring third day PM dispersion model for Site 4

Figure 2.66: Fall first day PM dispersion model for Site 4

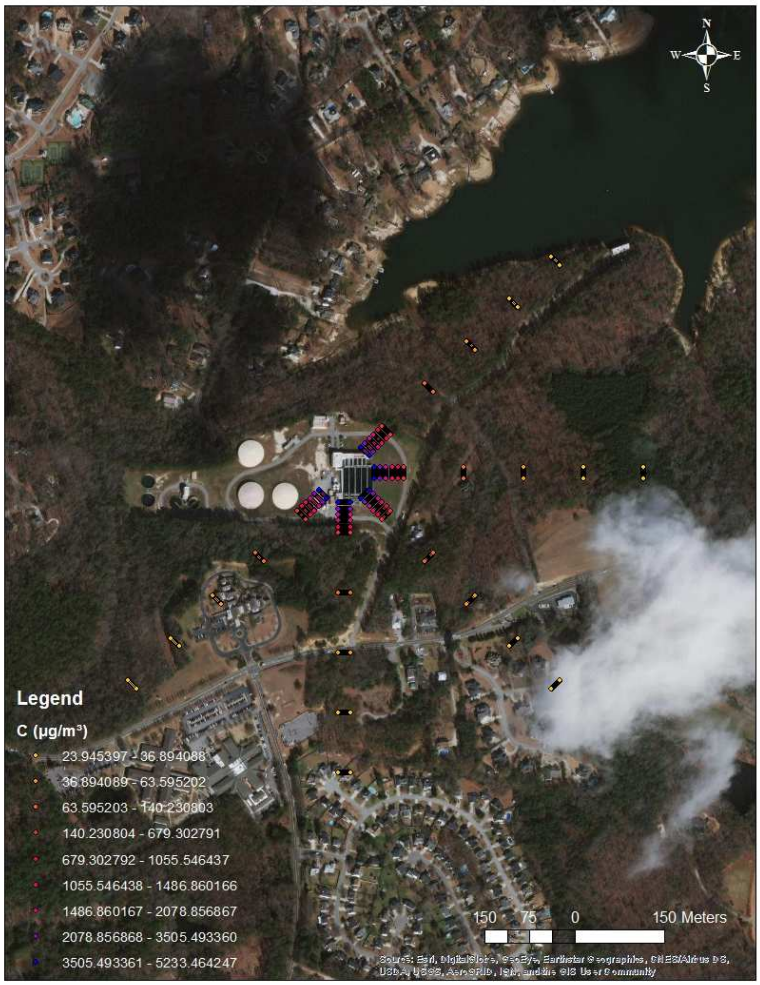

Figure 2.67: Fall second day PM dispersion model for Site 4

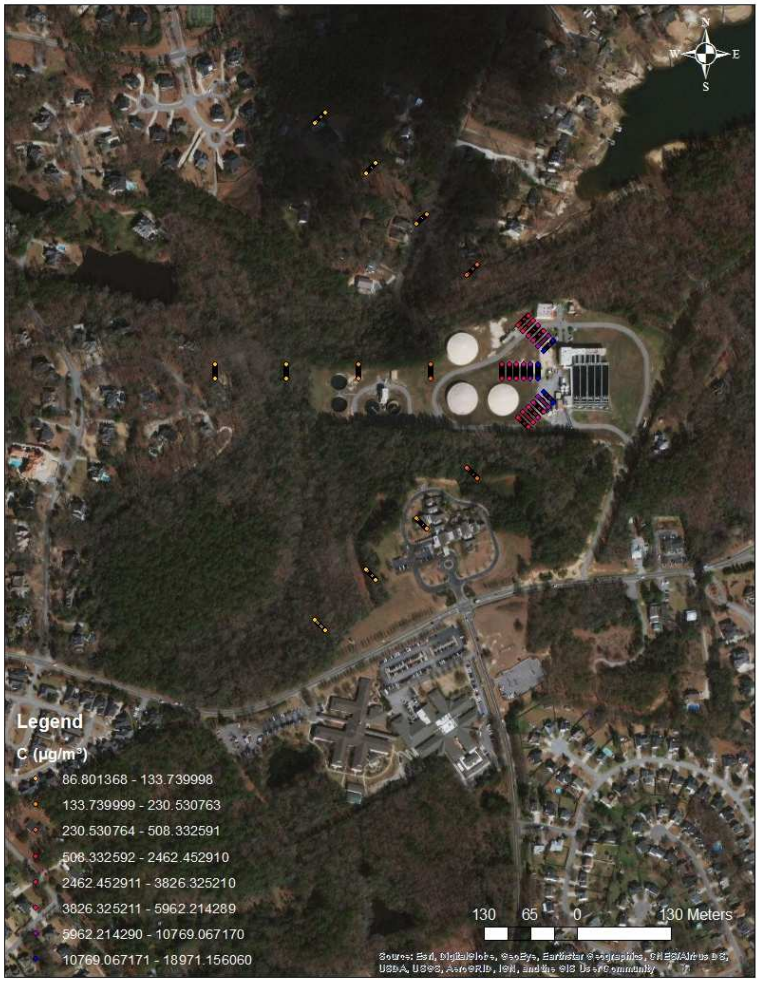

Figure 2.68: Fall third day PM dispersion model for Site 4

2.4. Discussion

The results of this study indicate that the measurements between all sites each season showed that Site 3 has the higher average total particulate count followed by Site 2, Site 1 and Site 4 in winter, spring and summer. This outcome is contrary to that of Han et al. (2019), who found that the maximum concentration was in summer followed by relatively high amounts in autumn and spring, where the minimum concentration of airborne bacteria was found in winter. Moreover, the study stated that the concentration

of airborne Escherichia coli was higher in the summer than in other seasons (Tang et al., 2020).

In accordance with the present results, previous studies have demonstrated that in terms of the abundance of particulate in the air based on their diameter, we found that the major diameters present in the air in winter is in Site 1 which seems to be consistent with (Meng et al., 2019) where they found that winter is the worst season with the higher PM10 concentrations in the air. On the other hand, Site 3 has a greater abundance of particulate variability in the air in summer, which supports evidence from previous observations of Han et al. (2019) as they conclude that the variability of the particulate size distributions for bioaerosols was higher in summer than the other seasons.

In addition, model results showed that Site 1 and Site 2 might pose potential human and environmental issues to the close communities due to the highest particulate distribution around the sites, and it is greater in winter, summer, and fall based on the wind direction measurements. Thus, there are several possible explanations for these results, seasonal variation in the total PM emissions, variability in the PM emissions by size and seasonal dispersion emissions, which reflected with those of (Nathan, 2018) and (Li et al., 2019) that the emission sources and metrological parameters (such as temperature, relative humidity [RH], and wind speed) could cause seasonal variations in the PM concentration and it is dispersal in the surrounding air.

Those findings have important implications for developing deep and detailed research in the future to analyze what those particulate matter contains because these results showed the total general particulate matter, not including if they hold bacteria, viruses, chemicals, and/or other contaminants. Understanding this major difference will help

comprehend each type of contaminant dispersion and behavior in the air, which will improve the protection measures for human and environmental health. Further studies, which take these variables into account, will need to be undertaken steady starting time of sampling for each process in each season to reduce the variation in the variables that affect the number of particulate matter and their concentration particularly in such study where the environmental and metrological factors are complicated and interrelated, and it is difficult to ignore their effect on the concentration and dispersion of the particulate.

CHAPTER 3

PROCESS AND SEASONAL VARIATION OF PARTICULATE MATTER EMISSION FROM WASTEWATER TREATMENT PLANTS

3.1. Introduction

Airborne particles in WWTPs may arise from wastewater, sludge, outside ambient air, and other sources. Identifying the origin of airborne pollutants is essential to quantify their concentrations for human health and environmental risks assessment. (Yang, et al., 2019). The release of particulate matters (PMs) and bioaerosols in the air from wastewater treatment processes is a result of the turbulence of wastewater flow. Additionally, wastewater treatment technology, aeration method, the quantity of aeration, and the type and concentration of microorganisms in the wastewater have an essential role in the concentration of PMs and bioaerosols in the surrounding air and environment (Michalkiewicz, et al., 2018).

Moreover, the structure, size, and concentration of microorganisms in the bioaerosols change based on the different stages of wastewater treatment. Mainly, the high concentration of bioaerosols in the air is noticed over mixed and aerated chambers of bioreactors where droplets are produced with a large variability of diameters (Michalkiewicz et al., 2018). Furthermore, airborne particles in the wastewater can also be transmitted to the air environment in and around WWTPs through aeration facilities, grit chambers, sediment tanks, and aeration tanks (Zhang, et al., 2018). According to

Michalkiewicz et al., (2018), the concentration of microorganisms in the bioaerosols produced by a mechanical mixing system was higher than in the aerosols that are generated by a fine-bubble aeration system due to forceful mixing of wastewater, overflowing and turbulence which causes the formation of a large number of harmful bioaerosols.

The dispersal of PMs differs among WWTP depending on the type of wastewater treated, treatment process selected, and meteorological parameters. According to (Wang, et al. 2018) study, the highest emission of microorganisms to the air occurs from aeration tanks where the oxygen is supplied by mechanical agitation. Also, they measured the airborne particles within the WWTP and discovered that the concentration of culturable bacteria was 110–846 CFU/m^3 with a higher concentration in biochemical reaction tank (BRT) and it was 846 ± 53 CFU/m^3, followed by fine screens (FS) with a concentration of 228 ± 37 CFU/m^3 and lastly by sludge treatment operations (sludge dewatering house (SDH)) with particle concentration of 141 ± 15 CFU/m^3. They stated the reason that the higher concentration of PMs on BRT is that it's the aerobic wastewater treatment section where the aeration process takes place. Moreover, they measured the concentration of the airborne particles in another WWTP that uses different aeration process for wastewater treatment for comparison. The second WWTP employs an oxidation ditch process that uses a vertical shaft brush device, and the water oxygenation occurs through the brush's vertical movement. At this site, the results showed that the culturable bacteria concentration was 27–579 CFU/m^3 with 579 CFU/m^3 at BRT and 404 CFU/m^3 at FS. Furthermore, previous research found human pathogenic bacteria in the air of WWTP. For example, a study in Poland revealed that the concentration of mesophilic bacteria in

the air exceeded 3 × 103 CFU/m^3. In addition, antibiotic-resistant strains have been isolated from bioaerosols above and around aeration tanks of the WWTP, and the concentration was higher than the residential community around the treatment plant (Zhang et al., 2018). Likewise, according to Han et al. (2019), the emission of airborne bacteria was monitored in a WWTP that used the A2O treatment process, which is the basic process to remove nitrogen and phosphorus biologically. They found that between 4.59×102 CFU/m^3 and 4.36×103 CFU/m^3 of airborne bacteria were found in the air above the aeration tank. Additionally, they measured the concentration downwind of the WWTP, and they detected that the highest concentration of bacteria was between 7.41×102 CFU/m^3 and 2.82×103 CFU/m^3 with the average concentration of 1.37×103 CFU/m^3.

In addition, some research assessed the concentration of airborne particles based on their sources among the treatment process and the seasonal variation. They concluded that coarse screen (CS), aerated grit chamber (AGC), primary settling tank (PST), anaerobic tank (AnT), and aeration tank (AeT) were the primary emission sources for PMs with emission levels ranging from 257 to 4878 CFU/m^3 and that there are positive correlations between those sites and bacterial concentrations in winter, spring and summer (Yang et al., 2019). Moreover, studies showed that the maximum concentrations of airborne particles in autumn were 2581 ± 401 CFU/m^3 at selector tank, 1952 ± 390 CFU/m^3 at aeration tank, 671 ± 134 CFU/m^3 at screw pump room, 449 ± 77 CFU/m^3 at the fine screen and 410 ± 90 CFU/m^3 at the coarse screen. On the other hand, the lowest number of bacterial particles in winter was in the surveillance building with 37 ± 7 CFU/m^3, site water supply with 55 ± 9 CFU/m^3, chlorination basin with 68 ± 8 CFU/m^3

and office building with 74 ± 12 CFU/m^3, while the highest number of bacterial particles in winter was in the aeration tank with a concentration of 1363 ±299 CFU/m^3 and screw pump with 1129 ± 200 CFU/m^3. Furthermore, in spring, the surveillance building with 37 ± 8 CFU/m^3 and chlorination basin with 59 ± 7 CFU/m^3 showed the lowest concentration of airborne particles. However, the highest concentration of airborne particles was at the screw pump with 1738 ± 350 CFU/m^3 and at a coarse screen process with 1324 ± 331 CFU/m^3 (Dehghani et al., 2018).

3.2. Materials and Methods

3.2.1. Sampling sites

The field sites used for this study consisted of three wastewater treatment plants (WWTPs) and one drinking water treatment plant (DWTP). The DWTP was used as a control for the background concentration of environmental particulate matter (PM) as compared to WWTPs. Though all the WWTPs included in this study use activated sludge treatment processes for their biological treatment, they use different methods of aeration. WWTP site 1 (Figure 3.1A), located in Mount Pleasant, SC uses bubble aeration in the activated sludge process and treats approximately 3 million gallons per day (MGD). WWTP site 2 (Figure 3.1B), also located in Mount Pleasant, SC, treats approximately 5 MGD and employs mixed methods in the same aeration tank. The injection of the air occurs through bubble aeration from the bottom of the tank and impellers from the top (surface agitation) are used for additional aeration. WWTP site 3 (Figure 3.1C) is located in Columbia, SC and serves around 60,000 customers and covers 120 square miles. The plant has a capacity of 60 MGD and treats an average of 35 MGD of wastewater. This site splits raw sewage into 2 separate treatment trains. Treatment train 1 uses surface

agitation for the aeration of activated sludge tanks and the treatment train 2 uses bubble aeration in the activated sludge tanks. The drinking water treatment facility used as a control in this study (site 4, Figure 3.1D) is located in Columbia, SC and has a total treatment capacity of 23 MGD. This facility uses a combination of chemical treatment for initial coagulation followed by mixing and sedimentation, chlorine addition and then a final filtration process.

Figure 3.1: Sampling sites. Panel A, Wastewater Treatment Plant (Site 1); Panel B, Wastewater Treatment plant (Site 2); Panel C, Wastewater Treatment Plant (Site 3); Panel D, Drinking Water Treatment Plant]

3.2.2. Meteorological Data Measurement

Meteorological conditions and particulate matter concentrations were monitored at each site across winter, spring, summer, and fall seasons to examine seasonal variability in particulate emissions (Figures 3.2 – 3.5). During each seasonal sampling event, monitoring occurred across three consecutive days to further examine daily variation in particulate emissions. Meteorological conditions (i.e., wind speed, wind

direction, temperature, relative humidity, and barometric pressure) were measured using the Kestrel 4500 Pocket Weather Tracker and the Kestrel 5500 Weather Meter. The Kestrel 4500 Pocket Weather Tracker was placed at the highest location at the center of the testing area to measure the overall prevailing site meteorological parameters across the entire site and sampling period. The Kestrel 5500 Weather Meter was used to collect individual metrological data at each unique sampling location within each field site. Individual meteorological measurements were used to examine within site variation across the different sampling locations to better model particulate emissions and dispersion.

3.2.3. Measurement of Particulate Matter Emissions

To measure particulate emissions, particle concentrations were obtained using the TSI Model 3330 Optical Particle Sizer Spectrometer (OPS). The TSI instrument has 12 channels that separate particles into 12 particle diameters (0.3, 0.4, 0.55, 0.7, 1, 1.3, 1.6, 2.2, 3, 4, 5.5, 7 and 10 micrometers [μm]). The sampling duration was one hour at each sampling location within each site, and the sampling location was varied each day based on the prevailing wind direction measured using the Kestrel 4500 to ensure isolation of downwind and upwind locations. Based on wind direction, one TSI instrument was placed in the upwind location while another TSI unit was placed in the downwind location to provide simultaneous measurement of upwind and downwind particulate matter concentration (Figures 3.2 - 3.5).

Figure 3.2: Field site 1 sampling location by seasons. Panel A, winter; Panel B, summer; Panel C, spring; Panel D, fall. White circles show the locations of the TSI upwind locations; red rectangles show the locations of the TSI downwind locations; Yellow stars represent the location of Kestrel weather meter measurements).

Figure 3.3: Field site 2 sampling location by seasons. Panel A, winter; Panel B, summer; Panel C, spring; Panel D, fall. White circles show the locations of the TSI upwind locations; red rectangles show the locations of the TSI downwind locations; Yellow stars represent the location of Kestrel weather meter measurements).

Figure 3.4: Field site 3 sampling location by seasons. Panel A, winter; Panel B, summer; Panel C, spring; Panel D, fall. White circles show the locations of the TSI upwind locations; red rectangles show the locations of the TSI downwind locations; Yellow stars represent the location of Kestrel weather meter measurements).

Figure 3.5: Field site 4 sampling location by seasons. Panel A, spring; Panel B, fall; Panel White circles show the locations of the TSI upwind locations; red rectangles show the locations of the TSI downwind locations; Yellow stars represent the location of Kestrel weather meter measurements).

3.2.4. Statistical Analysis

RStudio software (Version 1.2.5019, 2009-2019 RStudio, Inc) was used for the statistical analysis of the data. Analysis of variance (ANOVA) and Tukey tests were utilized to find the significant difference between study sites, seasons, the process of treatment, and different particulate diameters. In addition, Tableau 2020.2.1 software was used to generate figures for the results. In this chapter, we will examine the statistical differences between processes within each treatment site and between all sites together using total particulate counts and particulate count for each diameter.

3.3. Results

3.3.1. Seasonal Variation in Total PM Counts

Measurements of total particulate matter counts across seasons was used to examine the temporal variation in PM emissions at each process and they are shown in (Figures 3.6 – 3.8) where Site 1 (bubble aeration) has a higher median total particulate count in

summer (12394215.5) followed by fall (8092593), spring (7427707.5) and winter (5172864). For Site 2 (mixed of bubble aeration & surface agitation), the higher median total particulate count was in fall (17169109), summer (12889068), winter (11632140), and spring (9193843). On the other hand, measurements for Site 3 , where the bubble aeration tank is separate from the surface agitation tank, showed that the median total particulate number is higher in surface agitation tanks than bubble aeration in summer, spring and fall, whereas the median total particulate are higher in bubble aeration than surface agitation in winter. For surface agitation, the median amount of total particulate is higher in summer (11905448), followed by fall (10481688), spring (9988616) and winter (7542007) compared to the bubble aeration method where the higher median of total particulate is in winter (8069586), spring (6950029), fall (4853139) and summer (2719348). However, fall (4495514) was higher in the median total particulate count for drinking water treatment than spring (1792427).

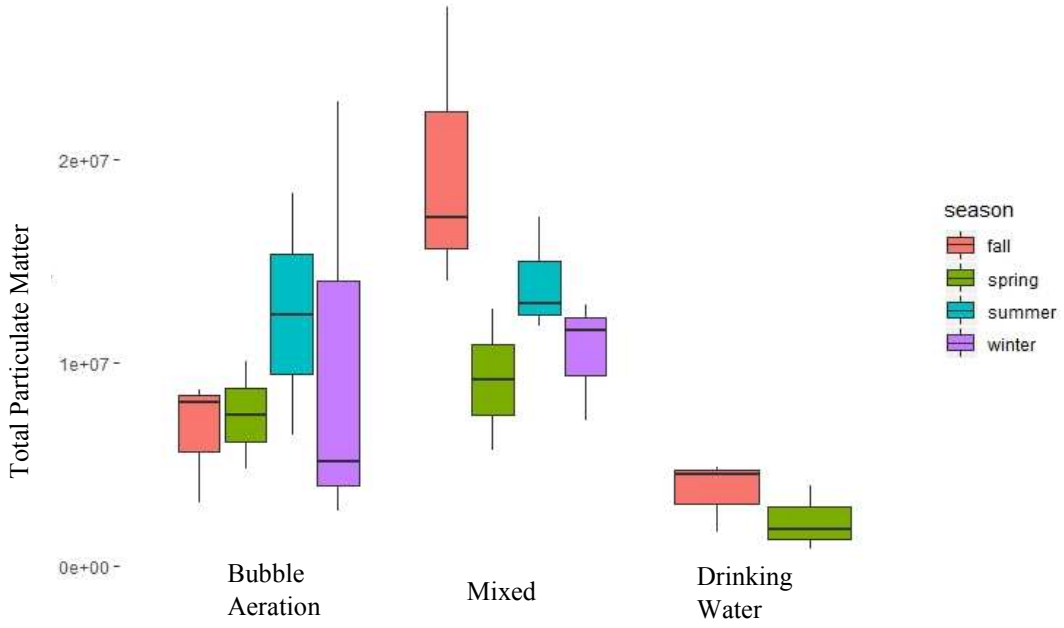

Figure 3.6: Total Particulate Matter (PMs) Count for treatment process (Site 1, Site 2 & Site 4) by seasons

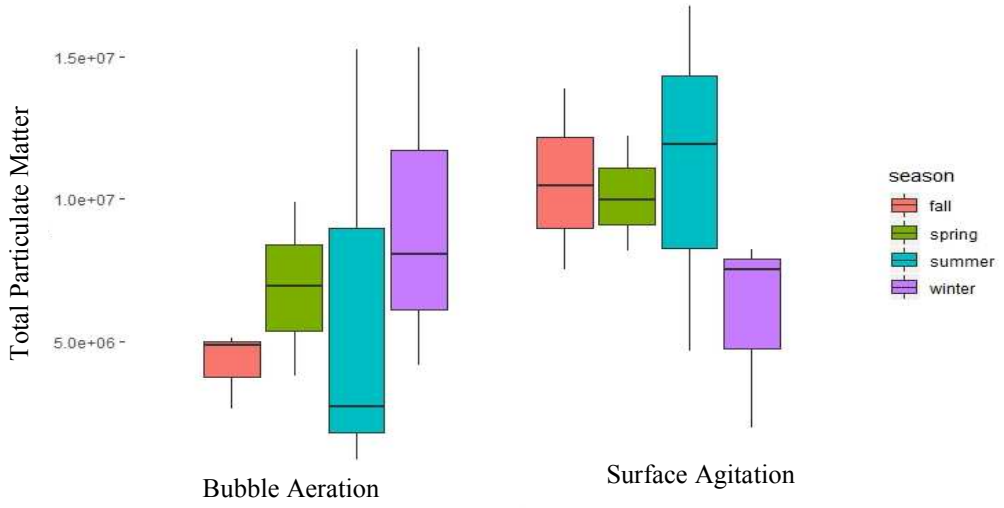

Figure 3.7: Total Particulate Matter (PMs) Count for treatment processes (Site 3) by seasons

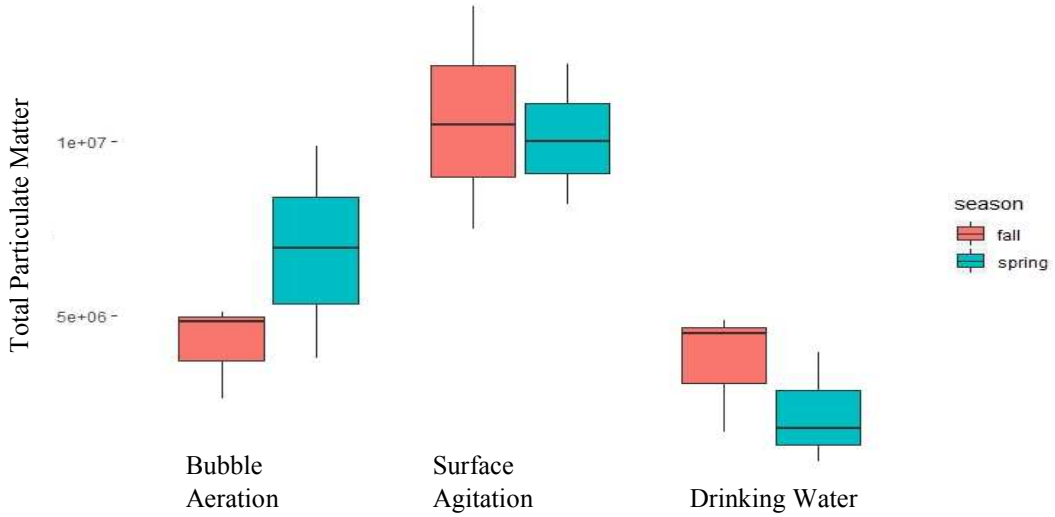

Figure 3.8: Total Particulate Matter (PMs) Count for treatment processes (Site 3 & Site 4) by seasons

3.3.2. Spatial Variation in Total PM Counts

To examine the spatial variation in PM emissions, comparisons between bubble aeration, a mixed tank containing bubble aeration and surface agitation, and drinking water (as a control) have been performed to find the differences based on the treatment methodology in each site (Figure 3.9). Also, similar comparisons have been applied between bubble aeration and surface agitation for a site that utilizes both process in separate tanks in addition to the drinking treatment process as a control (Figures 3.10 & 3.11). Results revealed that the mixed process is higher on average than bubble aeration and drinking water in fall summer and spring, while bubble aeration has a higher average in winter than the mixed tank. Likewise, in the facility that has both processes in isolated tanks, surface agitation average is higher than bubble aeration and drinking water in summer, fall and spring, while the median of total particulate numbers is higher in bubble aeration in winter than the surface agitation process.

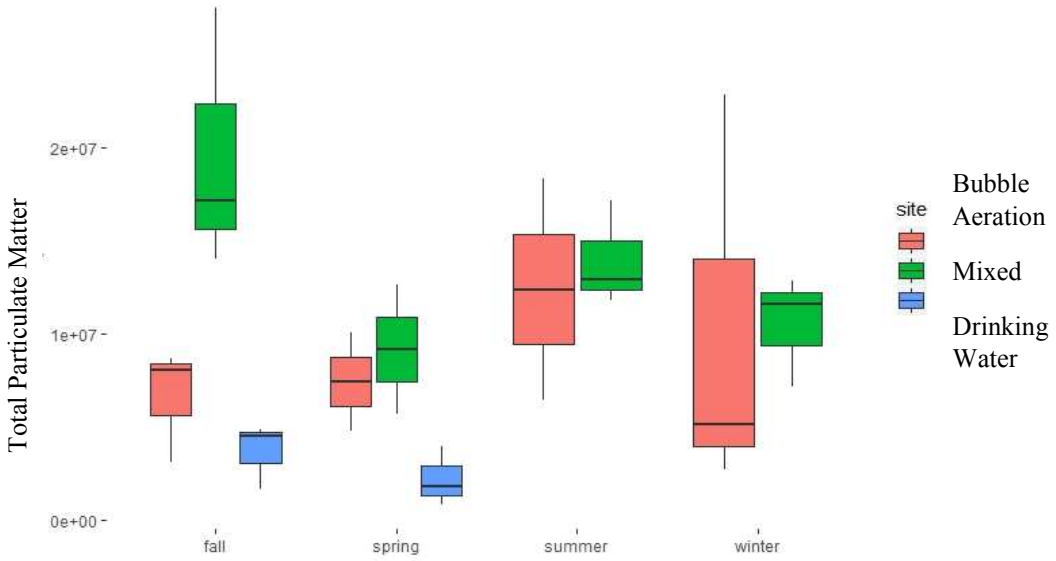

Figure 3.9: Total Particulate Matter (PMs) Count for seasons by treatment processes (Site 1, Site 2 & Site 4)

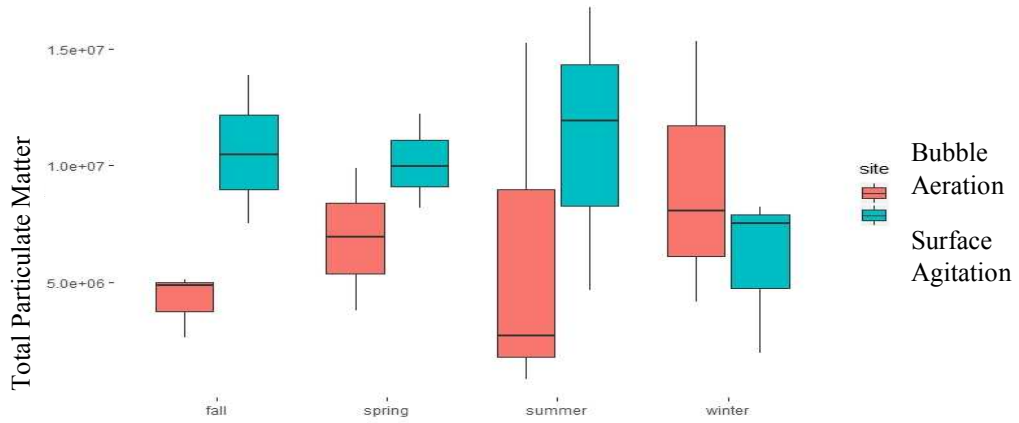

Figure 3.10: Total Particulate Matter (PMs) Count for seasons by treatment processes (Site 3)

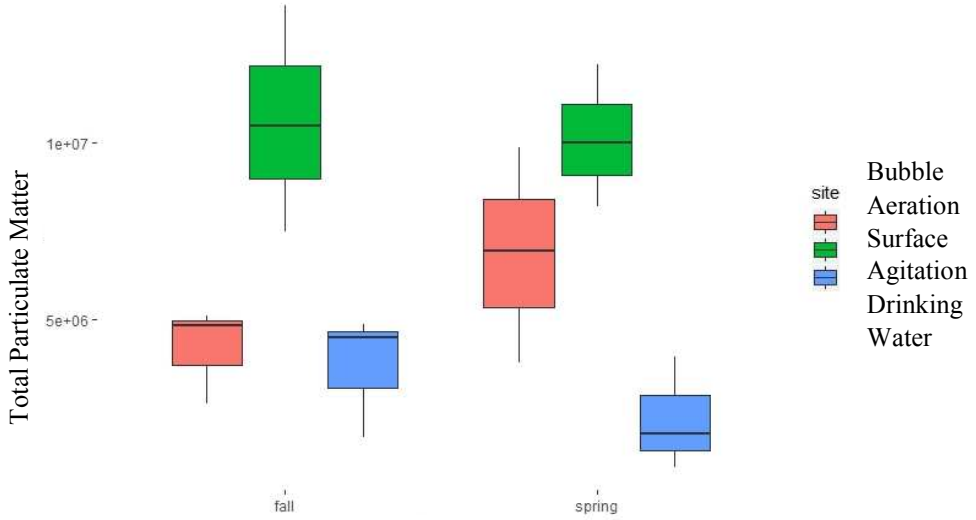

Figure 3.11: Total Particulate Matter (PMs) Count for seasons by treatment processes (Site 3 & Site 4)

3.3.3. Spatial and Temporal Variation by PM Diameter

Results showed that the major diameters present in the air are the smaller particulate with diameter of 0.3 µm and 0.4 µm in all processes and every season, as shown in the figures below (3.12, 3.14, 3.16 & 3.18). Therefore, we generated more

figures, excluding 0.3 µm and 0.4 µm particulate size, to observe the distribution profile of the other particulate sizes in the air. For bubble aeration in Site 1, winter has the higher particulate counts with higher particulate diameter abundance followed by fall, spring, and summer. The most particulate sizes have been found in the air are 0.55 µm, 2.2 µm, and 5.5 µm, respectively. Moreover, fall has the higher particulate counts in the mixed process in Site 2 with more particulate in diameter 4 µm, 2.2 µm, 3 µm, and 5.5 µm. Winter has slightly higher particulate numbers than spring after removing the smaller particulate, and summer shifted from the second higher season when we have all particulate sizes to the lowest season of particulate numbers with the bigger particulate diameter (Figure 3,13). In addition, the comparison in Site 3 was between bubble aeration tank and surface agitation tank, and the total particulate is higher in surface agitation than bubble aeration for all particulate sizes in fall, spring and summer, whereas bubble aeration has total particulate in winter than surface agitation. In fall, the most particulate in the air are 2.2 µm, 3 µm and 4 µm above surface agitation while in bubble aeration is 0.55 µm and 0. 7 µm. Moreover, 0.55 µm and 0.7 µm are higher in spring and summer in surface agitation than bubble aeration. However, the higher number of particulate in winter is 0.55 µm, and 2.2 µm and their presence are more over bubble aeration tanks than surface agitation tanks (Figure 3.17). On the other hand, the particulate count for the size 0.55 µm in the drinking water treatment facility (Site 4) is almost similar and the higher total particulate in fall are due to the higher abundance of the 0.7 µm particulate size compared to the spring (Figures 3.15 & 3.19).

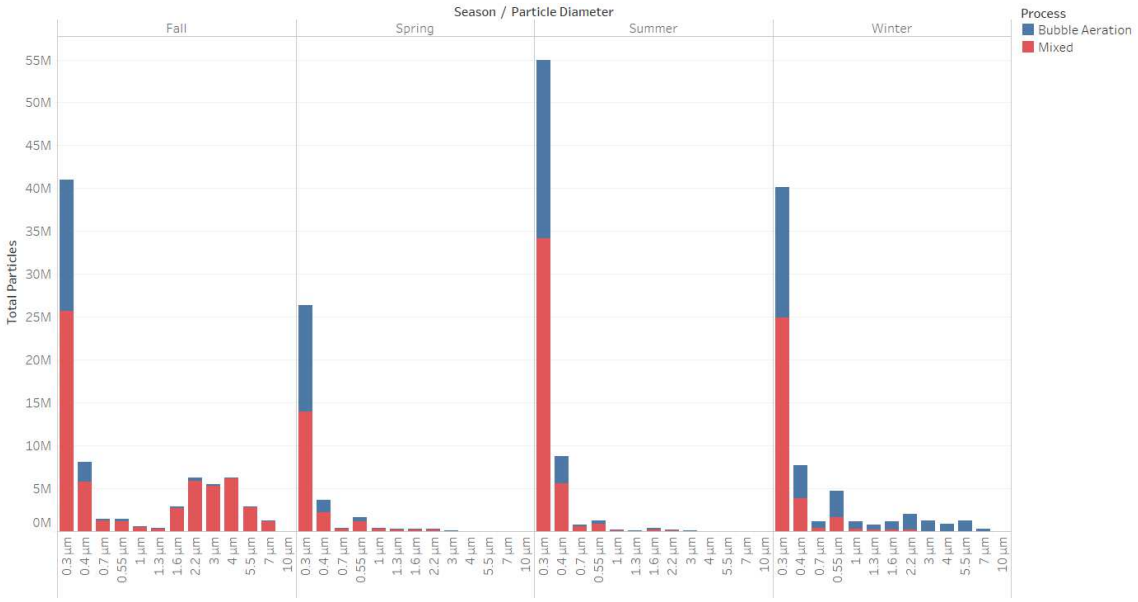

Figure 3.12: Total Particulate Matter (PMs) Count by particulate diameter for treatment processes (Site 1 & Site 2) by seasons

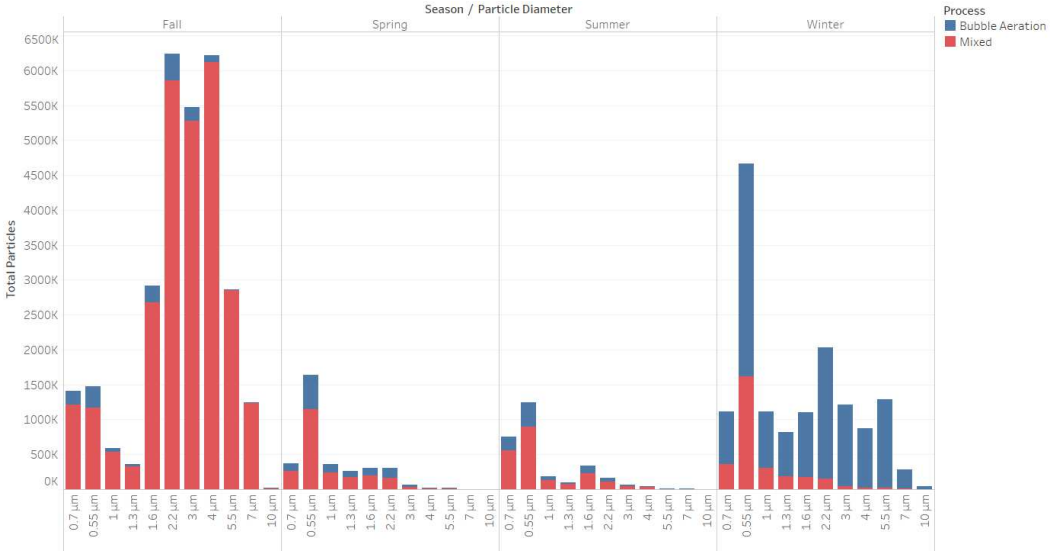

Figure 3.13: Total Particulate Matter (PMs) Count by particulate diameter for treatment processes (Site 1 & Site 2) by seasons (excluding 0.3 µm & 0.4 µm)

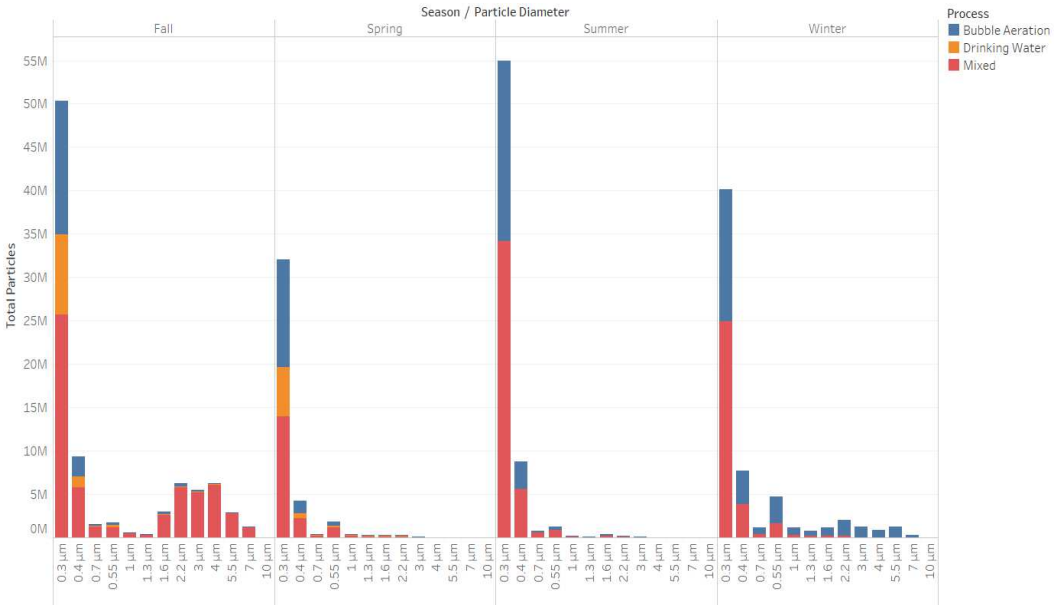

Figure 3.14: Total Particulate Matter (PMs) Count by particulate diameter for treatment processes (Site 1, Site 2 & Site 4) by seasons

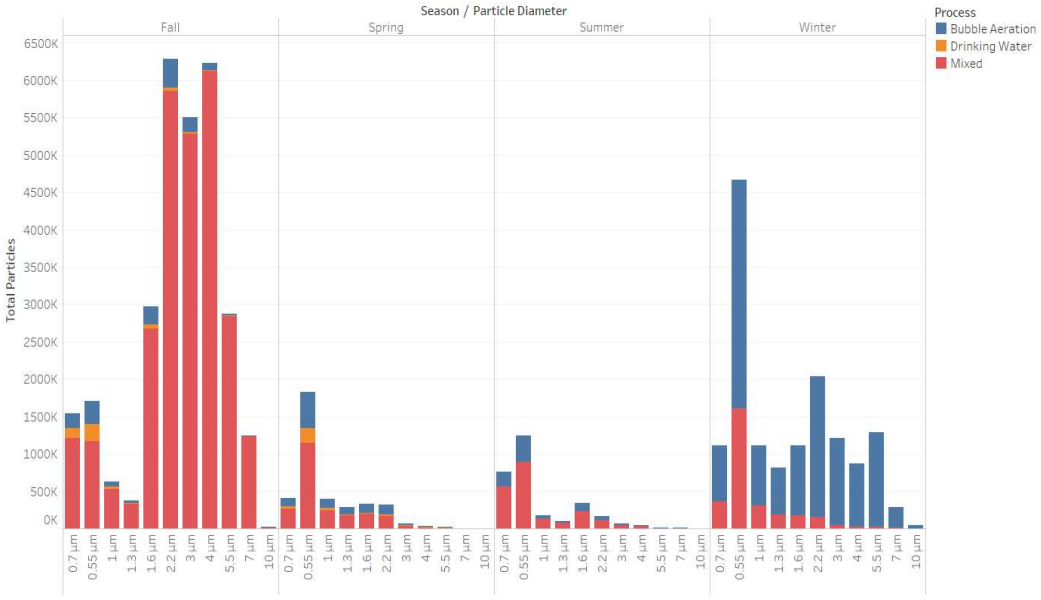

Figure 3.15: Total Particulate Matter (PMs) Count by particulate diameter for treatment process (Site 1, Site 2 & Site 4) by seasons (excluding 0.3 µm & 0.4 µm)

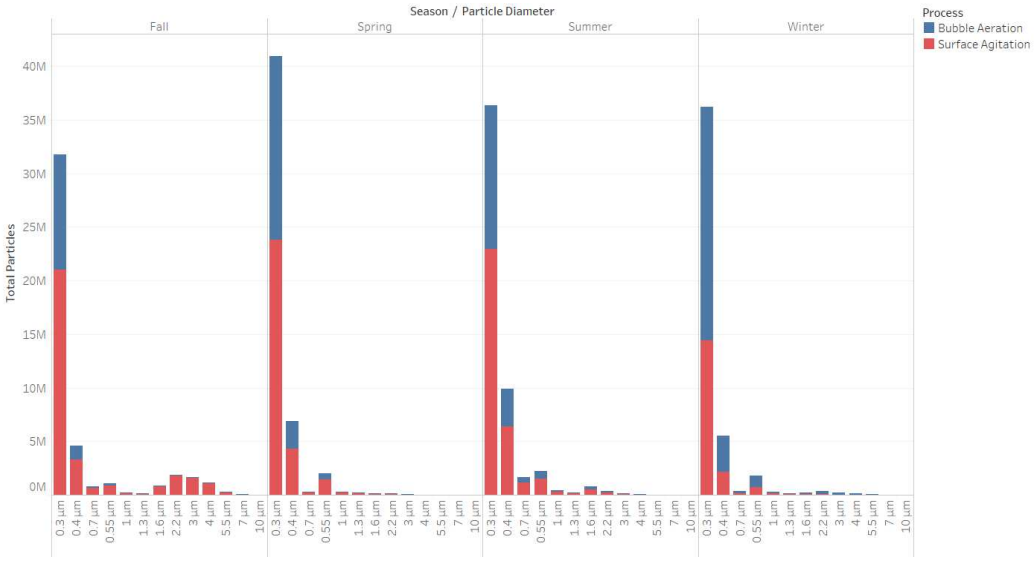

Figure 3.16: Total Particulate Matter (PMs) Count by particulate diameter for treatment processes (Site 3) by seasons

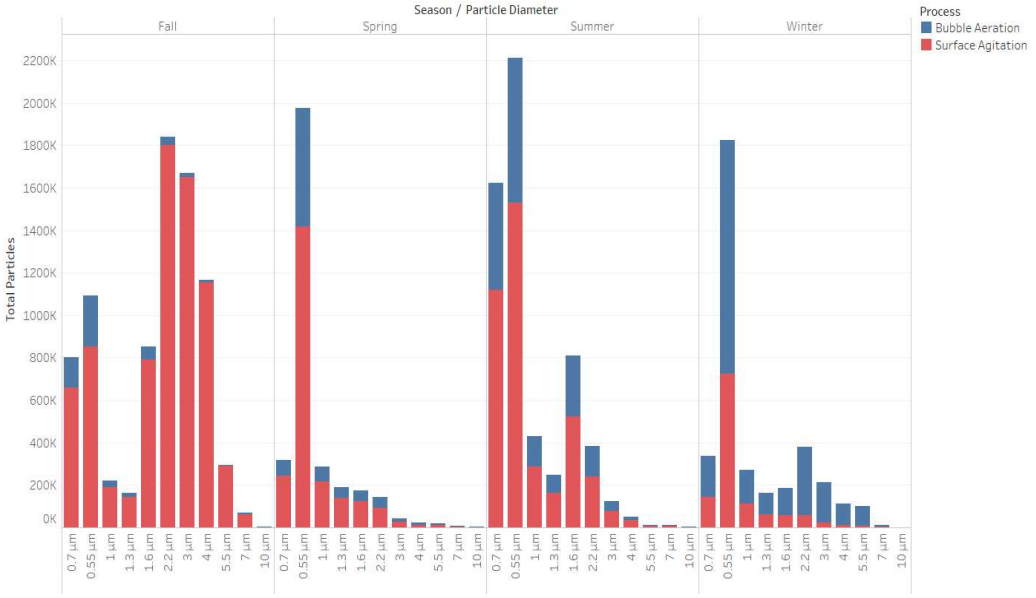

Figure 3.17: Total Particulate Matter (PMs) Count by particulate diameter for treatment process (Site 3) by seasons (excluding 0.3 µm & 0.4 µm)

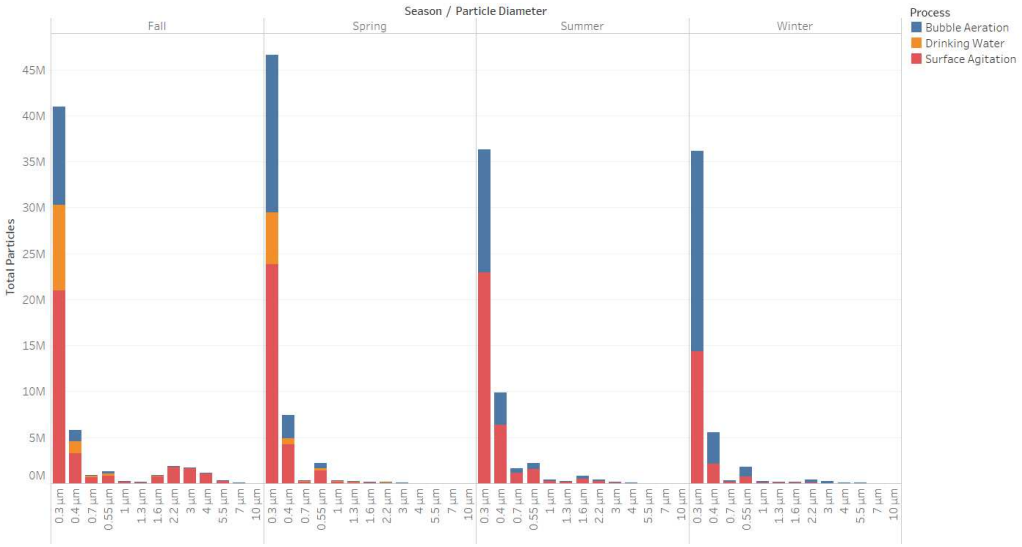

Figure 3.18: Total Particulate Matter (PMs) Count by particulate diameter for treatment processes (Site 3 & Site 4) by seasons

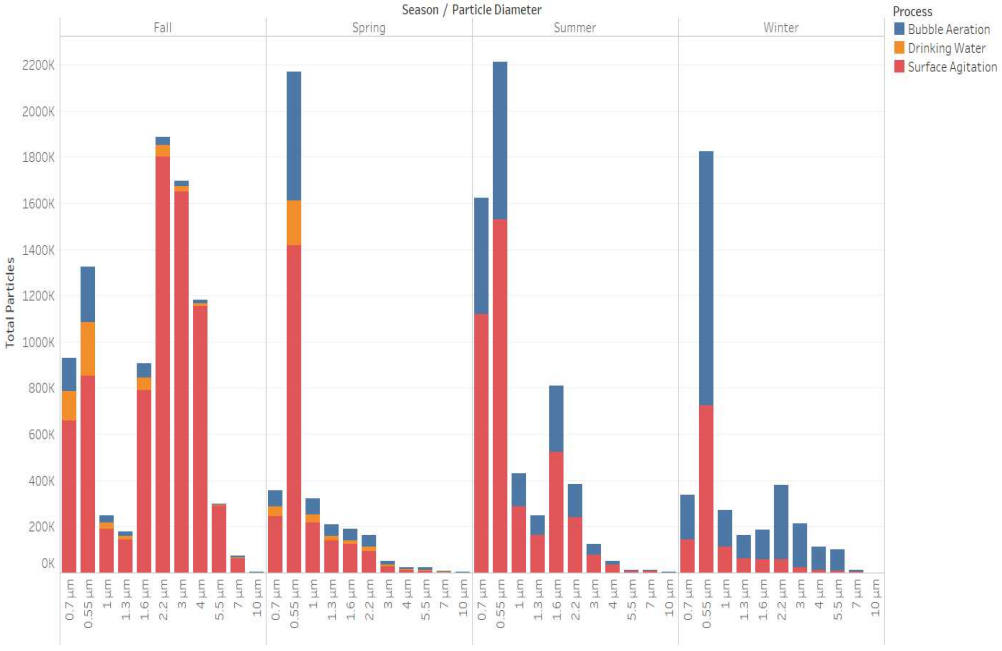

Figure 3.19: Total Particulate Matter (PMs) Count by particulate diameter for treatment process (Site 3 & Site 4) by seasons (excluding 0.3 µm & 0.4 µm)

3.3.4. Statistical analysis results

ANOVA and Tukey tests have been applied to detect the statistical differences for the total particle numbers between the processes in every site as treatment methodology and between processes seasonally. When we compared the treatment process in each facility, we found that there is a significant difference between process in each site, as shown in (Table 3.1) and the P-value is 7.03e-05 ($P < 0.05$). The differences are between drinking water treatment (Site 4) and bubble aeration (Site 1) process with adjusted P-value 0.0050502 and between drinking water treatment (Site 4) and mixed treatment method (Site 2) with adjusted P-value 0.0000429 (Table 3.2). On the other hand, for the facility (Site 3) that uses both processes (bubble aeration & surface agitation), there is no significant difference between the treatment process (P-value is 0.0963 [$P > 0.05$]) (Table 3.5). In terms of seasonal variation, in both situations, there is no significant difference between the treatment process and seasons, and the P values are 0.153 ($P > 0.05$) and 0.888 ($P > 0.05$), respectively (Tables 3.3 & 3.6).

Table 3.1: Analysis of variance (ANOVA) test results of total particulate matter by treatment processes (Site 1 & Site 2 & Site 4)

	Df	Sum Sq	Mean Sq	F value	P- value < 0.05
Process	2	1.960	0.980	14.62	**7.03e-05**
Residuals	24	1.608	0.067		

Bold: Significant difference

Table 3.2: Tukey test results of total particulate matter by treatment processes (Site 1 & Site 2 & Site 4)

Process	Difference	Lower	Upper	P- value < 0.05
Mixed – Bubble Aeration	0.2425917	-0.03987727	0.5250608	0.1019285
Drinking Water – Bubble Aeration	-0.4678642	-0.80170694	-0.1340216	**0.0050502**
Drinking Water - Mixed	-0.7104560	-1.03855884	-0.3823531	**0.0000429**

Bold: Significant difference

Table 3.3: Analysis of variance (ANOVA) test results of total particulate matter for treatment processes (Site 1 & Site 2 & Site 4) by season

	Df	Sum Sq	Mean Sq	F value	P- value < 0.05
Seasons	3	0.7171	0.239	1.928	0.153
Residuals	23	2.8513	0.124		

Table 3.4: Tukey test results of total particulate matter for treatment processes (Site 1 & Site 2 & Site 4) by season

Seasons	Difference	Lower	Upper	P- value < 0.05
Spring-Fall	-0.2411700	-0.73219759	0.2498575	0.5364036
Summer-Fall	0.2392996	-0.30416834	0.7827675	0.6217628
Winter-Fall	0.0633599	-0.45016901	0.5768888	0.9859496
Summer-Spring	0.4804696	-0.09005285	1.0509921	0.1202316
Winter-Spring	0.3045299	-0.23754981	0.8466097	0.4230151
Winter-Summer	-0.1759397	-0.76593947	0.4140601	0.8419526

Table 3.5: Analysis of variance (ANOVA) test results of total particulate matter by treatment processes (Site 3)

	Df	Sum Sq	Mean Sq	Lower	Upper	F value	P- value < 0.05
Process	1	0.2826	0.28255	-0.04199112	0.4760038	3.019	0.0963
Residuals	22	2.0587	0.09358				

Table 3.6: Analysis of variance (ANOVA) test results of total particulate matter for treatment processes (Site 3) by season

	Df	Sum Sq	Mean Sq	F value	P- value < 0.05
Seasons	3	0.0714	0.0238	0.21	0.888
Residuals	20	2.2699	0.1135		

Table 3.7: Tukey test results of total particulate matter for treatment processes (Site 3) by season

Seasons	Difference	Lower	Upper	P- value < 0.05
Spring-Fall	0.093367391	-0.4510336	0.6377684	0.9626409
Summer-Fall	-0.057147198	-0.6015482	0.4872538	0.9908966
Winter-Fall	-0.009681446	-0.5540824	0.5347195	0.9999541
Summer-Spring	-0.150514589	-0.6949156	0.3938864	0.8653054
Winter-Spring	-0.103048836	-0.6474498	0.4413521	0.9508129
Winter-Summer	0.047465752	-0.4969352	0.5918667	0.9947238

Furthermore, statistical analysis (ANOVA and Tukey tests) have been performed to test the significant difference for each particulate diameter between the processes in every site as treatment methodology and between processes seasonally. In terms of processes comparisons, we noted that for bubble aeration (Site 1) and mixed treatment tank (Site 2) there is a significant difference in fall (Table 3.17) and the P-value is 2.39e-05 ($P < 0.05$) while there is no significant difference between sites for the particulate

diameter in winter (Table 3.8) and the P-value is 0.201 (P > 0.05), spring (Table 3.11) and the P-value is 0.509 (P > 0.05), and summer (Table 3.14) and the P-value is 0.416 (P > 0.05). Likewise, in case of Site 3, where bubble aeration tank and surface agitation tank in the same facility but in distinct tanks, there is a significant difference in fall (Table 3.29), and the P-value is 2.44e-13 (P < 0.05) while there is no significant difference between processes for the particulate diameter in winter (Table 3.20) and the P-value is 0.381 (P > 0.05), spring (Table 3.23) and the P-value is 0.254 (P > 0.05), and summer (Table 3.26) and the P-value is 0.0502 (P > 0.05).

In addition, statistical analysis has been done to assess the significant difference between particulate diameter for processes among seasons. In case of bubble aeration (Site 1) and mixed treatment tank (Site 2), for winter (Table 3.9) showed that there is a significant difference with a P-value 1.06e-12 (P < 0.05) and the difference is between 0.3 µm and 0.7 µm, 1 µm, 1.3 µm, 1.6 µm, 2.2 µm, 3 µm, 4 µm, 5.5 µm, 7 µm, and 10 µm, between 0.4 µm and 3 µm, 4 µm, 5.5 µm, 7 µm, and 10 µm, between 0.55 µm and 4 µm, 5.5 µm 7 µm and 10 µm, between 0.7 µm and 7 µm and 10 µm, between 1 µm and 7 µm and 10 µm, between 1.3 µm and 7 µm and 10 µm, between 1.6 µm and 7 µm and 10 µm, between 2.2 µm and 7 µm and 10 µm and between 3 µm and 10 (Table 3.10). Also, the P value of spring (Table 3.12) is <2e-16 (P < 0.05) and the difference is in the particulate with diameter 0.3 µm and 0.4 µm, 0.55 µm, 0.7 µm, 1 µm, 1.3 µm, 1.6 µm, 2.2 µm, 3 µm, 4 µm, 5.5 µm, 7 µm and 10 µm, particulate of diameter 0.4 µm and 0.7 µm, 1 µm, 1.3 µm, 1.6 µm, 2.2 µm, 3 µm, 4 µm, 5.5 µm, 7 µm and 10 µm, particulate size of 0.55 µm and 1.3 µm , 1.6 µm , 2.2 µm, 3 µm, 4 µm, 5.5 µm, 7 µm and 10 µm, between particulate size of 0.7 µm and 4 µm, 5.5 µm, 7 µm and 10 µm, particulate

dimeter 1 µm and 4 µm, 5.5 µm, 7 µm and 10 µm, particulate size of 1.3 µm and 4 µm, 5.5 µm, 7 µm and 10 µm, between particulate size of 1.6 µm and 4 µm, 5.5 µm, 7 µm and 10 µm, particulate with 2.2 µm and 4 µm, 5.5 µm, 7 µm and 10 µm, particulate diameter of 3 µm and 7 µm and 10 µm, between particulate size 4 µm and 10 µm and between 5.5 µm and 10 µm (Table 3.13). Moreover, there is a significant difference in particulate sizes for summer with P-value <2e-16 ($P < 0.05$) (Table 3.15). We found that particulate with dimeter 0.3 µm are statistically different from 0.4 µm, 0.55 µm, 0.7 µm, 1 µm, 1.3 µm, 1.6 µm, 2.2 µm, 3 µm, 4 µm, 5.5 µm, 7 µm, and 10 µm, particulate size 0.4 µm is different from 0.55 µm, 0.7 µm, 1 µm, 1.3 µm, 1.6 µm, 2.2 µm, 3 µm, 4 µm, 5.5 µm, 7 µm, and 10 µm. There is a difference between particulate of 0.55 µm diameter and 1 µm, 1.3 µm, 1.6 µm, 2.2 µm, 3 µm, 4 µm, 5.5 µm, 7 µm, and 10 µm, between 0.7 µm and 1 µm, 1.3 µm, 2.2 µm, 3 µm, 4 µm, 5.5 µm, 7 µm, and 10 µm, between particulate size of 1 µm and 3 µm, 4 µm, 5.5 µm, 7 µm, and 10 µm, particulate of 1.3 µm and 4 µm, 5.5 µm, 7 µm, and 10 µm, the particulate diameter of 1.6 µm and 3 µm, 4 µm, 5.5 µm, 7 µm, and 10 µm, between 2.2 µm and 4 µm, 5.5 µm, 7 µm, and 10 µm, between 3 µm and 5.5 µm, 7 µm and 10 µm, between 4 µm and 5.5 µm, 7 µm and 10 µm, between particulate diameter of 5.5 µm and 10 µm and between 7 µm and 10 µm (Table 3.16). For fall, (Table 3.18) shows that there is a significant difference in the particulate bin size, and the P-value is 2.58e-07 ($P < 0.05$). The difference is between particulate diameter 0.3 µm and 1 µm, 1.3 µm, 4 µm, 5.5 µm, 7 µm, and 10 µm, particulate size 0.4 µm and 7 µm and 10 µm, particulate of diameter 0.55 µm and 10 µm, between 0.7 µm and 10 µm, between 1 µm and 10 µm, between 1.6 µm and 10 µm, particulate of 2.2 µm and 10 µm, between 3 µm and 10 µm and between 4 µm and 10 µm (Table 3.19).

Table 3.8: Analysis of variance (ANOVA) test results for Winter of particulate dimeter by treatment processes (Site 1 & Site 2)

	Df	Sum Sq	Mean Sq	Lower	Upper	F value	P- value < 0.05
Process	1	2.34	2.341	-0.8818116	0.1887674	1.662	0.201
Residuals	76	107.05	1.409				

Table 3.9: Analysis of variance (ANOVA) test results for Winter of particulate dimeter for treatment processes (Site 1 & Site 2) by bin size

	Df	Sum Sq	Mean Sq	F value	P- value < 0.05
Bin Size	12	76.33	6.361	12.51	**1.06e-12**
Residuals	65	33.06	0.509		

Bold: Significant difference

Table 3.10: Tukey test results for Winter of particulate dimeter for treatment processes (Site 1 & Site 2) by bin size

Bin Size	Difference	Lower	Upper	P- value < 0.05
0.3 µm – 0.4 µm	-0.766587306	-2.18247118	0.64929656	0.8104523
0.3 µm – 0.55 µm	-1.025629420	-2.44151329	0.39025445	0.3976846
0.3 µm – 0.7 µm	-1.635314808	-3.05119868	-0.21943094	**0.0105662**
0.3 µm – 1 µm	-1.657191573	-3.07307544	-0.24130770	**0.0089457**
0.3 µm – 1.3 µm	-1.826557543	-3.24244141	-0.41067367	**0.0023247**
0.3 µm – 1.6 µm	-1.783005836	-3.19888971	-0.36712197	**0.0033181**
0.3 µm – 2.2 µm	-1.777779205	-3.19366308	-0.36189534	**0.0034615**
0.3 µm – 3 µm	-2.320682818	-3.73656669	-0.90479895	**0.0000294**
0.3 µm – 4 µm	-2.638455864	-4.05433973	-1.22257199	**0.0000014**
0.3 µm – 5.5 µm	-2.690927964	-4.10681183	-1.27504409	**0.0000009**
0.3 µm – 7 µm	-3.261339238	-4.67722311	-1.84545537	**0.0000000**

0.3 µm – 10 µm	-3.828544651	-5.24442852	-2.41266078	**0.0000000**
0.4 µm – 0. 55 µm	-0.259042113	-1.67492598	1.15684176	0.9999868
0.4 µm – 0.7 µm	-0.868727501	-2.28461137	0.54715637	0.6566955
0.4 µm – 1 µm	-0.890604267	-2.30648814	0.52527960	0.6203509
0.4 µm – 1.3 µm	-1.059970237	-2.47585411	0.35591363	0.3464422
0.4 µm – 1.6 µm	-1.016418530	-2.43230240	0.39946534	0.4119863
0.4 µm – 2.2 µm	-1.011191899	-2.42707577	0.40469197	0.4201956
0.4 µm – 3 µm	-1.554095511	-2.96997938	-0.13821164	**0.0192712**
0.4 µm – 4 µm	-1.871868558	-3.28775243	-0.45598469	**0.0015956**
0.4 µm – 5.5 µm	-1.924340657	-3.34022453	-0.50845679	**0.0010244**
0.4 µm – 7 µm	-2.494751931	-3.91063580	-1.07886806	**0.0000057**
0.4 µm – 10 µm	-3.061957344	-4.47784121	-1.64607347	**0.0000000**
0.55 µm – 0.7 µm	-0.609685388	-2.02556926	0.80619848	0.9553280
0.55 µm – 1 µm	-0.631562154	-2.04744602	0.78432172	0.9426199
0.55 µm – 1.3 µm	-0.800928123	-2.21681199	0.61495575	0.7627113
0.55 µm – 1.6 µm	-0.757376417	-2.17326029	0.65850745	0.8223890
0.55 µm – 2.2 µm	-0.752149786	-2.16803366	0.66373408	0.8289869
0.55 µm – 3 µm	-1.295053398	-2.71093727	0.12083047	0.1058892
0.55 µm – 4 µm	-1.612826445	-3.02871031	-0.19694257	**0.0125135**
0.55 µm – 5.5 µm	-1.665298544	-3.08118241	-0.24941467	**0.0084065**
0.55 µm – 7 µm	-2.235709818	-3.65159369	-0.81982595	**0.0000645**
0.55 µm – 10 µm	-2.802915231	-4.21879910	-1.38703136	**0.0000003**
0.7 µm – 1 µm	-0.021876765	-1.43776064	1.39400710	1.0000000

0.7 µm – 1.3 µm	-0.191242735	-1.60712661	1.22464113	0.9999996
0.7 µm – 1.6 µm	-0.147691029	-1.56357490	1.26819284	1.0000000
0.7 µm – 2,2 µm	-0.142464398	-1.55834827	1.27341947	1.0000000
0.7 µm – 3 µm	-0.685368010	-2.10125188	0.73051586	0.9012502
0.7 µm – 4 µm	-1.003141056	-2.41902493	0.41274281	0.4329659
0.7 µm – 5.5 µm	-1.055613156	-2.47149703	0.36027071	0.3527486
0.7 µm – 7 µm	-1.626024430	-3.04190830	-0.21014056	**0.0113338**
0.7 µm – 10 µm	-2.193229843	-3.60911371	-0.77734597	**0.0000952**
1 µm – 1.3 µm	-0.169365970	-1.58524984	1.24651790	0.9999999
1 µm – 1.6 µm	-0.125814263	-1.54169813	1.29006961	1.0000000
1 µm – 2.2 µm	-0.120587632	-1.53647150	1.29529624	1.0000000
1 µm – 3 µm	-0.663491245	-2.07937511	0.75239263	0.9198688
1 µm – 4 µm	-0.981264291	-2.39714816	0.43461958	0.4683507
1 µm – 5.5 µm	-1.033736390	-2.44962026	0.38214748	0.3852818
1 µm – 7 µm	-1.604147665	-3.02003153	-0.18826379	**0.0133503**
1 µm – 10 µm	-2.171353078	-3.58723695	-0.75546921	**0.0001161**
1.3 µm – 1.6 µm	0.043551707	-1.37233216	1.45943558	1.0000000
1.3 µm – 2.2 µm	0.048778338	-1.36710553	1.46466221	1.0000000
1.3 µm – 3 µm	-0.494125275	-1.91000914	0.92175860	0.9916158
1.3 µm – 4 µm	-0.811898321	-2.22778219	0.60398555	0.7464876
1.3 µm – 5.5 µm	-0.864370421	-2.28025429	0.55151345	0.6638478
1.3 µm – 7 µm	-1.434781695	-2.85066556	-0.01889783	**0.0441364**
1.3 µm – 10 µm	-2.001987108	-3.41787098	-0.58610324	**0.0005246**
1.6 µm – 2.2 µm	0.005226631	-1.41065724	1.42111050	1.0000000

1.6 µm – 3 µm	-0.537676981	-1.95356085	0.87820689	0.9829932
1.6 µm – 4 µm	-0.855450028	-2.27133390	0.56043384	0.6783791
1.6 µm – 5.5 µm	-0.907922127	-2.32380600	0.50796174	0.5912277
1.6 µm – 7 µm	-1.478333402	-2.89421727	-0.06244953	**0.0328781**
1.6 µm – 10 µm	-2.045538814	-3.46142268	-0.62965494	**0.0003581**
2.2 µm – 3 µm	-0.542903612	-1.95878748	0.87298026	0.9816107
2.2 µm – 4 µm	-0.860676659	-2.27656053	0.55520721	0.6698840
2.2 µm – 5.5 µm	-0.913148758	-2.32903263	0.50273511	0.5824052
2.2 µm – 7 µm	-1.483560032	-2.89944390	-0.06767616	**0.0317162**
2.2 µm – 10 µm	2.050765445	0.63488158	3.46664932	**0.0003420**
3 µm – 4 µm	-0.317773046	-1.73365692	1.09811082	0.9998820
3 µm – 5.5 µm	-0.370245146	-1.78612902	1.04563872	0.9994359
3 µm – 7 µm	-0.940656420	-2.35654029	0.47522745	0.5359569
3 µm – 10 µm	1.507861833	0.09197796	2.92374570	**0.0267841**
4 µm – 5.5 µm	-0.052472099	-1.46835597	1.36341177	1.0000000
4 µm – 7 µm	-0.622883374	-2.03876724	0.79300050	0.9479312
4 µm – 10 µm	1.190088787	-0.22579508	2.60597266	0.1887853
5.5 µm – 7 µm	-0.570411274	-1.98629514	0.84547260	0.9728492
5.5 µm – 10 µm	1.137616687	-0.27826718	2.55350056	0.2449164
7 µm – 10 µm	0.567205413	-0.84867846	1.98308928	0.9740073

Bold: Significant difference

Table 3.11: Analysis of variance (ANOVA) test results for Spring of particulate dimeter by treatment processes (Site 1 & Site 2)

	Df	Sum Sq	Mean Sq	Lower	Upper	F value	P- value < 0.05
Process	1	0.64	0.6383	-0.4479961	0.891183	0.442	0.509
Residuals	50	72.24	1.4447				

Table 3.12: Analysis of variance (ANOVA) test results for Spring of particulate dimeter for treatment processes (Site 1 & Site 2) by bin size

	Df	Sum Sq	Mean Sq	F value	P- value < 0.05
Bin Size	12	69.37	5.781	64.36	**<2e-16**
Residuals	39	3.50	0.090		

Bold: Significant difference

Table 3.13: Tukey test results for Spring of particulate dimeter for treatment processes (Site 1 & Site 2) by bin size

Bin Size	Difference	Lower	Upper	P- value < 0.05
0.3 µm – 0.4 µm	-0.87032508	-1.61726593	-0.12338424	**0.0108174**
0.3 µm – 0.55 µm	-1.21184854	-1.95878939	-0.46490769	**0.0000866**
0.3 µm – 0.7 µm	-1.87791279	-2.62485364	-1.13097194	**0.0000000**
0.3 µm – 1 µm	-1.89296884	-2.63990969	-1.14602799	**0.0000000**
0.3 µm – 1.3 µm	-2.05405975	-2.80100060	-1.30711890	**0.0000000**
0.3 µm – 1.6 µm	-2.01872654	-2.76566739	-1.27178569	**0.0000000**
0.3 µm – 2.2 µm	-2.00116528	-2.74810613	-1.25422443	**0.0000000**
0.3 µm – 3 µm	-2.60171945	-3.34866030	-1.85477860	**0.0000000**
0.3 µm – 4 µm	-3.00303076	-3.74997161	-2.25608991	**0.0000000**
0.3 µm – 5.5 µm	-3.13637119	-3.88331204	-2.38943034	**0.0000000**

0.3 µm – 7 µm	-3.80964367	-4.55658451	-3.06270282	**0.0000000**
0.3 µm – 10 µm	-4.48098729	-5.22792814	-3.73404644	**0.0000000**
0.4 µm – 0. 55 µm	-0.34152345	-1.08846430	0.40541739	0.9155281
0.4 µm – 0.7 µm	-1.00758771	-1.75452855	-0.26064686	**0.0016661**
0.4 µm – 1 µm	-1.02264376	-1.76958461	-0.27570291	**0.0013470**
0.4 µm – 1.3 µm	-1.18373467	-1.93067551	-0.43679382	**0.0001310**
0.4 µm – 1.6 µm	-1.14840146	-1.89534230	-0.40146061	**0.0002198**
0.4 µm – 2.2 µm	-1.13084019	-1.87778104	-0.38389935	**0.0002841**
0.4 µm – 3 µm	-1.73139436	-0.98445351	-0.98445351	**0.0000000**
0.4 µm – 4 µm	-2.13270567	-2.87964652	-1.38576482	**0.0000000**
0.4 µm – 5.5 µm	-2.26604610	-3.01298695	-1.51910525	**0.0000000**
0.4 µm – 7 µm	-2.93931858	-3.68625943	-2.19237773	**0.0000000**
0.4 µm – 10 µm	-3.61066220	-4.35760305	-2.86372136	**0.0000000**
0.55 µm – 0.7 µm	-0.66606425	-1.41300510	0.08087660	0.1214804
0.55 µm – 1 µm	-0.68112030	-1.42806115	0.06582054	0.1038555
0.55 µm – 1.3 µm	-0.84221121	-1.58915206	-0.09527036	**0.0155674**
0.55 µm – 1.6 µm	-0.80687800	-1.55381885	-0.05993715	**0.0243097**
0.55 µm – 2.2 µm	-0.78931674	-1.53625759	-0.04237589	**0.0301746**
0.55 µm – 3 µm	-1.38987091	-2.13681176	-0.64293006	**0.0000062**
0.55 µm – 4 µm	-1.79118222	-2.53812307	-1.04424137	**0.0000000**
0.55 µm – 5.5 µm	-1.92452265	-2.67146350	-1.17758180	**0.0000000**
0.55 µm – 7 µm	-2.59779513	-3.34473598	-1.85085428	**0.0000000**
0.55 µm – 10 µm	-3.26913875	-4.01607960	-2.52219790	**0.0000000**

0.7 µm – 1 µm	-0.01505605	-0.76199690	0.73188480	1.0000000
0.7 µm – 1.3 µm	-0.17614696	-0.92308781	0.57079389	0.9996941
0.7 µm – 1.6 µm	-0.14081375	-0.88775460	0.60612710	0.9999705
0.7 µm – 2,2 µm	-0.12325249	-0.87019334	0.62368836	0.9999931
0.7 µm – 3 µm	-0.72380666	-1.47074751	0.02313419	0.0651636
0.7 µm – 4 µm	-1.12511797	-1.87205882	-0.37817712	**0.0003088**
0.7 µm – 5.5 µm	-1.25845840	-2.00539925	-0.51151755	**0.0000435**
0.7 µm – 7 µm	-1.93173087	-2.67867172	-1.18479003	**0.0000000**
0.7 µm – 10 µm	-2.60307450	-3.35001535	-1.85613365	**0.0000000**
1 µm – 1.3 µm	-0.16109091	-0.90803176	0.58584994	0.9998776
1 µm – 1.6 µm	-0.12575770	-0.87269855	0.62118315	0.9999914
1 µm – 2.2 µm	-0.10819644	-0.85513728	0.63874441	0.9999984
1 µm – 3 µm	-0.70875061	-1.45569145	0.03819024	0.0770762
1 µm – 4 µm	-1.11006191	-1.85700276	-0.36312107	**0.0003843**
1 µm – 5.5 µm	-1.24340234	-1.99034319	-0.49646150	**0.0000543**
1 µm – 7 µm	-1.91667482	-2.66361567	-1.16973397	**0.0000000**
1 µm – 10 µm	-2.58801845	-3.33495930	-1.84107760	**0.0000000**
1.3 µm – 1.6 µm	0.03533321	-0.71160764	0.78227406	1.0000000
1.3 µm – 2.2 µm	0.05289447	-0.69404638	0.79983532	1.0000000
1.3 µm – 3 µm	-0.54765970	-1.29460055	0.19928115	0.3527770
1.3 µm – 4 µm	-0.94897101	-1.69591186	-0.20203016	**0.0037650**
1.3 µm – 5.5 µm	-1.08231144	-1.82925229	-0.33537059	**0.0005741**
1.3 µm – 7 µm	-1.75558392	-2.50252476	-1.00864307	**0.0000000**
1.3 µm – 10 µm	-2.42692754	-3.17386839	-1.67998669	**0.0000000**

1.6 µm – 2.2 µm	0.01756126	-0.72937959	0.76450211	1.0000000
1.6 µm – 3 µm	-0.58299291	-1.32993376	0.16394794	0.2655089
1.6 µm – 4 µm	-0.98430422	-1.73124507	-0.23736337	**0.0023090**
1.6 µm – 5.5 µm	-1.11764465	-1.86458550	-0.37070380	**0.0003442**
1.6 µm – 7 µm	-1.79091712	-2.53785797	-1.04397628	**0.0000000**
1.6 µm – 10 µm	-2.46226075	-3.20920160	-1.71531990	**0.0000000**
2.2 µm – 3 µm	-0.60055417	-1.34749502	0.14638668	0.2279260
2.2 µm – 4 µm	-1.00186548	-1.74880633	-0.25492463	**0.0018057**
2.2 µm – 5.5 µm	-1.13520591	-1.88214676	-0.38826506	**0.0002666**
2.2 µm – 7 µm	-1.80847839	-2.55541924	-1.06153754	**0.0000000**
2.2 µm – 10 µm	2.47982201	1.73288116	3.22676286	**0.0000000**
3 µm – 4 µm	-0.40131131	-1.14825216	0.34562954	0.7889253
3 µm – 5.5 µm	-0.53465174	-1.28159259	0.21228911	0.3885136
3 µm – 7 µm	-1.20792422	-1.95486507	-0.46098337	**0.0000917**
3 µm – 10 µm	1.13232699	1.13232699	2.62620869	**0.0000000**
4 µm – 5.5 µm	-0.13334043	-0.88028128	0.61360042	0.9999836
4 µm – 7 µm	-0.80661291	-1.55355376	-0.05967206	**0.0243898**
4 µm – 10 µm	1.47795653	0.73101568	2.22489738	**0.0000017**
5.5 µm – 7 µm	-0.67327248	-1.42021333	0.07366837	0.1127565
5.5 µm – 10 µm	1.34461610	0.59767525	2.09155695	**0.0000121**
7 µm – 10 µm	-0.07559722	-0.07559722	1.41828447	0.1150386

Bold: Significant difference

Table 3.14: Analysis of variance (ANOVA) test results for Summer of particulate dimeter by treatment processes (Site 1 & Site 2)

	Df	Sum Sq	Mean Sq	Lower	Upper	F value	P- value < 0.05
Process	1	0.90	0.9023	-0.3462428	0.8272386	0.671	0.416
Residuals	63	84.73	1.3449				

Table 3.15: Analysis of variance (ANOVA) test results for Summer of particulate dimeter for treatment processes (Site 1 & Site 2) by bin size

	Df	Sum Sq	Mean Sq	F value	P- value < 0.05
Bin Size	12	83.92	6.993	212.7	**<2e-16**
Residuals	52	1.71	0.033		

Bold: Significant difference

Table 3.16: Tukey test results for Summer of particulate dimeter for treatment processes (Site 1 & Site 2) by bin size

Bin Size	Difference	Lower	Upper	P- value < 0.05
0.3 µm – 0.4 µm	-0.80966018	-1.2077000	-0.411620337	**0.0000003**
0.3 µm – 0.55 µm	-1.64776782	-2.0458077	-1.249727983	**0.0000000**
0.3 µm – 0.7 µm	-1.86050650	-2.2585463	-1.462466660	**0.0000000**
0.3 µm – 1 µm	-2.47636212	-2.8744020	-2.078322279	**0.0000000**
0.3 µm – 1.3 µm	-2.71537618	-3.1134160	-2.317336341	**0.0000000**
0.3 µm – 1.6 µm	-2.18294874	-2.5809886	-1.784908903	**0.0000000**
0.3 µm – 2.2 µm	-2.51064845	-2.9086883	-2.112608614	**0.0000000**
0.3 µm – 3 µm	-2.90064069	-3.2986805	-2.502600849	**0.0000000**
0.3 µm – 4 µm	-3.15362445	-3.5516643	-2.755584614	**0.0000000**
0.3 µm – 5.5 µm	-3.65982902	-4.0578689	-3.261789183	**0.0000000**
0.3 µm – 7 µm	-3.70818460	-4.1062244	-3.310144759	**0.0000000**

0.3 µm – 10 µm	-4.24123332	-4.6392732	-3.843193484	**0.0000000**
0.4 µm – 0. 55 µm	-0.83810765	-1.2361475	-0.440067808	**0.0000001**
0.4 µm – 0.7 µm	-1.05084632	-1.4488862	-0.652806484	**0.0000000**
0.4 µm – 1 µm	-1.66670194	-2.0647418	-1.268662104	**0.0000000**
0.4 µm – 1.3 µm	-1.90571600	-2.3037558	-1.507676166	**0.0000000**
0.4 µm – 1.6 µm	-1.37328857	-1.7713284	-0.975248728	**0.0000000**
0.4 µm – 2.2 µm	-1.70098828	-2.0990281	-1.302948439	**0.0000000**
0.4 µm – 3 µm	-2.09098051	-2.4890204	-1.692940674	**0.0000000**
0.4 µm – 4 µm	-2.34396428	-2.7420041	-1.945924439	**0.0000000**
0.4 µm – 5.5 µm	-2.85016885	-3.2482087	-2.452129008	**0.0000000**
0.4 µm – 7 µm	-2.89852442	-3.2965643	-2.500484583	**0.0000000**
0.4 µm – 10 µm	-3.43157315	-3.8296130	-3.033533309	**0.0000000**
0.55 µm – 0.7 µm	-0.21273868	-0.6107785	0.185301161	0.8124843
0.55 µm – 1 µm	-0.82859430	-1.2266341	-0.430554458	**0.0000002**
0.55 µm – 1.3 µm	-1.06760836	-1.4656482	-0.669568520	**0.0000000**
0.55 µm – 1.6 µm	-0.53518092	-0.9332208	-0.137141082	**0.0014069**
0.55 µm – 2.2 µm	-0.86288063	-1.2609205	-0.464840793	**0.0000001**
0.55 µm – 3 µm	-1.25287287	-1.6509127	-0.854833028	**0.0000000**
0.55 µm – 4 µm	-1.50585663	-1.9038965	-1.9038965	**0.0000000**
0.55 µm – 5.5 µm	-2.01206120	-2.4101010	-1.614021362	**0.0000000**
0.55 µm – 7 µm	-2.06041678	-2.4584566	-1.662376938	**0.0000000**
0.55 µm – 10 µm	-2.59346550	-2.9915053	-2.195425663	**0.0000000**
0.7 µm – 1 µm	-0.61585562	-1.0138955	-0.217815781	**0.0001295**

0.7 µm – 1.3 µm	-0.85486968	-1.2529095	0.456829843	**0.0000001**
0.7 µm – 1.6 µm	-0.32244224 -	-0.7204821	0.075597595	0.2281882
0.7 µm – 2,2 µm	-0.65014195	-1.0481818	-0.252102116	**0.0000453**
0.7 µm – 3 µm	-1.04013419	-1.4381740	-0.642094351	**0.0000000**
0.7 µm – 4 µm	-1.29311795	-1.6911578	-0.895078116	**0.0000000**
0.7 µm – 5.5 µm	-1.79932252	-2.1973624	-1.401282686	**0.0000000**
0.7 µm – 7 µm	-1.84767810	-2.2457179	-1.449638261	**0.0000000**
0.7 µm – 10 µm	-2.38072682	-2.7787667	-1.982686986	**0.0000000**
1 µm – 1.3 µm	-0.23901406	-0.6370539	0.159025776	0.6737628
1 µm – 1.6 µm	0.29341338	-0.1046265	0.691453214	0.3604347
1 µm – 2.2 µm	-0.03428634	-0.4323262	0.363753503	1.0000000
1 µm – 3 µm	-0.42427857	-0.8223184	-0.026238732	**0.0269975**
1 µm – 4 µm	-0.67726234	-1.0753022	-0.279222497	**0.0000195**
1 µm – 5.5 µm	-1.18346690	-1.5815067	-0.785427066	**0.0000000**
1 µm – 7 µm	-1.23182248	-1.6298623	-0.833782641	**0.0000000**
1 µm – 10 µm	-1.76487121	-2.1629110	-1.366831367	**0.0000000**
1.3 µm – 1.6 µm	0.53242744	0.1343876	0.930467276	**0.0015221**
1.3 µm – 2.2 µm	0.20472773 -	-0.1933121	0.602767565	0.8479019
1.3 µm – 3 µm	-0.18526451	-0.5833043	0.212775330	0.9168924
1.3 µm – 4 µm	-0.43824827	-0.8362881	-0.040208435	**0.0191515**
1.3 µm – 5.5 µm	-0.94445284	-1.3424927	-0.546413004	**0.0000000**
1.3 µm – 7 µm	-0.99280842	-1.3908483	-0.594768579	**0.0000000**
1.3 µm – 10 µm	-1.52585714	-1.9238970	-1.127817305	**0.0000000**
1.6 µm – 2.2 µm	-0.32769971	-0.7257395	0.070340127	0.2083248

1.6 µm – 3 µm	-0.71769195	-1.1157318	-0.319652108	**0.0000055**
1.6 µm – 4 µm	-0.97067571	-1.3687155	-0.572635873	**0.0000000**
1.6 µm – 5.5 µm	-1.47688028	-1.8749201	-1.078840442	**0.0000000**
1.6 µm – 7 µm	-1.52523586	-1.9232757	-1.127196017	**0.0000000**
1.6 µm – 10 µm	-2.05828458	-2.4563244	-1.660244743	**0.0000000**
2.2 µm – 3 µm	-0.38999223	-0.7880321	0.008047604	0.0599119
2.2 µm – 4 µm	-0.64297600	-1.0410158	-0.244936162	**0.0000565**
2.2 µm – 5.5 µm	-1.14918057	-1.5472204	-0.751140731	**0.0000000**
2.2 µm – 7 µm	-1.19753614	-1.5955760	-0.799496306	**0.0000000**
2.2 µm – 10 µm	1.73058487	1.3325450	2.128624708	**0.0000000**
3 µm – 4 µm	-0.25298377	-0.6510236	0.145056073	0.5915254
3 µm – 5.5 µm	-0.75918833 -	1.1572282 -	-0.361148496	**0.0000015**
3 µm – 7 µm	-0.80754391 -	-1.2055837	-0.409504071	**0.0000003**
3 µm – 10 µm	1.34059264	0.9425528	1.738632474	**0.0000000**
4 µm – 5.5 µm	-0.50620457	-0.9042444	-0.108164731	**0.0031825**
4 µm – 7 µm	-0.55456014	-0.9526000	-0.156520306	**0.0008042**
4 µm – 10 µm	1.08760887	0.6895690	1.485648708	**0.0000000**
5.5 µm – 7 µm	-0.04835558	-0.4463954	0.349684263	0.9999998
5.5 µm – 10 µm	0.58140430	0.1833645	0.979444139	**0.0003649**
7 µm – 10 µm	0.53304873	0.1350089	0.931088564	**0.0014953**

Bold: Significant difference

Table 3.17: Analysis of variance (ANOVA) test results for Fall of particulate dimeter by treatment processes (Site 1 & Site 2)

	Df	Sum Sq	Mean Sq	Lower	Upper	F value	P- value < 0.05
Process	1	29.03	29.030	0.6803467	1.759909	20.27	**2.39e-05**
Residuals	76	108.85	1.432				

Bold: Significant difference

Table 3.18: Analysis of variance (ANOVA) test results for Fall of particulate dimeter for treatment processes (Site 1 & Site 2) by bin size

	Df	Sum Sq	Mean Sq	F value	P- value < 0.05
Bin Size	12	74.54	6.212	6.375	**2.58e-07**
Residuals	65	63.34	0.974		

Bold: Significant difference

Table 3.19: Tukey test results for Fall of particulate dimeter for treatment processes (Site 1 & Site 2) by bin size

Bin Size	Difference	Lower	Upper	P- value < 0.05
0.3 µm – 0.4 µm	-0.72694429	-2.6868237	1.23293511	0.9859736
0.3 µm – 0.55 µm	-1.51872808	-3.4786075	0.44115132	0.2951318
0.3 µm – 0.7 µm	-1.63614935	-3.5960287	0.32373005	0.1967611
0.3 µm – 1 µm	-2.12895888	-4.0888383	-0.16907949	**0.0216302**
0.3 µm – 1.3 µm	-2.37868911	-4.3385685	-0.41880971	**0.0055586**
0.3 µm – 1.6 µm	-1.59952568	-3.5594051	0.36035372	0.2245765
0.3 µm – 2.2 µm	-1.53375462	-3.4936340	0.42612478	0.2810665
0.3 µm – 3 µm	-1.82223115	-3.7821105	0.13764825	0.0933003
0.3 µm – 4 µm	-2.04900494	-4.0088843	-0.08912554	**0.0324430**
0.3 µm – 5.5 µm	-2.59685232	-4.5567317	-0.63697292	**0.0015406**

0.3 µm – 7 µm	-2.95307006	-4.9129495	-0.99319066	**0.0001637**
0.3 µm – 10 µm	-4.15982877	-6.1197082	-2.19994937	**0.0000000**
0.4 µm – 0. 55 µm	-0.79178379	-2.7516632	1.16809561	0.9722566
0.4 µm – 0.7 µm	-0.90920506	-2.8690845	1.05067434	0.9250343
0.4 µm – 1 µm	-1.40201460	-3.3618940	0.55786480	0.4175633
0.4 µm – 1.3 µm	-1.65174482	-3.6116242	0.30813457	0.1857036
0.4 µm – 1.6 µm	-0.87258139	-2.8324608	1.08729800	0.9433630
0.4 µm – 2.2 µm	-0.80681033	-2.7666897	1.15306906	0.9679775
0.4 µm – 3 µm	-1.09528686	-3.0551663	0.86459254	0.7766210
0.4 µm – 4 µm	-1.32206065	-3.2819400	0.63781874	0.5116999
0.4 µm – 5.5 µm	-1.86990803	-3.8297874	0.08997137	0.0756552
0.4 µm – 7 µm	-2.22612577	-4.1860052	-0.26624638	**0.0129505**
0.4 µm – 10 µm	-3.43288448	-5.3927639	-1.47300508	**0.0000065**
0.55 µm – 0.7 µm	-0.11742127	-2.0773007	1.84245813	1.0000000
0.55 µm – 1 µm	-0.61023081	-2.5701102	1.34964859	0.9969754
0.55 µm – 1.3 µm	-0.85996103	-2.8198404	1.09991836	0.9488817
0.55 µm – 1.6 µm	-0.08079760	-2.0406770	1.87908179	1.0000000
0.55 µm – 2.2 µm	-0.01502654	-1.9749059	1.94485285	1.0000000
0.55 µm – 3 µm	-0.30350307	-2.2633825	1.65637633	0.9999979
0.55 µm – 4 µm	-0.53027686	-2.4901563	1.42960253	0.9992090
0.55 µm – 5.5 µm	-1.07812424	-3.0380036	0.88175516	0.7939375
0.55 µm – 7 µm	-1.43434198	-3.3942214	0.52553741	0.3815218
0.55 µm – 10 µm	-2.64110069	-4.6009801	-0.68122129	**0.0011767**

0.7 µm – 1 µm	-0.49280954	-2.4526889	1.46706986	0.9996194
0.7 µm – 1.3 µm	-0.74253976	-2.7024192	1.21733963	0.9833092
0.7 µm – 1.6 µm	0.03662367	-1.9232557	1.99650306	1.0000000
0.7 µm – 2,2 µm	0.10239473	-1.8574847	2.06227412	1.0000000
0.7 µm – 3 µm	-0.18608180	-2.1459612	1.77379760	1.0000000
0.7 µm – 4 µm	-0.41285559	-2.3727350	1.54702380	0.9999396
0.7 µm – 5.5 µm	-0.96070297	-2.9205824	0.99917643	0.8931688
0.7 µm – 7 µm	-1.31692071	-3.2768001	0.64295868	0.5179190
0.7 µm – 10 µm	-2.52367942	-4.4835588	-0.56380002	**0.0023900**
1 µm – 1.3 µm	-0.24973023	-2.2096096	1.71014917	0.9999998
1 µm – 1.6 µm	0.52943320	-1.4304462	2.48931260	0.9992213
1 µm – 2.2 µm	0.59520426	-1.3646751	2.55508366	0.9976008
1 µm – 3 µm	0.30672774	-1.6531517	2.26660713	0.9999977
1 µm – 4 µm	0.07995394	-1.8799255	2.03983334	1.0000000
1 µm – 5.5 µm	-0.46789343	-2.4277728	1.49198596	0.9997759
1 µm – 7 µm	-0.82411118	-2.7839906	1.13576822	0.9624641
1 µm – 10 µm	-2.03086988	-3.9907493	-0.07099049	**0.0354882**
1.3 µm – 1.6 µm	0.77916343	-1.1807160	2.73904283	0.9755054
1.3 µm – 2.2 µm	0.84493449	-1.1149449	2.80481388	0.9549429
1.3 µm – 3 µm	0.55645796	-1.4034214	2.51633736	0.9987346
1.3 µm – 4 µm	0.32968417	-1.6301952	2.28956357	0.9999948
1.3 µm – 5.5 µm	-0.21816321	-2.1780426	1.74171619	1.0000000
1.3 µm – 7 µm	-0.57438095	-2.5342603	1.38549845	0.9982854
1.3 µm – 10 µm	-1.78113966	-3.7410191	0.17873974	0.1111330

1.6 µm – 2.2 µm	0.06577106	-1.8941083	2.02565045	1.0000000
1.6 µm – 3 µm	-0.22270547	-2.1825849	1.73717393	0.9999999
1.6 µm – 4 µm	-0.44947926	-2.4093587	1.51040014	0.9998521
1.6 µm – 5.5 µm	-0.99732664	-2.9572060	0.96255276	0.8660849
1.6 µm – 7 µm	-1.35354438	0.60633502	0.60633502	0.4739577
1.6 µm – 10 µm	-2.56030309	-4.5201825	-0.60042369	**0.0019205**
2.2 µm – 3 µm	-0.28847653	-2.2483559	1.67140287	0.9999988
2.2 µm – 4 µm	-0.51525032	-2.4751297	1.44462908	0.9994050
2.2 µm – 5.5 µm	-1.06309769	-3.0229771	0.89678170	0.8085634
2.2 µm – 7 µm	-1.41931544	-3.3791948	0.54056396	0.3980968
2.2 µm – 10 µm	2.62607415	0.6661947	4.58595354	**0.0012899**
3 µm – 4 µm	-0.22677379	-2.1866532	1.73310560	0.9999999
3 µm – 5.5 µm	-0.77462117	-2.7345006	1.18525823	0.9766010
3 µm – 7 µm	-1.13083891	-3.0907183	0.82904049	0.7388656
3 µm – 10 µm	2.33759762	0.3777182	4.29747702	**0.0070124**
4 µm – 5.5 µm	-0.54784738	-2.5077268	1.41203202	0.9989119
4 µm – 7 µm	-0.90406512	-2.8639445	1.05581428	0.9278195
4 µm – 10 µm	2.11082383	0.1509444	4.07070322	**0.0237460**
5.5 µm – 7 µm	-0.35621774	-2.3160971	1.60366165	0.9999878
5.5 µm – 10 µm	1.56297645	-0.3969029	3.52285585	0.2549372
7 µm – 10 µm	1.20675871	-0.7531207	3.16663810	0.6516262

Bold: Significant difference

In the other treatment plant (Site 3), (Table 3.21) showed that there is a significance difference in winter with a P value <2e-16 ($P < 0.05$) and the difference is between 0.3 µm and 0.55 µm, 0.7 µm, 1 µm, 1.3 µm, 1.6 µm, 2.2 µm, 3 µm, 4 µm, 5.5

µm, 7 µm and 10 µm, between 0.4 µm and 0.7 µm, 1 µm, 1.3 µm, 1.6 µm, 2.2 µm, 3 µm, 4 µm, 5.5 µm, 7 µm and 10 µm, between 0.55 µm and 3 µm, 4 µm, 5.5 µm 7 µm and 10 µm, between 0.7 µm and 4 µm, 5.5 µm, 7 µm and 10 µm, between 1 µm and 4 µm, 5.5 µm, 7 µm and 10 µm, between 1.3 µm and 7 µm and 10 µm, between 1.6 µm and 7 µm and 10 µm, between 2.2 µm and 7 µm and 10 µm, between 3 µm and 10, between 4 µm and 10 µm and between 5.5 µm and 10 µm (Table 3.22). Also, the P value of spring (Table 3.24) is <2e-16 ($P < 0.05$) and the difference is in the particulate with diameter 0.3 µm and 0.4 µm, 0.55 µm, 0.7 µm, 1 µm, 1.3 µm, 1.6 µm, 2.2 µm, 3 µm, 4 µm, 5.5 µm, 7 µm and 10 µm, particulate of diameter 0.4 µm and 0.7 µm, 1 µm, 1.3 µm, 1.6 µm, 2.2 µm, 3 µm, 4 µm, 5.5 µm, 7 µm and 10 µm, particulate size of 0.55 µm and 0.7 µm, 1 µm, 1.3 µm , 1.6 µm , 2.2 µm, 3 µm, 4 µm, 5.5 µm, 7 µm and 10 µm, between particulate size of 0.7 µm and 3 µm, 4 µm, 5.5 µm, 7 µm and 10 µm, particulate dimeter 1 µm and 3 µm, 4 µm, 5.5 µm, 7 µm and 10 µm, particulate size of 1.3 µm and 3 µm, 4 µm, 5.5 µm, 7 µm and 10 µm, between particulate size of 1.6 µm and 4 µm, 5.5 µm, 7 µm and 10 µm, particulate with 2.2 µm and 4 µm, 5.5 µm, 7 µm and 10 µm, particulate diameter of 3 µm and 7 µm and 10 µm, between particulate size 4 µm and 10 µm and between 5.5 µm and 10 µm (Table 3.25). Moreover, there is a significance difference in particulate sizes for summer with P value <2e-16 ($P < 0.05$) (Table 3.27). We found that particulate with dimeter 0.3 µm is statistically different than 0.55 µm, 0.7 µm, 1 µm, 1.3 µm, 1.6 µm, 2.2 µm, 3 µm, 4 µm, 5.5 µm, 7 µm and 10 µm, particulate size 0.4 µm is different than 1 µm, 1.3 µm, 1.6 µm, 2.2 µm, 3 µm, 4 µm, 5.5 µm, 7 µm and 10 µm. There is a difference between particulate of 0.55 µm diameter and 3 µm, 4 µm, 5.5 µm, 7 µm and 10 µm, between 0.7 µm and 3 µm, 4 µm, 5.5 µm, 7 µm and 10 µm, between particulate size of 1

µm and 5.5 µm, 7 µm and 10 µm, particulate of 1.3 µm and 5.5 µm, 7 µm and 10 µm, particulate dimeter of 1.6 µm and 4 µm, 5.5 µm, 7 µm and 10 µm, between 2.2 µm and 5.5 µm, 7 µm and 10 µm, between 3 µm and 10 µm and between 4 µm and 10 µm (Table 3.28). For fall, (Table 3.30) show that there is a significance difference in the particulate bin size and the P value is 2.44e-13 ($P < 0.05$). the difference is between particulate diameter 0.3 µm and 0.55 µm, 0.7 µm, 1 µm, 1.3 µm, 4 µm, 5.5 µm, 7 µm and 10 µm, particulate size 0.4 µm and 1 µm, 1.3 µm, 3 µm, 4 µm, 5.5 µm, 7 µm and 10 µm, particulate of diameter 0.55 µm and 5.5 µm, 7 µm, 10 µm, between 0.7 µm and 7 µm, 10 µm, between 1 µm and 10 µm, between 1.3 µm and 10 µm, between 1.6 µm and 10 µm, particulate of 2.2 µm and 10 µm, between 3 µm and 10 µm and between 4 µm and 10 µm (Table 3.31).

Table 3.20: Analysis of variance (ANOVA) test results for Winter of particulate dimeter by treatment processes (Site 3)

	Df	Sum Sq	Mean Sq	Lower	Upper	F value	P- value < 0.05
Process	1	1.12	1.118	-0.7808359	0.3019632	0.776	0.381
Residuals	76	109.51	1.441				

Table 3.21: Analysis of variance (ANOVA) test results for Winter of particulate dimeter for treatment processes (Site 3) by bin size

	Df	Sum Sq	Mean Sq	F value	P- value < 0.05
Bin Size	12	97.92	8.160	41.75	**<2e-16**
Residuals	65	12.71	0.195		

Bold: Significant difference

Table 3.22: Tukey test results for Winter of particulate dimeter for treatment processes (Site 3) by bin size

Bin Size	Difference	Lower	Upper	P- value < 0.05
0.3 µm – 0.4 µm	-0.79688987	-1.6746583	0.08087855	0.1119951
0.3 µm – 0.55 µm	-1.26135253	-2.1391209	-0.38358411	**0.0003942**
0.3 µm – 0.7 µm	-1.97767197	-2.8554404	-1.09990355	**0.0000000**
0.3 µm – 1 µm	-2.07644900	-2.9542174	-1.19868058	**0.0000000**
0.3 µm – 1.3 µm	-2.31167775	-3.1894462	-1.43390933	**0.0000000**
0.3 µm – 1.6 µm	-2.32645143	-3.2042198	-1.44868301	**0.0000000**
0.3 µm – 2.2 µm	-2.27984634	-3.1576148	-1.40207793	**0.0000000**
0.3 µm – 3 µm	-2.68059566	-3.5583641	-1.80282724	**0.0000000**
0.3 µm – 4 µm	-2.99330520	-3.8710736	-2.11553678	**0.0000000**
0.3 µm – 5.5 µm	-3.09814708	-3.9759155	-2.22037867	**0.0000000**
0.3 µm – 7 µm	-3.71237739	-4.5901458	-2.83460897	**0.0000000**
0.3 µm – 10 µm	-4.36872714	-5.2464956	-3.49095872	**0.0000000**
0.4 µm – 0. 55 µm	-0.46446266	-1.3422311	0.41330576	0.8326517
0.4 µm – 0.7 µm	-1.18078210	-2.0585505	-0.30301368	**0.0012107**
0.4 µm – 1 µm	-1.27955912	-2.1573275	-0.40179071	**0.0003042**
0.4 µm – 1.3 µm	-1.51478787	-2.3925563	-0.63701946	**0.0000093**
0.4 µm – 1.6 µm	-1.52956155	-2.4073300	-0.65179314	**0.0000074**
0.4 µm – 2.2 µm	-1.48295647	-2.3607249	-0.60518805	**0.0000150**
0.4 µm – 3 µm	-1.88370579	-2.7614742	-1.00593737	**0.0000000**
0.4 µm – 4 µm	-2.19641533	-3.0741837	-1.31864691	**0.0000000**

0.4 µm – 5.5 µm	-2.30125721	-3.1790256 -	-1.42348879	**0.0000000**
0.4 µm – 7 µm	-2.91548751	-3.7932559	-2.03771910	**0.0000000**
0.4 µm – 10 µm	-3.57183727	-4.4496057	-2.69406885	**0.0000000**
0.55 µm – 0.7 µm	-0.71631944	-1.5940879	0.16144898	0.2246792
0.55 µm – 1 µm	-0.81509647	-1.6928649	0.06267195	0.0942258
0.55 µm – 1.3 µm	-1.05032521	-1.9280936	-0.17255680	0.0067204
0.55 µm – 1.6 µm	-1.06509889	-1.9428673	-0.18733048	0.0055757
0.55 µm – 2.2 µm	-1.01849381	-1.8962622	-0.14072539	0.0099771
0.55 µm – 3 µm	-1.41924313	-2.2970115	-0.54147471	**0.0000393**
0.55 µm – 4 µm	-1.73195267	-2.6097211	-0.85418425	**0.0000003**
0.55 µm – 5.5 µm	-1.83679455	-2.7145630	-0.95902614	**0.0000001**
0.55 µm – 7 µm	-2.45102485	-3.3287933	-1.57325644	**0.0000000**
0.55 µm – 10 µm	-3.10737461	-3.9851430	-2.22960619	**0.0000000**
0.7 µm – 1 µm	-0.09877703	-0.9765454	0.77899139	0.9999999
0.7 µm – 1.3 µm	-0.33400578	-1.2117742	0.54376264	0.9827116
0.7 µm – 1.6 µm	-0.34877946	-1.2265479	0.52898896	0.9756057
0.7 µm – 2,2 µm	-0.30217437	-1.1799428	0.57559404	0.9925516
0.7 µm – 3 µm	-0.70292369	-1.5806921	0.17484473	0.2493396
0.7 µm – 4 µm	-1.01563323	-1.8934016	-0.13786481	**0.0103326**
0.7 µm – 5.5 µm	-1.12047512	-1.9982435	-0.24270670	**0.0027210**
0.7 µm – 7 µm	-1.73470542	-2.6124738	-0.85693700	**0.0000003**
0.7 µm – 10 µm	-2.39105517	-3.2688236	-1.51328675	**0.0000000**
1 µm – 1.3 µm	-0.23522875	-1.1129972	0.64253967	0.9992804

1 μm – 1.6 μm	-0.25000243	-1.1277708	0.62776599	0.9986957
1 μm – 2.2 μm	-0.20339735	-1.0811658	0.67437107	0.9998353
1 μm – 3 μm	-0.60414666	-1.4819151	0.27362176	0.4794361
1 μm – 4 μm	-0.91685620	-1.7946246	-0.03908779	**0.0327426**
1 μm – 5.5 μm	-1.02169809	-1.8994665	-0.14392967	**0.0095924**
1 μm – 7 μm	-1.63592839	-2.5136968	-0.75815997	**0.0000014**
1 μm – 10 μm	-2.29227814	-3.1700466	-1.41450972	**0.0000000**
1.3 μm – 1.6 μm	-0.01477368	-0.8925421	0.86299474	1.0000000
1.3 μm – 2.2 μm	0.03183140 -	-0.8459370	0.90959982	1.0000000
1.3 μm – 3 μm	-0.36891791	-1.2466863	0.50885051	0.9625962
1.3 μm – 4 μm	-0.68162746	-1.5593959	0.19614096	0.2920935
1.3 μm – 5.5 μm	-0.78646934	-1.6642378	0.09129908	0.1233335
1.3 μm – 7 μm	-1.40069964	-2.2784681	-0.52293122	**0.0000519**
1.3 μm – 10 μm	-2.05704939	-2.9348178	-1.17928097	**0.0000000**
1.6 μm – 2.2 μm	0.04660508	-0.8311633	0.92437350	1.0000000
1.6 μm – 3 μm	-0.35414423	-1.2319126	0.52362419	0.9725390
1.6 μm – 4 μm	-0.66685377	-1.5446222	0.21091464	0.3242277
1.6 μm – 5.5 μm	-0.77169566	-1.6494641	0.10607276	0.1409604
1.6 μm – 7 μm	-1.38592596	-2.2636944	-0.50815754	**0.0000646**
1.6 μm – 10 μm	-2.04227571	-2.9200441	-1.16450729	**0.0000000**
2.2 μm – 3 μm	-0.40074931	-1.2785177	0.47701910	0.9326666
2.2 μm – 4 μm	-0.71345886	-1.5912273	0.16430956	0.2297990
2.2 μm – 5.5 μm	-0.81830074	-1.6960692	0.05946768	0.0913538
2.2 μm – 7 μm	-1.43253104	-2.3102995	-0.55476262	**0.0000322**

2.2 µm – 10 µm	2.08888079	1.2111124	2.96664921	**0.0000000**
3 µm – 4 µm	-0.31270954	-1.1904780	0.56505888	0.9899968
3 µm – 5.5 µm	-0.41755143	-1.2953198	0.46021699	0.9116355
3 µm – 7 µm	-1.03178173	-1.9095501	-0.15401331	**0.0084703**
3 µm – 10 µm	1.68813148	0.8103631	2.56589990	**0.0000006**
4 µm – 5.5 µm	-0.10484188	-0.9826103	0.77292653	0.9999999
4 µm – 7 µm	-0.71907218	-1.5968406	0.15869623	0.2198275
4 µm – 10 µm	1.37542194	0.4976535	2.25319035	**0.0000755**
5.5 µm – 7 µm	-0.61423030	-1.4919987	0.26353812	0.4528394
5.5 µm – 10 µm	1.27058005	0.3928116	2.14834847	**0.0003458**
7 µm – 10 µm	0.65634975	-0.2214187	1.53411817	0.3482390

Bold: Significant difference

Table 3.23: Analysis of variance (ANOVA) test results for Spring of particulate dimeter by treatment processes (Site 3)

	Df	Sum Sq	Mean Sq	Lower	Upper	F value	P- value < 0.05
Process	1	1.82	1.824	-0.2242729	0.835926	1.32	0.254
Residuals	76	104.98	1.381				

Table 3.24: Analysis of variance (ANOVA) test results for Spring of particulate dimeter for treatment processes (Site 3) by bin size

	Df	Sum Sq	Mean Sq	F value	P- value < 0.05
Bin Size	12	100.78	8.399	90.59	**<2e-16**
Residuals	65	6.03	0.093		

Bold: Significant difference

Table 3.25: Tukey test results for Winter of particulate dimeter for treatment processes (Site 3) by bin size

Bin Size	Difference	Lower	Upper	P- value < 0.05
0.3 µm – 0.4 µm	-0.78137256	-1.3858834	-0.17686169	**0.0022573**
0.3 µm – 0.55 µm	-1.35159210	-0.74708122	-0.74708122	**0.0000000**
0.3 µm – 0.7 µm	-2.18086422	-2.7853751	-1.57635335	**0.0000000**
0.3 µm – 1 µm	-2.21920093	-2.8237118	-1.61469006	**0.0000000**
0.3 µm – 1.3 µm	-2.38573493	-2.9902458	-1.78122405	**0.0000000**
0.3 µm – 1.6 µm	-2.41036296	-3.0148738	-1.80585208	**0.0000000**
0.3 µm – 2.2 µm	-2.48299487	-3.0875057	-1.87848399	**0.0000000**
0.3 µm – 3 µm	-3.00050526	-3.6050161	-2.39599438	**0.0000000**
0.3 µm – 4 µm	-3.32936075	-2.72484987	-2.72484987	**0.0000000**
0.3 µm – 5.5 µm	-3.37989579	-3.9844067	-2.77538491	**0.0000000**
0.3 µm – 7 µm	-3.79247094	-4.3969818	-3.18796006	**0.0000000**
0.3 µm – 10 µm	-4.16425482	-4.7687657	-3.55974395	**0.0000000**
0.4 µm – 0. 55 µm	-0.57021953	-1.1747304	0.03429135	0.0831206
0.4 µm – 0.7 µm	-1.39949166	-2.0040025	-0.79498078	**0.0000000**
0.4 µm – 1 µm	-1.43782837	-2.0423392	-0.83331749	**0.0000000**
0.4 µm – 1.3 µm	-1.60436236	-2.2088732	-0.99985148	**0.0000000**
0.4 µm – 1.6 µm	-1.62899040	-2.2335013	-1.02447952	**0.0000000**
0.4 µm – 2.2 µm	-1.70162231	-2.3061332	-1.09711143	**0.0000000**
0.4 µm – 3 µm	-2.21913269	-2.8236436	-1.61462182	**0.0000000**
0.4 µm – 4 µm	-2.54798819	-3.1524991	-1.94347731	**0.0000000**

0.4 µm – 5.5 µm	-2.59852322	-3.2030341	-1.99401235	**0.0000000**
0.4 µm – 7 µm	-3.01109838	-3.6156093	-2.40658750	**0.0000000**
0.4 µm – 10 µm	-3.38288226	-3.9873931	-2.77837138	**0.0000000**
0.55 µm – 0.7 µm	-0.82927213	-1.4337830	-0.22476125	**0.0008785**
0.55 µm – 1 µm	-0.86760884	-1.4721197	-0.26309796	**0.0004030**
0.55 µm – 1.3 µm	-1.03414283	-1.6386537	-0.42963195	**0.0000113**
0.55 µm – 1.6 µm	-1.05877086	-1.6632817	-0.45425999	**0.0000065**
0.55 µm – 2.2 µm	-1.13140277	-1.7359137	-0.52689190	**0.0000013**
0.55 µm – 3 µm	-1.64891316	-2.2534240	-1.04440228	**0.0000000**
0.55 µm – 4 µm	-1.97776866	-2.5822795	-1.37325778	**0.0000000**
0.55 µm – 5.5 µm	-2.02830369	-2.6328146	-1.42379281	**0.0000000**
0.55 µm – 7 µm	-2.44087884	-3.0453897	-1.83636797	**0.0000000**
0.55 µm – 10 µm	-2.81266273	-3.4171736	-2.20815185	**0.0000000**
0.7 µm – 1 µm	-0.03833671	-0.6428476	0.56617417	1.0000000
0.7 µm – 1.3 µm	-0.20487070	-0.8093816	0.39964018	0.9935053
0.7 µm – 1.6 µm	-0.22949874	-0.8340096	0.37501214	0.9830305
0.7 µm – 2,2 µm	-0.30213065	-0.9066415	0.30238023	0.8796991
0.7 µm – 3 µm	-0.81964103	-1.4241519	-0.21513016	**0.0010651**
0.7 µm – 4 µm	-1.14849653	-1.7530074	-0.54398565	**0.0000009**
0.7 µm – 5.5 µm	-1.19903156	-1.8035424	-0.59452069	**0.0000003**
0.7 µm – 7 µm	-1.61160672	-2.2161176	-1.00709584	**0.0000000**
0.7 µm – 10 µm	-1.98339060	-2.5879015	-1.37887972	**0.0000000**
1 µm – 1.3 µm	-0.16653399	-0.7710449	0.43797689	0.9990561

1 μm – 1.6 μm	-0.19116203	-0.7956729	0.41334885	0.9965120
1 μm – 2.2 μm	-0.26379394	-0.8683048	0.34071694	0.9508433
1 μm – 3 μm	-0.78130432	-1.3858152	-0.17679345	**0.0022603**
1 μm – 4 μm	-1.11015982	-1.7146707	-0.50564894	**0.0000021**
1 μm – 5.5 μm	-1.16069485	-1.7652057	-0.55618398	**0.0000007**
1 μm – 7 μm	-1.57327001	-2.1777809	-0.96875913	**0.0000000**
1 μm – 10 μm	-1.94505389	-2.5495648	-1.34054301	**0.0000000**
1.3 μm – 1.6 μm	-0.02462803	-0.6291389	0.57988284	1.0000000
1.3 μm – 2.2 μm	-0.09725994	-0.7017708	0.50725093	0.9999968
1.3 μm – 3 μm	-0.61477033	-1.2192812	-0.01025945	**0.0426526**
1.3 μm – 4 μm	-0.94362583	-1.5481367	-0.33911495	**0.0000816**
1.3 μm – 5.5 μm	-0.99416086	-1.5986717	-0.38964998	**0.0000273**
1.3 μm – 7 μm	-1.40673601	-2.0112469	-0.80222514	**0.0000000**
1.3 μm – 10 μm	-1.77851990	-2.3830308	-1.17400902	**0.0000000**
1.6 μm – 2.2 μm	-0.07263191	-0.6771428	0.53187897	0.9999999
1.6 μm – 3 μm	-0.59014230	-1.1946532	0.01436858	0.0621410
1.6 μm – 4 μm	-0.91899779	-1.5235087	-0.31448691	**0.0001378**
1.6 μm – 5.5 μm	-0.96953283	-1.5740437	-0.36502195	**0.0000467**
1.6 μm – 7 μm	-1.38210798	-1.9866189	-0.77759710	**0.0000000**
1.6 μm – 10 μm	-1.75389186	-2.3584027	-1.14938099	**0.0000000**
2.2 μm – 3 μm	-0.51751039	-1.1220213	0.08700049	0.1682520
2.2 μm – 4 μm	-0.84636588	-1.4508768	-0.24185500	**0.0006222**
2.2 μm – 5.5 μm	-0.89690092	-1.5014118	-0.29239004	**0.0002194**
2.2 μm – 7 μm	-1.30947607	-1.9139869	-0.70496519	**0.0000000**

2.2 µm – 10 µm	1.68125995	1.0767491	2.28577083	**0.0000000**
3 µm – 4 µm	-0.32885549	-0.9333664	0.27565538	0.8056060
3 µm – 5.5 µm	-0.37939053	-0.9839014	0.22512035	0.6236929
3 µm – 7 µm	-0.79196568	-1.3964766	-0.18745481	**0.0018378**
3 µm – 10 µm	1.16374957	0.5592387	1.76826044	**0.0000006**
4 µm – 5.5 µm	-0.05053504	-0.6550459	0.55397584	1.0000000
4 µm – 7 µm	-0.46311019	-1.0676211	0.14140069	0.3118240
4 µm – 10 µm	0.83489407	0.2303832	1.43940495	**0.0007846**
5.5 µm – 7 µm	-0.41257515	-1.0170860	0.19193573	0.4929799
5.5 µm – 10 µm	0.78435904	0.1798482	1.38886991	**0.0021306**
7 µm – 10 µm	0.37178388	-0.2327270	0.97629476	0.6532963

Bold: Significant difference

Table 3.26: Analysis of variance (ANOVA) test results for Summer of particulate dimeter by treatment processes (Site 3)

	Df	Sum Sq	Mean Sq	Lower	Upper	F value	P- value < 0.05
Process	1	5.27	5.274	-0.0004265784	1.04057	3.96	0.0502
Residuals	76	101.22	1.332				

Table 3.27: Analysis of variance (ANOVA) test results for Summer of particulate dimeter for treatment processes (Site 3) by bin size

	Df	Sum Sq	Mean Sq	F value	P- value < 0.05
Bin Size	12	90.47	7.539	30.59	**<2e-16**
Residuals	65	16.02	0.246		

Bold: Significant difference

Table 3.28: Tukey test results for Summer of particulate dimeter for treatment processes (Site 3) by bin size

Bin Size	Difference	Lower	Upper	P- value < 0.05
0.3 µm – 0.4 µm	-0.67278060	-1.65845447	0.312893261	0.4928274
0.3 µm – 0.55 µm	-1.29218920	-2.27786307	-0.306515339	**0.0018189**
0.3 µm – 0.7 µm	-1.38412370	-2.36979756	-0.398449839	**0.0005912**
0.3 µm – 1 µm	-1.95035622	-2.93603008	-0.964682355	**0.0000003**
0.3 µm – 1.3 µm	-2.18289055	-3.16856441	-1.197216688	**0.0000000**
0.3 µm – 1.6 µm	-1.67513104	-2.66080490	-0.689457172	**0.0000132**
0.3 µm – 2.2 µm	-1.99567001	-2.98134387	-1.009996148	**0.0000002**
0.3 µm – 3 µm	-2.46454370	-3.45021756	-1.478869833	**0.0000000**
0.3 µm – 4 µm	-2.84368191	-3.82935577	-1.858008043	**0.0000000**
0.3 µm – 5.5 µm	-3.41489928	-4.40057314	-2.429225413	**0.0000000**
0.3 µm – 7 µm	-3.44108125	-2.455407387	-2.455407387	**0.0000000**
0.3 µm – 10 µm	-3.84176583	-4.82743969	-2.856091965	**0.0000000**
0.4 µm – 0. 55 µm	-0.61940860	-1.60508246	0.366265263	0.6217688
0.4 µm – 0.7 µm	-0.71134310	-1.69701696	0.274330764	0.4035764
0.4 µm – 1 µm	-1.27757562	-2.26324948	-0.291901752	**0.0021649**
0.4 µm – 1.3 µm	-1.51010995	-2.49578381	-0.524436085	**0.0001184**
0.4 µm – 1.6 µm	-1.00235043	-1.98802430	-0.016676569	**0.0426738**
0.4 µm – 2.2 µm	-1.32288941	-2.30856327	-0.337215545	**0.0012564**
0.4 µm – 3 µm	-1.79176309	-2.77743696	-0.806089230	**0.0000027**
0.4 µm – 4 µm	-2.17090130	-3.15657517	-1.185227440	**0.0000000**

0.4 µm – 5.5 µm	-2.74211867	-3.72779254	-1.756444811	**0.0000000**
0.4 µm – 7 µm	-2.76830065	-3.75397451	-1.782626784	**0.0000000**
0.4 µm – 10 µm	-3.16898523	-4.15465909	-2.183311363	**0.0000000**
0.55 µm – 0.7 µm	-0.09193450	-1.07760836	0.893739364	1.0000000
0.55 µm – 1 µm	-0.65816702	-1.64384088	0.327506848	0.5279192
0.55 µm – 1.3 µm	-0.89070135	-1.87637521	0.094972514	0.1159171
0.55 µm – 1.6 µm	-0.38294183	-1.36861570	0.602732030	0.9795718
0.55 µm – 2.2 µm	-0.70348081	-1.68915467	0.282193054	0.4212493
0.55 µm – 3 µm	-1.17235449	-2.15802836	-0.186680631	**0.0072740**
0.55 µm – 4 µm	-1.55149270	-2.53716657	-0.565818840	**0.0000688**
0.55 µm – 5.5 µm	-2.12271007	-3.10838394	-1.137036211	**0.0000000**
0.55 µm – 7 µm	-2.14889205	-3.13456591	-1.163218185	**0.0000000**
0.55 µm – 10 µm	-2.54957663	-3.53525049	-1.563902763	**0.0000000**
0.7 µm – 1 µm	-0.56623252	-1.55190638	0.419441347	0.7442760
0.7 µm – 1.3 µm	-0.79876685	-1.78444071	0.186907014	0.2336739
0.7 µm – 1.6 µm	-0.29100733	-1.27668120	0.694666530	0.9981611
0.7 µm – 2,2 µm	-0.61154631	-1.59722017	0.374127554	0.6406009
0.7 µm – 3 µm	-1.08041999	-2.06609386	-0.094746131	**0.0195674**
0.7 µm – 4 µm	-1.45955820	-2.44523207	-0.473884341	**0.0002276**
0.7 µm – 5.5 µm	-2.03077557	-3.01644944	-1.045101712	**0.0000001**
0.7 µm – 7 µm	-2.05695755	-3.04263141	-1.071283685	**0.0000001**
0.7 µm – 10 µm	-2.45764213	-3.44331599	-1.471968263	**0.0000000**
1 µm – 1.3 µm	-0.23253433	-1.21820820	0.753139530	0.9998017

1 μm – 1.6 μm	0.27522518	-0.71044868	1.260899046	0.9989235
1 μm – 2.2 μm	-0.04531379	-1.03098766	0.940360070	1.0000000
1 μm – 3 μm	-0.51418748	-1.49986134	0.471486385	0.8454669
1 μm – 4 μm	-0.89332569	-1.87899955	0.092348175	0.1134251
1 μm – 5.5 μm	-1.46454306	-2.45021692	-0.478869195	**0.0002135**
1 μm – 7 μm	-1.49072503	-2.47639890	-0.505051169	**0.0001523**
1 μm – 10 μm	-1.89140961	-2.87708347	-0.905735747	**0.0000007**
1.3 μm – 1.6 μm	0.50775952	0.47791435	1.493433379	0.8561875
1.3 μm – 2.2 μm	0.18722054	-0.79845332	1.172894403	0.9999802
1.3 μm – 3 μm	-0.28165314	-1.26732701	0.704020718	0.9986541
1.3 μm – 4 μm	-0.66079135	-1.64646522	0.324882508	0.5215864
1.3 μm – 5.5 μm	-1.23200873	-2.21768259	-0.246334862	**0.0036936**
1.3 μm – 7 μm	-1.25819070	-2.24386456	-0.272516836	**0.0027218**
1.3 μm – 10 μm	-1.65887528	-2.64454914	-0.673201414	**0.0000164**
1.6 μm – 2.2 μm	-0.32053898	-1.30621284	0.665134887	0.9955027
1.6 μm – 3 μm	-0.78941266	-1.77508652	0.196261202	0.2492081
1.6 μm – 4 μm	-1.16855087	-2.15422473	-0.182877008	**0.0075884**
1.6 μm – 5.5 μm	-1.73976824	-2.72544210	-0.754094378	**0.0000054**
1.6 μm – 7 μm	-1.76595021	-2.75162408	-0.780276352	**0.0000038**
1.6 μm – 10 μm	-2.16663479	-3.15230866	-1.180960930	**0.0000000**
2.2 μm – 3 μm	-0.46887368	-1.45454755	0.516800178	0.9116452
2.2 μm – 4 μm	-0.84801189	-1.83368576	0.137661969	0.1629376
2.2 μm – 5.5 μm	-1.41922927	-2.40490313	-0.433555402	**0.0003804**
2.2 μm – 7 μm	-1.44541124	-2.43108510	-0.459737376	**0.0002728**

2.2 µm – 10 µm	1.84609582	0.86042195	2.831769680	**0.0000013**
3 µm – 4 µm	-0.37913821	-1.36481207	0.606535653	0.9811387
3 µm – 5.5 µm	-0.95035558	-1.93602944	0.035318283	0.0692224
3 µm – 7 µm	-0.97653755	-1.96221142	0.009136309	0.0544634
3 µm – 10 µm	1.37722213	0.39154827	2.362895995	**0.0006443**
4 µm – 5.5 µm	-0.57121737	-1.55689123	0.414456492	0.7334264
4 µm – 7 µm	-0.59739934	-1.58307321	0.388274519	0.6740107
4 µm – 10 µm	0.99808392	0.01241006	1.983757786	**0.0444518**
5.5 µm – 7 µm	-0.02618197	-1.01185584	0.959491890	1.0000000
5.5 µm – 10 µm	0.42686655	-0.55880731	1.412540415	0.9534488
7 µm – 10 µm	0.40068458	-0.58498928	1.386358441	0.9709050

Bold: Significant difference

Table 3.29: Analysis of variance (ANOVA) test results for Fall of particulate dimeter by treatment processes (Site 3)

	Df	Sum Sq	Mean Sq	Lower	Upper	F value	P- value < 0.05
Process	1	12.02	12.023	0.308528	1.261902	10.76	**0.00156**
Residuals	76	84.89	1.117				

Bold: Significant difference

Table 3.30: Analysis of variance (ANOVA) test results for Fall of particulate dimeter for treatment processes (Site 3) by bin size

	Df	Sum Sq	Mean Sq	F value	P- value < 0.05
Bin Size	12	69.01	5.751	13.39	**2.44e-13**
Residuals	65	27.91	0.429		

Bold: Significant difference

Table 3.31: Tukey test results for Fall of particulate dimeter for treatment processes (Site 3) by bin size

Bin Size	Difference	Lower	Upper	P- value < 0.05
0.3 µm – 0.4 µm	-0.86517867	-2.1660947	0.43573732	0.5343030
0.3 µm – 0.55 µm	-1.52608076	-2.8269967	-0.22516477	**0.0086920**
0.3 µm – 0.7 µm	-1.70771451	-3.0086305	-0.40679852	**0.0017821**
0.3 µm – 1 µm	-2.33931304	-3.6402290	-1.03839705	**0.0000035**
0.3 µm – 1.3 µm	-2.51417653	-3.8150925	-1.21326055	**0.0000006**
0.3 µm – 1.6 µm	-1.94306967	-3.2439857	-0.64215368	**0.0001935**
0.3 µm – 2.2 µm	-1.99859104	-3.2995070	-0.69767505	**0.0001121**
0.3 µm – 3 µm	-2.22219207	-3.5231081	-0.92127608	**0.0000117**
0.3 µm – 4 µm	-2.41073303	-3.7116490	-1.10981704	**0.0000016**
0.3 µm – 5.5 µm	-2.90447457	-4.2053906	-1.60355858	**0.0000000**
0.3 µm – 7 µm	-3.09352883	-4.3944448	-1.79261285	**0.0000000**
0.3 µm – 10 µm	-3.85345656	-5.1543725	-2.55254057	**0.0000000**
0.4 µm – 0. 55 µm	-0.66090208	-1.9618181	0.64001390	0.8673854
0.4 µm – 0.7 µm	-0.84253584	-2.1434518	0.45838015	0.5759085
0.4 µm – 1 µm	-1.47413437	-2.7750504	-0.17321838	**0.0133242**
0.4 µm – 1.3 µm	-1.64899786	-2.9499139	-0.34808188	**0.0030169**
0.4 µm – 1.6 µm	-1.07789099	-2.3788070	0.22302499	0.2057868
0.4 µm – 2.2 µm	-1.13341237	-2.4343284	0.16750362	0.1499044
0.4 µm – 3 µm	-1.35701340	-2.6579294	-0.05609741	**0.0331945**
0.4 µm – 4 µm	-1.54555436	-2.8464703	-0.24463837	**0.0073820**

0.4 µm – 5.5 µm	-2.03929590	-3.3402119	-0.73837991	**0.0000749**
0.4 µm – 7 µm	-2.22835016	-3.5292661	-0.92743417	**0.0000110**
0.4 µm – 10 µm	-2.98827789	-4.2891939	-1.68736190	**0.0000000**
0.55 µm – 0.7 µm	-0.18163375	-1.4825497	1.11928223	0.9999994
0.55 µm – 1 µm	-0.81323228	-2.1141483	0.48768370	0.6295510
0.55 µm – 1.3 µm	-0.98809578	-2.2890118	0.31282021	0.3245748
0.55 µm – 1.6 µm	-0.41698891	-1.7179049	0.88392708	0.9960538
0.55 µm – 2.2 µm	-0.47251028	-1.7734263	0.82840570	0.9882210
0.55 µm – 3 µm	-0.69611132	-1.9970273	0.60480467	0.8220658
0.55 µm – 4 µm	-0.88465227	-2.1855683	0.41626371	0.4987972
0.55 µm – 5.5 µm	-1.37839381	-2.6793098	-0.07747783	**0.0282570**
0.55 µm – 7 µm	-1.56744808	-2.8683641	-2.8683641	**0.0061311**
0.55 µm – 10 µm	-2.32737580	-3.6282918	-1.02645982	**0.0000039**
0.7 µm – 1 µm	-0.63159853	-1.9325145	0.66931746	0.8993787
0.7 µm – 1.3 µm	-0.80646202	-2.1073780	0.49445396	0.6418139
0.7 µm – 1.6 µm	-0.23535516	-1.5362711	1.06556083	0.9999884
0.7 µm – 2,2 µm	-0.29087653	-1.5917925	1.01003946	0.9998865
0.7 µm – 3 µm	-0.51447756	-1.8153935	0.78643843	0.9764921
0.7 µm – 4 µm	-0.70301852	-2.0039345	0.59789747	0.8123439
0.7 µm – 5.5 µm	-1.19676006	-2.4976760	0.10415593	0.1013430
0.7 µm – 7 µm	-1.38581432	-2.6867303	-0.08489834	**0.0267047**
0.7 µm – 10 µm	-2.14574205	-3.4466580	-0.84482606	**0.0000256**
1 µm – 1.3 µm	-0.17486350	-1.4757795	1.12605249	0.9999996

1 μm – 1.6 μm	0.39624337	-0.9046726	1.69715936	0.9975340
1 μm – 2.2 μm	0.34072200	-0.9601940	1.64163799	0.9994269
1 μm – 3 μm	0.11712097	-1.1837950	1.41803695	1.0000000
1 μm – 4 μm	-0.07141999	-1.3723360	1.22949600	1.0000000
1 μm – 5.5 μm	-0.56516153	-1.8660775	0.73575446	0.9523867
1 μm – 7 μm	-0.75421579	-2.0551318	0.54670019	0.7329121
1 μm – 10 μm	-1.51414352	-2.8150595	-0.21322753	**0.0095993**
1.3 μm – 1.6 μm	0.57110687	-0.7298091	1.87202286	0.9486989
1.3 μm – 2.2 μm	0.51558549	-0.7853305	1.81650148	0.9760925
1.3 μm – 3 μm	0.29198446	-1.0089315	1.59290045	0.9998819
1.3 μm – 4 μm	0.10344351	-1.1974725	1.40435949	1.0000000
1.3 μm – 5.5 μm	-0.39029803	-1.6912140	0.91061795	0.9978598
1.3 μm – 7 μm	-0.57935230	-1.8802683	0.72156369	0.9432565
1.3 μm – 10 μm	-1.33928003	-2.6401960	-0.03836404	**0.0378615**
1.6 μm – 2.2 μm	-0.05552138	-1.3564374	1.24539461	1.0000000
1.6 μm – 3 μm	-0.27912241	-1.5800384	1.02179358	0.9999266
1.6 μm – 4 μm	-0.46766336	-1.7685794	0.83325262	0.9892005
1.6 μm – 5.5 μm	-0.96140490	-2.2623209	0.33951108	0.3663231
1.6 μm – 7 μm	-1.15045917	-2.4513752	0.15045682	0.1353266
1.6 μm – 10 μm	-1.91038690	-3.2113029	-0.60947091	**0.0002658**
2.2 μm – 3 μm	-0.22360103	-1.5245170	1.07731496	0.9999934
2.2 μm – 4 μm	-0.41214199	-1.7130580	0.88877400	0.9964527
2.2 μm – 5.5 μm	-0.90588353	-2.2067995	0.39503246	0.4607107
2.2 μm – 7 μm	-1.09493779	-2.3958538	0.20597819	0.1872209

2.2 µm – 10 µm	1.85486552	0.5539495	3.15578151	**0.0004530**
3 µm – 4 µm	-0.18854096	-1.4894569	1.11237503	0.9999990
3 µm – 5.5 µm	-0.68228250	-1.9831985	0.61863349	0.8407298
3 µm – 7 µm	-0.87133676	-2.1722527	0.42957923	0.5230326
3 µm – 10 µm	1.63126449	0.3303485	2.93218048	**0.0035279**
4 µm – 5.5 µm	-0.49374154	-1.7946575	0.80717445	0.9830703
4 µm – 7 µm	-0.68279580	-1.9837118	0.61812018	0.8400566
4 µm – 10 µm	1.44272353	0.1418075	2.74363952	**0.0171417**
5.5 µm – 7 µm	-0.18905426	-1.4899703	1.11186172	0.9999990
5.5 µm – 10 µm	0.94898199	-0.3519340	2.24989798	0.3866324
7 µm – 10 µm	0.75992773	-0.5409883	2.06084371	0.7233531

Bold: Significant difference

3.4. Discussion

The current study found that total particulate matters emission from mechanical aeration processes is higher in average than bubble aeration processes which is consistent with that of Michalkiewicz et al., (2018) and Wang et al., (2018), where they found that concentration of microorganisms in the bioaerosols produced by a mechanical mixing system was higher than in the aerosols that are generated by fine-bubble aeration system due to the powerful mixing and turbulence in the surface of the treatment tank which causes the formation of a large number of bioaerosols.

Another important finding was that fall, summer and spring have higher total particulate in the aeration tanks with mechanical agitation than bubble aeration tanks when they are in separate facilities, while the mechanical agitation process is higher than bubble aeration process in summer, fall and spring when they are in the same treatment

facility. This finding was also reported by Yang et al. (2019) and Dehghani et al. (2018). A possible explanation for the switch in the order between fall and summer might be the effect of metrological factors (such as wind speed, temperature, etc.,) which have an impact on the dispersion of the particulate on the air which will affect the particulate counts at the time of sampling. Moreover, the time of sampling was not constant for each process and season, which can be one of the reasons for the order change between seasons.

Furthermore, the major diameters present in the air are the smaller particulate 0.3 µm and 0.4 µm in all processes and every season. In addition, particles matters with dimeters 0.55 µm, 0.7 µm, 1 µm, 1.3 µm, 1.6 µm, 2.2 µm, 3 µm, 4 µm, 5.5 µm, 7 µm, and 10 µm have been measured and observed in the air with variations in the count between processes and seasons due to the effect of metrological factors (such as wind speed, temperature, etc.,). In accordance with the present results, previous studies have demonstrated that the dispersal of PMs differs among WWTP depending on the type of wastewater treated, treatment process selected, and meteorological parameters. (Wang et al., 2018). Moreover, the structure, size, and concentration of microorganisms in the bioaerosols are changing based on the different stages of wastewater treatment where a higher concentration of bioaerosols in the air is noticed over mixed and aerated chambers of bioreactors where droplets are produced with a large variability of diameters (Michalkiewicz et al., 2018).

Those findings have important implications for developing deep and detailed research in the future to analyze what those particulate matter contains because these results showed the total general particulate matter, not including if they hold bacteria,

viruses, chemicals, and/or other contaminants. Understanding this major difference will help comprehend each type of contaminant dispersion and behavior in the air, which will improve the protection measures for human and environmental health. Further studies, which take these variables into account, will need to be undertaken steady starting time of sampling for each process in each season to reduce the variation in the variables that affect the number of particulate matter and their concentration particularly in such study where the environmental and metrological factors are complicated and interrelated, and it is difficult to ignore their effect on the particulate count.

CHAPTER 4

DAILY AND SEASONAL VARIATION OF PARTICULA MATTER EMISSION FROM WASTEWATER TREATMENT PLANTS

4.1. Introduction

Airborne particles in WWTPs may arise from wastewater, sludge, outside ambient air, and other sources. Identifying the origin of airborne pollutants is essential to quantify their concentrations for human health and environmental risk assessment (Yang et al., 2019). Additionally, wastewater treatment technology, aeration method, the quantity of aeration, and the type and concentration of microorganisms in the wastewater have an essential role in the concentration of PMs and bioaerosols in the surrounding air and environment (Michalkiewicz et al., 2018).

Generally, particulate matter (PMs) concentrations in the air vary due to several factors. These factors are emission sources, metrological parameters (such as temperature, relative humidity [RH], and wind speed) (Nathan, 2018), human activities, and seasonal variations (Li et al., 2019). According to Han et al., (2020), the airborne bacteria concentrations were different due to the seasonal variations. According to (Han, et al., 2019) study, they studied concentration, size distribution, population, and exposure risk from bacteria and fungi in bioaerosols of WWTPs that use anaerobic-anoxic-oxic (A2O) process, which uses the activated sludge method to treat wastewater and it is the

most widely used process in WWTPs, and they found that the airborne bacteria concentrations were different due to the seasonal variations.

Due to the potential adverse environmental impacts of the atmospheric particulate (such as PM10 and/or PM2.5), studies investigated daily, weekly, seasonal and annual variability in wastewater characteristics and emissions based on the water consumption pattern (Atinkpahoun, et al., 2018). According to (Mansha, et al., 2012), data reveals that PM2.5 measurements varied daily from 27.4 μg/m³ to 175.5 μg/m³ with an average of 83.53 μg/m³ and the observed PM2.5 concentrations were 5 and 2 times higher in winter and autumn than the prescribed limits of the United States Environmental Protection Agency (USEPA) while in summer it was 1.5 times higher from the standard limit. Moreover, they found that average daily total suspended particles (TSP) concentrations at the Karachi site ranged from 627 to 938 μg/m³ with a mean of 668 μg/m³ compared to 428–998 μg/m³ with a mean of 691 μg/m³ at the Islamabad.

Moreover, some studies conclude that bacteria-carrying particles in the air of a WWTP have a diameter between 3.3 μm and 4.7 μm, which means that they are a potential cause of infections because they can enter the lungs easily when inhaled. In addition, these small particulate can travel by the wind to several kilometers, causing potential environmental and human health issues to site workers and neighboring residents (Korzeniewska, 2011).

4.2. Materials and Methods

4.2.1. Sampling sites

The field sites used for this study consisted of three wastewater treatment plants (WWTPs) and one drinking water treatment plant (DWTP). The DWTP was used as a control for the background concentration of environmental particulate matter (PM) as compared to WWTPs. Though all the WWTPs included in this study use activated sludge treatment processes for their biological treatment, they use different methods of aeration. WWTP site 1 (Figure 4.1A), located in Mount Pleasant, SC uses bubble aeration in the activated sludge process and treats approximately 3 million gallons per day (MGD). WWTP site 2 (Figure 4.1B), also located in Mount Pleasant, SC, treats approximately 5 MGD and employs mixed methods in the same aeration tank. The injection of the air occurs through bubble aeration from the bottom of the tank and impellers from the top (surface agitation) are used for additional aeration. WWTP site 3 (Figure 4.1C) is located in Columbia, SC and serves around 60,000 customers and covers 120 square miles. The plant has a capacity of 60 MGD and treats an average of 35 MGD of wastewater. This site splits raw sewage into 2 separate treatment trains. Treatment train 1 uses surface agitation for the aeration of activated sludge tanks and the treatment train 2 uses bubble aeration in the activated sludge tanks. The drinking water treatment facility used as a control in this study (site 4, Figure 4.1D) is located in Columbia, SC and has a total treatment capacity of 23 MGD. This facility uses a combination of chemical treatment for initial coagulation followed by mixing and sedimentation, chlorine addition and then a final filtration process.

Figure 4.1: Sampling sites. Panel A, Wastewater Treatment Plant (Site 1); Panel B, Wastewater Treatment plant (Site 2); Panel C, Wastewater Treatment Plant (Site 3); Panel D, Drinking Water Treatment Plant]

4.2.2. Meteorological Data Measurement

Meteorological conditions and particulate matter concentrations were monitored at each site across winter, spring, summer, and fall seasons to examine seasonal variability in particulate emissions (Figures 4.2 – 4.5). During each seasonal sampling event, monitoring occurred across three consecutive days to further examine daily variation in particulate emissions. Meteorological conditions (i.e., wind speed, wind direction, temperature, relative humidity, and barometric pressure) were measured using the Kestrel 4500 Pocket Weather Tracker and the Kestrel 5500 Weather Meter. The Kestrel 4500 Pocket Weather Tracker was placed at the highest location at the center of the testing area to measure the overall prevailing site meteorological parameters across the entire site and sampling period. The Kestrel 5500 Weather Meter was used to collect

individual metrological data at each unique sampling location within each field site. Individual meteorological measurements were used to examine within site variation across the different sampling locations to better model particulate emissions and dispersion.

4.2.3. Measurement of Particulate Matter Emissions

To measure particulate emissions, particle concentrations were obtained using the TSI Model 3330 Optical Particle Sizer Spectrometer (OPS). The TSI instrument has 12 channels that separate particles into 12 particle diameters (0.3, 0.4, 0.55, 0.7, 1, 1.3, 1.6, 2.2, 3, 4, 5.5, 7 and 10 micrometers [μm]). The sampling duration was one hour at each sampling location within each site, and the sampling location was varied each day based on the prevailing wind direction measured using the Kestrel 4500 to ensure isolation of downwind and upwind locations. Based on wind direction, one TSI instrument was placed in the upwind location while another TSI unit was placed in the downwind location to provide simultaneous measurement of upwind and downwind particulate matter concentration (Figures 4.2 - 4.5).

Figure 4.2: Field site 1 sampling location by seasons. Panel A, winter; Panel B, summer; Panel C, spring; Panel D, fall. White circles show the locations of the TSI upwind locations; red rectangles show the locations of the TSI downwind locations; Yellow stars represent the location of Kestrel weather meter measurements).

Figure 4.3: Field site 2 sampling location by seasons. Panel A, winter; Panel B, summer; Panel C, spring; Panel D, fall. White circles show the locations of the TSI upwind locations; red rectangles show the locations of the TSI downwind locations; Yellow stars represent the location of Kestrel weather meter measurements).

Figure 4.4: Field site 3 sampling location by seasons. Panel A, winter; Panel B, summer; Panel C, spring; Panel D, fall. White circles show the locations of the TSI upwind locations; red rectangles show the locations of the TSI downwind locations; Yellow stars represent the location of Kestrel weather meter measurements).

Figure 4.5: Field site 4 sampling location by seasons. Panel A, spring; Panel B, fall; Panel White circles show the locations of the TSI upwind locations; red rectangles show the locations of the TSI downwind locations; Yellow stars represent the location of Kestrel weather meter measurements).

4.2.4. Statistical Analysis

RStudio software (Version 1.2.5019, 2009-2019 RStudio, Inc) was used for the statistical analysis of the data. Analysis of variance (ANOVA) and Tukey tests were utilized to find the significant difference between study sites, seasons, the process of treatment and different particulate diameters. In addition, Tableau 2020.2.1 software was used to generate figures for the results. In this chapter, we will examine the daily statistical differences between treatment sites and between all sites together using total particulate counts and particulate count for each diameter.

4.3. Results

4.3.1. Seasonal Variation in Total PM Counts

Daily measurements for particulate matters count showed that the third day is higher in Site 1 (Figure 4.6) on winter (22846483), summer (18308224), and spring (10088296) where the second day is higher in fall (8699839). Similarly, the third day is higher in Site 2 in summer (17137069), spring (12672578), and winter (12884192) while the second day is higher in fall (27511373) (Figure 4.7). In addition, for Site 3 we found that the first day is higher in the total particulate in winter (22871352) and fall (16509428), where the second day is higher in summer (19899225) and the third day on spring (22079806) (Figure 4.8). Moreover, Site 4 (Figure 4.9) showed that the first day is higher in fall (4890134) and the third day in spring (3981577).

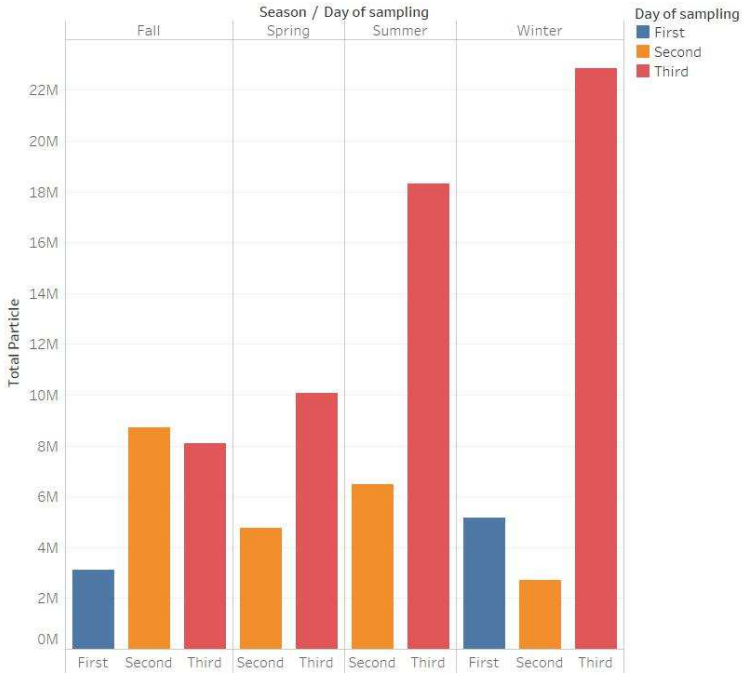

Figure 4.6: Daily total particulate matter for Site 1 by seasons

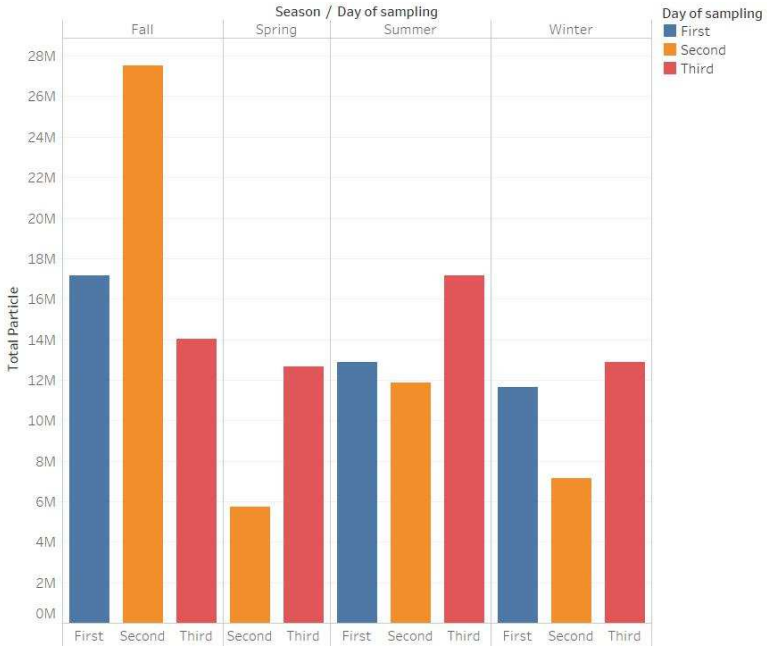

Figure 4.7: Daily total particulate matter for Site 2 by seasons

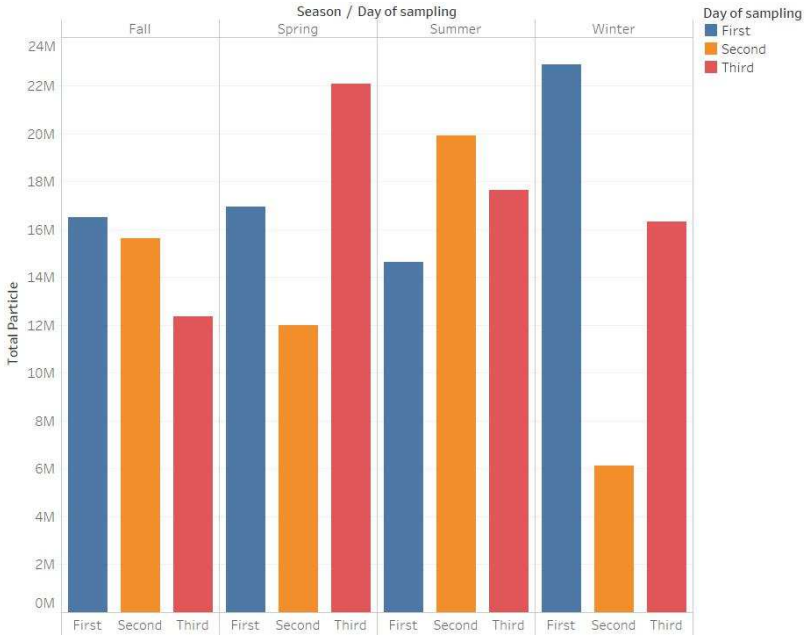

Figure 4.8: Daily total particulate matter for Site 3 by seasons

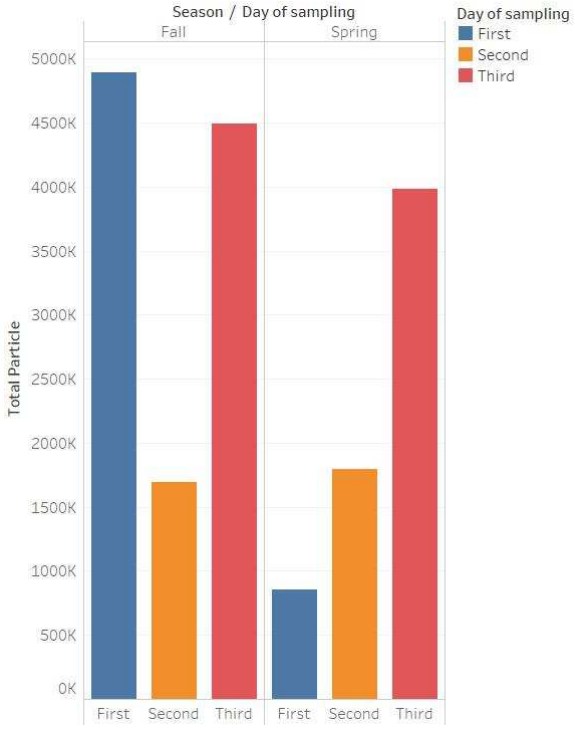

Figure 4.9: Daily total particulate matter for Site 4 by seasons

4.3.2. Spatial Variation in Total PM Counts

For seasonal daily variation between sites, we found that the third day is higher in Site 1 (22846483) and Site 2 (12884192) in winter (Figure 4.10) while the first day is higher in Site 3 (22871352). For spring, the third day was higher in all sites, as shown in (Figure 4.11). Furthermore, the third day is higher in Site 1 (18308224) and Site 2 (17137069), and the second day is the highest on Site 3 (19899225) in summer (Figure 4.12). In fall (Figure 4.13), the second day is higher in Site 1 (8699839) and Site 2 (27511373), where the first day is higher in Site 3 (16509428) and Site 4 (4890134).

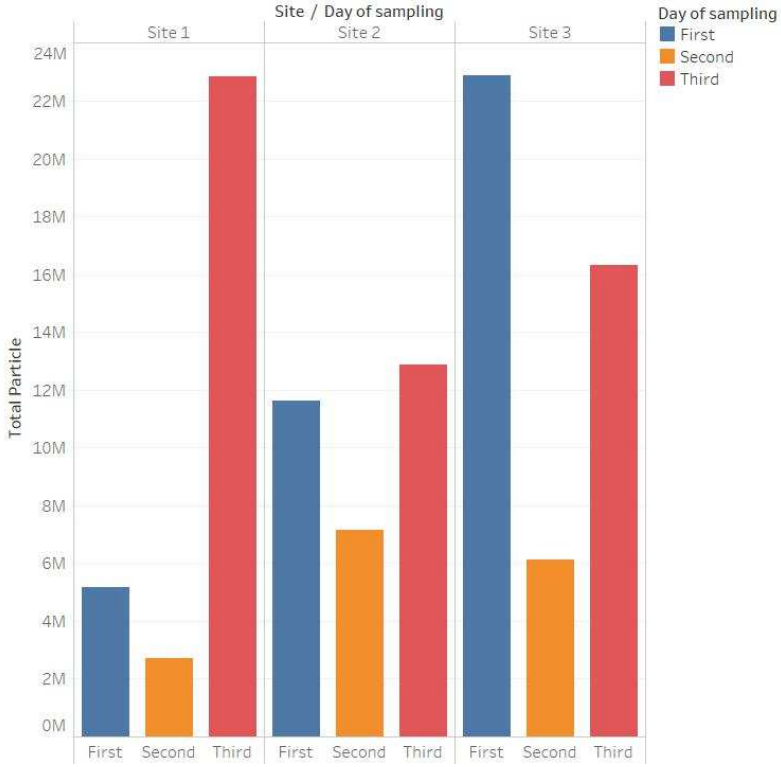

Figure 4.10: Daily total particulate matter for winter by sites

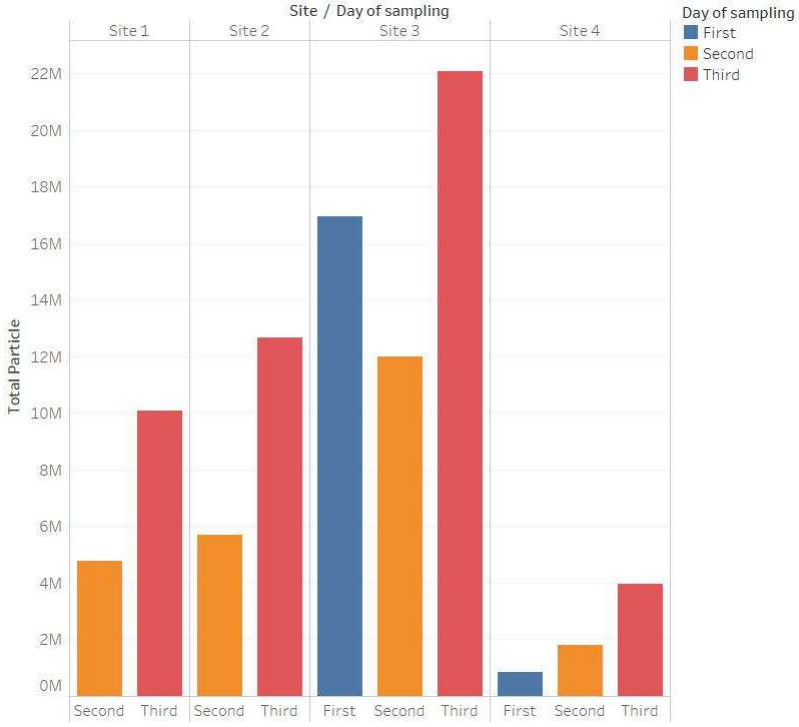

Figure 4.11: Daily total particulate matter for spring by sites

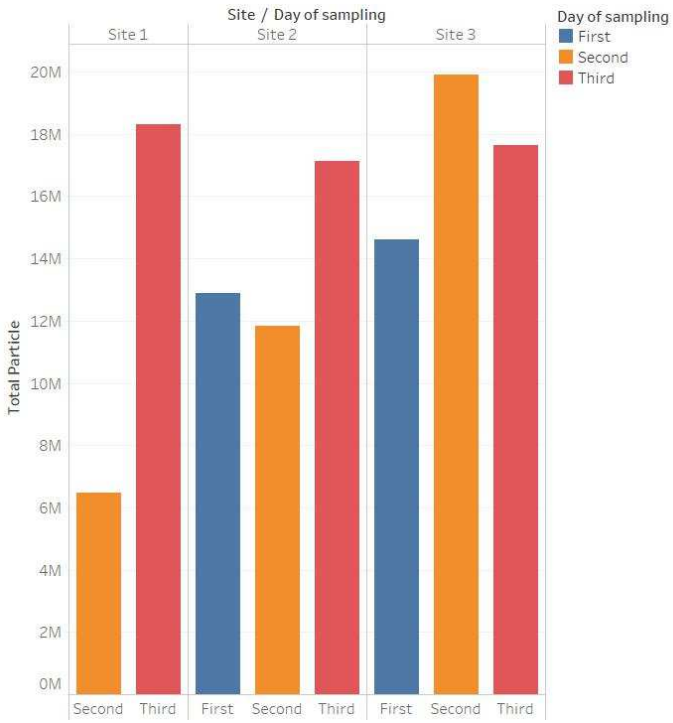

Figure 4.12: Daily total particulate matter for summer by sites

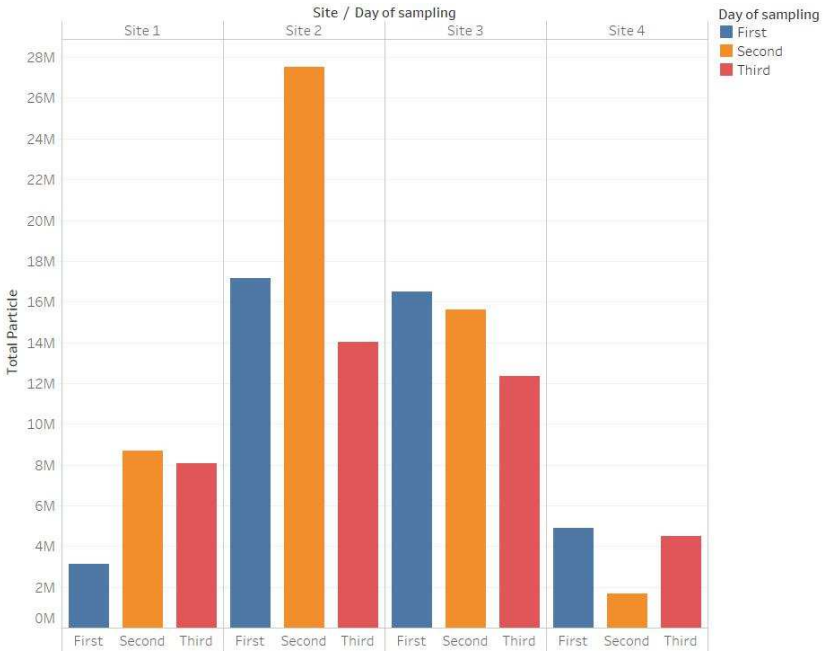

Figure 4.13: Daily total particulate matter for fall by sites

4.3.3. Spatial and Temporal Variation by PM Diameter

For daily particulate size diversity, particulate with a diameter of 0.3 μm and 0.4 μm are the higher in each day in all sites for every season (Figures 4.14, 4.16, 4.18, 4.20, 4.22, 4.24, 4.26 & 4.28). Thus, we eliminate those smaller sizes to assess the presence of the other particulate diameter measured. Results for the difference in each site by season showed that the third day on winter for Site 1 (Figure 4.15) has higher particulate sizes variety with higher abundance of particulate of 0.55 μm, 2.2 μm, and 5.5 μm. For Site 2 (Figure 4.17), the second day on fall has the highest particulate sizes diversity in the air compared to the other seasons and the highest particulate sizes measured are 2.2 μm, 3 μm, 4 μm, and 5.5 μm. Similarly, the first day on fall has the highest particulate size variety for Site 3 (Figure 4.19) with higher particulate of 1.6 μm, 2.2 μm, 3 μm, and 4 μm. In addition, the particulate sizes distribution is slightly equivalent in Site 4 (Figure 4.21) on fall and spring with more particulate of 0.55 μm and 0.7 μm. On the other hand, we compared the daily seasonal variation particulate distribution between sites in the air, and we found that the third day on winter for Site 1 (Figure 4.23) is the highest with a higher abundance of particulate of 0.55 μm, 2.2 μm, and 5.5 μm. For Spring, the third day for Site 2 and Site 3 has a higher variety on particulate diameter and with more particles of 0.55 μm (Figure 4.25). Moreover, the second day and third day in Site 3 are almost equal in summer (Figure 4.27) with higher particulate on diameter 0.55 μm and 0.7 μm. Furthermore, the second day on fall in Site 2 (Figure 4.29) has the highest particulate sizes diversity in the air and the highest particulate sizes measured are 2.2 μm, 3 μm, 4 μm, and 5.5 μm.

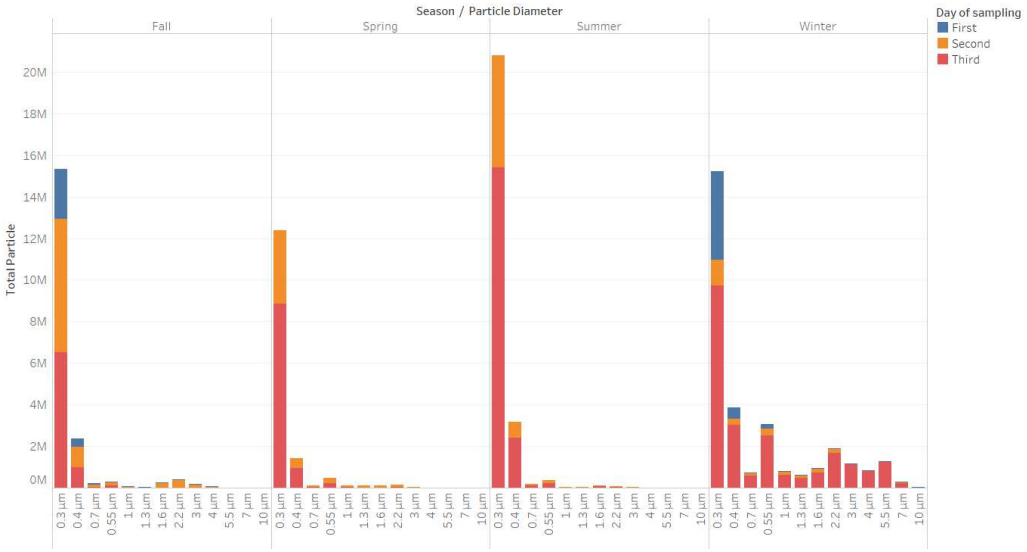

Figure 4.14: Daily total particulate matter by diameter for Site 1 by seasons

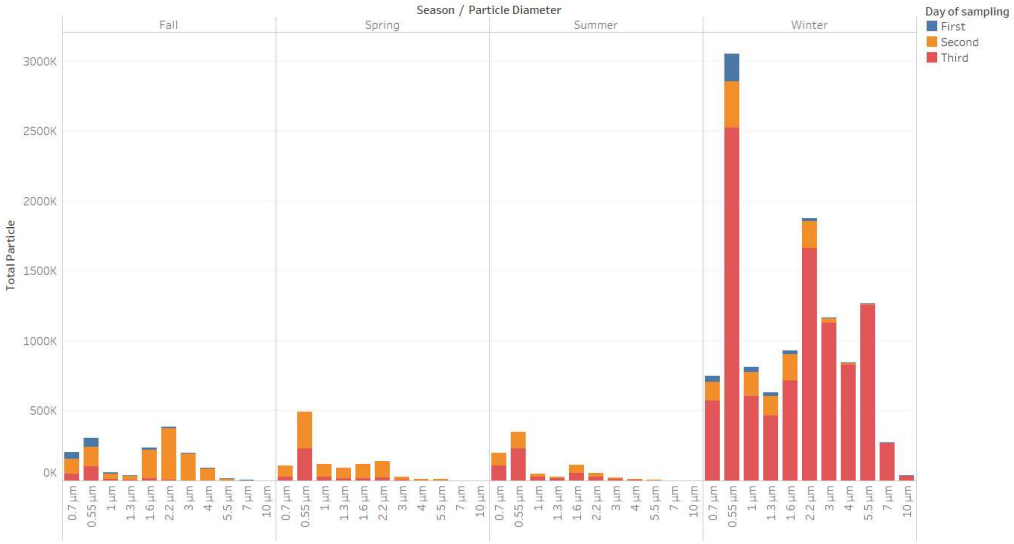

Figure 4.15: Daily total particulate matter by diameter for Site 1 by seasons (excluding 0.3 µm & 0.4 µm)

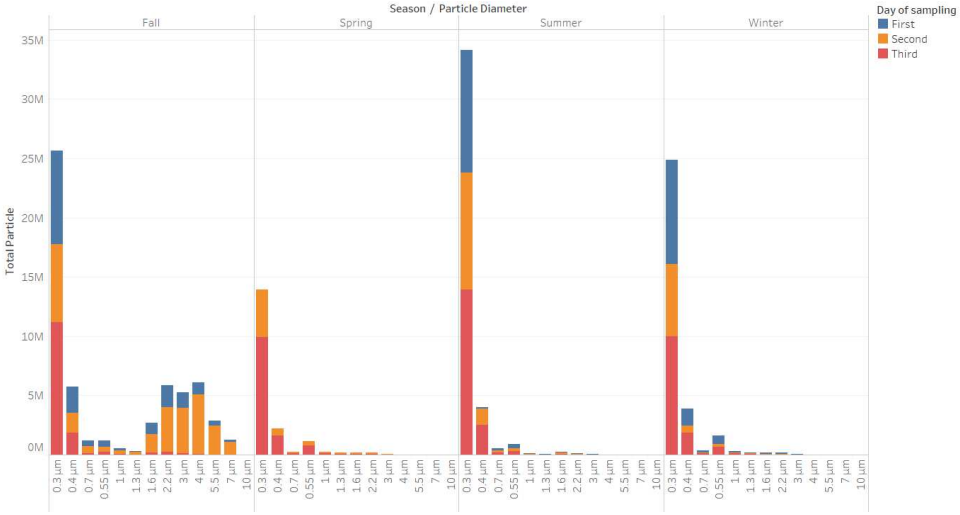

Figure 4.16: Daily total particulate matter by diameter for Site 2 by seasons

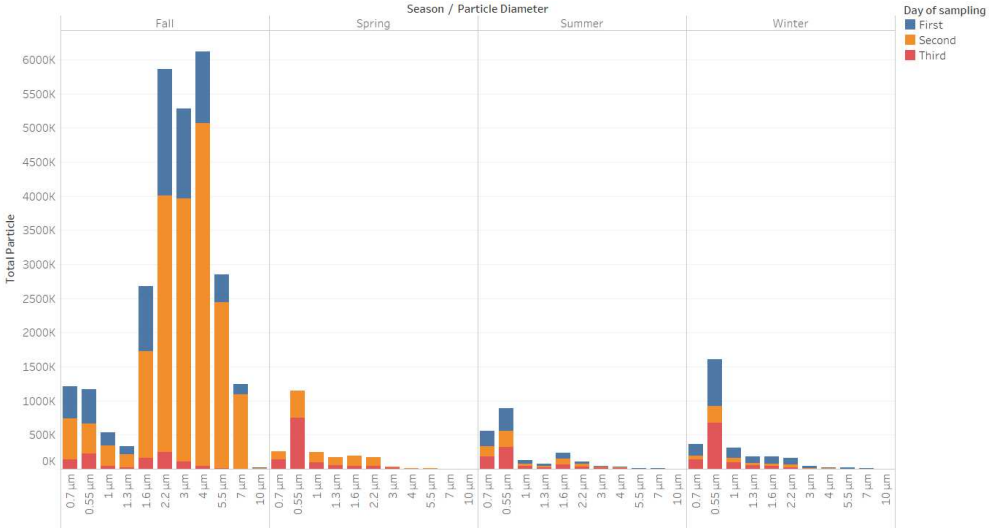

Figure 4.17: Daily total particulate matter by diameter for Site 2 by seasons (excluding 0.3 µm & 0.4 µm)

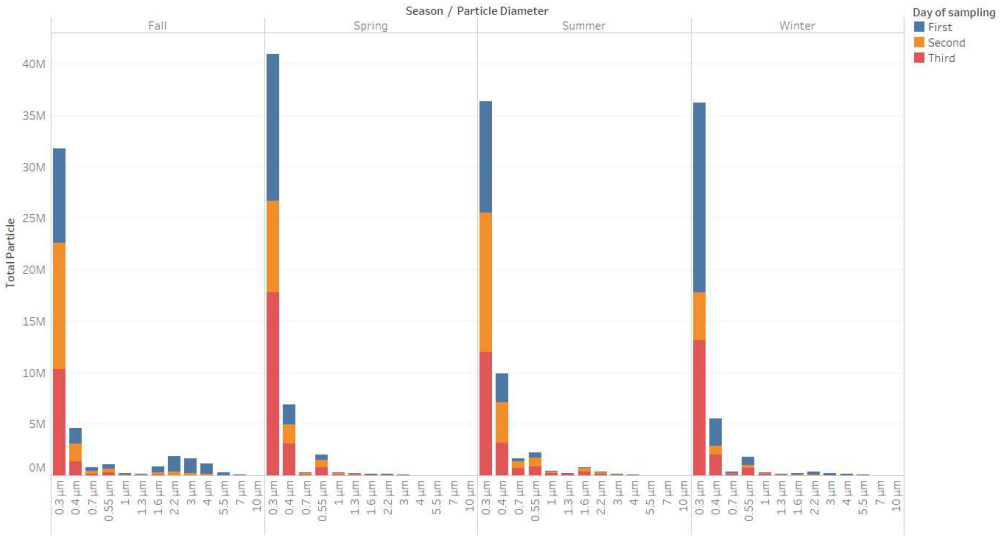

Figure 4.18: Daily total particulate matter by diameter for Site 3 by seasons

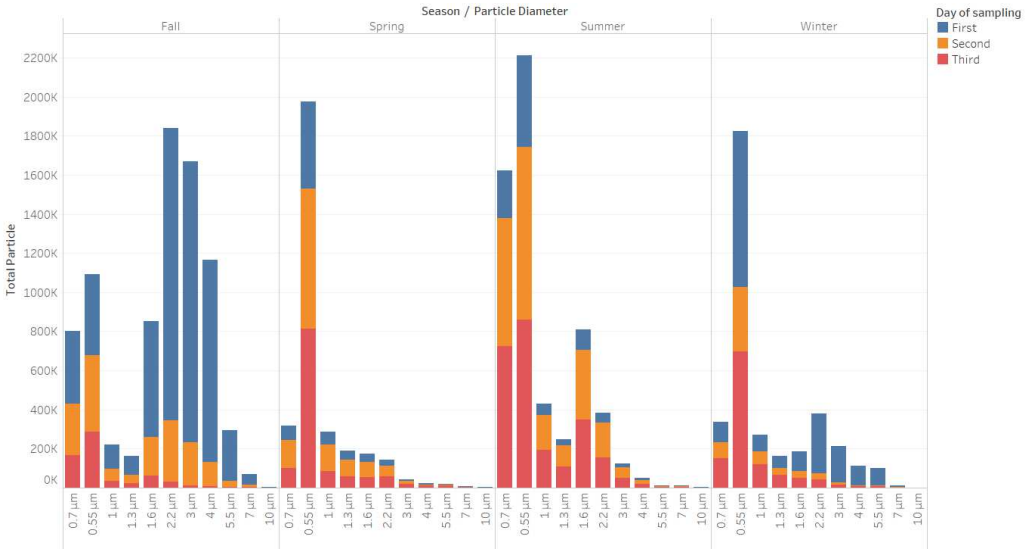

Figure 4.19: Daily total particulate matter by diameter for Site 3 by seasons (excluding 0.3 µm & 0.4 µm)

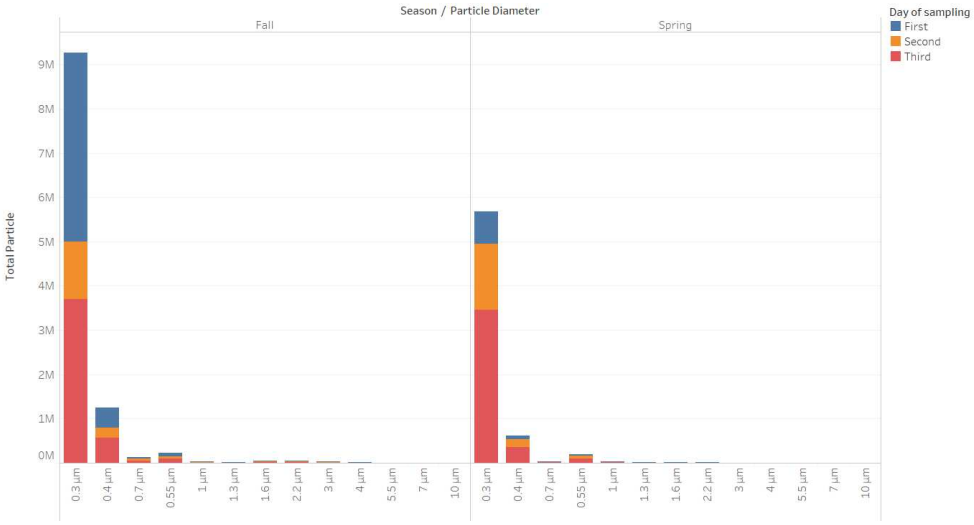

Figure 4.20: Daily total particulate matter by diameter for Site 4 by seasons

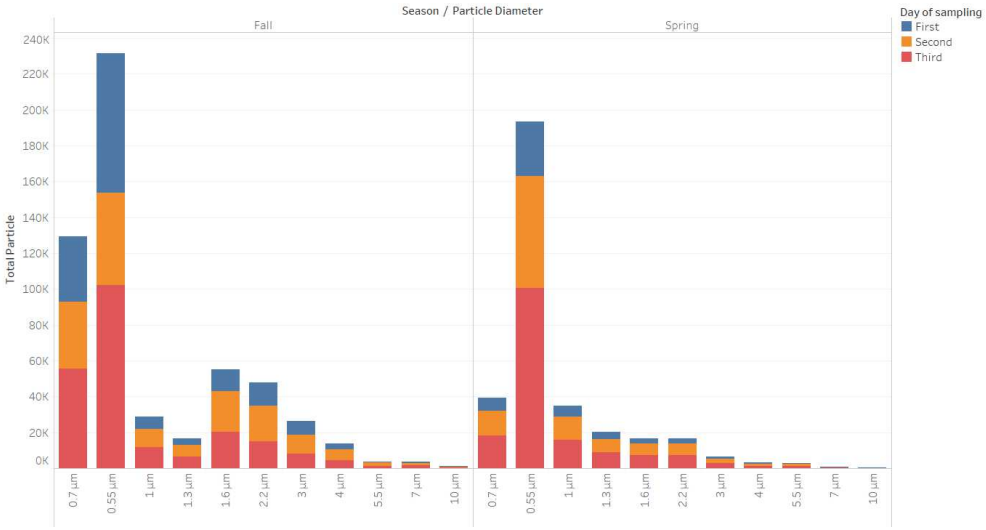

Figure 4.21: Daily total particulate matter by diameter for Site 4 by seasons (excluding 0.3 µm & 0.4 µm)

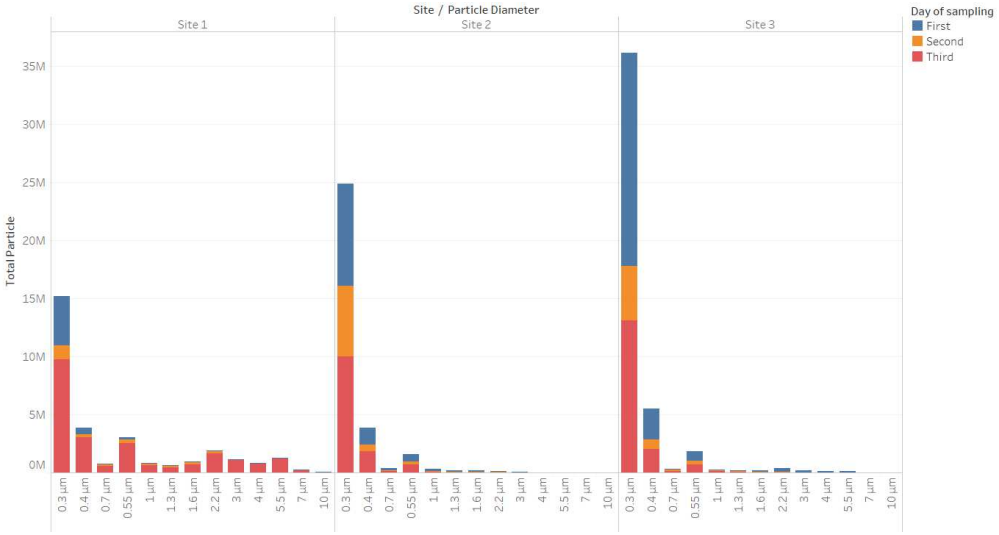

Figure 4.22: Daily total particulate matter by diameter for winter by sites

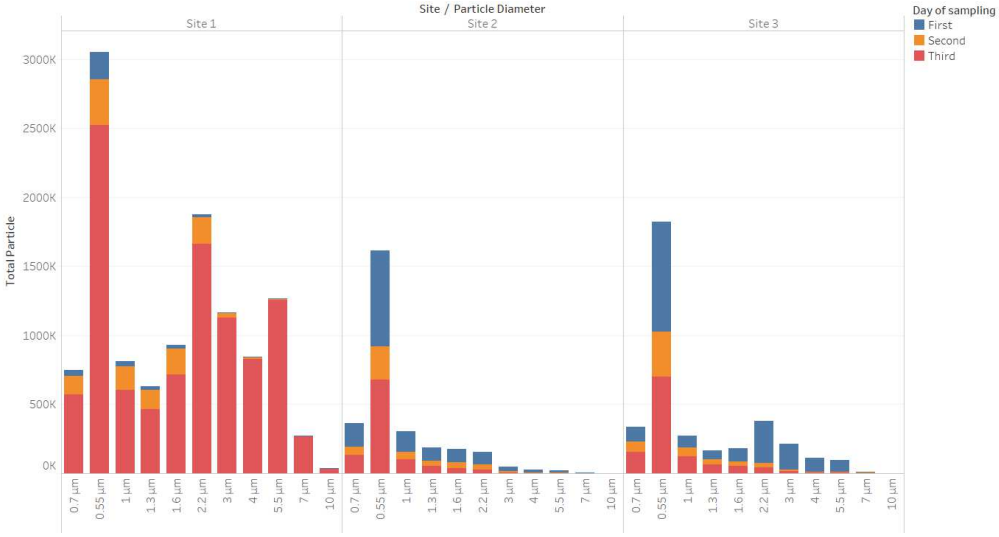

Figure 4.23: Daily total particulate matter by diameter for winter by sites (excluding 0.3 µm & 0.4 µm)

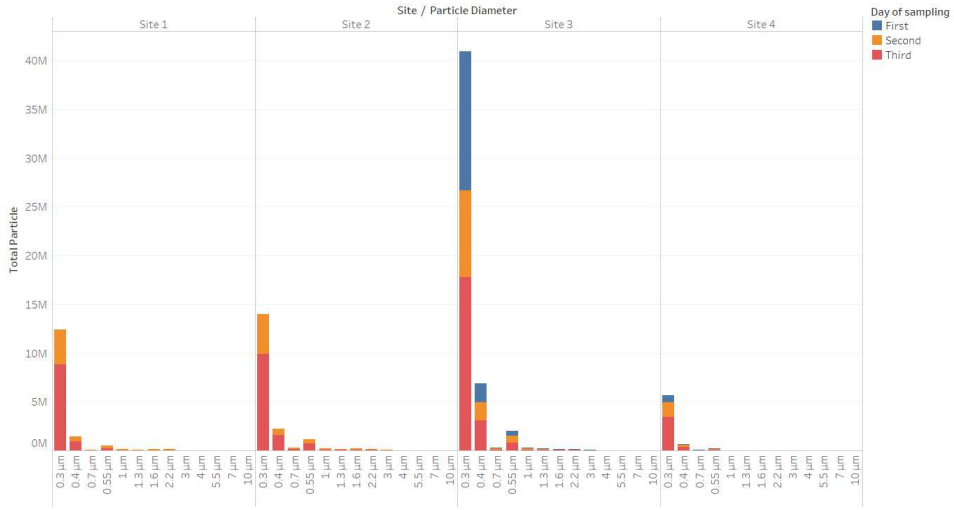

Figure 4.24: Daily total particulate matter by diameter for spring by sites

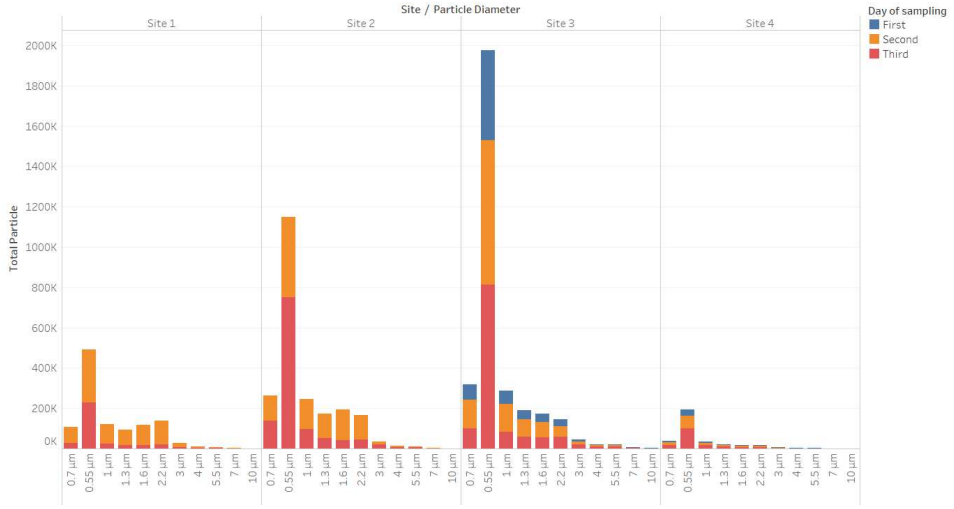

Figure 4.25: Daily total particulate matter by diameter for spring by sites (excluding 0.3 µm & 0.4 µm)

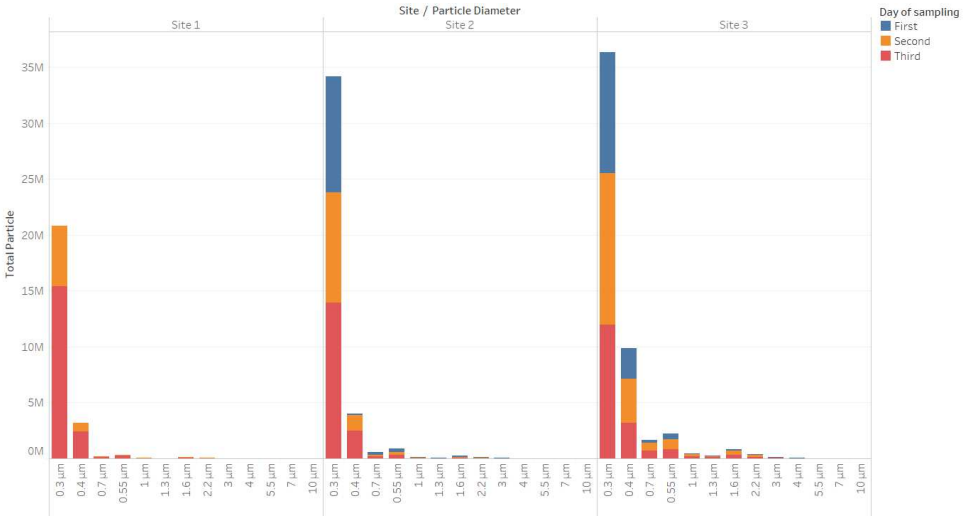

Figure 4.26: Daily total particulate matter by diameter for summer by sites

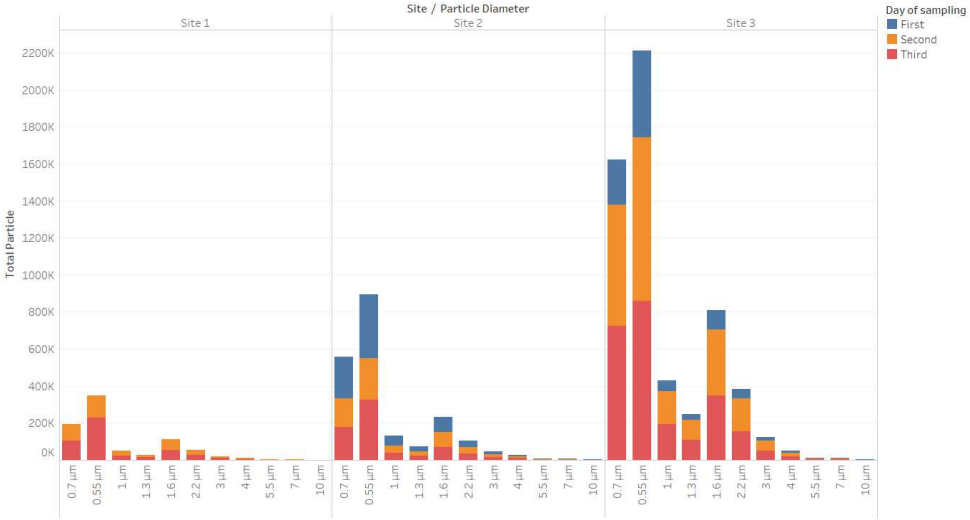

Figure 4.27: Daily total particulate matter by diameter for summer by sites (excluding 0.3 µm & 0.4 µm)

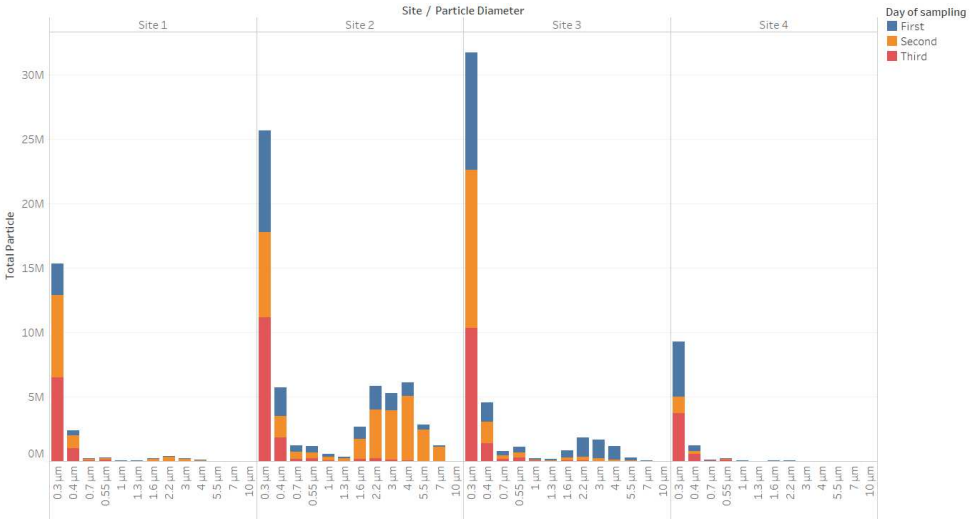

Figure 4.28: Daily total particulate matter by diameter for fall by sites

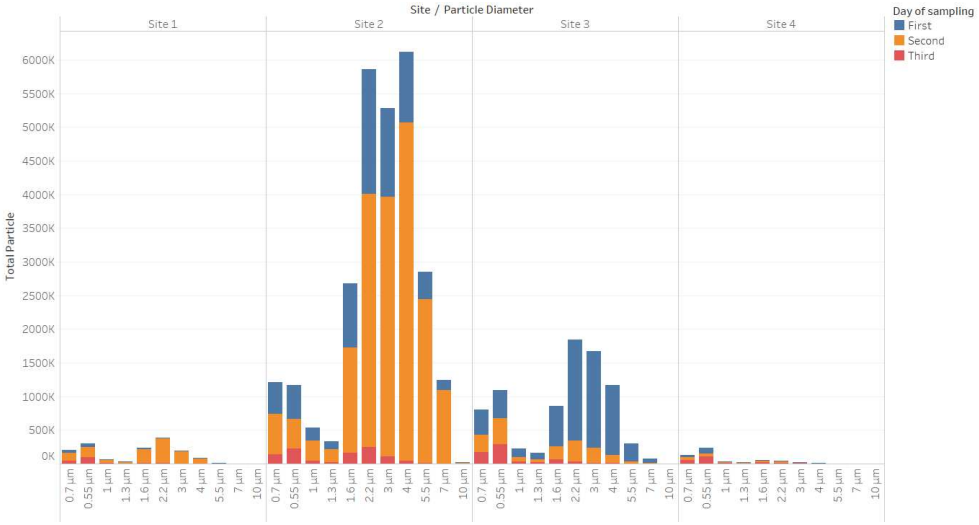

Figure 4.29: Daily total particulate matter by diameter for fall by sites (excluding 0.3 µm & 0.4 µm)

4.3.4. Statistical analysis results

ANOVA and Tukey tests have been performed to find the statistical differences on the daily variation measurements for total particulate number and total particulate counts by diameter for sites and seasons. Findings revealed that there is a significant difference in total daily particulate in Site 1 with P value 0.0305 ($P < 0.05$) (Table 4.1) and the difference is between the first and third days of measurements with P-value 0.0495485 ($P < 0.05$) (Table 4.2). In the other side, we found that there is a significant difference in the total particulate by diameter on fall with P-value 0.024 ($P < 0.05$) (Table 4.31) and the difference is between the measurements of the second and third day with P-value 0.0187435 ($P < 0.05$) (Table 4.32).

Table 4.1: Analysis of variance (ANOVA) test results for Site 1 of daily total particulate matter

	Df	Sum Sq	Mean Sq	F value	P- value < 0.05
Day	2	0.5146	0.2573	5.983	**0.0305**
Residuals	7	0.3010	0.0430		

Bold: Significant difference

Table 4.2: Tukey test results for Site 1 of daily total particulate matter

Days	Difference	Lower	Upper	P- value < 0.05
Second-First	0.1119209	-0.416959105	0.6408010	0.8124917
Third-First	0.5300763	0.001196265	1.0589564	**0.0495485**
Third-Second	0.4181554	-0.013673379	0.8499841	0.0567872

Bold: Significant difference

Table 4.3: Analysis of variance (ANOVA) test results for Site 2 of daily total particulate matter

	Df	Sum Sq	Mean Sq	F value	P- value < 0.05
Day	2	0.03233	0.01616	0.43	0.665
Residuals	8	0.30099	0.03762		

Table 4.4: Tukey test results for Site 2 of daily total particulate matter

Days	Difference	Lower	Upper	P- value < 0.05
Second-First	-0.10567613	-0.5289959	0.3176437	0.7627647
Third-First	0.01157335	-0.4117464	0.4348932	0.9966424
Third-Second	0.11724948	-0.2746685	0.5091675	0.6816476

Table 4.5: Analysis of variance (ANOVA) test results for Site 3 of daily total particulate matter

	Df	Sum Sq	Mean Sq	F value	P- value < 0.05
Day	2	0.1693	0.08466	0.875	0.502
Residuals	3	0.2902	0.09673		

Table 4.6: Tukey test results for Site 3 of daily total particulate matter

Days	Difference	Lower	Upper	P- value < 0.05
Second-First	-0.1534380	-0.4474477	0.1405716	0.3546918
Third-First	-0.0190679	-0.3130775	0.2749417	0.9821225
Third-Second	0.1343701	-0.1596395	0.4283798	0.4422154

Table 4.7: Analysis of variance (ANOVA) test results for Site 4 of daily total particulate matter

	Df	Sum Sq	Mean Sq	F value	P- value < 0.05
Day	2	0.05595	0.02797	1.261	0.329
Residuals	9	0.19960	0.02218		

Table 4.8: Tukey test results for Site 4 of daily total particulate matter

Days	Difference	Lower	Upper	P- value < 0.05
Second-First	-0.06890496	-1.3685296	1.230720	0.9735394
Third-First	0.31687170	-0.9827529	1.616496	0.6164797
Third-Second	0.38577666	-0.9138479	1.685401	0.5114506

Table 4.9: Analysis of variance (ANOVA) test results for winter of daily total particulate matter

	Df	Sum Sq	Mean Sq	F value	P- value < 0.05
Day	2	0.325	0.1625	0.769	0.499
Residuals	7	1.478	0.2112		

Table 4.10: Tukey test results for winter of daily total particulate matter

Days	Difference	Lower	Upper	P- value < 0.05
Second-First	-0.3554138	-0.95484689	0.2440193	0.2419377
Third-First	0.1809213	-0.41851183	0.7803543	0.6451806
Third-Second	0.5363351	-0.06309802	1.1357682	0.0747905

Table 4.11: Analysis of variance (ANOVA) test results for spring of daily total particulate matter

	Df	Sum Sq	Mean Sq	F value	P- value < 0.05
Day	2	0.05249	0.02624	1.086	0.406
Residuals	5	0.12085	0.02417		

Table 4.12: Tukey test results for spring of daily total particulate matter

Days	Difference	Lower	Upper	P- value < 0.05
Second-First	0.1125676	-1.0595837	1.284719	0.9571290
Third-First	0.4333588	-0.7387926	1.605510	0.5500231
Third-Second	0.3207912	-0.6362664	1.277849	0.6072948

Table 4.13: Analysis of variance (ANOVA) test results for summer of daily total particulate matter

	Df	Sum Sq	Mean Sq	F value	P- value < 0.05
Day	2	0.4467	0.22335	3.901	0.0821
Residuals	6	0.3435	0.05725		

Table 4.14: Tukey test results for summer of daily total particulate matter

Days	Difference	Lower	Upper	P- value < 0.05
Second-First	-0.07637899	-0.5381708	0.3854128	0.8566920
Third-First	0.10992844	-0.3518633	0.5717202	0.7332942
Third-Second	0.18630743	-0.2267317	0.5993466	0.3796919

Table 4.15: Analysis of variance (ANOVA) test results for fall of daily total particulate matter

	Df	Sum Sq	Mean Sq	F value	P- value < 0.05
Day	2	4.0	2.001	1.426	0.244
Residuals	140	196.5	1.403		

Table 4.16: Tukey test results for fall of daily total particulate matter

Days	Difference	Lower	Upper	P- value < 0.05
Second-First	0.0414073926	-0.7351363	0.8179511	0.9878715
Third-First	0.0412976824	-0.7352460	0.8178414	0.9879352
Third-Second	-0.0001097101	-0.7766534	0.7764340	0.9999999

Table 4.17: Analysis of variance (ANOVA) test results for Site 1 of daily total particulate matter by diameter

	Df	Sum Sq	Mean Sq	F value	P- value < 0.05
Day	2	0.0046	0.00228	0.015	0.985
Residuals	9	1.3924	0.15471		

Table 4.18: Tukey test results for Site 1 of daily total particulate matter by diameter

Days	Difference	Lower	Upper	P- value < 0.05
Second-First	0.55309123	-0.1524691	1.2586515	0.1549540
Third-First	0.54585020	-0.1597101	1.2514105	0.1624947
Third-Second	-0.00724103	-0.5833286	0.5688465	0.9995102

Table 4.19: Analysis of variance (ANOVA) test results for Site 2 of daily total particulate matter by diameter

	Df	Sum Sq	Mean Sq	F value	P- value < 0.05
Day	2	1.33	0.6666	0.549	0.58
Residuals	75	90.99	1.2132		

Table 4.20: Tukey test results for Site 2 of daily total particulate matter by diameter

Days	Difference	Lower	Upper	P- value < 0.05
Second-First	-0.1608222	-0.7553125	0.4336680	0.7978344
Third-First	-0.4136561	-1.0081464	0.1808341	0.2289927
Third-Second	-0.2528339	-0.8032249	0.2975571	0.5229591

Table 4.21: Analysis of variance (ANOVA) test results for Site 3 of daily total particulate matter by diameter

	Df	Sum Sq	Mean Sq	F value	P- value < 0.05
Day	2	5.71	2.854	2.112	0.126
Residuals	114	154.03	1.351		

Table 4.22: Tukey test results for Site 3 of daily total particulate matter by diameter

Days	Difference	Lower	Upper	P- value < 0.05
Second-First	-0.13981464	-0.6615687	0.3819394	0.8015144
Third-First	-0.17045313	-0.6922071	0.3513009	0.7200170
Third-Second	-0.03063849	-0.5523925	0.4911155	0.9894085

Table 4.23: Analysis of variance (ANOVA) test results for Site 4 of daily total particulate matter by diameter

	Df	Sum Sq	Mean Sq	F value	P- value < 0.05
Day	2	0.86	0.4294	0.34	0.712
Residuals	153	193.33	1.2636		

Table 4.24: Tukey test results for Site 4 of daily total particulate matter by diameter

Days	Difference	Lower	Upper	P- value < 0.05
Second-First	0.23533343	-0.4951378	0.9658047	0.7222822
Third-First	0.30576380	-0.4247074	1.0362350	0.5786114
Third-Second	0.07043037	-0.6600409	0.8009016	0.9711357

Table 4.25: Analysis of variance (ANOVA) test results for winter of daily total particulate matter by diameter

	Df	Sum Sq	Mean Sq	F value	P- value < 0.05
Day	2	3.28	1.639	1.114	0.332
Residuals	127	186.87	1.471		

Table 4.26: Tukey test results for winter of daily total particulate matter by diameter

Days	Difference	Lower	Upper	P- value < 0.05
Second-First	-0.2190058	-0.84410634	0.4060948	0.6839948
Third-First	0.3189139	-0.30618668	0.9440144	0.4488265
Third-Second	0.5379197	-0.08718089	1.1630202	0.1065699

Table 4.27: Analysis of variance (ANOVA) test results for spring of daily total particulate matter by diameter

	Df	Sum Sq	Mean Sq	F value	P- value < 0.05
Day	2	6.28	3.141	2.047	0.133
Residuals	127	194.85	1.534		

Table 4.28: Tukey test results for spring of daily total particulate matter by diameter

Days	Difference	Lower	Upper	P- value < 0.05
Second-First	0.42480410	-0.2661498	1.1157580	0.3146387
Third-First	0.35237524	-0.3385786	1.0433291	0.4498052
Third-Second	-0.07242885	-0.6365903	0.4917326	0.9502066

Table 4.29: Analysis of variance (ANOVA) test results for summer of daily total particulate matter by diameter

	Df	Sum Sq	Mean Sq	F value	P- value < 0.05
Day	2	0.19	0.0949	0.07	0.932
Residuals	101	136.20	1.3485		

Table 4.30: Tukey test results for summer of daily total particulate matter by diameter

Days	Difference	Lower	Upper	P- value < 0.05
Second-First	-0.05089830	-0.7502774	0.6484808	0.9836163
Third-First	0.04777097	-0.6516081	0.7471500	0.9855532
Third-Second	0.09866927	-0.5268744	0.7242129	0.9253952

Table 4.31: Analysis of variance (ANOVA) test results for fall of daily total particulate matter by diameter

	Df	Sum Sq	Mean Sq	F value	P- value < 0.05
Day	2	11.54	5.771	3.82	**0.024**
Residuals	153	231.16	1.511		

Bold: Significant difference

Table 4.32: Tukey test results for fall of daily total particulate matter by diameter

Days	Difference	Lower	Upper	P- value < 0.05
Second-First	0.2543584	-0.3161632	0.82487998	0.5433620
Third-First	-0.4061527	-0.9766743	0.16436890	0.2142698
Third-Second	-0.6605111	-1.2310327	-0.08998949	**0.0187435**

Bold: Significant difference

4.4. Discussion

The current study found that there is a daily variation in the PM numbers between sites and season. E.g., the second day is higher in fall for Site 1, wherein Site 2, the third

day, is higher in on summer, and the second day is higher in fall. These results reflect those of Mansha et al., (2012) who also found that PM2.5 measurements varied daily from 27.4 μg/m³ to 175.5 μg/m³ with an average of 83.53 μg/m³ and the observed PM2.5 concentrations were 5 and 2 times higher in winter and autumn than while in summer it was 1.5 times higher from the standard limit. Moreover, they found that average daily total suspended particles (TSP) concentrations at the Karachi site ranged from 627 to 938 μg/m³ with a mean of 668 μg/m³ compared to 428–998 μg/m³ with a mean of 691 μg/m³ at the Islamabad. This result may be explained by the fact that the atmospheric particulate (such as PM10 and/or PM2.5) emissions varied daily, weekly, seasonal and annually based on the water consumption pattern (Atinkpahoun et al., 2018), emission sources, metrological parameters (such as temperature, relative humidity [RH], and wind speed) (Nathan, 2018), human activities and seasonal variations (Li et al., 2019).

Another important finding was that particulate with a diameter of 2.2 μm, 3 μm, 4 μm, and 5.5 μm were emitted to the air from WWTP in noticeable quantity which inconsistent with the findings of (Korzeniewska, 2011) that bacteria-carrying particles in the air of a WWTP have a diameter between 3.3 μm and 4.7. Thus, they are a potential cause of infections because they can enter the lungs easily, and they can travel by the wind to several kilometers, causing potential environmental and human health issues to WWTP workers and to neighboring residents.

Those findings have important implications for developing deep and detailed researches in the future to analyze what those particulate matter contains because these results showed the total general particulate matter, not including if they hold bacteria, viruses, chemicals, and/or other contaminants. Understanding this major difference will

help comprehend each type of contaminant dispersion and behavior in the air, which will improve the protection measures for human and environmental health. Further studies, which take these variables into account, will need to be undertaken steady starting time of sampling for each process in each season to reduce the variation in the variables that affect the number of particulate matter and their concentration particularly in such study where the environmental and metrological factors are complicated and interrelated, and it is difficult to ignore their effect on the particulate count.

REFERENCES

Amoatey, P., Omidvarborna, H., & Baawain, M. (2018). The modeling and health risk assessment of PM2. 5 from Tema Oil Refinery. *Human and Ecological Risk Assessment: An International Journal*, 24(5), 1181-1196.

Atinkpahoun, C. N., Le, N. D., Pontvianne, S., Poirot, H., Leclerc, J. P., Pons, M. N., & Soclo, H. H. (2018). Population mobility and urban wastewater dynamics. *Science of the Total Environment*, *622*, 1431-1437.

Barancheshme, F., & Munir, M. (2018). Strategies to combat antibiotic resistance in the wastewater treatment plants. *Frontiers in microbiology*, 8, 2603.

Bitta, J., Pavlíková, I., Svozilík, V., & Jančík, P. (2018). Air pollution dispersion modelling using spatial analyses. *ISPRS International Journal of Geo-Information*, 7(12), 489.

Chonova, T., Labanowski, J., Cournoyer, B., Chardon, C., Keck, F., Laurent, É., ... & Bouchez, A. (2018). River biofilm community changes related to pharmaceutical loads emitted by a wastewater treatment plant. *Environmental Science and Pollution Research*, 25(10), 9254-9264.

Daly, A., & Zannetti, P. (2007). Air pollution modeling–An overview. *Ambient air pollution*, 15-28.

Dehghani, M., Sorooshian, A., Ghorbani, M., Fazlzadeh, M., Miri, M., Badiee, P., ... & Delikhoon, M. (2018). Seasonal variation in culturable bioaerosols in a wastewater treatment plant. *Aerosol and air quality research*, *18*(11), 2826-2839.

Dickman, R. N. (2013). Estimation of Aerosolized Antibiotic Resistant Bacteria Concentrations from Wastewater Treatment Facilities Using Spatially-Based Dispersion Modeling.

Eslami, A., Foumani, B. S., Khazraei, R., Pourjafar, Z., Ghaebi, K., Dehghanzad, S., ... & Kheirandish, R. (2011). Implementation of GIS in natural resources. *Annals of Biological Research*, 2(5), 533-540.

Filipkowska, Z., Janczukowicz, W., Krzemieniewski, M., & Pesta, J. (2000). Microbiological air pollution in the surroundings of the wastewater treatment plant with activated-sludge tanks aerated by horizontal rotors. *Polish Journal of Environmental Studies*, 9(4), 273-280.

Fletcher-Lartey, S. M., & Caprarelli, G. (2016). Application of GIS technology in public health: successes and challenges. *Parasitology*, 143(4), 401–415.

Godoi, A. F. L., Grasel, A. M., Polezer, G., Brown, A., Potgieter-Vermaak, S., Scremim, D. C., ... & Godoi, R. H. M. (2018). Human exposure to hydrogen sulphide concentrations near wastewater treatment plants. *Science of the Total Environment*, 610, 583-590.

Han, Y., Yang, T., Chen, T., Li, L., & Liu, J. (2019). Characteristics of submicron aerosols produced during aeration in wastewater treatment. *Science of The Total Environment*, 696, 134019.

Han, Y., Yang, K., Yang, T., Zhang, M., & Li, L. (2019). Bioaerosols emission and exposure risk of a wastewater treatment plant with A2O treatment process. *Ecotoxicology and environmental safety*, *169*, 161-168.

Kirby, R. S., Delmelle, E., & Eberth, J. M. (2017). Advances in spatial epidemiology and geographic information systems. *Annals of Epidemiology*, 27(1), 1–9.

Korzeniewska, E. (2011). Emission of bacteria and fungi in the air from wastewater treatment plants-a review. *Front Biosci (Schol Ed)*, *3*, 393-407.

Li, H., Zhou, X. Y., Yang, X. R., Zhu, Y. G., Hong, Y. W., & Su, J. Q. (2019). Spatial and seasonal variation of the airborne microbiome in a rapidly developing city of China. *Science of the Total Environment*, *665*, 61-68.

Li, J., Zhou, L., Zhang, X., Xu, C., Dong, L., & Yao, M. (2016). Bioaerosol emissions and detection of airborne antibiotic resistance genes from a wastewater treatment plant. *Atmospheric Environment*, 124, Part B, 404–412.

Ma, D., & Zhang, Z. (2016). Contaminant dispersion prediction and source estimation with integrated Gaussian-machine learning network model for point source emission in atmosphere. *Journal of hazardous materials*, 311, 237-245.

Mansha, M., Ghauri, B., Rahman, S., & Amman, A. (2012). Characterization and source apportionment of ambient air particulate matter (PM2. 5) in Karachi. *Science of the total environment*, *425*, 176-183.

Masclaux, F. G., Hotz, P., Gashi, D., Savova-Bianchi, D., & Oppliger, A. (2014). Assessment of airborne virus contamination in wastewater treatment plants. *Environmental Research*, 133, 260–265.

Matacchiera, F., Manes, C., Beaven, R. P., Rees-White, T. C., Boano, F., Mønster, J., & Scheutz, C. (2019). AERMOD as a Gaussian dispersion model for planning tracer gas dispersion tests for landfill methane emission quantification. *Waste Management*, 87, 924-936.

Maués, C. S., Guimarães, C. S., & Martinez-Amariz, A. (2019, November). Study for the dispersion of particulate matter emissions from a steel industry using Gaussian Plume equation through computational modeling. In Journal of Physics: *Conference Series* (Vol. 1386, No. 1, p. 012137). IOP Publishing.

Meng, X., Wu, Y., Pan, Z., Wang, H., Yin, G., & Zhao, H. (2019). Seasonal characteristics and particle-size distributions of particulate air pollutants in Urumqi. *International journal of environmental research and public health*, *16*(3), 396.

Michałkiewicz, M., Kruszelnicka, I., & Widomska, M. (2018). The variability of the concentration of bioaerosols above the chambers of biological wastewater treatment. *Ecological Chemistry and Engineering S*, *25*(2), 267-278.

Miklos, D. B., Remy, C., Jekel, M., Linden, K. G., Drewes, J. E., & Hübner, U. (2018). Evaluation of advanced oxidation processes for water and wastewater treatment–A critical review. *Water research*, *139*, 118-131.

Nathan, P. (2018). *Fine Bioaerosols in Outdoor Air-Characterization, Influence of Seasonal Variation and Chemical Co-pollutants in Urban and Rural Airsheds* (Doctoral dissertation).

Ni, Z. Z., Luo, K., Zhang, J. X., Feng, R., Zheng, H. X., Zhu, H. R., ... & Cen, K. F. (2018). Assessment of winter air pollution episodes using long-range transport modeling in Hangzhou, China, during World Internet Conference, 2015. *Environmental pollution*, 236, 550-561.

Rushton, G. (2003). Public Health, GIS, and Spatial Analytic Tools. *Annual Review of Public Health*, 24(1), 43–56.

Saha, P. K., Khlystov, A., Snyder, M. G., & Grieshop, A. P. (2018). Characterization of air pollutant concentrations, fleet emission factors, and dispersion near a North Carolina interstate freeway across two seasons. *Atmospheric Environment*, 177, 143-153.

Singh, K. (2018). Air pollution modeling. *International Journal of Advance Research, Ideas and Innovations in Technology*, 4(3).

Tang, Q., Huang, K., Liu, J., Shen, D., Dai, P., Li, Y., & Li, C. (2020). Seasonal variations of microbial assemblage in fine particulate matter from a nursery pig house. *Science of The Total Environment*, *708*, 134921.

Teggi, S., Costanzini, S., Ghermandi, G., Malagoli, C., & Vinceti, M. (2018). A GIS-based atmospheric dispersion model for pollutants emitted by complex source areas. *Science of the Total Environment*, 610, 175-190.

Tran, N. H., Reinhard, M., & Gin, K. Y. H. (2018). Occurrence and fate of emerging contaminants in municipal wastewater treatment plants from different geographical regions-a review. *Water research*, *133*, 182-207.

Turolla, A., Cattaneo, M., Marazzi, F., Mezzanotte, V., & Antonelli, M. (2018). Antibiotic resistant bacteria in urban sewage: role of full-scale wastewater treatment plants on environmental spreading. *Chemosphere*, 191, 761-769.

Vantarakis, A., Paparrodopoulos, S., Kokkinos, P., Vantarakis, G., Fragou, K., & Detorakis, I. (2016). Impact on the Quality of Life When Living Close to a Municipal Wastewater Treatment Plant. *Journal of Environmental and Public Health*, 2016, e8467023.

Wang, Y., Li, L., Han, Y., Liu, J., & Yang, K. (2018). Intestinal bacteria in bioaerosols and factors affecting their survival in two oxidation ditch process municipal wastewater treatment plants located in different regions. *Ecotoxicology and environmental safety*, 154, 162-170.

Wark, K., C.F. Warner, and W.T. Davis, Air Pollution Its Control and Origin Third ed. 1998: Addison Wesley Longman

Wastewater Treatment Water Use https://www.usgs.gov/special-topic/water-science-school/science/wastewater-treatment-water-use?qt-science_center_objects=0#qt-science_center_objects

Yang, K., Li, L., Wang, Y., Xue, S., Han, Y., & Liu, J. (2019). Airborne bacteria in a wastewater treatment plant: Emission characterization, source analysis and health risk assessment. *Water research*, *149*, 596-606.

Zhang, M., Zuo, J., Yu, X., Shi, X., Chen, L., & Li, Z. (2018). Quantification of multi-antibiotic resistant opportunistic pathogenic bacteria in bioaerosols in and around a pharmaceutical wastewater treatment plant. *Journal of Environmental Sciences*, *72*, 53-63.